UNIVERSITAT POLITÈCNICA DE CATALUNYA BARCELONATECH

Development of polymeric coatings with combined antifouling/antibacterial properties for titanium dental implants

Judit Buxadera Palomero

UNIVERSITAT POLITÈCNICA DE CATALUNYA BARCELONATECH

PhD Thesis
Materials Science and Engineering Doctoral Program

DEVELOPMENT OF POLYMERIC COATINGS WITH COMBINED ANTIFOULING/ANTIBACTERIAL PROPERTIES FOR TITANIUM DENTAL IMPLANTS

Thesis presented to obtain the qualification of Doctor from the Technical University of Catalonia

Candidate: Judit Buxadera Palomero
Supervisors: Daniel Rodríguez Rius
F. Javier Gil Mur

Abstract

Titanium dental implants are a commonly used solution for the replacement of lost teeth. Even though the success rate is high, the number of infections related to the placement of the implant is still remarkable and may impair the proper function of the device, leading to health and economic costs. The infections related to medical devices start with a bacterial adhesion and proliferation on the material surface, leading to the formation of a complex biofilm able to protect the bacteria from the host immune response and the treatment with antibiotic. Due to the difficulty of treatment of the implant site once the biofilm is settled, one of the strategies to avoid the infection is to deal with the initial bacterial adhesion.

This PhD thesis deals with the development of polymeric antibacterial coatings on titanium for dental implants, focusing on the achievement of fast and cost-effective procedures. With this aim, different coating strategies have been developed, tested and compared.

A pre-treatment of the titanium surface was optimized in the first part of the thesis in order to achieve a clean surface and to enhance the chemical reactivity of the titanium oxide. With this aim, low pressure plasma activation was the selected method. The use of plasma activation allows for the removal of organic contaminants while increasing the surface energy of the treated surfaces.

For the preparation of the polymeric antibacterial coatings, two different antifouling polymers have been used, namely, polyethylene glycol (PEG) and poly-2-hydroxyethylmetacrylate (PHEMA). PEG coatings were prepared by three different techniques, a wet chemical technique (silanization), a plasma enhanced chemical vapor deposition and an electrochemical process (electrodeposition). The three methods rendered an ultra-thin coating able to resist the bacterial adhesion. On the other hand, PHEMA-like coatings were prepared in a novel set-up by treating the liquid monomer by a plasma jet.

Moreover, the different coatings were biofunctionalized in order to achieve multifunctionality and enhance the performance of the coating. For instance, the combination of PEG with a cell adhesion peptide (RGD) reported a better human fibroblast adhesion while maintaining the antifouling properties of the coating. PEG was also used as a platform for the immobilization of antimicrobial peptides (AMP). The bonding of the polymer with the AMP was optimized, achieving a surface able to reduce the bacterial adhesion and to kill the bacteria still able to adhere to the surface. Finally, the combination of two different plasma polymerized coatings with antibiotics (either Doxycycline or Vancomycin) was used as a drug delivery system.

Resum

Els implants dentals de titani són la solució més estesa per substituir peces dentals. Tot i que les taxes d'èxit són elevades, el nombre d'infeccions relacionades amb la col·locació de l'implant és elevat, i influeix en el mal funcionament de l'implant, amb un elevat cost tan a nivell econòmic com de salut.

Les infeccions associades als dispositius sanitaris comencen amb una adhesió i proliferació dels bacteris a la superfície del material, que comporta la formació d'un biofilm capaç de protegir els bacteris de l'acció del sistema immunitari de l'hoste i del tractament amb antibiòtics.

Aquesta tesi doctoral es basa en el desenvolupament de recobriments polimèrics antibacterians en titani per aplicacions dentals, buscant aconseguir mètodes ràpids i econòmics. Per tal d'assolir aquest objectiu, s'han desenvolupat, provat i comparat diferents estratègies per obtenir els recobriments.

En la primera part de la tesi s'ha optimitzat un pretractament de la superfície del titani, per tal d'obtenir una superfície neta i millorar la reactivitat química de l'òxid de titani. El mètode seleccionat per l'activació ha estat l'activació per plasma, que permet eliminar els contaminants orgànics i augmentar l'energia superficial de les mostres tractades.

Els polímers seleccionats per als recobriments han estat el polietilenglicol (PEG) i el 2-hidroxietilmetacrilat (PHEMA), que tenen propietats *antifouling*. Per preparar els recobriments de PEG s'han utilitzat tres mètodes diferents: la silanització, la polimerització per plasma i l'electrodeposició. Els tres mètodes han donat com a resultat una capa fina capaç de resistir l'adhesió bacteriana. Per altra banda, els recobriments amb PHEMA s'han preparat amb una nova metodologia, tractant el líquid amb un plasma jet.

Els diversos recobriments s'han biofuncionalitzat per tal d'aconseguir una multifuncionalitat i millorar el seu funcionament. La combinació del PEG amb un pèptid d'adhesió cel·lular ha permès millorar l'adhesió de fibroblasts i mantenir les propietats *antifouling* del recobriment. La immobilització de pèptids antibacterians al PEG permet obtenir una superfície resistent a l'adhesió bacteriana i amb efecte antibacterià sobre els bacteris capaços d'adherir-se al recobriment. Per últim, la combinació de dos recobriments preparats per polimerització per plasma amb dos antibiòtics (vancomicina o doxiciclina) permet obtenir un sistema d'alliberació de fàrmacs a la superfície del titani.

Agraïments

Al llarg de la tesi he tingut la sort de creuar-me amb molt bones persones, que m'han ajudat a tirar endavant i a créixer tan personal com professionalment. Per tot el suport que he rebut, us vull dedicar aquestes paraules.

Als meus directors de tesi, el Dr. Daniel Rodríguez i el Dr. Xavier Gil. Al Dr. Daniel Rodríguez, per haver-me donat l'oportunitat de realitzar aquesta tesi. Per haver confiat en mi des del principi i pel suport incondicional que m'ha donat. Per haver-me deixat espai per desenvolupar-me com a investigadora, estant sempre disposat a compartir el seus coneixements i el seu esperit crític. Al Dr. Xavier Gil, per haver-me acollit al grup de recerca. Pel seu suport i el seu bon humor.

A la Dra. Cristina Canal, per haver-me guiat al llarg de la tesi. Per tenir sempre una estona per ajudar-me, animar-me i donar-me consells, sempre amb un somriure. Per totes les oportunitats que m'ha donat al llarg d'aquests anys, i per estar al meu costat.

A la Dra. Mª Pau Ginebra, per haver-me obert les portes del grup. Perquè el seu esforç i dedicació són un exemple a seguir i aconsegueixen mantenir el bon ritme de treball del grup.

A tots els companys del grup de Biomaterials, Biomecànica i Enginyeria de Teixits, per totes les estones que hem compartit. Pel bon ambient de treball que tenim i per estar sempre disposats a donar un cop de mà. Als post-docs i professors del grup, a en Carles, la Marta, en Jordi, la Montse, la Clara, en José María, en Giuseppe, la Elisa i en Román, per la seva bona disposició en tot moment. Als professors i companys de l'EUETIB, la Gemma, en Jordi Llumà, en Jordi Jorba, en José Maria i en Toni, per acollir-me, aconsellar-me i ajudar-me sempre que m'ha calgut.

Als doctorands amb qui he compartit els laboratoris, els bons i els mals moments. Al Romain, la Mireia, la Roberta, la Mar, en Diego, en Yago, en Zhitong i l'Angelica. A la Maria, per totes les estones que va invertir en ajudar-me, al Pablo pels seus consells, a la Carolina, la Sara, en David, en Yassine, la Maria Isabel i la Natalia, per tot el suport i ajuda que m'heu ofert. Al Cédric, per la seva ajuda amb el plasma i per tots els bon moments que hem passat junts.

Menció especial a l'Anna, per arrancar-me un somriure en qualsevol ocasió, per estar sempre disposada a escoltar-me i per tots els bons moments que hem passat juntes. A la Joanna, per "aguantar-me" en els bons i els mals moments i per ajudar-me a tirar endavant. A Priya, por todos los momentos que hemos compartido. Por darle un toque de humor y realidad a la vida. A l'Elia, per ensenyar-me una manera més fàcil de veure la vida. Per estar sempre disposada a xerrar una estona. Al Casi, per haver estat sempre al meu costat. A en Lluís, per tenir sempre una estoneta per xerrar. A la Noelia, per tenir sempre un recurs per arreglar els papers que fem malament. Per la paciència que té i per ser més que una companya (y por quererme como soy...).

A tots els projectistes que han compartit el seu dia a dia amb mi, l'Adriana, la Cristina i la Patricia, hem après molt juntes. Especialment a en Sergi, perquè amb les

teves bromes m'has ajudat a estimar una mica més la meva feina (PEG PEG PEG). Per tenir la paciència d'aprendre junts quan feies el projecte i per haver seguit al meu costat. Als projectistes amb qui he compartit estones de laboratori (i de bacteris), especialment a en Marc Avilés i a la Bea.

Als d'empreses, perquè encara que vaig estar poc temps amb vosaltres, vaig poder aprendre molt. A en Marc i en Lluís, per haver-me donat l'oportunitat de treballar amb vosaltres. A en Miquel, per tot el suport que m'ha donat, tan durant el procés de demanar la beca de doctorat com després. Per estar sempre disposat a donar un cop de mà. I molt especialment a la Mònica, per fer-me sempre costat.

A tots els tècnics, la Txell per aconseguir que funcionin els laboratoris i que no ens hi fem mal. Per tenir sempre un moment i per ser sempre tan eficient, fas que la feina sigui molt més fàcil. A en Kim, per tots els "invents" que ha desenvolupat pels laboratoris, sempre a punt per donar un cop de mà. A l'Isaac, per fer que les sessions de SEM siguin molt més divertides. A en Pedro, pel seu bon humor i la seva bona disposició. A la Montse, en Trifon i la Carla, per tota l'ajuda que m'han prestat i per tenir sempre un moment per mi.

To the people from the University of Bari. To Dr. Pietro Favia and Dr. Fabio Palumbo for their advice and for giving me the opportunity of working with them. To Chiara, for sharing her time in the labs, and to Ilaria, Marta, Giuseppe, Teresa, Savino and Danilo, for their help and for showing me the italian life.

To the people from the INP in Greifswald. To Dr. Stephan Reuter for making possible my stage in the institute. To Dr. Martin Polak and Dr. Katja Fricke for their advice and for opening the doors of their labs. To the rest of the people from the group, for making my daily life there easier. Especially to Johanna and Monica, for all the time that we shared together and for taking me into account.

A les meves amigues de sempre, la Gisela, la Neus i la Núria, perquè esteu sempre al meu costat. M'heu ajudat a passar els mals moments i heu compartit els bons amb mi. Per no dubtar mai que puc aconseguir el que em proposi. A en Martín, en Josep i en Francesc, per adoptar-me com una amiga més.

Als meus pares, per ser un exemple de superació i dedicació. Perquè sé que esteu orgullosos de mi, i jo n'estic de vosaltres. Pel vostre suport incondicional, i per estar sempre al meu costat. Sense vosaltres no hauria arribat on sóc. A en Jordi, l'Arnau, la Noelia i la Laura, per fer-me costat i estar pendents de mi. I als petits, en Gerard, en Bernat i la Berta, per tota l'alegria i la felicitat que m'heu aportat. A mis tíos y primos, porque aunque estando lejos siguen apoyándome.

A tots vosaltres, i a tothom que ha contribuït a fer possible aquesta tesi, moltes gràcies!

Publications and communications derived from this thesis

Publications in indexed journals

1. J. Buxadera-Palomero, C. Calvo, S. Torrent-Camarero, F. J. Gil, C. Mas-Moruno, C. Canal, D. Rodríguez, *Biofunctional polyethylene glycol coatings on titanium: An in vitro-based comparison of functionalization methods*. Colloids and Surfaces B: Biointerfaces 152 (2017): 367-375. DOI: 10.1016/j.colsurfb.2017.01.042
2. J. Buxadera-Palomero, C. Canal, S Torrent-Camarero, B. Garrido, F. J. Gil, D. Rodríguez. *Antifouling coatings for dental implants: Polyethylene glycol-like coatings on titanium by plasma polymerization*, Biointerphases,10(2):029505 (2015). DOI: 10.1116/1.4913376
3. C. Labay, J. Buxadera-Palomero, M. Aviles, C. Canal, M. P. Ginebra, *Modulation of release kinetics by plasma polymerization of ampicillin-loaded b-TCP ceramics,* J. Phys. D: Appl. Phys. 49, 304004 (2016)

Papers in preparation

1. J. Buxadera-Palomero, P. Carrasco, K. Albó, F. J. Gil, D. Rodríguez, *Polyethylene glicol pulsed electrodeposition for the design of antifouling coatings on titanium*
2. J. Buxadera-Palomero, P. Carrasco, F. J. Gil, C. Mas-Moruno, D. Rodríguez, *Antifouling coatings as a platform for antimicrobial peptides*
3. J. Buxadera-Palomero, C. Labay, C. Canal, F. J. Gil, D. Rodriguez, *Modulation of doxycycline release from titanium implants by a plasma polymerized polyethylene glycol coating*

Book chapters

1. Judit Buxadera-Palomero, Cristina Canal, F. Javier Gil, Daniel Rodríguez, *Dental implants: Plasma Polymerization for antibacterial coatings*, Encyclopedia of Plasma Technology, J. Leon Shohet, Ed. 328-338 (2016)

Conference papers

1. Judit Buxadera-Palomero, Cristina Canal, F.Javier Gil, Daniel Rodríguez, *Obtención y caracterización de un recubrimiento de poli(etilenglicol) sobre titanio por polimerización por plasma*. Actas del XXXVI Congreso de la Sociedad Ibérica de Biomecánica y Biomateriales. F.Javier Rojas, Carmen Gutiérrez (eds.), ISBN 978-84-338-5595-4, pp. 92.
2. Judit Buxadera-Palomero, Sergi Torrent, F.Javier Gil, Daniel Rodríguez. *Desarrollo de un tratamiento antiadherente en superficies de titanio para aplicaciones biomédicas*. Actas de las Jornadas de Investigación EUETIB 2013, Beatriz Garrido, Antonio Travieso, Ricardo Torres (eds.), ISBN 978-84-695-9922-8, pp.33-36.

Oral Comunicacions in national and international conferences

1. Judit Buxadera-Palomero, Chiara Loporto, Cristina Canal, Daniel Rodríguez, F. Javier Gil, Pietro Favia, Fabio Palumbo, *Atmospheric Pressure Plasma Processing of Titanium Alloys for Biomedical Application*, Bioplasmas & plasmas with liquids - Joint Conference of COST ACTIONS TD1208

"Electrical discharges with liquids for future applications" & MP1101 Biomedical Applications of Atmospheric Pressure Plasma Technology, Bertinoro, Italy, 13th-17th September 2015

2. Judit Buxadera-Palomero, Patricia Carrasco, Cristina Canal, Carles Mas-Moruno, F. Javier Gil, Daniel Rodríguez, *Antifouling coatings as a platform for antimicrobial peptides immobilization*, 27th European Conference on Biomaterials, Krakow, Poland, 30 august-3 september 2015
3. Judit Buxadera-Palomero, F.Javier Gil, Cristina Canal, Daniel Rodríguez. *Obtención de un recubrimiento antifouling sobre titanio para aplicaciones biomédicas*. XIII Congreso Nacional de Materiales. 18-20 junio 2014, Barcelona.
4. Judit Buxadera-Palomero, Sergi Torrent, F.Javier Gil, Daniel Rodríguez, *Desarrollo de un tratamiento antiadherente en superficies de titanio para aplicaciones biomédicas*. Jornadas de Investigación EUETIB 2013. 3-4 diciembre 2013, Barcelona.
5. Judit Buxadera-Palomero, Cristina Canal, F.Javier Gil, Daniel Rodríguez. *Obtención y caracterización de un recubrimiento de poli(etilenglicol) sobre titanio por polimerización por plasma*. XXXVI Congreso de la Sociedad Ibérica de Biomecánica y Biomateriales, 25-27 octubre 2013, Granada.
6. Judit Buxadera-Palomero, Cristina Canal, Xavier Gil, Daniel Rodríguez, *Antifouling surfaces by plasma polymerization on dental implants*, Summer school: Contribution of calcium phosphate-based materials to new bone regeneration strategies (June 10-12 2013, Barcelona)

Poster presentations in national and international conferences

1. J. Buxadera-Palomero, C. Labay, C. Canal, F. J. Gil, D. Rodriguez, *Modulation of doxycycline release from titanium implants by a plasma polymerized polyethylene glycol coating*, 6th International Conference on plasma medicine, 4-9 september 2016, Bratislava (Slovakia)
2. C. Labay, J. Buxadera-Palomero, M. Avilés, C. Canal, M. P. Ginebra, *Plasma polymerization on b-TCP for the design of antibiotic delivery systems in bone repair surgery*, 6th International Conference on plasma medicine, 4-9 september 2016, Bratislava (Slovakia)
3. F. Palumbo, C. LoPorto, C. Canal, J. Buxadera-Palomero, P. Jelinek, E. Sardella, G. Camporeale, P. Favia, *Bio-composite coatings for biomedical applications*, 6th International Conference on plasma medicine, 4-9 september 2016, Bratislava (Slovakia)
4. C. Robo, M. Espanol, J. Buxadera-Palomero, C. Öhman, M. P. Ginebra, C. Persson, *The effect of two fatty acids on the antibacterial properties of calcium phosphate cements*, European Chapter Meeting of the Tissue Engineering and Regenerative Medicine International Society 2016 28 June - 1 July, 2016 Uppsala (Sweden)

5. Judit Buxadera-Palomero, Sergi Torrent-Camarero, Adriana Carreter, Cristina Canal, F. Javier Gil, Daniel Rodriguez, *Recubrimientos antiadherentes sobre titanio: métodos de deposición de Polietilenglicol*, XXXVIII Congreso de la Sociedad Ibérica de Biomecánica y Biomateriales, Barcelona, 6-8 november 2015
6. Judit Buxadera-Palomero, Cristina Canal, F. Javier Gil, Daniel Rodríguez. *Antibacterial coatings on Titanium obtained by plasma polymerization of Tetraglyme*. COST TD1208 2nd annual meeting "Electrical discharges with liquids for future applications" Barcelona, 23rd-26th February 2015.
7. Judit Buxadera-Palomero, Sergi Torrent, Cristina Calvo, Adriana Carreter, F. Javier Gil, Cristina Canal, Daniel Rodríguez, *Antifouling coatings on titanium: deposition methods of poly(ethylene glycol)*, 7th IBEC Symposium Bioengineering for future medicine, 29th September 2014, Barcelona
8. Judit Buxadera-Palomero, Sergi Torrent, Cristina Calvo, F. Javier Gil, Cristina Canal, Daniel Rodríguez, *Deposition methods of poly(ethylene glycol) antifouling coatings on titanium*, 26th European Conference on Biomaterials, 30 august-4 september 2014, Liverpool
9. Judit Buxadera-Palomero, F.Javier Gil, Cristina Canal, Daniel Rodríguez. *Poly(ethylene glycol) coatings on Titanium by plasma polymerization*, 18th European Summer School Low Temperature Plasma Physics: Basics and applications, 5-10 Octubre 2013, Bad Honnef (Alemania).

Awards

Young researcher presentation award in the 6th International Conference on plasma medicine, Bratislava (Slovakia), for the poster presentation *Modulation of doxycycline release from titanium implants by a plasma polymerized polyethylene glycol coating.*

SCOPE AND AIM OF THE THESIS

The main aim of this PhD Thesis is to develop new coatings on titanium to achieve a proper soft tissue integration by reducing the rate of adhered bacteria and/or enhancing the cell adhesion to be employed in the head of an enhanced dental implant. This will be investigated by producing and functionalizing polymeric coatings on titanium surfaces by different methods.

To accomplish this main objective, a number of specific objectives have been defined:

1. To study the effects of plasma activation on the titanium surface in terms of the surface properties.
2. To develop a novel silanized PEG to efficiently coat titanium surfaces and the functionalization of the coating with a cell adhesion peptide.
3. To obtain an electrodeposited PEG bis(aminopropyl) terminated coating on titanium and use the coating as a platform for the immobilization of antimicrobial peptides (Magainin 2 and human Lactoferrin 1-11).
4. To obtain a PEG-like coating by plasma polymerization using different precursors and characterize their physical and chemical properties as well as their biological suitability for the defined application. The coating is evaluated as a drug delivery of antibacterial drugs.
5. To use atmospheric pressure plasma in contact with liquids to develop novel antibacterial coatings on titanium.
6. To discuss the main properties of each coating, the suitability of the methods and the performance *in vitro* of the coatings.

TABLE OF CONTENTS

List of tables

List of figures

List of abbreviations

AMP: AntiMicrobial Peptide

ANOVA: ANalysis Of VAriance

AP: Acquired Pellicle

APPJ: Atmospheric Pressure Plasma Jet

ATR: Attenuated Total Reflectance

BE: Binding Energy

BHI: Brain Heart Infusion

BSA: Bovine Serum Albumin

CFU: Colony Forming Units

CW: Continuous Wave

DAPI: 4'-6-diamidino-2-phenylindole

DBD: Dielectric Barrier Discharge

EDC: 1-ethyl-3(3-dimethylaminopropyl) carbodiimide

FITC: Fluorescein Isotiocyanate

FTIR: Fourier Transformed Infrared spectroscopy

HEMA: 2-HydroxyEthylMethacrylate

hFFs: human Foreskin Fibroblasts

hLF1-11: human LactoFerrin

KE: Kinetic Energy

LDH: Lactate DeHydrogenase

MIC: Minimum Inhibitory Concentration

mPER: mammalian Protein Extraction Reagent

MRS: Man-Rogosa-Sharpe broth

NHS: N- hydroxy-succinimide

OES: Optical Emission Spectroscopy

PBS: Phosphate Buffered Saline

PECVD: Plasma Enhanced Chemical Vapor Deposition

PEG: PolyEthylene Glycol

RGD: arginine, glycine and aspartic acid

SAOS: Sarcoma OSteogenic

SEM: Scanning Electron Microscopy

sccm: standard cubic centimeter per minute

sLm: Standard liter per minute

SMP: N-succinimidyl- 3-maleimidopropionate

TCPS: Tissue Culture PolyStyrene

TH: Todd-Hewitt broth

ToF-SIMS: Time of Flight Secondary Ion Mass Spectrometry

XPS: X-Ray Photoelectron Spectroscopy

INTRODUCTION

This section describes the state of the art regarding dental implant placement, the infection related to dental implants and the main strategies to avoid and treat such infections, focusing on the titanium surface treatments and coatings.

1. INTRODUCTION

1.1. Dental implants

A dental implant is a medical device used to substitute the root of lost teeth, in order to restore mastication, to improve aesthetics and to aid speech. Implants act as the support for the tooth to be substituted, allowing the anchorage to the maxillary or the mandibular bone [1].

Implant-supported structures are basically composed by three parts, namely, the crown, the abutment and the implant. The crown acts as the prosthesis and substitutes the visible part of the tooth. The abutment connects the crown with the implant. The implant, that can have screw or cylindrical shape, is placed into the bone to anchor the structure (Figure 1.1). Nowadays, the most used design for dental implants is the screw-shaped one, with a typical diameter of 3-5mm and a length of 6-16mm depending on the anatomic and clinical conditions.

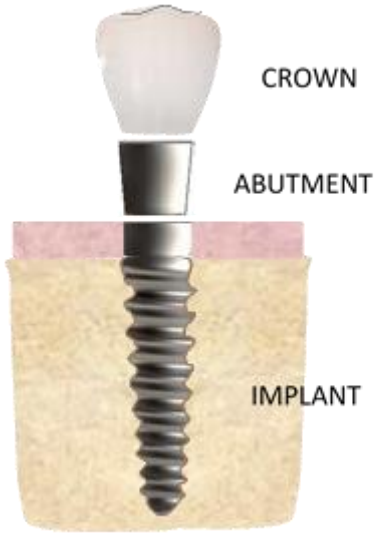

Figure 1.1. Components of an implant supported dental reconstruction. Adapted from [2]

The main requirements for a material used as dental implant are the biocompatibility, biofunctionality and the ability to osseointegrate, i.e. have a strong biomechanical bond between implant and jaw bone. The material of choice for this application is commercially pure titanium [3]. Titanium is covered by a layer of titanium oxide which is formed on the surface of the metal within milliseconds following exposure to air, water or other electrolytes [2]. This oxide layer facilitates adsorption of specific biomolecules and subsequent cell attachment and spreading, rendering titanium an excellent biomaterial with osseointegration properties [3].

Even though a dental implant resembles the structure of the natural tooth, there are some differences in the interaction of the implant/tooth and the surrounding tissues (Figure 1.2). For the soft tissue/tooth interface, a bundle of fibers inserted into the root

cementum between the alveolar crest and cement enamel junction is connecting the gingiva to the tooth, while the transmucosal part of the implant (abutment or neck of the implant) protrudes through the overlying mucosa which heals around the implant without a cementum attachment.

In the case of the bone/tooth interface, there is a periodontal ligament that attaches the tooth to the alveolar bone. This periodontal ligament is based on collagen fibers, has a blood supply and a proprioceptive mechanism which can detect changes in the forces applied to the tooth. In contrast, the implant connects directly to the alveolar bone through osseointegration [4–6].

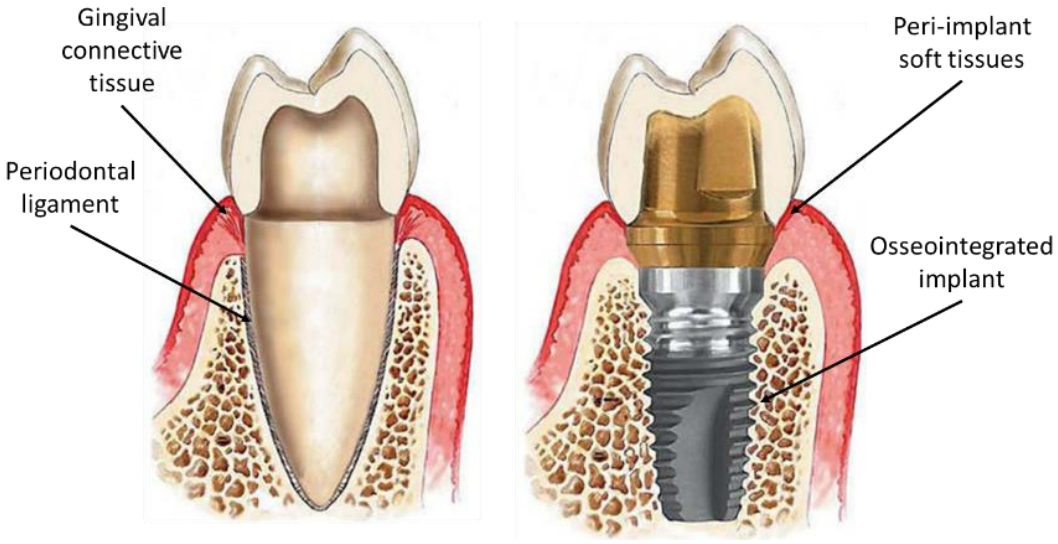

Figure 1.2. Dental implant structure compared to natural tooth (Adapted from [7])

1.2. Failure of dental implants

The success rates of dental implants are high, ranging from 90% to 98% depending on the kind of study reported. In a systematic review performed by Berglundh *et al.* [8] a mean survival rate of 96.5% was found after periods of follow-up higher than 5 years. In another review by Moraschini *et al.* [9], survival rates of 94.6% and 91.2% were found for follow-up periods of more than 10 and 20 years respectively.

Despite the high success rate, only 66.4% of the patients are completely free of reported complications [10]. The main causes for the failure of the implants are the lack of tissue integration of the surface and the possibility of a biomaterial-centered infection. These two processes were associated in the term “race for the surface” by Gristina [11], where the competition between the cell tissue integration and the bacterial adhesion is described. If the biomaterial surface is occupied by the cells, it will be less available for the bacteria colonization. Regarding the factors influencing failure of dental implants, two kinds of complications can be found: biological complications (Figure 1.3) and technical complications (fracture of suprastructures, losing of retention, screw loosening) [12].

1.3. Infection related to dental implants

While the stability of the implant is achieved through the osseointegration, the maintenance of a barrier mechanism is achieved through a proper interaction between the head of the implant and the gingiva, which is known as biological sealing or biosealing [13]. The lack of biosealing can lead to the infiltration of bacteria to the peri-implant pocket and, subsequently, to the dental plaque formation. Plaque accumulation causes the inflammation of the soft tissue surrounding the implant (mucositis) and, if not treated, leads to the infection of the supporting bone (periimplantitis) [14].

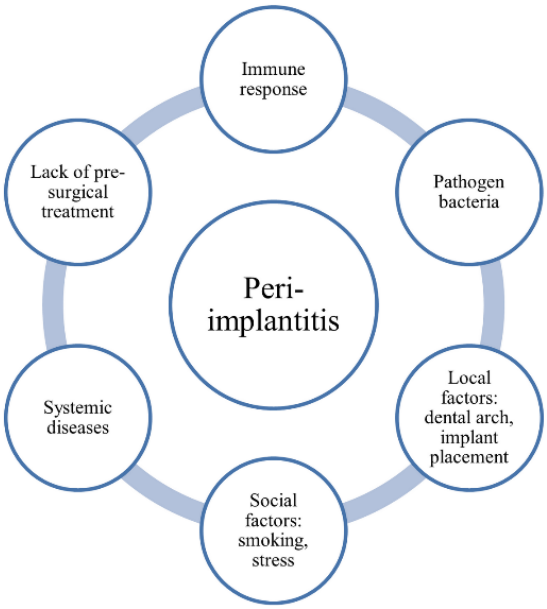

Figure 1.3. Main causes associated with the peri-implantitis [2]

The dental plaque is a type of biofilm hosted in the oral cavity. A biofilm is a multi-specie bacterial community embedded in an extracellular substance produced by the bacteria. The dental plaque is characterized by its high biodiversity (around 700 species) and high cell density (10^{11}cells/g wet wt) [15]. Biofilm formation is an adaptive response of the bacteria, since it provides survival optimization, better access to the nutrients and an improved protection against the external aggressions (host immune system or antibiotics) [16–18]. The bacteria in a biofilm undergo a change on the physiological activity (biofilm phenotypes). These changed phenotypes are associated with the virulence and pathogenicity of the bacteria [19–22].

The formation of a biofilm comprises four stages (Figure 1.4). The first stage of the biofilm formation occurs right after the placement of the implant, when an unspecific adsorption of proteins takes place and forms the acquired pellicle (AP) (Figure 1.4a). The AP contains saliva and enzymes which mediates the bacterial adhesion through a group of biochemical reactions. The interaction of the proteins with the biomaterial surface is a complex process which depends on the microtopography, surface free

energy, roughness, chemical composition of the surface and mechanical properties of the material [23–25].

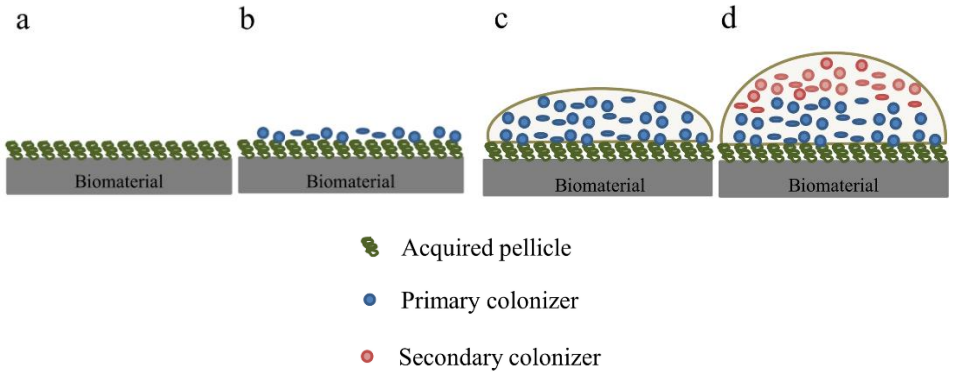

Figure 1.4. Stages of the biofilm formation. a) formation of the acquired pellicle, b) adhesion of primary colonizers, c) formation of the protective layer, d) adhesion of the secondary colonizers [2]

The first bacteria adhering to the AP are called primary or early colonizers (Figure *1.4*b). These bacteria release molecular signaling products that can be detected by the surrounding bacteria in a process known as quorum sensing. When the frequency of signaling reaches a threshold, a gene regulation is triggered, and the bacteria start to produce extracellular fibers known as pili, which are used for the attachment to the substrate and to the other bacteria. After the pili formation, the bacteria secrete an extracellular matrix of proteins, polysaccharides and nucleic acids (Figure *1.4*c). As a final stage, secondary or late colonizers adhere to the biofilm forming the complete biofilm (Figure *1.4*d).

A dynamic biofilm composition has been reported for dental implant surfaces. The biofilm is formed by a complex bacterial ecology, including early colonizers such as *Streptococcus sanguinis* [25–27], which attach to the surface and guide the later colonizers, such as *Porphyromonas gingivalis*, *Fusobacterium nucleatum* and *Aggregatibacter actinomycetemonitans* [28,29]. Other species, such as *Lactobacillus salivarius*, have an important role on the formation and maintenance of the biofilm through the interaction with other strains and their by-products [30–32]. During the peri-implant disease, the bacterial flora shifts to a more pathogenic one. This fact, and the communication of the bacteria through the quorum sensing mechanism, allows the bacteria to increase the virulence aimed at favoring their growth at the expense of the tissue destruction [33].

The main problem associated with the presence of bacteria and the formation of a biofilm is not the biofilm itself, but the host response induced by the bacteria. During the progression of the peri-implantitis, the tissue homeostasis is turned into tissue destruction [34]. The host response involves the stimulation of cells to produce inflammatory associated products such as cytokines, interleukins and prostaglandins,

which in turn induce the release of enzymes from the cells in the periodontum. This enzymes, called matrix metalloproteinases, are degrading agents of the periodontal connective tissue [35,36].

1.4. Antibacterial treatments for dental implants

There are different approaches to confer antibacterial properties to the titanium surface, but all of them are intended to avoid the initial interaction between the implant surface and the bacteria, either repelling or killing them, in order to prevent the biofilm formation. Thus, antimicrobial surfaces are designed with the principle that they should either repel the microbes or kill them on contact. According to these two strategies, the coatings can be classified as biopassive or bioactive respectively [37–39].

1.4.1. Surface modification

The passivating titanium oxide layer present naturally on the titanium surface exhibits photocatalytic effects when it has the crystalline phase anatase. To obtain this crystalline structure, an amorphous layer is deposited by anodization, followed by a thermal treatment that produces a crystalline order in the layer. An implant with this anatase oxide layer can be UV irradiated *in situ* in order to kill the bacteria present on the surface. The use of the UV treatment is limited when the implant is osseointegrated or within a deep peri-implant pocket, since the light is not able to reach the infected area [40–45].

Topography is an important factor on the interaction of the bacteria and the titanium surface. The shape and the rigidity of the bacterial cells allow designing specific topographies to avoid bacterial adhesion. It is generally accepted that an average roughness of 200 nm is the threshold value to modify the bacterial adhesion [46,47].

Moreover, differences between eukaryotic cells and bacteria enable the possibility to achieve topographies that promote the cell adhesion while avoiding bacteria adhesion. Several studies reported the influence of a surface patterning in the nano and micrometric scale, showing the changes in the shape and the size of the aggregates and the orientation of the cell substructures involved in the bacterial movement [48,49].

The modification of the chemical composition of the outer layer of the implant by doping it with inorganic antimicrobial agents confers antibacterial properties to titanium. These dopants show a good antimicrobial activity, and they are biocompatible and stable. The best well-known dopant is silver, which shows a significant antibacterial effect by the interaction of silver ions with bacterial DNA, inhibiting DNA synthesis or by direct interaction with bacterial membrane proteins [47,50–52]. Copper [53,54], fluorine [55] and iodine [56,57] has been also used for their antibacterial properties.

1.4.2. Polymeric coatings

Polymers can be deposited onto a surface by different techniques. Traditional approaches, such as dip-coating, spin-coating, chemical vapor deposition, physical vapor deposition or electropolymerization can be used for the deposition of polymers. Another group of techniques involves self-assembling molecules, including self-assembled monolayers and layer-by-layer films. There is also the possibility of chemical grafting in order to obtain polymer brushes. Grafting includes two groups, namely, grafting from (surface initiated polymerization) and grafting to (grafting of pre-synthesized polymer to the surface) [58].

1.4.2.1. Antifouling coatings

Bacterial attachment to a surface is mediated by different types of interactions, which can be specific (through a protein) or non-specific. Antifouling coatings are polymeric films able to reduce the protein adsorption. The main properties of the antifouling coatings are the hydrophilicity, the ability to form bonds with water and the conformational flexibility [59].

Repulsion of proteins by antifouling polymers is thought to be caused by a steric stabilization force. This force has mainly two contributions, namely, an excluded volume component and a mixing interaction component. Excluded volume component is related to an elastic response from the loss of conformation entropy when the proteins are close to the surface, i.e. the loss of conformational freedom of the polymeric chains due to the protein adsorption leads to the protein repulsion. Mixing interaction component is caused by the reduction of available conformations of the molecule segments owing to either compression or interpenetration of the protein chains [60,61].

The polymers used to achieve low fouling surfaces can be either hydrophilic polymers or zwitterionic polymers. Antifouling polymers such as polyethylene glycol or polyhydroxyethyl methacrylate possess antifouling properties due to the possibility to form hydrogen bonds with water [62,63]. Zwitterionic polymers are molecules with positive and negative charges but with an overall neutral charge, which are able to have tightly interactions with water, giving the antifouling character [64].

1.4.2.2. Cationic polymers

Cationic polymers kill bacteria by damaging the cell membrane through lysis, which induces the release of the intracellular components in solution. The adsorption of cationic polymers at the bacterial cell surface is explained by the net negative charge of the bacterial membrane, due to the presence of the teichoic acid membrane protein in Gram-positive bacteria and negatively charged phospholipids at the outer membrane of Gram-negative bacteria. Once the polymer is attached to the surface it can penetrate the cell membrane causing its disruption [38].

Most cationic polymers are generally based on quaternary ammonium, guanidinium, phosphonium or sulphonium groups grafted on the polymer backbone

[65–69]. The strategies employed for the preparation of cationic polymer coatings on titanium include the use of poly(hexamethylenebiguanadine) [70], electropolymerization of pyrrole [71], and the use of poly(ethylene imine) [72,73].

1.4.3. Bioactive molecules immobilization

1.4.3.1. Antibiotics

For the coating of the titanium surface with antibiotics, different broad spectra antibiotics have been used, like gentamicin, cephalothin, carbenicillin, amoxicillin, cefamandole, tobramycin or vancomycin [74–76]. The antibiotic can be immobilized on the surface through biodegradable polymers, sol-gel coatings or nanotubes to achieve a releasing surface [74,77–79], or can be covalently bonded for a longer shelf life [80–82], as the releasing coatings have a fast release (from some hours up to some days). The use of antibiotics has two main problems: the drug resistance of the bacteria and the achievement of a release during a long period of time at a concentration higher than the minimum inhibitory concentration (MIC).

1.4.3.2. Antiseptics

In order to avoid the drug resistance associated with the antibiotic use in coatings, some nonantibiotic organic antimicrobial agents like chlorhexidine, chloroxylenol and poly(hexamethylenebiguadine) have been used [83–85]. These molecules have been immobilized by adsorption on the titanium oxide layer [86,87] surface induced mineralization with hydroxyapatite containing chlorhexidine [88] or via covalent bonding with biomolecules like collagen [70]. Some studies reported the cell damage [84] caused by the nonantibiotic antimicrobial agents, so it is important to clarify its biocompatibility. Another important issue is to control the release and concentration of the drug at the target site.

1.4.3.3. Antimicrobial peptides

Antimicrobial peptides (AMPs) are endogenous polypeptides produced by multicellular organisms in order to protect a host from pathogenic microbes [89]. Generally, an AMP is defined as a peptide of less than 50 aminoacids with an overall positive charge, imparted by the presence of multiple lysine (K) and arginine (R) residues (Figure 1.5), and a substantial portion (at least 50%) of hydrophobic residues [90].

AMPs are natural molecules, but can be also synthetic, modulating the antibacterial properties by chemical modification. The use of antimicrobial peptides has grown the last decades motivated by the resistance to conventional antibiotics, which induces a need of new kind of antibiotic molecules [91]. AMPs protects humans from microbial infections, showing in most of the cases a growth inhibition against Gram positive and Gram negative species [92]. Moreover, antifungal [93], antiviral [94], antiparasitic [95] and anticancer [96] activities of AMPs have also been described, as

well as the role in chemotactic activity [97], apoptosis [98] and wound healing [99]. The ability to neutralize bacterial toxins and up-regulate the host defense response has also been reported [100].

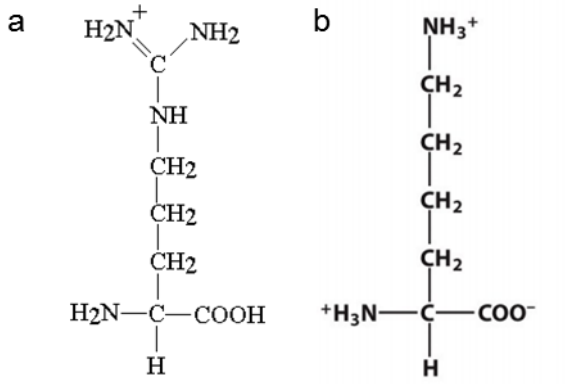

Figure 1.5. Molecular structure of the aminoacids with a positive charge in the side chain group at physiological pH. Arginine (a) and Lysine (b)

Host defense peptides have been isolated from a vast variety of tissues in humans, including skin, eyes, ears, mouth, airways, lung, intestines and the urinary tract. Usually, AMPs are expressed as precursor proteins and the mature form is released by protease processing [101]. Several families of AMPs are expressed in the oral epithelium, such as α-defensin, β-defensin, calcoprotein, histatin, lactoferrin or cathelicidin [102].

The mechanism of action of the AMP is based on the interaction of the peptide with the cell membrane. Bacterial membranes are organized in such a way that the outermost leaflet of the bilayer is heavily populated by lipids with negatively charged phospholipid head groups. In contrast, the outer leaflet of the membranes of plants and animals is composed mainly of lipids with no net charge; most of the lipids with negatively charged head groups are segregated into the inner leaflet, facing the cytoplasm (Figure 1.6) [103–105].

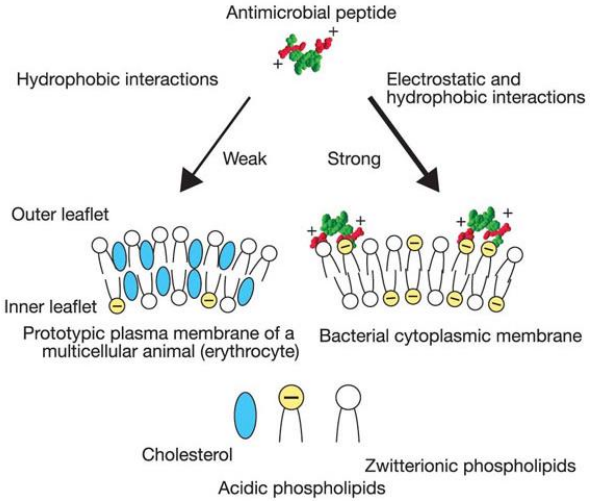

Figure 1.6. Differences on the interaction of an AMP with eukaryotic and prokaryotic cells [89]

The differences on the composition of the cell membrane of eukaryote and prokaryote cells induce differences on the interaction of the AMPs with both types of cells. With the eukaryotic cells, the interaction is weak since it is driven by hydrophobic interactions. In turn, the interaction with the negatively charged bacteria membrane allows for a stronger electrostatic interaction. This fact allows the use of antimicrobial peptides as the coating of a biomaterial, since the threshold toxicity concentration for the mammalian cells is higher than the one for the bacteria [106].

A model that explains the activity of most antimicrobial peptides is the Shai-Matsuzaki-Huang (SMH) model. The model proposes the interaction of the peptide with the membrane, followed by displacement of lipids, alteration of membrane structure, and in certain cases entry of the peptide into the target cell [104,107,108] (Figure 1.7).

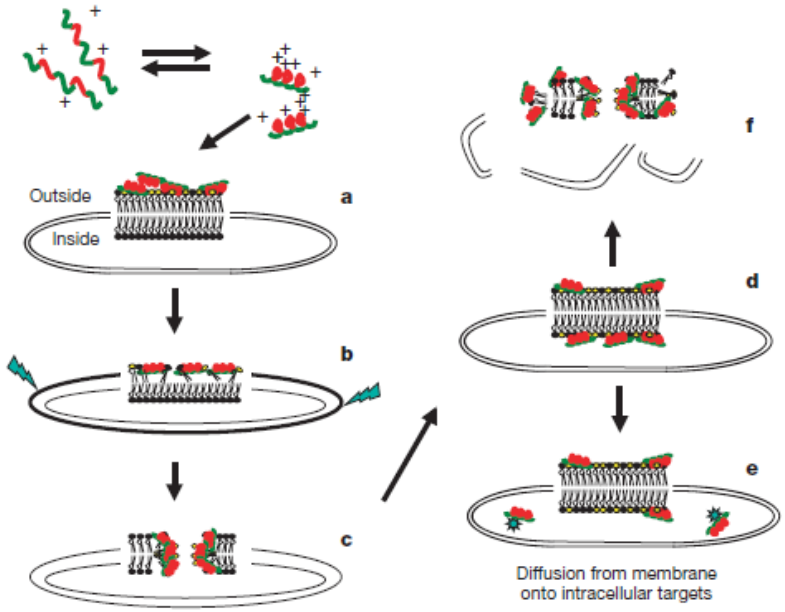

Figure 1.7. Mechanisms of action of AMP (Adapted from [100])

All antimicrobial peptides interact with membranes, but they can be divided in two types according to their mechanism of action: membrane disruptive and non-membrane disruptive [106] (Figure 1.8). The action of AMP, additionally, can be seen as a whole group with multiple actions on cells ranging from membrane permeation to cell wall and division effects to macromolecular synthesis inhibition. Each AMP has a different mechanism of action in each bacterial strain [90].

The action mechanism of the AMP can be related to the secondary structure. α-helical peptides cause the disruption of the bacterial membrane, causing the formation of barrel-like bundles in the bacterial membrane [104]. β-sheet peptides also cause the disruption of the bacterial membrane. They are perpendicularly inserted or tilted into the lipid bilayer to form toroidal pores [108]. Extended peptides are not active against the membrane, but they can penetrate it and interact with bacterial proteins inside [109].

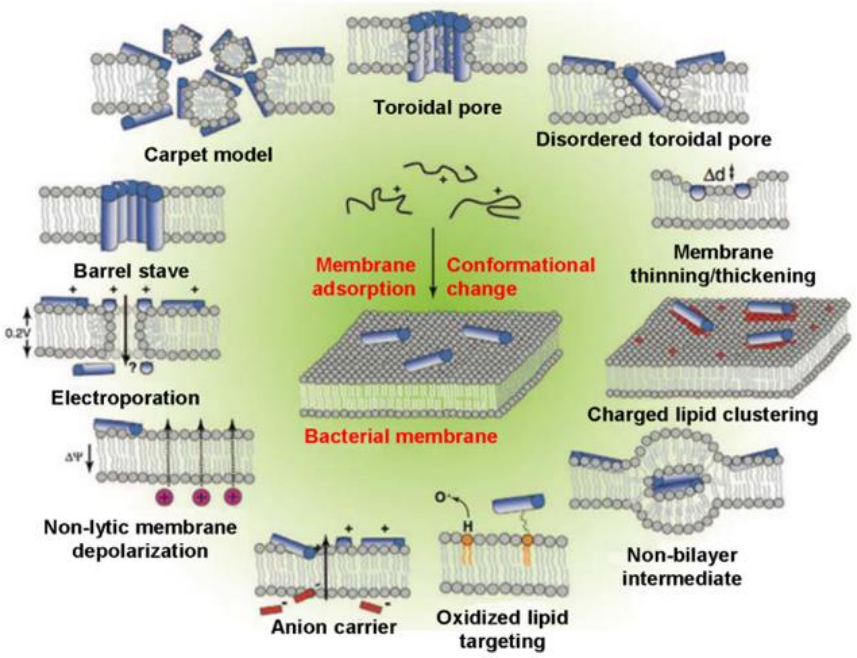

Figure 1.8. Key mechanisms of bacterial membrane disruption by AMPs (adapted from [90]

Magainin is an AMP that was isolated and characterized by Zasloff [110] on the skin of the frog Xenopus laevis. Two similar peptides, differing only in two aminoacids have been described (Table 1.1), namely Magainin 1 and Magainin 2 [111]. The studies dealing with the antibacterial activity of the peptide revealed a broad spectrum activity against several clinical isolates, and no bacterial resistance was induced after repeated passages with subinhibitory concentrations [112,113].

Table 1.1. Aminoacid sequence of the two magainin peptides. An understrike indicates an aminoacid change.

Peptide Name	Aminoacid sequence
Magainin 1	GIGKFLHSAGKFGKAFVGEIMKS
Magainin 2	GIGKFLHSAKKFGKAFVGEIMNS

Lactoferrin is an iron-binding glycoprotein that can be found in most of the exocrine secretions, including saliva, tears and nasal secretions. This protein is a source of cationic and hydrophobic antimicrobial peptides, which are released following enzymatic proteolysis [109]. The most studied lactoferrin derived AMP are lactoferrin 1-11, lactoferrampin and lactoferricin (Table 1.2).

Table 1.2. Aminoacid sequence of the most common Lactoferrin derived AMPs

Peptide Name	Aminoacid sequence
Lactoferrin 1-11	GRRRSVQWCAV
Lactoferrampin	WNLLRQAQEKFGKDKSP
Lactoferricin	KCFQWQRNMRKVRGPPVSCIKRDS

Lactoferrin 1-11 is the N-terminal peptide of lactoferrin, comprising the first eleven residues of the molecule. The effectiveness of the peptide is associated to the arginine residues in the N-terminal [114], and it has been tested against different bacterial strains, including methicillin-resistant *Staphylococcus aureus* [115].

The strategies for the application of AMPs on titanium implants comprises their use on multilayered drug delivery systems [116], the covalent immobilization through silanization of the titanium surface [27,117], or through a polymeric coating such as polyacrylamide brushes, polyethylene glycol (PEG) or chitosan [118–121].

1.5. Techniques for the preparation of polyethylene glycol coatings on titanium

Different preparation methods for the coating of titanium with PEG have been developed. The simplest way of coating the surface is by physisorption of PEG [122–124] or of a copolymer [125–129]. Self-assembling of certain copolymers such as Poly(L-lysine)-Poly(ethylene glycol) have also been studied [130–132]. Another group of techniques include grafting of PEG, by either UV-induced graft polymerization [133], cathecol chemistry [134], or phosphonate chemistry [135,136]. Electrochemical processes have been applied to the titanium surfaces, such as the electrodeposition of PEG bis-amine terminated [136] or the electropolymerization of polypyrrole-poly(ethylene glycol) [137]. Some of these techniques are described in the following sections.

1.5.1. Plasma polymerization

Plasma is the fourth state of matter, characterized by the total or partial ionization of the atoms or molecules from a gas phase. The presence of radicals, free electrons, charged particles, photons, and radicals explain the high reactivity of plasmas and their suitability for application in many fields.

Plasma can be classified in two groups depending on their temperature, namely, high temperature or thermal plasmas and non-equilibrium or glow discharge plasma. Fusion plasmas are in thermal equilibrium, i.e. the electrons and the gas phase have the same temperature, whereas in discharge plasmas the temperature of the electrons is higher than the temperature of the gas phase [138]. This kind of plasmas, also called cold plasmas due to their gas temperature being close to ambient temperature, are usually generated and sustained by applying an electrical discharge to a neutral gas. Cold plasmas are suitable for the treatment of temperature-sensitive substrates such as polymers or biological systems, like tissues or cells, and has been widely studied for surface treatments [139,140].

Gas discharges can be produced by direct current (DC) or alternating current (AC) with a wide range of frequencies. Typically, radiofrequency and microwave discharges are used, but other frequencies are also useful. For DC, the voltage difference

between the two electrodes induces collisions of the electrons with the particles, leading to ionization and excitation. For AC, the role of electrodes is less important, as electrons can oscillate in the plasma, giving rise to electrodeless discharges (e.g. capacitively coupled discharges) [138].

Low temperature plasma can be produced either at low or at atmospheric pressure. In low-pressure plasmas, the concentration of species is low, and hence, collisions between particles are reduced, fact that maintains the temperature close to the room temperature. For atmospheric plasmas, a higher number of collisions induce an increase in the temperature. One of the strategies to maintain the plasma at low temperature is by decreasing the distance between the electrodes, so low-temperature atmospheric pressure plasmas can be achieved in some special configurations [141,142].

In the last years, there has been an increasing interest on the atmospheric pressure plasma systems, mainly to avoid the expensive pumping systems required for the low-pressure devices. However, at atmospheric pressure the breakdown voltage is higher, requiring in most of the cases the use of an ignition tool. Moreover, the glow discharge produced at low pressure may turn into hot filamentary arches (streamers) at atmospheric pressure. The streamers are undesirable because they lead to inhomogeneous treatments and to local damage to thermally sensitive substrates. There are some ways to avoid the streamers, such as the use of helium as discharge gas, use of microwave power, dielectric barriers limiting the current or special shapes of the electrodes [143].

Plasma surface treatments can be classified into plasma activation, plasma etching and plasma polymerization [144–146]. Plasma treatment of titanium with non-polymerizing gases leading to surface activation (often designated as plasma cleaning) is a useful technique to eliminate organic contaminants and enhance the chemical reactivity by the grafting of oxygen reactive groups on the surface. The elimination of organic contamination enhances biological performance of the improvement of the bare titanium and the chemical reactivity of the titanium surfaces. Plasma activation can be performed either at low pressure or at atmospheric pressure, and both techniques have shown good results [139,140].

Plasma polymerization is a method for deposition of polymer films involving plasma dissociation and excitation of a monomer (or precursor) and the subsequent deposition and polymerization of the excited species on the surface of the substrate. The final structure of the polymer is different when compared with a conventional polymer obtained by radical polymerization or polycondensation (Figure 1.9).

However, by controlling the plasma parameters, a certain retention of the functionality of the precursor can be maintained, as well as the properties of the polymer [147,148]. Well-designed plasma polymerized coatings of application in dental implants

should enhance cell adhesion (osteoblast or fibroblast) [150], and if possible, provide also antibacterial properties [151].

Till date, fundamental plasma polymerization studies with PEG precursors include the use of flat surfaces (gold or silicon) or glass substrates, in order to analyze the properties of the coatings depending on the plasma system and parameters. Application studies of PEG plasma polymerized coatings have dealt mainly with microfluidics, chips for biosensors and, to some extent, biomaterials for the blood contact devices (Table 1.3).

Table 1.3. Precursors for the production of PEG-like layers on different substrates

Precursor	Substrate	References
Monoglyme	Glass coverslip	[152]
Diglyme	Glass coverslip	[152]
	Silicon wafer	[153–155]
	Silicon wafer and indium tin oxide	[156]
Triglyme	Glass coverslip	[152]
	Polyamide-based composite membrane	[157]
Tetraglyme	Glass coverslip	[152]
	Nitinol	[158]
	Glass/PTFE hybrid microfluidic chip	[159]
	Silicon wafer	[154]
	Polypropylene surgical mesh	[160]
	Polyethylene	[161]
	Ionomer membrane (sulfonated tetrafluoroethylene based fluoro-polymer)	[162]
Diethylene glycol vinyl ether	Polyethylene terephthalate	[163]
	Polyethylene terephthalate, silicon wafer	[164]
Diethylene glycol monovinyl ether	Mica, silicon wafer, glass	[165]
	Gold coated glass slide, silicon wafer	[166]
Triethylene glycol monoallyl ether	Polyethylene terephthalate	[167]
1,4-p-Dioxane	Ionomer membrane (sulfonated tetrafluoroethylene based fluoro-polymer)	[162]

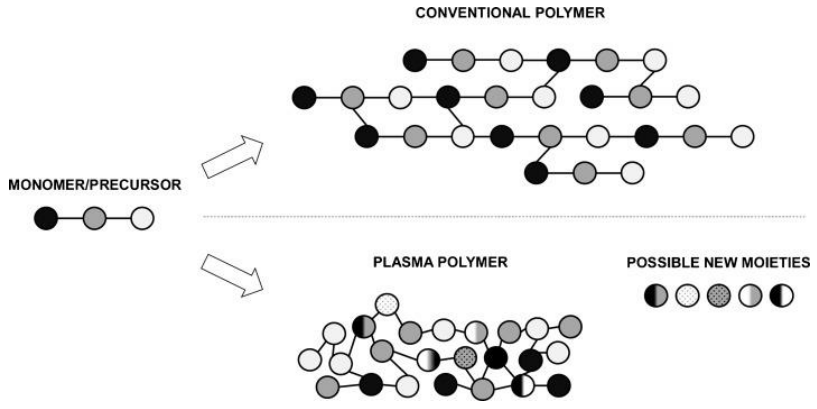

Figure 1.9. Differences between a conventional polymer and the corresponding plasma polymer [149]

1.5.2. Silane coupling agents

Silane coupling agents are molecules with the general formula $R_nSiX_{(4-n)}$. X is the functional group involved in the reaction with the substrate. It is a hydrolysable group (such as alkoxy, amine or chlorine), which is replaced by a bond between the substrate and the silicon atom. R is an organic moiety that enables the further bond with a polymer or another molecule with a suitable functional group.

Titanium is naturally covered by a titanium oxide layer, conferring it a low reactivity and preventing the formation of covalent bonds, fact that might hinder a possible surface functionalization [168]. Silane coupling agents have been used to bond to hydroxyl groups, which can be obtained on the titanium oxide surface by plasma activation [169], plasma polymerization [170] or sodium hydroxide treatment [27,171].

The strategies for bonding PEG through a silane usually involve the reaction of alkanosilanes with the titanium surface, which in turn are meant to react with modified end groups of PEG. The application of this process was used by Groll *et al.* using N-[3-(trimethoxysilyl)propyl] ethylenediamine to react with an isocyanate modified PEG-star [172]. 3-(2-aminoethylamino)-propyltrimethoxysilane was also used for the immobilization of PEG on a NaOH treated titanium surface [171].

A slightly different approach has been used for the preparation of PEG-coatings on silicon wafers. It was initially developed by Zhang *et al.* [173], by using PEG and silicon tetrachloride ($SiCl_4$), which in turn reacted with the silanols of the silicon surface. This method was also used by Kocijan *et al.* [174] to coat stainless steel. A significant reduction of protein and bacterial adhesion was observed for the immobilization of the silanized PEG on both silicon and stainless steel. Methods for the silanization of silica surfaces can also be applied to titanium, due to the presence of a titanium oxide layer [175].

1.5.3. Electrodeposition

Electrodeposition is a wet process in which an external electrical field attracts charged particles towards an electrode, to incorporate metallic ions in the surface or to obtain a coating. It is performed in an electrolytic cell, which has three parts: an electrolyte and two electrodes, anode and cathode. The electrolyte is a solution of water or other solvents with the ions dissolved [176]. When an external voltage is applied to the electrodes, the ions are attracted to the electrode with the opposite charge. Electrodeposition is usually made with metallic ions, but it can also be used for the preparation of polymeric coatings, either for the electropolymerization of charged monomers or the electrodeposition of partially charged polymers [177,178].

Electrochemical treatments are able to produce a great variety of coatings, such as hydroxyapatite [179], phospholipid-based polymers [180] and silver-doped surfaces [47]. Electrodeposition of polymers can be performed via electropolymerization [181,182] or by electrostatic attraction of the polymer to the sample, which acts as one

of the electrodes of the system [183]. Production of PEG-coatings by means of electrodeposition was developed by Tanaka *et al.* [129,184,185]. This coating showed a reduced biofilm formation of *Streptococcus gordonii* and *Streptococcus mutans* on titanium surfaces [186]. The use of PEG electrodeposition implies the use of water as a solvent and represents a simple and fast procedure.

1.6. References

[1] P.A. Norowski, J.D. Bumgardner, *Biomaterial and antibiotic strategies for peri-implantitis: a review*., J. Biomed. Mater. Res. B. Appl. Biomater. 88 (2009) 530–43. doi:10.1002/jbm.b.31152.

[2] J. Buxadera-Palomero, C. Canal, F.J. Gil, D. Rodriguez, *Dental Implants: Plasma Polymerization for Antibacterial Coatings*, in: J.L. Shohet (Ed.), Encycl. Plasma Technol., Taylor & Francis Group, 2016.

[3] S.G. Steinemann, *Titanium--the material of choice?*, Periodontol. 2000. 17 (1998) 7–21. doi:10.1111/j.1600-0757.1998.tb00119.x.

[4] R. Palmer, *Dental implants: Teeth and implants*, Br. Dent. J. 187 (1999) 183–188. doi:10.1038/sj.bdj.4800236.

[5] A.F. Mavrogenis, R. Dimitriou, J. Parvizi, G.C. Babis, *Biology of implant osseointegration*., J. Musculoskelet. Neuronal Interact. 9 (2009) 61–71.

[6] J. Schatzker, *Osseointegration of metal*., Can. J. Surg. 38 Suppl 1 (1995) S49-54.

[7] MengDentistry, Single Tooth Implant | Meng Dental ~ Located in Missoula Montana, (n.d.). http://www.mengdental.com/implant/missoula_dentist_dental_implant-single-tooth-implant (accessed October 18, 2016).

[8] T. Berglundh, L. Persson, B. Klinge, *A systematic review of the incidence of biological and technical complications in implant dentistry reported in prospective longitudinal studies of at least 5 years*, J. Clin. Periodontol. 29 (2002) 197–212. doi:10.1034/j.1600-051X.29.s3.12.x.

[9] V. Moraschini, L.A. da C. Poubel, V.F. Ferreira, E. dos S.P. Barboza, *Evaluation of survival and success rates of dental implants reported in longitudinal studies with a follow-up period of at least 10 years: a systematic review*, Int. J. Oral Maxillofac. Surg. 44 (2015) 377–388. doi:10.1016/j.ijom.2014.10.023.

[10] T. Albrektsson, N. Donos, *Implant survival and complications. The Third EAO consensus conference 2012*, Clin. Oral Implants Res. 23 (2012) 63–65. doi:10.1111/j.1600-0501.2012.02557.x.

[11] A. G. Gristina, *Biomaterial-centered infection: microbial adhesion versus tissue integration*., Science. 237 (1987) 1588–95. doi:10.1126/science.3629258.

[12] Y. Zhou, J. Gao, L. Luo, Y. Wang, *Does Bruxism Contribute to Dental Implant Failure? A Systematic Review and Meta-Analysis*, Clin. Implant Dent. Relat. Res. 18 (2015) n/a-n/a. doi:10.1111/cid.12300.

[13] T. Berglundh, J. Lindhe, I. Ericsson, C.P. Marinello, B. Liljenberg, P. Thornsen, *The soft tissue barrier at implants and teeth*, Clin. Oral Implants Res. 2 (1991) 81–90. doi:10.1034/j.1600-0501.1991.020206.x.

[14] H.-P. Weber, D.L. Cochran, *The soft tissue response to osseointegrated dental implants*, J. Prosthet. Dent. 79 (1998) 79–89. doi:10.1016/S0022-3913(98)70198-2.

[15] Y.-H. Li, X. Tian, *Quorum sensing and bacterial social interactions in biofilms*., Sensors (Basel). 12 (2012) 2519–38. doi:10.3390/s120302519.

[16] L. Hall-Stoodley, P. Stoodley, J.I. Paez, O. Ustahüseyin, C. Serrano, X.-A. Ton, *et al.*, *Evolving concepts in biofilm infections*., Cell. Microbiol. 11 (2015) 1034–43. doi:10.1111/j.1462-5822.2009.01323.x.

[17] A. Lee, H.-L. Wang, *Biofilm related to dental implants*., Implant Dent. 19 (2010) 387–93. doi:10.1097/ID.0b013e3181effa53.

[18] J.W. Costerton, L. Montanaro, C.R. Arciola, *Biofilm in implant infections: its production and regulation*., Int. J. Artif. Organs. 28 (2005) 1062–8.

[19] M.R. Parsek, P.K. Singh, *Bacterial biofilms: an emerging link to disease pathogenesis*.,

Annu. Rev. Microbiol. 57 (2003) 677–701. doi:10.1146/annurev.micro.57.030502.090720.

[20] M.R. Parsek, E.P. Greenberg, *Sociomicrobiology: the connections between quorum sensing and biofilms*, Trends Microbiol. 13 (2005) 27–33. doi:10.1016/j.tim.2004.11.007.

[21] C.D. Nadell, J.B. Xavier, K.R. Foster, *The sociobiology of biofilms*, FEMS Microbiol. Rev. 33 (2009) 206–224. doi:10.1111/j.1574-6976.2008.00150.x.

[22] L.C.M. Antunes, R.B.R. Ferreira, M.M.C. Buckner, B.B. Finlay, *Quorum sensing in bacterial virulence*, Microbiology. 156 (2010) 2271–2282. doi:10.1099/mic.0.038794-0.

[23] M. Lorenzetti, I. Dogša, T. Stošicki, D. Stopar, M. Kalin, S. Kobe, *et al.*, *The Influence of Surface Modification on Bacterial Adhesion to Titanium-Based Substrates*, ACS Appl. Mater. Interfaces. 7 (2015) 1644–1651. doi:10.1021/am507148n.

[24] P.F. Amoroso, A. Pier-Francesco, R.J. Adams, M.G.J. Waters, D.W. Williams, *Titanium surface modification and its effect on the adherence of Porphyromonas gingivalis: an in vitro study*., Clin. Oral Implants Res. 17 (2006) 633–7. doi:10.1111/j.1600-0501.2006.01274.x.

[25] K. Hori, S. Matsumoto, *Bacterial adhesion: From mechanism to control*, Biochem. Eng. J. 48 (2010) 424–434. doi:10.1016/j.bej.2009.11.014.

[26] P.E. Kolenbrander, R.N. Andersen, L.V.H. Moore, *Intrageneric coaggregation among strains of human oral bacteria: Potential role in primary colonization of the tooth surface*, Appl. Environ. Microbiol. 56 (1990) 3890–3894.

[27] M. Godoy-Gallardo, C. Mas-Moruno, M.C. Fernández-Calderón, C. Pérez-Giraldo, J.M. Manero, F. Albericio, *et al.*, *Covalent immobilization of hLf1-11 peptide on a titanium surface reduces bacterial adhesion and biofilm formation*., Acta Biomater. 10 (2014) 3522–34. doi:10.1016/j.actbio.2014.03.026.

[28] P.E. Kolenbrander, J. London, *Adhere today, here tomorrow: oral bacterial adherence*., J. Bacteriol. 175 (1993) 3247–52.

[29] G. Mayanagi, T. Sato, H. Shimauchi, N. Takahashi, *Microflora profiling of subgingival and supragingival plaque of healthy and periodontitis subjects by nested PCR*, Int. Congr. Ser. 1284 (2005) 195–196. doi:10.1016/j.ics.2005.06.069.

[30] L.C. Pham, R.J.M. van Spanning, W.F.M. Röling, A.C. Prosperi, Z. Terefework, J.M. Ten Cate, *et al.*, *Effects of probiotic Lactobacillus salivarius W24 on the compositional stability of oral microbial communities*., Arch. Oral Biol. 54 (2009) 132–7. doi:10.1016/j.archoralbio.2008.09.007.

[31] S. Harder, R. Podschun, L. Grancicova, C. Mehl, M. Kern, *Analysis of the intraimplant microflora of two-piece dental implants*., Clin. Oral Investig. 17 (2013) 1135–42. doi:10.1007/s00784-012-0805-2.

[32] A. Almståhl, M. Wikström, B. Fagerberg-Mohlin, *Microflora in oral ecosystems in subjects with radiation-induced hyposalivation*., Oral Dis. 14 (2008) 541–9. doi:10.1111/j.1601-0825.2007.01416.x.

[33] M.T. Pöllänen, M.A. Laine, R. Ihalin, V.J. Uitto, *Host-bacteria Crostalk at the Dentogingival Junction*, Int. J. Dent. 2012 (2012) 14. doi:10.1155/2012/821383.

[34] G. Hajishengallis, *Complement and periodontitis*, Biochem. Pharmacol. 80 (2010) 1992–2001. doi:10.1016/j.bcp.2010.06.017.

[35] N. Silva, L. Abusleme, D. Bravo, N. Dutzan, J. Garcia-Sesnich, R. Vernal, *et al.*, *Host response mechanisms in periodontal diseases*., J. Appl. Oral Sci. 23 (2015) 329–55. doi:10.1590/1678-775720140259.

[36] C. Damgaard, P. Holmstrup, T.E. Van Dyke, C.H. Nielsen, *The complement system and*

its role in the pathogenesis of periodontitis: current concepts, J. Periodontal Res. 50 (2015) 283–293. doi:10.1111/jre.12209.

[37] M. Charnley, M. Textor, C. Acikgoz, *Designed polymer structures with antifouling-antimicrobial properties*, React. Funct. Polym. 71 (2011) 329–334. doi:10.1016/j.reactfunctpolym.2010.10.013.

[38] N. Gour, K.X. Ngo, C. Vebert-Nardin, *Anti-Infectious Surfaces Achieved by Polymer Modification*, Macromol. Mater. Eng. 299 (2014) 648–668. doi:10.1002/mame.201300285.

[39] B.D. Ratner, A.S. Hoffman, *Biomaterials Science: An introduction to materials in medicine*, 2nd ed., Academic Press, San Diego, 1996.

[40] S. Bakardjieva, J. Šubrt, V. Štengl, M.J. Dianez, M.J. Sayagues, *Photoactivity of anatase–rutile TiO2 nanocrystalline mixtures obtained by heat treatment of homogeneously precipitated anatase*, Appl. Catal. B Environ. 58 (2005) 193–202. doi:10.1016/j.apcatb.2004.06.019.

[41] A. Fujishima, T.N. Rao, D.A. Tryk, *Titanium dioxide photocatalysis*, J. Photochem. Photobiol. C Photochem. Rev. 1 (2000) 1–21. doi:10.1016/S1389-5567(00)00002-2.

[42] B. Del Curto, M.F. Brunella, C. Giordano, M.P. Pedeferri, V. Valtulina, L. Visai, *et al.*, *Decreased bacterial adhesion to surface-treated titanium*., Int. J. Artif. Organs. 28 (2005) 718–30.

[43] B. Wälivaara, B.-O. Aronsson, M. Rodahl, J. Lausmaa, P. Tengvall, *Titanium with different oxides: in vitro studies of protein adsorption and contact activation*, Biomaterials. 15 (1994) 827–834. doi:10.1016/0142-9612(94)90038-8.

[44] S. Bonetta, S. Bonetta, F. Motta, A. Strini, E. Carraro, *Photocatalytic bacterial inactivation by TiO2-coated surfaces*., AMB Express. 3 (2013) 59. doi:10.1186/2191-0855-3-59.

[45] K.P. Kühn, I.F. Chaberny, K. Massholder, M. Stickler, V.W. Benz, H.-G. Sonntag, *et al.*, *Disinfection of surfaces by photocatalytic oxidation with titanium dioxide and UVA light*., Chemosphere. 53 (2003) 71–7. doi:10.1016/S0045-6535(03)00362-X.

[46] C.M. Bollen, P. Lambrechts, M. Quirynen, *Comparison of surface roughness of oral hard materials to the threshold surface roughness for bacterial plaque retention: a review of the literature*., Dent. Mater. 13 (1997) 258–69.

[47] M. Godoy-Gallardo, A.G. Rodríguez-Hernández, L.M. Delgado, J.M. Manero, F. Javier Gil, D. Rodríguez, *Silver deposition on titanium surface by electrochemical anodizing process reduces bacterial adhesion of Streptococcus sanguinis and Lactobacillus salivarius*., Clin. Oral Implants Res. 0 (2014) 1–10. doi:10.1111/clr.12422.

[48] C. Lüdecke, J. Bossert, M. Roth, K.D. Jandt, *Physical vapor deposited titanium thin films for biomedical applications: Reproducibility of nanoscale surface roughness and microbial adhesion properties*, Appl. Surf. Sci. 280 (2013) 578–589. doi:10.1016/j.apsusc.2013.05.030.

[49] L. Badihi Hauslich, M.N. Sela, D. Steinberg, G. Rosen, D. Kohavi, *The adhesion of oral bacteria to modified titanium surfaces: role of plasma proteins and electrostatic forces*, Clin. Oral Implants Res. 24 (2013) 49–56. doi:10.1111/j.1600-0501.2011.02364.x.

[50] M. Bosetti, A. Massè, E. Tobin, M. Cannas, *Silver coated materials for external fixation devices: in vitro biocompatibility and genotoxicity*., Biomaterials. 23 (2002) 887–92.

[51] A. Melaiye, W.J. Youngs, *Silver and its application as an antimicrobial agent*, Expert Opin. Ther. Pat. 15 (2005) 125–130. doi:10.1517/13543776.15.2.125.

[52] S.L. Percival, P.G. Bowler, D. Russell, *Bacterial resistance to silver in wound care*., J. Hosp. Infect. 60 (2005) 1–7. doi:10.1016/j.jhin.2004.11.014.

[53] X.B. Tian, Z.M. Wang, S.Q. Yang, Z.J. Luo, R.K.Y. Fu, P.K. Chu, *Antibacterial copper-*

containing titanium nitride films produced by dual magnetron sputtering, Surf. Coatings Technol. 201 (2007) 8606–8609. doi:10.1016/j.surfcoat.2006.09.322.

[54] J.P. Ruparelia, A.K. Chatterjee, S.P. Duttagupta, S. Mukherji, *Strain specificity in antimicrobial activity of silver and copper nanoparticles*., Acta Biomater. 4 (2008) 707–16. doi:10.1016/j.actbio.2007.11.006.

[55] M. Yoshinari, Y. Oda, T. Kato, K. Okuda, *Influence of surface modifications to titanium on antibacterial activity in vitro*, Biomaterials. 22 (2001) 2043–2048. doi:10.1016/S0142-9612(00)00392-6.

[56] H. Tsuchiya, T. Shirai, H. Nishida, H. Murakami, T. Kabata, N. Yamamoto, *et al.*, *Innovative antimicrobial coating of titanium implants with iodine*., J. Orthop. Sci. 17 (2012) 595–604. doi:10.1007/s00776-012-0247-3.

[57] G. McDonnell, A.D. Russell, *Antiseptics and disinfectants: activity, action, and resistance*., Clin. Microbiol. Rev. 12 (1999) 147–79.

[58] B. Zhao, W.. Brittain, *Polymer brushes: surface-immobilized macromolecules*, Prog. Polym. Sci. 25 (2000) 677–710. doi:10.1016/S0079-6700(00)00012-5.

[59] I. Banerjee, R.C. Pangule, R.S. Kane, *Antifouling coatings: recent developments in the design of surfaces that prevent fouling by proteins, bacteria, and marine organisms*., Adv. Mater. 23 (2011) 690–718. doi:10.1002/adma.201001215.

[60] N.A. Alcantar, E.S. Aydil, J.N. Israelachvili, *Polyethylene glycol-coated biocompatible surfaces*., J. Biomed. Mater. Res. 51 (2000) 343–51. doi:10.1002/1097-4636(20000905)51:3.

[61] A.S. Lea, J.D. Andrade, V. Hlady, *Compression of polyethylene glycol chains grafted onto silicon nitride surface as measured by scanning force microscopy*, Colloids Surfaces A Physicochem. Eng. Asp. 93 (1994) 349–357. doi:10.1016/0927-7757(94)02878-8.

[62] S.. Jeon, J.. Lee, J.. Andrade, P.. De Gennes, *Protein—surface interactions in the presence of polyethylene oxide: I. Simplified theory*, J. Colloid Interface Sci. 142 (1991) 149–158. doi:10.1016/0021-9797(91)90043-8.

[63] S.. Jeon, J.. Andrade, *Protein—surface interactions in the presence of polyethylene oxide: II. Effect of protein size*, J. Colloid Interface Sci. 142 (1991) 159–166. doi:10.1016/0021-9797(91)90044-9.

[64] C. Leng, S. Sun, K. Zhang, Z. Chen, *Molecular level studies on interfacial hydration of zwitterionic and other antifouling polymers in situ*, Acta Biomater. 40 (2016) 6–15. doi:10.1016/j.actbio.2016.02.030.

[65] L.M. Timofeeva, N.A. Kleshcheva, A.F. Moroz, L. V. Didenko, *Secondary and Tertiary Polydiallylammonium Salts: Novel Polymers with High Antimicrobial Activity*, Biomacromolecules. 10 (2009) 2976–2986. doi:10.1021/bm900435v.

[66] T. Ikeda, A. Ledwith, C.H. Bamford, R.A. Hann, *Interaction of a polymeric biguanide biocide with phospholipid membranes*, Biochim. Biophys. Acta - Biomembr. 769 (1984) 57–66. doi:10.1016/0005-2736(84)90009-9.

[67] A. Kanazawa, T. Ikeda, T. Endo, *Antibacterial activity of polymeric sulfonium salts*, J. Polym. Sci. Part A Polym. Chem. 31 (1993) 2873–2876. doi:10.1002/pola.1993.080311126.

[68] A. Kanazawa, T. Ikeda, T. Endo, *Novel polycationic biocides: Synthesis and antibacterial activity of polymeric phosphonium salts*, J. Polym. Sci. Part A Polym. Chem. 31 (1993) 335–343. doi:10.1002/pola.1993.080310205.

[69] A. Kanazawa, T. Ikeda, T. Endo, *Polymeric phosphonium salts as a novel class of cationic biocides. IV. Synthesis and antibacterial activity of polymers with phosphonium salts in the main chain*, J. Polym. Sci. Part A Polym. Chem. 31 (1993) 3031–3038.

doi:10.1002/pola.1993.080311219.
[70] M. Morra, C. Cassinelli, G. Cascardo, A. Carpi, M. Fini, G. Giavaresi, *et al.*, *Adsorption of cationic antibacterial on collagen-coated titanium implant devices*., Biomed. Pharmacother. 58 (2004) 418–22. doi:10.1016/j.biopha.2004.08.002.
[71] E. De Giglio, M.. Guascito, L. Sabbatini, G. Zambonin, *Electropolymerization of pyrrole on titanium substrates for the future development of new biocompatible surfaces*, Biomaterials. 22 (2001) 2609–2616. doi:10.1016/S0142-9612(00)00449-X.
[72] C. Brunot, L. Ponsonnet, C. Lagneau, P. Farge, C. Picart, B. Grosgogeat, *Cytotoxicity of polyethyleneimine (PEI), precursor base layer of polyelectrolyte multilayer films*, Biomaterials. 28 (2007) 632–640. doi:10.1016/j.biomaterials.2006.09.026.
[73] J. Lin, S. Qiu, K. Lewis, A.M. Klibanov, *Bactericidal properties of flat surfaces and nanoparticles derivatized with alkylated polyethylenimines*., Biotechnol. Prog. 18 (n.d.) 1082–6. doi:10.1021/bp025597w.
[74] S. Radin, P. Ducheyne, *Controlled release of vancomycin from thin sol-gel films on titanium alloy fracture plate material*., Biomaterials. 28 (2007) 1721–9. doi:10.1016/j.biomaterials.2006.11.035.
[75] M. Stigter, J. Bezemer, K. de Groot, P. Layrolle, *Incorporation of different antibiotics into carbonated hydroxyapatite coatings on titanium implants, release and antibiotic efficacy*., J. Control. Release. 99 (2004) 127–37. doi:10.1016/j.jconrel.2004.06.011.
[76] M. Stigter, K. de Groot, P. Layrolle, *Incorporation of Tobramycin into biomimetic hydroxyapatite coating on titanium*, Biomaterials. 23 (2002) 4143–4153.
[77] M. Lucke, G. Schmidmaier, S. Sadoni, B. Wildemann, R. Schiller, N.P. Haas, *et al.*, *Gentamicin coating of metallic implants reduces implant-related osteomyelitis in rats*., Bone. 32 (2003) 521–31.
[78] K.C. Popat, M. Eltgroth, T.J. Latempa, C.A. Grimes, T.A. Desai, *Decreased Staphylococcus epidermis adhesion and increased osteoblast functionality on antibiotic-loaded titania nanotubes*., Biomaterials. 28 (2007) 4880–8. doi:10.1016/j.biomaterials.2007.07.037.
[79] K.C. Popat, L. Leoni, C.A. Grimes, T.A. Desai, *Influence of engineered titania nanotubular surfaces on bone cells*., Biomaterials. 28 (2007) 3188–97. doi:10.1016/j.biomaterials.2007.03.020.
[80] V. Antoci, C.S. Adams, J. Parvizi, H.M. Davidson, R.J. Composto, T.A. Freeman, *et al.*, *The inhibition of Staphylococcus epidermidis biofilm formation by vancomycin-modified titanium alloy and implications for the treatment of periprosthetic infection*., Biomaterials. 29 (2008) 4684–90. doi:10.1016/j.biomaterials.2008.08.016.
[81] O.P. Edupuganti, V. Antoci, S.B. King, B. Jose, C.S. Adams, J. Parvizi, *et al.*, *Covalent bonding of vancomycin to Ti6Al4V alloy pins provides long-term inhibition of Staphylococcus aureus colonization*., Bioorg. Med. Chem. Lett. 17 (2007) 2692–6. doi:10.1016/j.bmcl.2007.03.005.
[82] B. Jose, V. Antoci, A.R. Zeiger, E. Wickstrom, N.J. Hickok, *Vancomycin covalently bonded to titanium beads kills Staphylococcus aureus*., Chem. Biol. 12 (2005) 1041–8. doi:10.1016/j.chembiol.2005.06.013.
[83] R.O. Darouiche, G. Green, M.D. Mansouri, *Antimicrobial activity of antiseptic-coated orthopaedic devices*, Int J Antimicrob Agents. 10 (1998) 83–86.
[84] L.G. Harris, L. Mead, E. Müller-Oberländer, R.G. Richards, *Bacteria and cell cytocompatibility studies on coated medical grade titanium surfaces*., J. Biomed. Mater. Res. A. 78 (2006) 50–8. doi:10.1002/jbm.a.30611.
[85] W.-H. Kim, S.-B. Lee, K.-T. Oh, S.-K. Moon, K.-M. Kim, K.-N. Kim, *The release behavior of CHX from polymer-coated titanium surfaces*, Surf. Interface Anal. 40 (2008)

202–204. doi:10.1002/sia.2809.

[86] A. Kozlovsky, Z. Artzi, O. Moses, N. Kamin-Belsky, R.B.-N. Greenstein, *Interaction of chlorhexidine with smooth and rough types of titanium surfaces*., J. Periodontol. 77 (2006) 1194–200. doi:10.1902/jop.2006.050401.

[87] M.E. Barbour, D.J. O'Sullivan, D.C. Jagger, *Chlorhexidine adsorption to anatase and rutile titanium dioxide*, Colloids Surfaces A Physicochem. Eng. Asp. 307 (2007) 116–120. doi:10.1016/j.colsurfa.2007.05.010.

[88] A.A. Campbell, L. Song, X.S. Li, B.J. Nelson, C. Bottoni, D.E. Brooks, *et al.*, *Development, characterization, and anti-microbial efficacy of hydroxyapatite-chlorhexidine coatings produced by surface-induced mineralization*., J. Biomed. Mater. Res. 53 (2000) 400–7.

[89] M.-D. Seo, H.-S. Won, J.-H. Kim, T. Mishig-Ochir, B.-J. Lee, *Antimicrobial peptides for therapeutic applications: a review*., Molecules. 17 (2012) 12276–86. doi:10.3390/molecules171012276.

[90] J.-P.S. Powers, R.E.. W. Hancock, *The relationship between peptide structure and antibacterial activity*., Peptides. 24 (2003) 1681–91. doi:10.1016/j.peptides.2003.08.023.

[91] M. Zasloff, *Antimicrobial peptides of multicellular organisms*, Nature. 415 (2002) 389–395. doi:10.1038/415389a.

[92] G. Wang, X. Li, Z. Wang, *APD2: the updated antimicrobial peptide database and its application in peptide design*., Nucleic Acids Res. 37 (2009) D933-7. doi:10.1093/nar/gkn823.

[93] A. Lupetti, A. Paulusma-Annema, M.M. Welling, S. Senesi, J.T. van Dissel, P.H. Nibbering, *Candidacidal activities of human lactoferrin peptides derived from the N terminus*., Antimicrob. Agents Chemother. 44 (2000) 3257–63. doi:10.1128/AAC.44.12.3257-3263.2000.

[94] K.V.K. Mohan, S.S. Rao, C.D. Atreya, *Antiviral activity of selected antimicrobial peptides against vaccinia virus*, Antiviral Res. 86 (2010) 306–311. doi:10.1016/j.antiviral.2010.03.012.

[95] A.J. Ullal, E.J. Noga, *Antiparasitic activity of the antimicrobial peptide HbbetaP-1, a member of the beta-haemoglobin peptide family*., J. Fish Dis. 33 (2010) 657–64. doi:10.1111/j.1365-2761.2010.01172.x.

[96] J. Lehmann, M. Retz, S.S. Sidhu, H. Suttmann, M. Sell, F. Paulsen, *et al.*, *Antitumor activity of the antimicrobial peptide magainin II against bladder cancer cell lines*., Eur. Urol. 50 (2006) 141–7. doi:10.1016/j.eururo.2005.12.043.

[97] De Yang, Q. Chen, A.P. Schmidt, G.M. Anderson, J.M. Wang, J. Wooters, *et al.*, *LL-37, the neutrophil granule- and epithelial cell-derived cathelicidin, utilizes formyl peptide receptor-like 1 (FPRL1) as a receptor to chemoattract human peripheral blood neutrophils, monocytes, and T cells*., J. Exp. Med. 192 (2000) 1069–74.

[98] P.G. Barlow, Y. Li, T.S. Wilkinson, D.M.E. Bowdish, Y.E. Lau, C. Cosseau, *et al.*, *The human cationic host defense peptide LL-37 mediates contrasting effects on apoptotic pathways in different primary cells of the innate immune system*., J. Leukoc. Biol. 80 (2006) 509–20. doi:10.1189/jlb.1005560.

[99] M.J. Oudhoff, M.E. Blaauboer, K. Nazmi, N. Scheres, J.G.M. Bolscher, E.C.I. Veerman, *The role of salivary histatin and the human cathelicidin LL-37 in wound healing and innate immunity*., Biol. Chem. 391 (2010) 541–8. doi:10.1515/BC.2010.057.

[100] C.P.J.M. Brouwer, M. Rahman, M.M. Welling, *Discovery and development of a synthetic peptide derived from lactoferrin for clinical use*., Peptides. 32 (2011) 1953–63. doi:10.1016/j.peptides.2011.07.017.

[101] G. Wang, *Human antimicrobial peptides and proteins*., Pharmaceuticals (Basel). 7 (2014) 545–94. doi:10.3390/ph7050545.
[102] R.B. Presland, B.A. Dale, *Epithelial structural proteins of the skin and oral cavity: function in health and disease*., Crit. Rev. Oral Biol. Med. 11 (2000) 383–408.
[103] A. Dubin, P. Mak, G. Dubin, M. Rzychon, J. Stec-Niemczyk, B. Wladyka, *et al.*, *New generation of peptide antibiotics*, Acta Biochim. Pol., 2005: pp. 633–638.
[104] C.D. Fjell, J.A. Hiss, R.E.W. Hancock, G. Schneider, *Designing antimicrobial peptides: form follows function*, Nature Publishing Group, 2012. doi:10.1038/nrd3653.
[105] F. Milletti, *Cell-penetrating peptides: classes, origin, and current landscape*., Drug Discov. Today. 17 (2012) 850–60. doi:10.1016/j.drudis.2012.03.002.
[106] M. Zasloff, B. Martin, H.C. Chen, *Antimicrobial activity of synthetic magainin peptides and several analogues*., Proc. Natl. Acad. Sci. U. S. A. 85 (1988) 910–913. doi:10.1073/pnas.85.3.910.
[107] Y. Shai, *Mechanism of the binding, insertion and destabilization of phospholipid bilayer membranes by α-helical antimicrobial and cell non-selective membrane-lytic peptides*, Biochim. Biophys. Acta - Biomembr. 1462 (1999) 55–70. doi:10.1016/S0005-2736(99)00200-X.
[108] L.T. Nguyen, E.F. Haney, H.J. Vogel, K.J. Williams, R.P. Bax, R.E. Hancock, *et al.*, *The expanding scope of antimicrobial peptide structures and their modes of action*., Trends Biotechnol. 29 (2011) 464–72. doi:10.1016/j.tibtech.2011.05.001.
[109] T.J. Falla, D.N. Karunaratne, R.E. Hancock, *Mode of action of the antimicrobial peptide indolicidin*., J. Biol. Chem. 271 (1996) 19298–303.
[110] M. Zasloff, *Magainins, a class of antimicrobial peptides from Xenopus skin: isolation, characterization of two active forms, and partial cDNA sequence of a precursor*., Proc. Natl. Acad. Sci. U. S. A. 84 (1987) 5449–53.
[111] L.M. Gottler, A. Ramamoorthy, *Structure, membrane orientation, mechanism, and function of pexiganan — A highly potent antimicrobial peptide designed from magainin*, Biochim. Biophys. Acta - Biomembr. 1788 (2009) 1680–1686. doi:10.1016/j.bbamem.2008.10.009.
[112] Y. Ge, D.L. MacDonald, K.J. Holroyd, C. Thornsberry, H. Wexler, M. Zasloff, *In vitro antibacterial properties of pexiganan, an analog of magainin*., Antimicrob. Agents Chemother. 43 (1999) 782–8.
[113] P.C. Fuchs, A.L. Barry, S.D. Brown, *In vitro Antimicrobial Activity of MSI-78, a Magainin Analog*, Antimicrob. Agents Chemother. 42 (1998) 1213–1216.
[114] P.H. Nibbering, E. Ravensbergen, M.M. Welling, L.A. Van Berkel, P.H.C. Van Berkel, E.K.J. Pauwels, *et al.*, *Human lactoferrin and peptides derived from its N terminus are highly effective against infections with antibiotic-resistant bacteria*, Infect. Immun. 69 (2001) 1469–1476. doi:10.1128/IAI.69.3.1469-1476.2001.
[115] H.P. Stallmann, C. Faber, A.L.J.J. Bronckers, J.M.A. de Blieck-Hogervorst, C.P.J.M. Brouwer, A.V.N. Amerongen, *et al.*, *Histatin and lactoferrin derived peptides: Antimicrobial properties and effects on mammalian cells*, Peptides. 26 (2005) 2355–2359. doi:10.1016/j.peptides.2005.05.014.
[116] M. Kazemzadeh-Narbat, B.F.L. Lai, C. Ding, J.N. Kizhakkedathu, R.E.W. Hancock, R. Wang, *Multilayered coating on titanium for controlled release of antimicrobial peptides for the prevention of implant-associated infections*., Biomaterials. 34 (2013) 5969–77. doi:10.1016/j.biomaterials.2013.04.036.
[117] M. Gabriel, K. Nazmi, E.C. Veerman, A. V Nieuw Amerongen, A. Zentner, *Preparation of LL-37-grafted titanium surfaces with bactericidal activity*., Bioconjug. Chem. 17 (2006) 548–50. doi:10.1021/bc050091v.

[118] G. Gao, D. Lange, K. Hilpert, J. Kindrachuk, Y. Zou, J.T.J.J. Cheng, *et al.*, *The biocompatibility and biofilm resistance of implant coatings based on hydrophilic polymer brushes conjugated with antimicrobial peptides*, Biomaterials. 32 (2011) 3899–3909. doi:10.1016/j.biomaterials.2011.02.013.

[119] F. Costa, I.F. Carvalho, R.C. Montelaro, P. Gomes, M.C.L. Martins, *Covalent immobilization of antimicrobial peptides (AMPs) onto biomaterial surfaces*, Acta Biomater. 7 (2011) 1431–1440. doi:10.1016/j.actbio.2010.11.005.

[120] F. Costa, S. Maia, J. Gomes, P. Gomes, M.C.L. Martins, *Characterization of hLF1–11 immobilization onto chitosan ultrathin films, and its effects on antimicrobial activity*, Acta Biomater. 10 (2014) 3513–3521. doi:10.1016/j.actbio.2014.02.028.

[121] J. Peyre, V. Humblot, C. Méthivier, J.-M. Berjeaud, C.-M. Pradier, *Co-grafting of amino-poly(ethylene glycol) and Magainin I on a TiO2 surface: tests of antifouling and antibacterial activities.*, J. Phys. Chem. B. 116 (2012) 13839–47. doi:10.1021/jp305597y.

[122] G. Fytas, S.H. Anastasiadis, R. Seghrouchni, D. Vlassopoulos, J. Li, B.J. Factor, *et al.*, *Probing Collective Motions of Terminally Anchored Polymers*, Science (80-.). 274 (1996) 2041–2044. doi:10.1126/science.274.5295.2041.

[123] A. Razatos, Y. Ong, F. Boulay, D. L. Elbert, J. A. Hubbell, M. M. Sharma, *et al.*, *Force Measurements between Bacteria and Poly(ethylene glycol)-Coated Surfaces*, (2000). doi:10.1021/LA000818Y.

[124] P. Kingshott, S. McArthur, H. Thissen, D.G. Castner, H.J. Griesser, *Ultrasensitive probing of the protein resistance of PEG surfaces by secondary ion mass spectrometry*., Biomaterials. 23 (2002) 4775–85.

[125] M.R. Nejadnik, *Polymer brush-coatings to prevent biomaterials associated infection*, 2009.

[126] X. Liu, A.H. Vesterinen, J. Genzer, J. V. Seppälä, O.J. Rojas, *Adsorption of PEO-PPO-PEO triblock copolymers with end-capped cationic chains of poly(2-dimethylaminoethyl methacrylate)*, Langmuir. 27 (2011) 9769–9780. doi:10.1021/la201596x.

[127] A.K. Muszanska, H.J. Busscher, A. Herrmann, H.C. van der Mei, W. Norde, *Pluronic-lysozyme conjugates as anti-adhesive and antibacterial bifunctional polymers for surface coating.*, Biomaterials. 32 (2011) 6333–41. doi:10.1016/j.biomaterials.2011.05.016.

[128] I. Wong, C.M. Ho, *Surface molecular property modifications for poly (dimethylsiloxane)(PDMS) based microfluidic devices*, Microfluid. Nanofluidics. 7 (2009) 291–306. doi:10.1007/s10404-009-0443-4.Surface.

[129] A. Kawawe, I. Nakagawa, Z. Kanno, Y. Tsutsumi, T. Hanawa, T. Ono, *Evaluation of biofilm formation in the presence of saliva on poly(ethylene glycol)deposited titanium*, Dent. Mater. J. 33 (2014) 638–47. doi:10.4012/dmj.2014-025.

[130] N.-P. Huang, R. Michel, J. Voros, M. Textor, R. Hofer, A. Rossi, *et al.*, *Poly(l -lysine)-g -poly(ethylene glycol) Layers on Metal Oxide Surfaces: Surface-Analytical Characterization and Resistance to Serum and Fibrinogen Adsorption*, Langmuir. 17 (2001) 489–498. doi:10.1021/la000736+.

[131] B.F. Bell, M. Schuler, S. Tosatti, M. Textor, Z. Schwartz, B.D. Boyan, *Osteoblast response to titanium surfaces functionalized with extracellular matrix peptide biomimetics*, Clin. Oral Implants Res. 22 (2011) 865–872. doi:10.1111/j.1600-0501.2010.02074.x.

[132] M. Schuler, G.R. Owen, D.W. Hamilton, M. de Wild, M. Textor, D.M. Brunette, *et al.*, *Biomimetic modification of titanium dental implant model surfaces using the RGDSP-peptide sequence: a cell morphology study*., Biomaterials. 27 (2006) 4003–15.

doi:10.1016/j.biomaterials.2006.03.009.
[133] F. Zhang, Z.L. Shi, P.H. Chua, E.T. Kang, K.G. Neoh, *Functionalization of Titanium Surfaces via Controlled Living Radical Polymerization: From Antibacterial Surface to Surface for Osteoblast Adhesion*, Ind. Eng. Chem. Res. 46 (2007) 9077–9086. doi:10.1021/ie070795j.
[134] H. Lee, K.D. Lee, K.B. Pyo, S.Y. Park, H. Lee, *Catechol-grafted poly(ethylene glycol) for PEGylation on versatile substrates*., Langmuir. 26 (2010) 3790–3. doi:10.1021/la904909h.
[135] V. Zoulalian, S. Zürcher, S. Tosatti, M. Textor, S. Monge, J.-J. Robin, *Self-assembly of poly(ethylene glycol)-poly(alkyl phosphonate) terpolymers on titanium oxide surfaces: synthesis, interface characterization, investigation of nonfouling properties, and long-term stability*., Langmuir. 26 (2010) 74–82. doi:10.1021/la902110j.
[136] Y. Tanaka, H. Doi, Y. Iwasaki, S. Hiromoto, T. Yoneyama, K. Asami, *et al.*, *Electrodeposition of amine-terminated poly(ethylene glycol) to titanium surface*, Mater. Sci. Eng. C. 27 (2007) 206–212. doi:10.1016/j.msec.2006.03.007.
[137] C. Ungureanu, C. Pirvu, M. Mindroiu, I. Demetrescu, *Antibacterial polymeric coating based on polypyrrole and polyethylene glycol on a new alloy TiAlZr*, Prog. Org. Coatings. 75 (2012) 349–355. doi:10.1016/j.porgcoat.2012.07.015.
[138] N.S.J. Braithwaite, V.E.A. H, F.R. N, L.M.A. and L.A. J, R.Y. P, *Introduction to gas discharges*, Plasma Sources Sci. Technol. 9 (2000) 517–527. doi:10.1088/0963-0252/9/4/307.
[139] H.-M. Huang, S.-C. Hsieh, N.-C. Teng, S.-W. Feng, K.-L. Ou, W.-J. Chang, *Biological surface modification of titanium surfaces using glow discharge plasma*., Med. Biol. Eng. Comput. 49 (2011) 701–706. doi:10.1007/s11517-011-0742-2.
[140] M. Pykönen, H. Silvaani, J. Preston, P. Fardim, M. Toivakka, *Plasma activation induced changes in surface chemistry of pigment coating components*, Colloids Surfaces A Physicochem. Eng. Asp. 352 (2009) 103–112. doi:10.1016/j.colsurfa.2009.10.008.
[141] A. Bogaerts, E. Neyts, R. Gijbels, J. van der Mullen, *Gas discharge plasmas and their applications, Spectrochim*. Acta Part B At. Spectrosc. 57 (2002) 609–658. doi:10.1016/S0584-8547(01)00406-2.
[142] C. Tendero, C. Tixier, P. Tristant, J. Desmaison, P. Leprince, *Atmospheric pressure plasmas: A review*, Spectrochim. Acta Part B At. Spectrosc. 61 (2006) 2–30. doi:10.1016/j.sab.2005.10.003.
[143] L. Bárdos, H. Baránková, *Plasma processes at atmospheric and low pressures*, Vacuum. 83 (2008) 522–527. doi:10.1016/j.vacuum.2008.04.063.
[144] L. Dai, H.J. Griesser, A.W.H. Mau, *Surface Modification by Plasma Etching and Plasma Patterning*, J. Phys. Chem. 101 (1997) 9548–9554.
[145] R. Hippler, S. Pfau, M. Schmidt, K.H. Schoenback, *Low temperature plasma physics: fundamental aspects and applications*, Wiley-VCH Verlag GmbH & Co. KGaA, 2001.
[146] M.J. Shenton, C.J. Stevens, *Surface modification of polymer surfaces: atmospheric plasma versus vacuum plasma treatments*, J. Phys. D. Appl. Phys. 34 (2001) 2761.
[147] H.K. Yasuda, *Some Important Aspects of Plasma Polymerization*, Plasma Process. Polym. 2 (2005) 293–304. doi:10.1002/ppap.200400071.
[148] P. Favia, M. Creatore, F. Palumbo, V. Colaprico, R. d'Agostino, *Process control for plasma processing of polymers*, Surf. Coatings Technol. 142–144 (2001) 1–6. doi:10.1016/S0257-8972(01)01191-4.
[149] B. Nisol, F. Reniers, *Challenges in the characterization of plasma polymers using XPS*, J. Electron Spectros. Relat. Phenomena. 200 (2015) 311–331. doi:10.1016/j.elspec.2015.05.002.

[150] S. Cha, Y.-S. Park, *Plasma in dentistry*, Clin. Plasma Med. 2 (2014) 4–10. doi:10.1016/j.cpme.2014.04.002.
[151] Y. Ma, M. Chen, J.E. Jones, A.C. Ritts, Q. Yu, H. Sun, *Inhibition of Staphylococcus epidermidis biofilm by trimethylsilane plasma coating*, Antimicrob. Agents Chemother. 56 (2012) 5923–5937. doi:10.1128/AAC.01739-12.
[152] E.E. Johnston, J.D. Bryers, B.D. Ratner, *Plasma deposition and surface characterization of oligoglyme, dioxane, and crown ether nonfouling films*, Langmuir. 21 (2005) 870–881. doi:10.1021/la036274s.
[153] D.J. Menzies, M. Jasieniak, H.J. Griesser, J.S. Forsythe, G. Johnson, G.A. McFarland, et al., *A ToF-SIMS and XPS study of protein adsorption and cell attachment across PEG-like plasma polymer films with lateral compositional gradients*, Surf. Sci. 606 (2012) 1798–1807. doi:10.1016/j.susc.2012.07.017.
[154] D.J. Menzies, A. Nelson, H.-H.H.-H. Shen, K.M. McLean, J.S. Forsythe, T. Gengenbach, et al., *An X-ray and neutron reflectometry study of "PEG-like" plasma polymer films*., J. R. Soc. Interface. 9 (2012) 1008–19. doi:10.1098/rsif.2011.0509.
[155] D.J. Menzies, B. Cowie, C. Fong, J.S. Forsythe, T.R. Gengenbach, K.M. McLean, et al., *One-Step Method for Generating PEG-Like Plasma Polymer Gradients: Chemical Characterization and Analysis of Protein Interactions*, Langmuir. 26 (2010) 13987–13994. doi:10.1021/la102033d.
[156] Y. Li, B.W. Muir, C.D. Easton, L. Thomsen, D.R. Nisbet, J.S. Forsythe, *A study of the initial film growth of PEG-like plasma polymer films via XPS and NEXAFS*, Appl. Surf. Sci. 288 (2014) 288–294. doi:10.1016/j.apsusc.2013.10.022.
[157] L. Zou, I. Vidalis, D. Steele, A. Michelmore, S.P.P. Low, J.Q.J.C.Q.J.C. Verberk, *Surface hydrophilic modification of RO membranes by plasma polymerization for low organic fouling*, J. Memb. Sci. 369 (2011) 420–428. doi:10.1016/j.memsci.2010.12.023.
[158] J. Yang, J. Wang, S. Tong, *Surface properties of bio-implant Nitinol modified by ECR cold plasma*, Mater. Sci. Technol. 20 (2004) 1427–1430. doi:10.1179/026708304X4303.
[159] M. Salim, G. Mishra, G.J.S. Fowler, B. O'sullivan, P.C. Wright, S.L. McArthur, *Non-fouling microfluidic chip produced by radio frequency tetraglyme plasma deposition*., Lab Chip. 7 (2007) 523–525. doi:10.1039/b615328c.
[160] C. Labay, J.M. Canal, M. Modic, U. Cvelbar, M. Quiles, M. Armengol, et al., *Antibiotic-loaded polypropylene surgical meshes with suitable biological behaviour by plasma functionalization and polymerization*., Biomaterials. 71 (2015) 132–44. doi:10.1016/j.biomaterials.2015.08.023.
[161] G. Da Ponte, E. Sardella, F. Fanelli, A. Van Hoeck, R. d'Agostino, S. Paulussen, et al., *Atmospheric pressure plasma deposition of organic films of biomedical interest*, Surf. Coatings Technol. 205 (2011) S525–S528. doi:10.1016/j.surfcoat.2011.03.112.
[162] T.I. Valdes, W. Ciridon, B.D. Ratner, J.D. Bryers, *Surface modification of a perfluorinated ionomer using a glow discharge deposition method to control protein adsorption*., Biomaterials. 29 (2008) 1356–66. doi:10.1016/j.biomaterials.2007.11.035.
[163] Z. Ademovic, J. Wei, B. Winther-Jensen, X. Hou, P. Kingshott, *Surface Modification of PET Films Using Pulsed AC Plasma Polymerisation Aimed at Preventing Protein Adsorption*, Plasma Process. Polym. 2 (2005) 53–63. doi:10.1002/ppap.200400038.
[164] Y.J. Wu, R.B. Timmons, J.S. Jen, F.E. Molock, *Non-fouling surfaces produced by gas phase pulsed plasma polymerization of an ultra low molecular weight ethylene oxide containing monomer*, Colloids Surfaces B Biointerfaces. 18 (2000) 235–248. doi:10.1016/S0927-7765(99)00150-2.
[165] Z. Zhang, B. Menges, R.B. Timmons, W. Knoll, R. Förch, *Surface Plasmon Resonance Studies of Protein Binding on Plasma Polymerized Di(ethylene glycol) Monovinyl Ether*

Films, (2003). doi:10.1021/LA026980D.
[166] Li-Qiang Chu, A. Wolfgang Knoll, R. Förch, L.Q. Chu, W. Knoll, R. Förch, *Pulsed plasma polymerized di(ethylene glycol) monovinyl ether coatings for nonfouling surfaces*, Chem. Mater. 18 (2006) 4840–4844. doi:10.1021/cm061217g.
[167] D. Beyer, W. Knoll, H. Ringsdorf, J.H. Wang, R.B. Timmons, P. Sluka, *Reduced protein adsorption on plastics via direct plasma deposition of triethylene glycol monoallyl ether*., J. Biomed. Mater. Res. 36 (1997) 181–9.
[168] Y. Tsutsumi, Y. Tanaka, H. Saito, H. Doi, H. Imai, T. Hanawa, *Active Hydroxyl Groups on Surface Oxide Film of Titanium, 316L Stainless Steel, and Cobalt-Chromium-Molybdenum Alloy and Its Effect on the Immobilization of Poly(Ethylene Glycol)*, Mater. Trans. 49 (2008) 805–811.
[169] J. Buxadera-Palomero, C. Canal, S. Torrent-Camarero, B. Garrido, F. Javier Gil, D. Rodríguez, *Antifouling coatings for dental implants: Polyethylene glycol-like coatings on titanium by plasma polymerization*., Biointerphases. 10 (2015) 29505. doi:10.1116/1.4913376.
[170] Y.-W.W. Yang, G. Camporeale, E. Sardella, G. Dilecce, J.-S.S. Wu, F. Palumbo, et al., *Deposition of Hydroxyl Functionalized Films by Means of Water Aerosol-Assisted Atmospheric Pressure Plasma*, Plasma Process. Polym. 11 (2014) 1102–1111. doi:10.1002/ppap.201400066.
[171] J. Chen, J. Cao, J. Wang, M.F. Maitz, L. Guo, Y. Zhao, et al., *Biofunctionalization of titanium with PEG and anti-CD34 for hemocompatibility and stimulated endothelialization*., J. Colloid Interface Sci. 368 (2012) 636–47. doi:10.1016/j.jcis.2011.11.039.
[172] J. Groll, J. Fiedler, E. Engelhard, T. Ameringer, S. Tugulu, H.-A. Klok, et al., *A novel star PEG-derived surface coating for specific cell adhesion*., J. Biomed. Mater. Res. A. 74 (2005) 607–17. doi:10.1002/jbm.a.30335.
[173] M. Zhang, T. Desai, M. Ferrari, *Proteins and cells on PEG immobilized silicon surfaces*, Biomaterials. 19 (1998) 953–960. doi:10.1016/S0142-9612(98)00026-X.
[174] A. Kocijan, M. Conradi, D. Mandrino, T. Kosec, *Comparison and characterization of biocompatible polymer coatings on AISI 316L stainless steel*, J. Coatings Technol. Res. 12 (2015) 1123–1131. doi:10.1007/s11998-015-9698-8.
[175] D.M. Brunette, P. Tengvall, M. Textor, P. Thomsen, *Titanium in Medicine*, Springer Berlin Heidelberg, Berlin, Heidelberg, 2001. doi:10.1007/978-3-642-56486-4.
[176] I. Krylova, *Painting by electrodeposition on the eve of the 21st century*, Prog. Org. Coatings. 42 (2001) 119–131. doi:10.1016/S0300-9440(01)00146-1.
[177] S. Cosnier, *Affinity Biosensors Based on Electropolymerized Films*, Electroanalysis. 17 (2005) 1701–1715. doi:10.1002/elan.200503308.
[178] F. Beck, *Electrodeposition of polymer coatings*, Electrochim. Acta. 33 (1988) 839–850. doi:10.1016/0013-4686(88)80080-X.
[179] R. Drevet, F. Velard, S. Potiron, D. Laurent-Maquin, H. Benhayoune, *In vitro dissolution and corrosion study of calcium phosphate coatings elaborated by pulsed electrodeposition current on Ti6Al4V substrate*., J. Mater. Sci. Mater. Med. 22 (2011) 753–61. doi:10.1007/s10856-011-4251-5.
[180] Y. Fukuhara, M. Kyuzo, Y. Tsutsumi, A. Nagai, P. Chen, T. Hanawa, *Phospholipid polymer electrodeposited on titanium inhibits platelet adhesion*., J. Biomed. Mater. Res. B. Appl. Biomater. (2015). doi:10.1002/jbm.b.33423.
[181] F. Zhang, S. Gu, Y. Ding, Z. Zhang, L. Li, *A novel sensor based on electropolymerization of β-cyclodextrin and L-arginine on carbon paste electrode for determination of fluoroquinolones*., Anal. Chim. Acta. 770 (2013) 53–61. doi:10.1016/j.aca.2013.01.052.

[182] S. He, P. Zhou, L. Wang, X. Xiong, Y. Zhang, Y. Deng, et al., *Antibiotic-decorated titanium with enhanced antibacterial activity through adhesive polydopamine for dental / bone implant Antibiotic-decorated titanium with enhanced antibacterial activity through adhesive polydopamine for dental / bone implant*, J. R. Soc. Interface. (2014). doi:10.1098/rsif.2014.0169.

[183] S. Saxer, C. Portmann, S. Tosatti, K. Gademann, S. Zürcher, M. Textor, *Surface Assembly of Catechol-Functionalized Poly(l -lysine)- graft -poly(ethylene glycol) Copolymer on Titanium Exploiting Combined Electrostatically Driven Self-Organization and Biomimetic Strong Adhesion*, Macromolecules. 43 (2010) 1050–1060. doi:10.1021/ma9020664.

[184] V. Zoulalian, S. Monge, S. Zürcher, M. Textor, J.J. Robin, S. Tosatti, *Functionalization of titanium oxide surfaces by means of poly(alkyl-phosphonates).*, J. Phys. Chem. B. 110 (2006) 25603–5. doi:10.1021/jp066811s.

[185] Y. Tanaka, Y. Matsuo, T. Komiya, Y. Tsutsumi, H. Doi, T. Yoneyama, et al., *Characterization of the spatial immobilization manner of poly(ethylene glycol) to a titanium surface with immersion and electrodeposition and its effects on platelet adhesion*., J. Biomed. Mater. Res. A. 92 (2010) 350–8. doi:10.1002/jbm.a.32375.

[186] Y. Tanaka, K. Matin, M. Gyo, A. Okada, Y. Tsutsumi, H. Doi, et al., *Effects of electrodeposited poly(ethylene glycol) on biofilm adherence to titanium*., J. Biomed. Mater. Res. A. 95 (2010) 1105–13. doi:10.1002/jbm.a.32932.

MATERIALS AND METHODS

This section describes the materials used in the thesis, as well as the coating procedures, the biofunctionalization of the coatings, the characterization techniques for the coating characterization and the *in vitro* characterization used and developed within the thesis.

2. MATERIALS AND METHODS

2.1. Sample preparation

Dental implants are usually made from commercially pure titanium. Therefore, the substrates used for all the experiments were commercially pure titanium grade 2. Samples were cut from rods to produce disks of 10 mm diameter and 2 mm thickness. The surface of each disk was grinded with silicon carbide wet grinding paper (P600, P800, P1200 and P2500, Buehler, USA) and polished in a subsequent stage with a colloidal silica suspension (0.05 μm size, Buehler). Polished samples were cleaned with a sequence of organic solvents: toluene, isopropanol, water, ethanol and acetone (Sigma Aldrich, USA) in an ultrasonic bath for 15 min each. Samples treated up to this stage were used as control group (Ti).

2.2. Plasma activation

2.2.1. Plasma equipment

Low pressure plasma treatments were performed in a customized commercial reactor Diener Femto (Diener, Germany) operating with a radiofrequency power supply (13.56MHz). The cylindrical quartz reaction chamber has a volume of 2L (30x15cm). The plasma operates in the capacitively coupled mode with a stainless steel electrode surrounding the chamber and the back wall and the chamber door acting as grounded electrodes. Two gas lines equipped with mass flow controllers (MFC, MKS, USA) are used to enter the gases into the reaction chamber, allowing for the use of a single gas or mixtures of gases. A bubbling system in the gas line 2 allows for the introduction of the vapor of a liquid precursor for plasma polymerization (Figure 2.1).

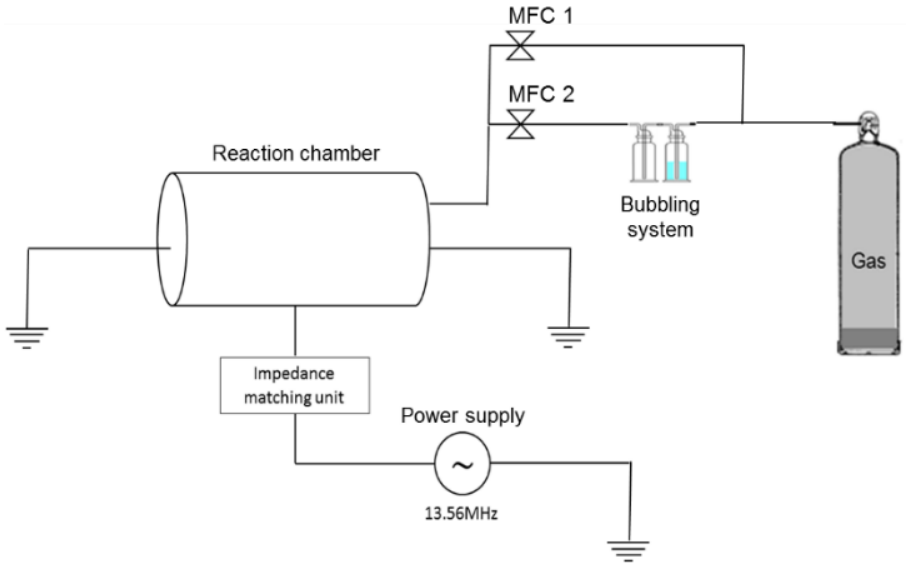

Figure 2.1. Configuration of the plasma system used for the study

2.2.2. Plasma phase characterization

The excited species generated in the plasma phase present electronic transitions within the visible spectrum. Each gas and specie has different characteristic electronic excitation energies and emission wavelengths, which can be measured by means of Optical Emission Spectroscopy (OES).

OES was done with a spectrophotometer Black Comet UV-Vis with a spectral range in the 200-1000 nm zone (StellarNet Inc.) connected to an optical fibre. Measurements were taken through the quartz door of the reaction chamber. The spectra were analysed with the software Spectrawiz.

2.2.3. Plasma activation parameters

To ascertain the most suitable treatment for activation of Ti, different conditions were tested in continuous wave (CW) plasma mode, at 0.40 mbar, and using different plasma gases, treatment times and discharge powers (Table 2.1).

Table 2.1. Plasma parameters employed in the activation treatments of titanium. Sample codes used in the thesis are indicated

Gas	Power (W)	Time of treatment (min)	Sample code
Oxygen	100	0.5	O_2PA100_05
Oxygen	100	2	O_2PA100_2
Oxygen	100	5	O_2PA100_5
Oxygen	200	0.5	O_2PA200_05
Oxygen	200	2	O_2PA200_2
Oxygen	200	5	O_2PA200_5
Argon	100	0.5	ArPA100_05
Argon	100	2	ArPA100_2
Argon	100	5	ArPA100_5
Argon	200	0.5	ArPA200_05
Argon	200	2	ArPA200_2
Argon	200	5	ArPA200_5

2.3. Methods for the preparation of PEG coatings

2.3.1. PEG silanization

Titanium is naturally covered by a titanium oxide layer, conferring it a low reactivity and preventing the formation of covalent bonding [1]. Silane coupling agents have been used to bond to hydroxyl groups on the substrate surface, which can be obtained on the titanium oxide surface by plasma activation [2], plasma polymerization [3] or sodium hydroxide treatment [4,5].

Polyethylene glycol silanization protocol was an adaptation of the work by Zhang *et al.* for the PEG immobilization on silicon wafers [6]. For the silanization of PEG, solution of 0.98% of PEG (Mw=1000g/mol, Sigma Aldrich) in anhydrous toluene (99.8%, Sigma Aldrich) was mixed with 136µL of trimethylamine (Sigma Aldrich) during 1h. After this time, 20µL of silicon tetrachloride (Sigma Aldrich) was added and left to react for 5min. The major product of the reaction is PEG-$OSiCl_3$ (Scheme 1). This

solution was filtered and the plasma activated samples were immersed in this solution for 2h.

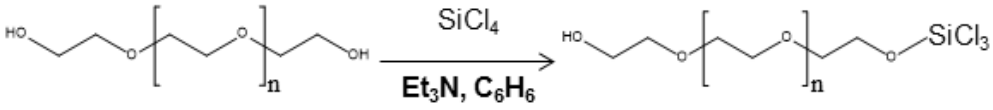

Scheme 1. PEG silanization reaction

The reagents used in this process are air sensitive, thus, all the process was carried out in glass apparatus and prevented from exposure to the atmosphere. The silanization procedure was done in a triple-neck round bottom flask maintained under vacuum and purged with nitrogen prior the introduction of the PEG solution (Figure 2.2). After the reaction, the solution was absorbed by the vacuum with a plastic tube through the filter in order to eliminate a side-product of the reaction, $Et_3N\text{-}OSiCl_3$, which is insoluble in toluene. In the Erlenmeyer flask, the plasma activated titanium were immersed in the solution of the silanized PEG for either 30min (SPEG30) or 2h (SPEG120).

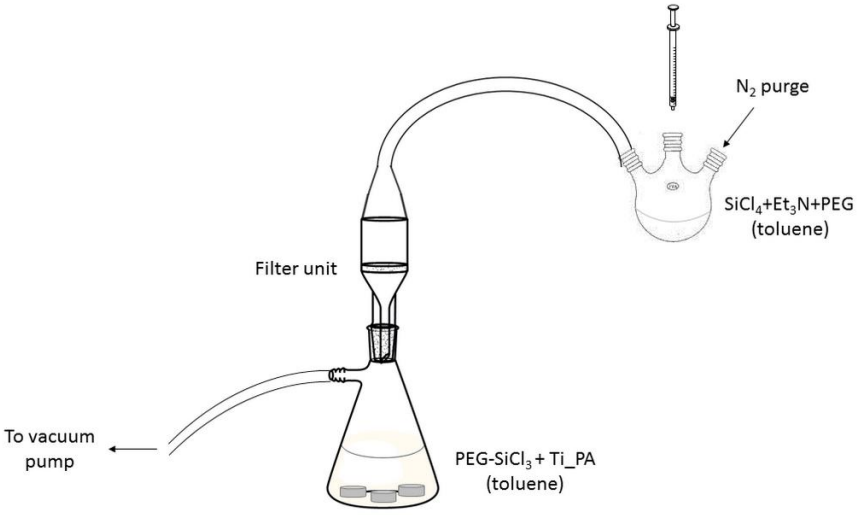

Figure 2.2. System for the coating of titanium samples with silanized PEG

2.3.2. PEG electrodeposition

The electrodeposition was done in a two electrode electrolytic cell connected to a power supply. Electrodeposition process has been adapted from Tanaka et al. [7]. To prepare the electrolyte, 2% w/w of PEG-amine and 0.3M of NaCl were dissolved in water. Control sample for the electrodeposition optimization was the continuous electrodeposition at 5V during 5 min. Sample code for this condition is EPEG5.

Pulsed electrodeposition was performed with a square wave (Figure 2.3). Different conditions were tested by varying the t_1 and t_2 and the ΔV (Table 2.2). The pulsed times were tested for a ΔV=-5V, and using t_1=t_2=4, 6 and 8ms respectively. The potential difference was tested at t_1=t_2=4ms, and taking values of ΔV=-7.5, -5 and -2.5V.

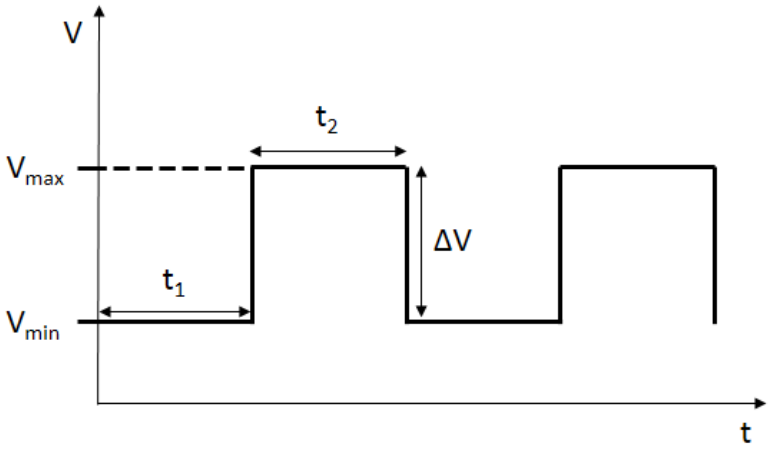

Figure 2.3. Square wave used for the pulsed electrodeposition.

Table 2.2. Conditions used for the electrodeposition of the titanium samples. V_{min} is the voltage applied during t_1, V_{max} is the maximum voltage applied during t_2.

Sample code	V_{min} (V)	V_{max} (V)	t_1=t_2 (ms)
EPEG_5	0	-5	-
EPEG2.5_4	-2.5	-5	4
EPEG5_4	0	-5	4
EPEG5_6	0	-5	6
EPEG5_8	0	-5	8
EPEG7.5_4	2.5	-5	4

To control the voltage wave form, a virtual instrument was generated with the software Laboratory Virtual Instrument Engineering Workbench (LabVIEW®, National Instruments) (Figure 2.4), and the output signal was controlled by an oscilloscope (DSO1052B, Agilent Technologies).

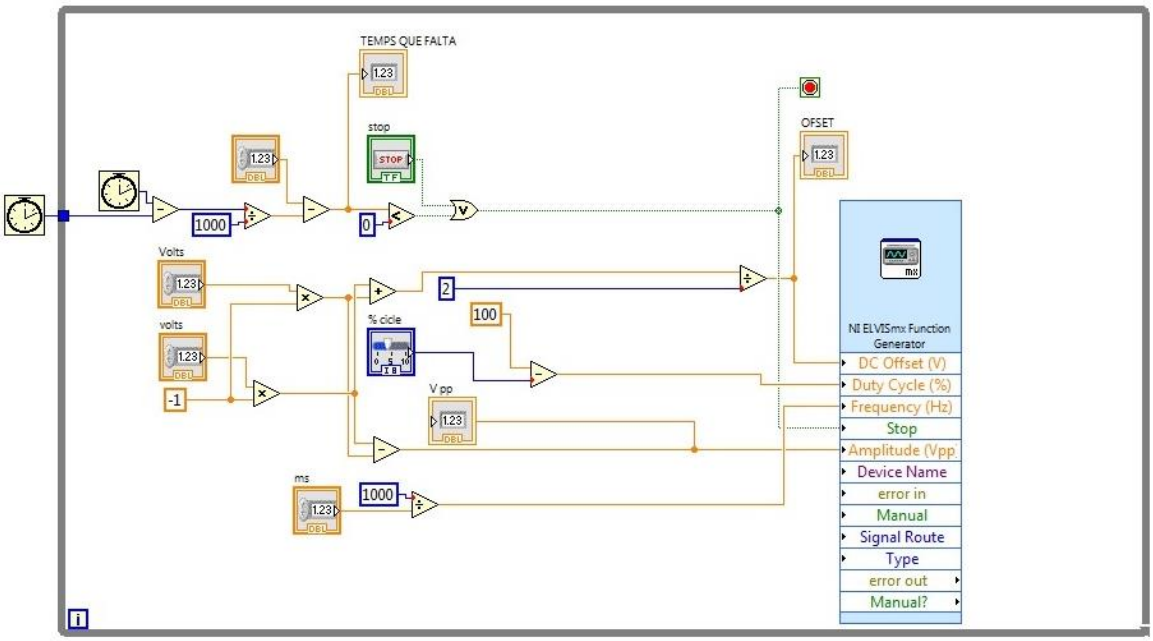

Figure 2.4. Graphical flow diagram of the virtual interface designed for the electrodeposition control

The user interface of the LabVIEW® virtual instrument (Figure 2.5) allows for the control of the maximum and minimum voltage, the cycle time, the duty cycle percentage and the time of the assay.

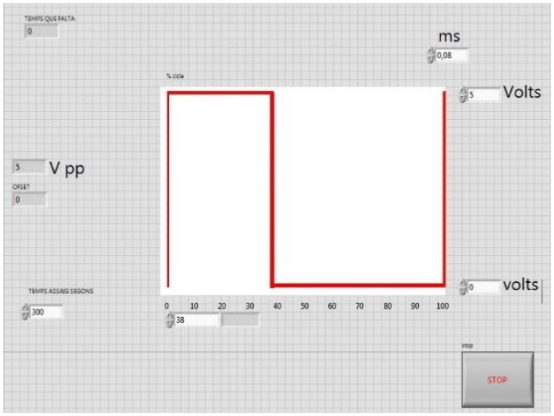

Figure 2.5. User interface (front panel) for the electrodeposition control.

2.3.3. Low pressure plasma polymerization

Plasma polymerization, also known as Plasma Enhanced Chemical Vapor Deposition (PECVD), is the formation of high molecular weight products from low molecular weight precursors in non-thermal discharges (below 100ºC) [8]. The main aim of PECVD is to produce ultrathin (from a few nanometer up to some micrometer), pinhole-free polymer layers with a regular structure but with variable composition, resembling the properties of conventional polymers [9,10].

In this thesis, two different precursors for the preparation of PEG-like layers on the titanium surface have been used, i.e. tetraethylene glycol dimethyl ether and diethylene glycol dimethyl ether (Figure 2.6). Due to the difference on the vapor pressure of this two precursors, the concentration of the precursor in the gas phase on the reaction chamber is different, and also the thickness of the coatings.

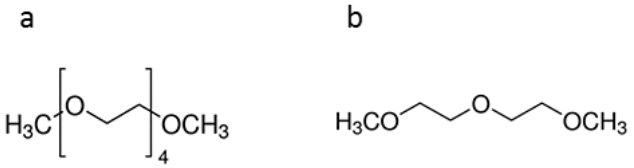

Figure 2.6. Tetraethylene glycol dimethyl ether (a) and Diethylene glycol dimethyl ether (b)

2.3.3.1. Tetraglyme

Plasma polymerization treatments were performed by using Argon (Ar) as carrier gas, which was bubbled through the monomer tetraethylene glycol dimethyl ether (tetraglyme, Sigma Aldrich) after the plasma activation treatment.

Pulsed power was employed to perform the polymerization treatments, with a duty cycle of 0.1% at a pulse-on time of 20 μs and pulse-off of 20 ms. Pressure was kept at 0.40 mbar during treatments, and different conditions were evaluated to produce the coatings (Table 2.3).

Table 2.3. Plasma parameters employed in the plasma polymerization treatments with tetraglyme. Sample codes used in the thesis are indicated.

Peak power (W)	Time of treatment (min)	Sample code
100	30	PPT100_30
100	60	PPT100_60
150	30	PPT150_30
150	60	PPT150_60
200	30	PPT200_30
200	60	PPT200_60

2.3.3.2. Diglyme

Diethylene glycol dimethyl ether (Diglyme, Sigma Aldrich) was used as the plasma polymerization precursor for the drug delivery system. The precursor was introduced in the reaction chamber with argon as carrier gas. Plasma polymerization was done in the continuous mode at 150W and 1.30 mbar using a multi-stage treatment (Table 2.4).

Table 2.4. Plasma parameters employed in the plasma polymerization treatments with diglyme. Sample codes used in the thesis are indicated.

Steps of plasma treatments	Sample code
1 x 1h	PPD150_60
2 x 30 min	PPD150_2x30
3 x 20 min	PPD150_3x20

2.4. Incorporation of bioactive and antibacterial molecules on PEG coatings

2.4.1. Doxycycline adsorption

Doxycycline hyclate (Sigma Aldrich, Figure 2.7) was dissolved in water at a concentration of 50 µg/mL. A drop of 10 µL was placed on top of the titanium sample and kept overnight for drying before performing the plasma polymerization of diglyme as described in section 2.3.3.2.

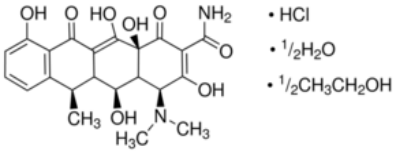

Figure 2.7. Doxycycline hyclate molecule

2.4.2. RGD physisorption

The RGD (arginine, glycine and aspartic acid, Figure 2.8) peptide was prepared by solid-phase peptide synthesis and characterized as explained in previous studies [11]. For the physisorption of RGD, Ti and PEG-coated samples were immersed overnight at room temperature in a solution of 100µM of the peptide in Phosphate Buffered Saline (PBS, Gibco, UK). After the immersion, samples were cleaned twice with PBS.

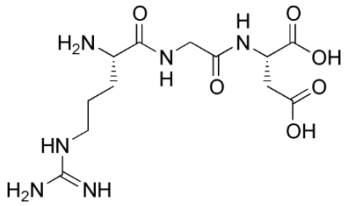

Figure 2.8. RGD peptide chemical structure

2.4.3. AMP immobilization

2.4.3.1. AMP composition

Magainin 2 and human Lactoferrin 1-11 have been purchased from GenScript (USA). Two different terminations have been purchased from each peptide depending on the functionalization strategy, by adding an extra cysteine in the C-terminal of the original sequence of each peptide (Table 2.5). The peptide code are used for the identification of the peptides through this thesis.

Table 2.5. Peptide sequences and modifications used in this thesis

Peptide name	Peptide code	Aminoacid sequence	C-terminal modification	N-terminal modification
Magainin 2	MG-1	GIGKFLHSAKKFGKAFVGEIMNS	None	Acetylation
Magainin 2	MG-2	CGIGKFLHSAKKFGKAFVGEIMNS	Amidation	Acetylation
Lactoferrin 1-11	LF-1	GRRRRSVQWCA	None	Acetylation
Lactoferrin 1-11	LF-2	CGRRRRSVQWCA	Amidation	Acetylation

2.4.3.2. AMP immobilization

Two different strategies have been used for the bonding of AMPs with the amino group in PEG, using the N-terminal and the C-terminal of each peptide. For the linking with the C-terminal (Figure 2.9), an esterification of the carboxylate group of the peptide (LF-1 and MG-1) was performed by reaction of N-hydroxy-succinimide (NHS) in presence of 1-ethyl-3-(3-dimethylaminopropyl)carbodiimide (EDC), following the protocol provided by Thermo Scientific.

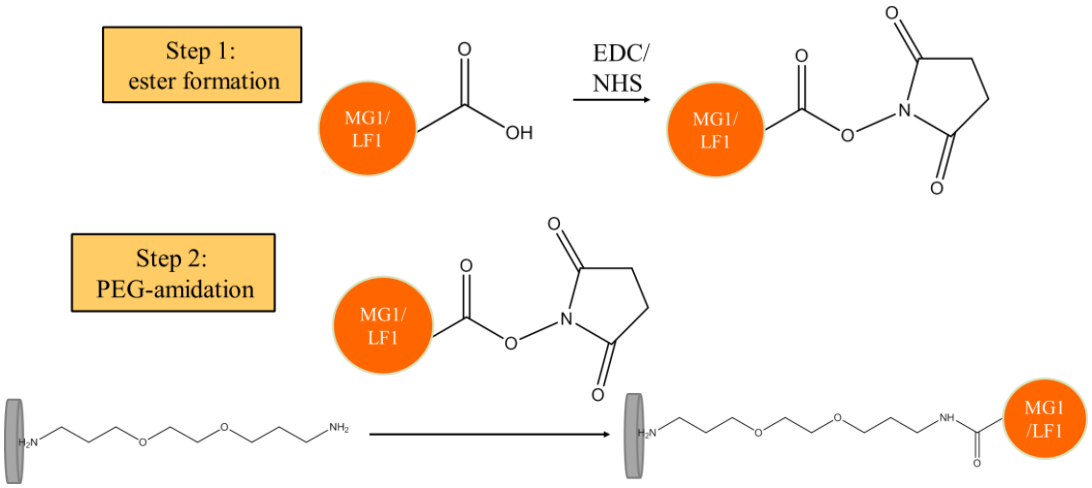

Figure 2.9. C-terminal modification by activation of the carboxylic acid with EDC/NHS

An activation solution was prepared (Table 2.6), using PBS at pH=6.5 as a solvent. This solution is left during 15min, and then the same volume of PBS at pH=8 is added. The PEG-coated titanium samples are immersed on the final solution for 2h.

Table 2.6. Concentrations used for the preparation of the activation solution

Peptide	Peptide concentration (µM)	EDC concentration (mM)	NHS concentration (mM)
MG-1	200	4	6
LF-1	200	2	3

For the linking with the N-terminal, an extra cysteine was added to the N-terminal of the two peptides (LF-2 and MG-2). A crosslinking of the amino of the PEG was done with N-succinimidyl-3-maleimidopropionate (7.5mM in N,N-dimethylformamide). Afterwards, a 100µM in PBS (pH=6.5) solution of the peptide was added to the PEG-coated titanium samples during 2h (Figure 2.10).

Figure 2.10. Crosslinking of the thiol from the cysteine with N-succinimidyl-3-maleimidopropionate

2.5. Atmospheric pressure plasma polymerization

Atmospheric pressure plasma is a promising technique for the deposition of polymeric coatings. It allows the use of high vapor pressure liquids in direct contact with the plasma. Considering the increasing interest of this kind of techniques, two stages were done during this thesis in order to develop novel antibacterial coatings on titanium by means of atmospheric plasma systems. An Aerosol assisted Dielectric Barrier Discharge (DBD) was employed in a short stay at the University of Bari (Italy), and an atmospheric pressure plasma jet (APPJ) was employed in a stay at the Institute of Low Temperature Plasma in Greifswald (Germany).

2.5.1. Aerosol assisted Dielectric Barrier Discharge Plasma

The Aerosol assisted DBD atmospheric plasma reactor used in this thesis was design and built at the University of Bari (Italy). It consists of two parallel plate silver electrodes, 8×13 cm^2 wide, and 4 mm apart, both covered with 0.6 mm thick alumina sheets. (Figure 2.11).

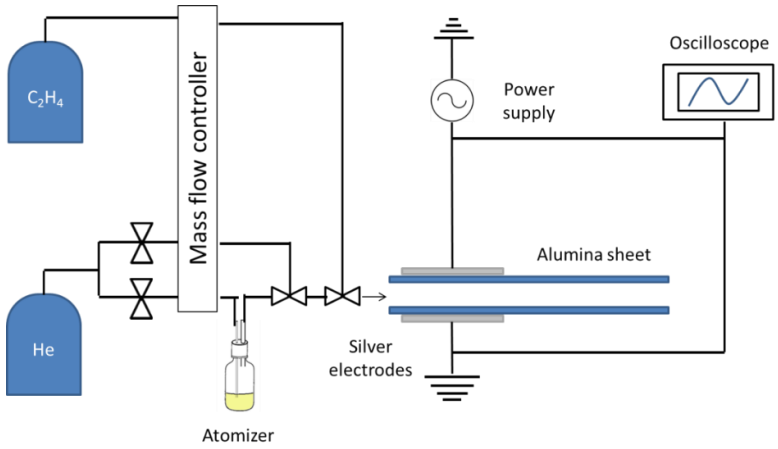

Figure 2.11. Scheme of the DBD plasma reactor (Adapted from [3])

The gas feed is let in between the electrodes from one side, and the opposite side was connected to an aspirator hood. Helium (99.999%, Air Liquide) at 5 sLm was used as carrier gas and ethylene (99.95%, Air Liquide) at 10 sccm was used as deposition precursor. Both gases were fed through electronic mass flow controllers (MKS Instruments). The samples were treated directly in the plasma, about 1 cm apart from the edge of the silver electrode (Figure 2.12).

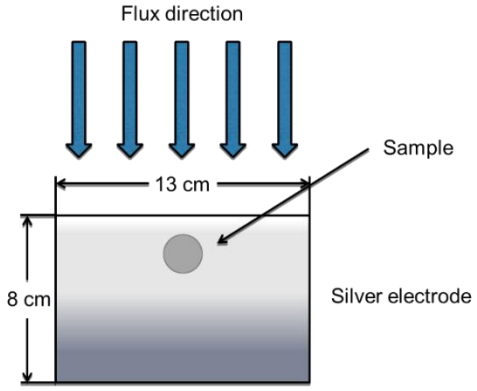

Figure 2.12. Sample position on the silver electrode in the plasma region

The parameters that were studied for the preparation of ethylene-vancomycin composite coatings were the use of a pulsed or a continuous process, with an overall process time of 40 min, and the presence of a protective layer on top of the coatings (TC) to modulate the vancomycin release (Table 2.7).

Table 2.7. Plasma parameters employed in the plasma polymerization treatments with ethylene and vancomycin. Sample codes used in the thesis are indicated.

Sample code	t_{on} (ms)	t_{off} (ms)	Deposition time of TC (min)
PE_Van_10/80	10	80	0
PE_Van_cont	-	-	0
PE_Van_10/80_TC2	10	80	2
PE_Van_cont_TC4	-	-	4
PE_Van_10/80_TC4	10	80	4

2.5.2. Atmospheric pressure plasma jet

The atmospheric pressure plasma jet (Figure 2.13) consists of two ring electrodes around a quartz capillary of 1 mm in diameter. The upper electrode is capacitively coupled to a radiofrequency power supply (27.12MHz) through a matching network while the bottom electrode is grounded.

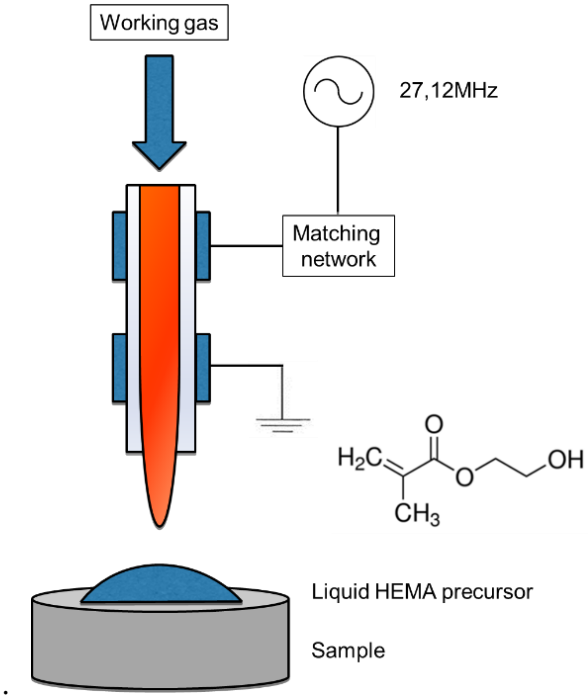

Figure 2.13. Atmospheric pressure plasma jet used for the treatment of liquid HEMA

The coating was prepared by placing a drop of the liquid HEMA (98%, Sigma Aldrich) on the sample and treating the sample during 5 min with the argon plasma. The parameters selected for the study were the plasma power, the gas flow rate, the distance between the sample and the electrode and the HEMA drop volume (Table 2.8).

Table 2.8. Plasma parameters employed in the plasma polymerization treatments with HEMA. Sample codes used in the thesis are indicated.

Sample code	Power (W)	Gas flow (sLm)	Distance (mm)	Time (min)	V_{HEMA} (µL)
S1	10	1	4	5	8
S2	7	0.7	4	5	8
S3	10	1	3	5	10
S4	10	1	3	2.5+2.5	5+5

2.6. Surface characterization

It is well-known that surface parameters like surface energy, composition, roughness and topography play a major role on the interaction of the implants with the biological surrounding [12]. This section describes the techniques used in this thesis for the characterization of the surface properties of the titanium and the different coated samples.

2.6.1. Water contact angle

The surface energy of a solid can be determined by different methods, but measurement of contact angles of liquids with a solid surface is one of the most extended technique. Contact angle is measured by establishing the tangent of a liquid drop with a solid surface (Figure 2.14).

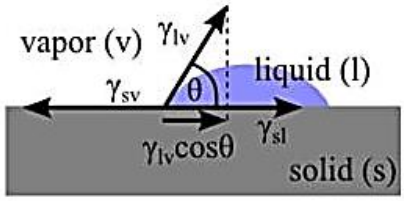

Figure 2.14. Measurement of the water contact angle [13]

The contact angle of a liquid drop with a solid substrate is defined by the mechanical equilibrium of the drop under three interfacial tensions: solid-vapour (γ_{SV}), solid-liquid (γ_{SL}) and liquid-vapour (γ_{LV}). The equilibrium relation is given by the Young equation, where θ is the contact angle [14]:

$$\gamma_{LV} \cdot cos\theta = \gamma_{SV} \cdot \gamma_{SL}$$

Surface wettability was determined by the sessile-drop method using an OCA15 (Dataphysics instrument Company, Germany) equipment with ultra-pure MilliQ (Millipore Corporation) water. A 2 µl droplet of water was deposited at 1 µl/s on the surface of the studied specimens. The drop image was captured by a video camera and analyzed using the SCA20 software (Dataphysics instrument Company, Germany). Three measurements were carried out on three different samples for each condition.

2.6.2. Scanning Electron Microscopy/Focused Ion Beam

Scanning electron microscopy (SEM) is based on the interaction of an electron beam with a surface. Among the processes that take place when the electron beam interacts with the sample, SEM uses the secondary electrons, which are emitted from the sample, and the backscattered electrons, which are electrons from the beam that are reflected. These two interactions give information on the topography and the changes in phase on the substrate. Focused ion beam (FIB) systems have a similar set-up, but use a beam of ions (usually gallium) instead of electrons. Operated at high beam current, FIB is able to remove part of the material and allows for the preparation of cross-sections.

2.6.3. Chemical composition

2.6.3.1. Fourier transformed infrared spectroscopy

Infrared radiation is able to interact with the normal vibration modes of the covalent bonds, i.e. the stretching or bending of the bonds. The frequency of the vibration depends on the mass of the atoms in the bond (reduced mass, µ) and the bonding force (k) (Equation 1)

$$\omega = \frac{1}{2\pi}\sqrt{\frac{k}{\mu}} \qquad \text{Equation 1}$$

Depending on the frequency of vibration of each bond, the molecule absorbs infrared light at different wavelengths, allowing the identification of functional groups (e. g. ether, alcohol or hydrocarbon among others).

For the plasma polymerized tetraglyme, Fourier Transformed Infrared Spectra (FTIR) were recorded using a FTIR Nicolet 6700 in the transmittance mode, (128 scans and resolution 1 with data spacing 0.482 cm^{-1}). Potassium Bromide (KBr) disks were used as the substrate for plasma polymerization instead of Ti for the FTIR measurements.

For the rest of PEG-coated samples, FTIR was performed by using the Attenuated reflection mode (ATR) with a germanium crystal directly on the titanium coated sample (512 scans and resolution 1 with data spacing of 0.964 cm^{-1})

2.6.3.2. X-Ray photoelectron spectroscopy

X-ray photoelectron spectroscopy (XPS) is a technique that retrieves information about the elemental composition of a surface. It is based on the photoelectric effect, i.e. the emission of electrons from the core level of an atom when irradiated with and X-Ray source (usually aluminum or magnesium). The emitted photoelectron has a kinetic energy (KE) related to the binding energy (BE) (Equation 2). BE is given by the chemical environment of the atom, making possible the identification of the bonding state of the atoms in the surface (up to 10nm).

$$KE = h\upsilon - BE - \phi \qquad \text{Equation 2}$$

ϕ is the work function which depends both on the spectrometer and the sample.

XPS spectra in this thesis were acquired in ultra-high vacuum ($5.0 \cdot 10^{-9}$ mbar) with an XR50 Mg anode source operating at 150 W and a Phoibos 150 MCD-9 detector (D8 advance, SPECS Surface Nano Analysis GmbH, Germany). Spectra were recorded at pass energy of 25 eV with a step size of 1.0 eV for survey spectra and 0.1 eV for high resolution spectra. The recorded core levels were C 1s, O 1s and Ti 2p. C 1s peak was used as a reference. CasaXPS software (Casa Software Ldt, UK) was used for the determination of atomic elemental composition applying the manufacturer set of relative sensitivity factors.

2.6.3.3. Film thickness by X-Ray photoelectron spectroscopy

Film thickness was estimated by the attenuation of the XPS titanium signal according to the Equation 3, where I_{Ti} is the intensity of Ti2p from the clean surface (Ti_PA), I_{Ti}^{0} is the intensity of the Ti2p from PEG coated substrate, L_{Ti} is the electron attenuation length for Ti peaks and θ is the take-off angle for XPS measurements.

$$I_{Ti} = I_{Ti}^{0}\exp\left(-\frac{t}{L_{Ti}sin\theta}\right) \quad \text{Equation 3}$$

Electron attenuation length was assumed as 2.8Å according to Ruiz-Taylor *et al.* [15] and the take-off angle was 90º for all the measurements.

2.6.3.4. Time of flight secondary ion mass spectrometry

Time-of-flight Secondary Ion Mass Spectrometry (ToF-SIMS) uses an ion beam to ionize atoms and fragments of molecules from a surface. These charged fragments are extracted and analyzed with a Time-of-flight detector able to detect differences on the mass of the fragments at high resolution.

Spectral surface analysis was done using Bi_3 cluster ions as primary ions using bunched mode. Image acquisition was made over 500x500um for homogeneity analysis. Images were acquired with 256x256 pixel size and 20 scans. Spectra were acquired from 50x50um area region for better mass resolution. Both positive and negative spectra were acquired.

2.7. In vitro biological characterization

The coatings and functionalization of the titanium samples performed in this thesis are intended to have an antifouling effect or a combination of antifouling and bactericidal effect in order to reduce the rate of infections related to the placement of a dental implants. However, this kind of coatings may have a negative effect on the interaction of the implant with the surrounding tissue, inducing toxic effects or an inadequate response of the surrounding cells. *In vitro* biological performance of the coatings focuses in the biocompatibility of the coatings (cytotoxicity and cell adhesion) and the bacteria-coating interaction (bacterial adhesion, agar diffusion test and growth inhibition).

2.7.1. Protein adsorption

2.7.1.1. Fluorescence microscopy

Protein adsorption on the Ti surface was tested by immersing the samples in bovine serum albumin (BSA, Sigma Aldrich, USA). BSA was stained with Fluorescein Isotiocyanate (FITC) with the Kit Pierce Antibody Labeling Kit (Thermo Scientific, USA). The staining was performed by dissolving BSA in a phosphate-borate buffer, mixed with a FITC solution and purified in a resin to remove the non-reacted FITC. Samples were then immersed in 150 µl of FITC-BSA at a concentration of 100 µg/ml during 1 h in darkness. Protein was fixed with paraformaldehyde (Sigma Aldrich, USA). After each step samples were washed with phosphate buffered saline (PBS). Coverslips were mounted on the samples in Mowiol (Merck Millipore Corporation, Bedford, MA, USA) mounting medium. Samples were photographed with a Nikon E-600 fluorescence microscope, and an Olympus DP72 camera (Nikon Corporation Instruments Company,

USA). To assess the protein adsorption, four images were taken for each sample and the average pixel intensity was analyzed by the software Image-J (NIH, MD, USA).

2.7.1.2. XPS measurement of the adsorbed protein

Protein adsorption was performed with human fibronectin (Fibronectin from human serum, Sigma Aldrich). 50µl of fibronectin solution at 100µg/ml in Phosphate Buffered Solution (PBS, Gibco, UK) were placed on the samples and incubated for 2h at room temperature. Afterwards, the samples were washed twice with PBS and analyzed by XPS. %N1s was taken as an indicative for the presence of the protein. Two samples for each condition were analyzed.

2.7.2. Biocompatibility

2.7.2.1. Cytotoxicity

Potential cytotoxic effects of the samples were evaluated according to ISO 10993-5 standard on fibroblasts (hFFs, Merck Millipore Corporation, Bedford, MA, USA) and human osteosarcoma cell line (SAOS-2, ATCC, USA) as osteoblast-like cellular model, using three samples for each condition. All specimens were disinfected by immersion in ethanol 70% during 30min. Extracts of the samples at concentrations of 1:1, 1:10, 1:100 and 1:1000 were prepared by immersing the samples in Dulbecco's Modified Eagle Medium (DMEM, Invitrogen, Carlsbad, CA, USA) for the hFFs and McCoy's (Invitrogen, Carlsbad, CA, USA) for SAOS-2 at 37 °C for 72 h. 5000 cells/well were seeded on a 96-well tissue polystyrene (TCPS) dish and incubated with media for 24 h. Afterwards, culture media were replaced by the extract dilutions. After 24 h, cells were lysed with mammalian protein extraction reagent (mPER, Thermo Scientific, USA) and cell viability was measured by the activity of the enzyme lactate dehydrogenase (LDH) with a Cytotoxity Detection Kit (Thermo Scientific, USA). Cells seeded in the TCPS were used as the positive control, and culture media is used as the negative control. The cell viability was calculated following the Equation 4, were Abs is the measured absorbance for the samples (Abs_{sample}) and the positive (Abs_{C+}) and negative control (Abs_{C-}).

$$Cell\ viability = \frac{Abs_{sample} - Abs_{C-}}{Abs_{C+} - Abs_{C-}} \qquad \text{Equation 4}$$

2.7.2.2. Cell adhesion

Cell adhesion was studied by seeding $5 \cdot 10^3$ cells on triplicate specimens, and incubated for 6 h in a 48-well culture plate. Ti and the culture dish (TCPS) were used as controls. Cells used were hFFs and SAOS-2. Cell numbers were assessed with the Cytotoxity Detection Kit (LDH).

Specimens were prepared for SEM by fixing the cells with 4% paraformaldehyde in PBS, and a sequence for dehydrating the cells was performed by immersing the samples in 50%, 70%, 90%, 96% and 100% (v/v) ethanol during 15 min each step. As the final step, samples were immersed in HDMS overnight and carbon coated.

2.7.3. Antifouling/antibacterial effects

2.7.3.1. Bacterial strains and media

Bacterial strains used in this thesis were *Streptococcus sanguinis (S. sanguinis*, CCUG 17826, Culture Collection University of Göteborg (CUG), Göteborg, Sweden), *Lactobacillus salivarius (L. salivarius*, CECT 4063, Colección Española de Cultivos Tipo (CECT), Valencia, Spain), *Staphylococcus aureus* (*S. aureus*, CCUG 15915), and *Escherichia coli* (*E. coli*, CECT 101, Valencia, Spain).

The selection of such bacterial strains was based either on the relevance of the strain in the oral infections or for being model of specific strains. As reported in section 1.3, *S. sanguinis*, *S. aureus* and *L. salivarius* are strains related to oral infections and maintenance of biofilms. Moreover, *S. aureus* and *E. coli* are models for gram positive and gram negative bacteria.

Incubation media were Todd-Hewitt broth (TH, Scharlab SL, Spain) for *S. sanguinis*, Man-Rogosa-Sharpe broth (MRS, Scharlab SL) for *L. salivarius*, and Brain-Heart Infusion (BHI, Scharlab SL) for both *S. aureus* and *E. coli*. Solid agar plates were prepared by mixing the corresponding culture media for each strain with 7.5 g/L of agar (Agar bacteriological, Scharlab SL). The cultures for all the strains were incubated from three colonies overnight at 37ºC before the assays.

2.7.3.2. Bacterial adhesion

Bacteria suspensions were diluted to an absorbance of 0.20±0.01 at 600nm using a Laxco MicroSpek DSM-Cuvette Cell Density Meter (Cole Parmer, USA), giving approximately $1 \cdot 10^8$ Colony Forming Units (CFU). Either 1 mL or 5µL of the bacterial suspension were placed on top of the samples and left 2h at 37ºC. After this time samples were cleaned twice with PBS. Adherent bacteria were detached by vortexing the disks for 5 min in 1 mL of PBS. Detached bacteria were then seeded using serial dilutions in bacterial media-agar plates. The plates were then incubated overnight at 37ºC and the resulting CFU were counted. Three samples for each condition were studied.

2.7.3.3. Agar diffusion test

Bacteria incubated overnight were diluted to an absorbance of 0.20±0.01 at 600nm, giving approximately $1 \cdot 10^8$ CFU/mL. 100µL of the suspension were seeded on the agar plate and the samples were placed upside down on the bacteria. The plates were incubated overnight at 37ºC and the inhibition zone was measured by a picture using the software ImageJ (Figure 2.15).

The inhibition zone was calculated from the diameter of the inhibition zone (ϕ_{iz}) and the diameter of the sample (ϕ_s), according to the Equation 5 [16]

$$Inhibition\ zone\ site = \frac{\Phi_{iz} - \Phi_s}{2} \qquad \text{Equation 5}$$

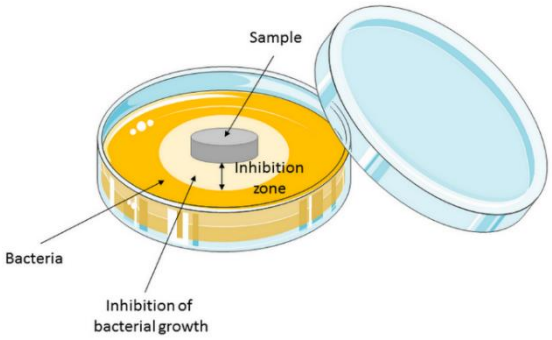

Figure 2.15. Representation of the inhibition zone for the agar diffusion test

2.7.3.4. Growth inhibition (double-well test)

In order to test the dynamic antibacterial activity of eluents from the samples, a double-well test was designed. With this objective, two adjacent wells from a 48 well multiwell plate (Nunc) were connected by melting the walls, in order to have two connected wells, one for the titanium sample and the other one for the measurement of the growth curve of the bacteria by spectrophotometry. Bacteria for this assay were grown overnight and diluted to an optical density of 0.02, corresponding to 10^6CFU/mL (pre-exponential growth phase). 1mL was placed on each well and the absorbance at 600nm was monitored by a multiplate reader every 10min (Multimode microplate reader, Synergy™ HTX). Before each measurement, the plate was shaken for 3s in order to ensure the homogeneity of the suspension.

2.7.3.5. Minimum inhibitory concentration (MIC)

Analysis of the minimum inhibitory concentration of the antimicrobial peptides was carried out through recording bacterial growth curve (as reported in section 2.7.3.4) in presence of increasing concentration of the peptide.

2.7.4. Co-culture studies

Cell-bacteria co-culture experiment was an adaptation from [17,18]. For cell adhesion studies, $2 \cdot 10^4$cells were seeded on each sample and left for 24h at 37ºC. For co-culture experiments, a suspension of either *S. aureus* or *E. coli* was adjusted to an optical density of 0.2 in BHI, giving approximately $1 \cdot 10^8$cells/ml. 5µl ($5 \cdot 10^5$cells/sample) of the bacterial suspension were seeded on each sample. After 2h at 37ºC, samples were washed three times in order to eliminate the non-attached bacteria, and hFFs in modified DMEM (DMEM with 2% BHI) at $2 \cdot 10^4$cells/sample were seeded and incubated for 24h. After the incubation time, all the samples were washed twice with PBS, fixed and stained with Phalloidin-Rhodamin (Invitrogen) and DAPI (Invitrogen) for observation. Images were taken with a Leica TCS SPE confocal microscope and analyzed with Image J software. Five images were taken for each sample for the quantification, using duplicates for each condition.

2.8. Statistical analysis

Statistical analysis was performed with Minitab 17^{TM} software (Minitab Inc, State College, PA, USA). Data were analyzed by Student's t-test and one-way ANOVA tables with Tukey's multiple comparison tests in order to evaluate statistically significant differences between sample groups. The differences were considered as statistically significant when $p<0.05$. The results are expressed as the average ± standard deviation of at least three independent samples, except for XPS results which were done with two samples.

2.9. References

[1] Y. Tsutsumi, Y. Tanaka, H. Saito, H. Doi, H. Imai, T. Hanawa, *Active Hydroxyl Groups on Surface Oxide Film of Titanium, 316L Stainless Steel, and Cobalt-Chromium-Molybdenum Alloy and Its Effect on the Immobilization of Poly(Ethylene Glycol)*, Mater. Trans. 49 (2008) 805–811.

[2] J. Buxadera-Palomero, C. Canal, S. Torrent-Camarero, B. Garrido, F. Javier Gil, D. Rodríguez, *Antifouling coatings for dental implants: Polyethylene glycol-like coatings on titanium by plasma polymerization*, Biointerphases. 10 (2015) 29505. doi:10.1116/1.4913376.

[3] Y.-W.W. Yang, G. Camporeale, E. Sardella, G. Dilecce, J.-S.S. Wu, F. Palumbo, et al, *Deposition of Hydroxyl Functionalized Films by Means of Water Aerosol-Assisted Atmospheric Pressure Plasma*, Plasma Process. Polym. 11 (2014) 1102–1111. doi:10.1002/ppap.201400066.

[4] M. Godoy-Gallardo, C. Mas-Moruno, M.C. Fernández-Calderón, C. Pérez-Giraldo, J.M. Manero, F. Albericio, *et al.*, *Covalent immobilization of hLf1-11 peptide on a titanium surface reduces bacterial adhesion and biofilm formation*, Acta Biomater. 10 (2014) 3522–34. doi:10.1016/j.actbio.2014.03.026.

[5] J. Chen, J. Cao, J. Wang, M.F. Maitz, L. Guo, Y. Zhao, *et al.*, *Biofunctionalization of titanium with PEG and anti-CD34 for hemocompatibility and stimulated endothelialization*, J. Colloid Interface Sci. 368 (2012) 636–47. doi:10.1016/j.jcis.2011.11.039.

[6] M. Zhang, T. Desai, M. Ferrari, *Proteins and cells on PEG immobilized silicon surfaces*, Biomaterials. 19 (1998) 953–960. doi:10.1016/S0142-9612(98)00026-X.

[7] Y. Tanaka, H. Doi, Y. Iwasaki, S. Hiromoto, T. Yoneyama, K. Asami, *et al.*, *Electrodeposition of amine-terminated poly(ethylene glycol) to titanium surface*, Mater. Sci. Eng. C. 27 (2007) 206–212. doi:10.1016/j.msec.2006.03.007.

[8] A. Fridman, *Plasma Chemistry*, Cambridge University Press, 2008.

[9] R. Förch, A.N. Chifen, A. Bousquet, H.L. Khor, M. Jungblut, L.-Q. Chu, *et al.*, *Recent and Expected Roles of Plasma-Polymerized Films for Biomedical Applications*, Chem. Vap. Depos. 13 (2007) 280–294. doi:10.1002/cvde.200604035.

[10] J. Friedrich, *Mechanisms of Plasma Polymerization - Reviewed from a Chemical Point of View*, Plasma Process. Polym. 8 (2011) 783–802. doi:10.1002/ppap.201100038.

[11] C. Mas-Moruno, R. Fraioli, F. Albericio, J.M. Manero, F.J. Gil, *Novel peptide-based platform for the dual presentation of biologically active peptide motifs on biomaterials*, ACS Appl. Mater. Interfaces. 6 (2014) 6525–36. doi:10.1021/am5001213.

[12] K. Kieswetter, Z. Schwartz, D.D. Dean, B.D. Boyan, *The role of implant surface characteristics in the healing of bone*, Crit. Rev. Oral Biol. Med. 7 (1996) 329–45.

[13] F. Rupp, R.A. Gittens, L. Scheideler, A. Marmur, B.D. Boyan, Z. Schwartz, *et al.*, *A review on the wettability of dental implant surfaces I: theoretical and experimental aspects*, Acta Biomater. 10 (2014) 2894–906. doi:10.1016/j.actbio.2014.02.040.

[14] T. Young, *An Essay on the Cohesion of Fluids*, Philos. Trans. 95 (1805) 65–87.

[15] L.A. Ruiz-Taylor, T.L. Martin, P. Wagner, *X-ray Photoelectron Spectroscopy and Radiometry Studies of Biotin-Derivatized Poly(l -lysine)-grafted-Poly(ethylene glycol) Monolayers on Metal Oxides*, Langmuir. 17 (2001) 7313–7322. doi:10.1021/la010620t.

[16] D. Pastorino, C. Canal, M. P. Ginebra, *Drig delivery from injectable calcium phosphate foams by tailoring the macroporosity-drug interaction*, Acta Biomaterialia, 12 (2015), 250-259

[17] B. Zhao, H.C. van der Mei, G. Subbiahdoss, J. de Vries, M. Rustema-Abbing, R. Kuijer, *et al.*, *Soft tissue integration versus early biofilm formation on different dental implant*

materials, Dent. Mater. 30 (2014) 716–27. doi:10.1016/j.dental.2014.04.001.

[18] M. Godoy-Gallardo, J. Guillem-Marti, P. Sevilla, J.M. Manero, F.J. Gil, D. Rodriguez, *Anhydride-functional silane immobilized onto titanium surfaces induces osteoblast cell differentiation and reduces bacterial adhesion and biofilm formation*, Mater. Sci. Eng. C. 59 (2016) 524–32. doi:10.1016/j.msec.2015.10.051.

RESULTS AND DISCUSSION

The results and discussion of the thesis are described in this section. Chapter 3 presents the characterization of the sample preparation by plasma activation. Chapters 4-7 describe and discuss the results regarding the preparation of antifouling coatings on titanium, and are organized according to the coating strategy. Finally, in chapter 8 an overall discussion is given by comparing the coating strategies in terms of the coating properties and the *in vitro* performance.

3. TITANIUM SURFACE ACTIVATION BY LOW TEMPERATURE PLASMA

Plasma activation is a widely used process in the sample pre-treatment for the preparation of coatings or for surface cleaning of biomaterials. This process is based on the reactions of the reactive species of plasmas (i.e. atoms, radicals, charged particles or electrons) with the contamination present on the surface of a biomaterial. If the reaction of the molecules is producing volatile products, these can be pumped away from the plasma chamber [1]. On the other hand, the treatment of surfaces with plasma and the subsequent interaction of the oxygen or humidity of air may lead to the formation of oxygen functionalities that can be used to link polymers or biomolecules to the titanium surface. In this chapter, the process of plasma activation of titanium is studied.

3.1. Plasma phase characterization

Optical emission spectroscopy spectra for the plasma discharge of argon and oxygen evaluated in this thesis was recorded in order to identify the main species emitting light in the plasma phase. The oxygen spectrum (Figure 3.1a) shows mainly two peaks.

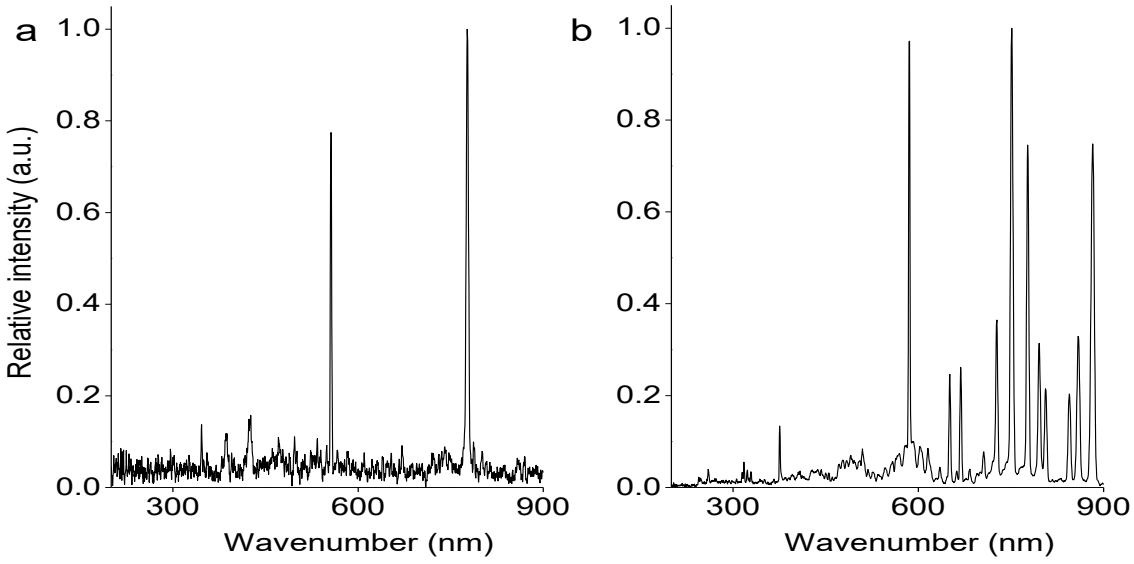

Figure 3.1. OES spectra of oxygen plasma (a) and argon plasma (b)

The peak showing the higher intensity at 777nm corresponds to the first transition line of the monoatomic oxygen (Equation 6).

$$3p^5P \rightarrow 3s^5S \qquad \text{Equation 6}$$

The other peak present in the spectrum is related to the first transition of the first ionization of oxygen (O_2^+) (Equation 7). These two peaks have been assigned accordingly to previous references [2].

$$b^4\Sigma_g^- \rightarrow a_4\pi_u \qquad \text{Equation 7}$$

In the argon spectrum (Figure 3.1b), mainly two regions can be found. The first region, in the range 690-900nm, corresponds to the transition from $3p^5 4p$ to $3p^5 4s$. The second region, in the range of 400-650nm, which is less intense, and corresponds both to the transition $3p^5 5p$ to $3p^5 4s$ and the spectral lines of ionized argon. Band assignation (Table 3.1) has been done according to the studies by Crintea *et al* [3].

Table 3.1. Assigned peaks of the main transitions of the OES spectra of argon

λ (nm) (Theoretical)	λ (nm) (Experimental)	Associated transition
454.5	455	$3p^5 5p \rightarrow 3p^5 4s$ Lines of Ar^+
465.7	466	
472.6	472	
476.4	477.5	
496.5	495.5	
501.7	502.5	
528.7	528.5	
706.7	705	$3p^5 4p \rightarrow 3p^5 4s$
727.3	727	
751.5	751	
794.8	796	
794.8	796	
810.6	806	
842.5	844.5	

3.2. Characterization of plasma activated Ti surfaces

3.2.1. Wettability

Wettability of the samples is an indicator of surface functionalization (herein activation, since the presence of polar moieties and the reduction of organic contamination renders an increase on the wettability. The wettability was increased with all the plasma activation (PA) treatments with non-polymerizing gases at different powers from an initial value of water contact angle of 57º for the Ti to a superhydrophilic surface (below 5º) following the plasma activation treatment (Figure 3.2). The best wettability was obtained for the argon activation at 100 W (ArPA5_100), as these samples display the lowest water contact angle.

3.2.2. Chemical composition

Chemical composition was analyzed by XPS on plasma activated samples and on untreated Ti, and revealed the presence of oxygen, carbon and titanium, which probably account for the presence of titanium oxide and of adsorbed contaminants on the surface. The XPS of the plasma activated samples was performed on two of the studied conditions: O_2PA5_200 and ArPA5_100, which are the most effective activation conditions according to the wettability results. In both conditions, due to the cleaning

effect of the treatment, a decrease of the carbon amount on the titanium surface can be observed comparing the untreated Ti to the plasma activated sample (Table 3.1).

Table 3.2. Atomic concentration (in %) of the carbon, oxygen and titanium amount present on the Ti, O_2PA5_200 and ArPA5_100

At. Comp (%)	C 1s	O 1s	Ti 2p
Ti	23 ± 2	59 ± 1	18 ± 1
O_2PA5_200	13 ± 2	64 ± 1	23 ± 1
ArPA5_100	15 ± 1	62 ± 1	22 ± 1

The lower attenuation of the substrate signal due to the elimination of organic contaminants on the surface, made the titanium and oxygen signals more intense, yielding higher atomic concentration. Differences between the O_2PA5_200 and the ArPA5_100 are not statistically significant. Following the results on wettability and XPS, the condition selected for further work in the titanium activation was ArPA5_100.

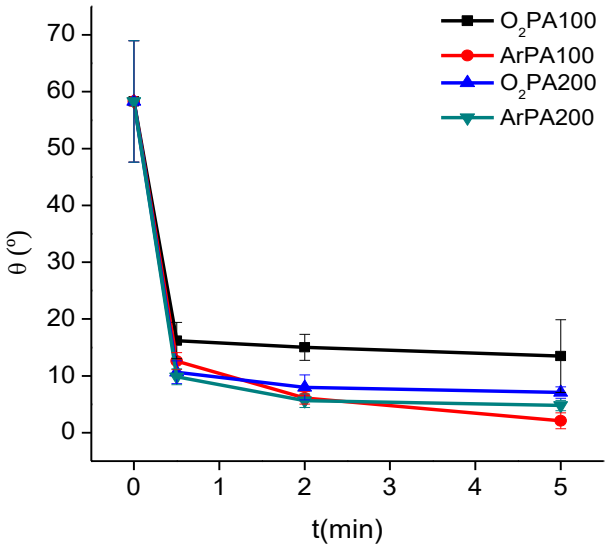

Figure 3.2. Water contact angle of the activated samples as a function of plasma activation time with different gases (oxygen and argon) and different powers (100, 200W)

Activation of titanium is an important step for its subsequent chemical functionalization, as titanium is naturally covered by a titanium oxide layer with low chemical reactivity [4,5]. As shown by XPS (Table 3.1), plasma activation has two main effects on the titanium surface, as removes organic contaminants (hydrocarbons) adsorbed on the surface [6,7], and produces a reactive surface which can be then used in a subsequent step for the bonding with a polymeric layer [1,4,8]. This treatment renders a higher hydrophilicity, as shown by the water contact angle measurements (figure 2a). The cleaning and activation process was followed by water contact angle, where it can be observed that all the different plasma activation conditions tested yield a water contact angle lower than that of untreated Ti (Figure 3.2). Oxygen and argon were evaluated for activation and argon showed to be more effective. While higher power correlates with higher wettability, employing argon as plasma gas leads to contact

angles as low as 5º already at the lowest power evaluated here. This fact can be explained by the differences in the breakdown potential of the two gases. As argon has a lower breakdown voltage than oxygen, the plasma dissociation is easier and the number of active species is higher. Thus, the enhanced activation can be achieved with argon at lower plasma powers [9–12].

3.3. Aging of the plasma activated samples

Since plasma activation will be used as the first step for the different PEG coatings processes studied in this thesis, the evolution of the sample wettability with storage time after plasma treatment (herein aging) was analyzed. An increase on the water contact angle can be observed for all the plasma treatment time conditions (Figure 3.3).

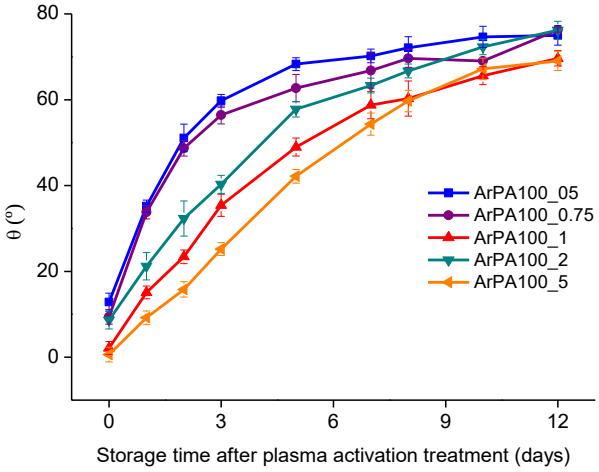

Figure 3.3. Aging of the activation process for the condition ArPA100 and different times of plasma treatment.

The change on the wettability can be explained by a loss of the most reactive functional groups formed on the surface and the adsorption of a layer of contaminants from air, process known as hydrophobic recovery [13,14]. The decrease in the wettability is faster for shorter treatments. For instance, a plasma activated sample for 30 s (ArPA0.5_100) shows the same water contact angle than titanium after 2 days of storage, while the sample activated for 5 min (ArPA5_100) evolves slower and does not reach the wettability of the untreated titanium until 7 days after plasma activation treatment. Within the first day after the plasma activation for 5 min, the difference in water contact angle is not significant. Hence, the subsequent functionalization treatments of the samples can be performed during the same day of the plasma treatment.

3.4. References

[1] B.O. Aronsson, J. Lausmaa, B. Kasemo, *Glow discharge plasma treatment for surface cleaning and modification of metallic biomaterials*, J. Biomed. Mater. Res. 35 (1997) 49–73.

[2] E. Vassallo, A. Cremona, F. Ghezzi, D. Ricci, *Characterization by optical emission spectroscopy of an oxygen plasma used for improving PET wettability*, Vacuum. 84 (2010) 902–906. doi:10.1016/j.vacuum.2009.12.008.

[3] D.L. Crintea, U. Czarnetzki, S. Iordanova, I. Koleva, D. Luggenhölscher, U.K. and B.M.D. Muraoka K, *et al.*, *Plasma diagnostics by optical emission spectroscopy on argon and comparison with Thomson scattering*, J. Phys. D. Appl. Phys. 42 (2009) 45208. doi:10.1088/0022-3727/42/4/045208.

[4] B. Kasemo, J. Lausmaa, *Biomaterial and implant surfaces: On the role of cleanliness, contamination, and preparation procedures*, J. Biomed. Mater. Res. 22 (1988) 145–158. doi:10.1002/jbm.820221307.

[5] F. Rupp, L. Scheideler, N. Olshanska, M. de Wild, M. Wieland, J. Geis-Gerstorfer, *Enhancing surface free energy and hydrophilicity through chemical modification of microstructured titanium implant surfaces*, J. Biomed. Mater. Res. A. 76 (2006) 323–34. doi:10.1002/jbm.a.30518.

[6] V.S. Smentkowski, C.A. Moore, *In-situ plasma cleaning of samples to remove hydrocarbon and/or polydimethylsiloxane prior to ToF-SIMS analysis*, J. Vac. Sci. Technol. A Vacuum, Surfaces, Film. 31 (2013) 06F105. doi:10.1116/1.4822516.

[7] W. Petasch, B. Kegel, H. Schmid, K. Lendenmann, H.. Keller, *Low-pressure plasma cleaning: a process for precision cleaning applications*, Surf. Coatings Technol. 97 (1997) 176–181. doi:10.1016/S0257-8972(97)00143-6.

[8] P. Cools, N. De Geyter, E. Vanderleyden, P. Dubruel, R. Morent, *Surface Analysis of Titanium Cleaning and Activation Processes: Non-thermal Plasma Versus Other Techniques*, Plasma Chem. Plasma Process. 34 (2014) 917–932. doi:10.1007/s11090-014-9552-2.

[9] B.T. Chaid, N.A.A. Al-Tememee, M.K. Khalaf, F.T. Ibrahim, *Electrical Discharges Characterization of Planar Sputtering System*, Int. J. Recent Res. Rev. V (2013) 17–21.

[10] H.B. Smith, C. Charles, R.W. Boswell, *Breakdown behavior in radio-frequency argon discharges*, Phys. Plasmas. 10 (2003) 875. doi:10.1063/1.1531615.

[11] K.T.A.L. Burm, *Calculation of the Townsend Discharge Coefficients and the Paschen Curve Coefficients*, Contrib. to Plasma Phys. 47 (2007) 177–182. doi:10.1002/ctpp.200710025.

[12] J.D. Pace, A.B. Parker, *The breakdown of argon at low pressure*, J. Phys. D. Appl. Phys. 6 (1973) 1525–1536. doi:10.1088/0022-3727/6/12/315.

[13] D. Bodas, C. Khan-Malek, *Formation of more stable hydrophilic surfaces of PDMS by plasma and chemical treatments*, Microelectron. Eng. 83 (2006) 1277–1279. doi:10.1016/j.mee.2006.01.195

[14] F. Palumbo, R. Di Mundo, D. Capelluti, R. d'Agostino, *Superhydrophobic and superhydrophilic polycarbonate by tayloring chemistry and nano-texture with plasma processing*, Plasma Proc. And Pol. 8, 118-126 (2011)

4. SURFACE FUNCTIONALIZATION OF TITANIUM BY PEG SILANIZATION

Silanization is a technique based on the interaction of the hydroxyl groups with a silane. For the case of titanium, alkanosilanes are commonly used for the further immobilization of biomolecules or polymers [1,2]. In this chapter, the use of the silanization technique for the immobilization of PEG on titanium is reported. The approach taken in this thesis is based on the work by Sharma and coworkers dealing with the use of silanized PEG for silicon substrates [3–5].

4.1. Surface characterization

4.1.1. Wettability

Water contact angle of the PEG coated samples (Figure 4.1) decreased in comparison to untreated titanium. The coated samples reached values around 15º for the two treatment times used in the study of silanization. No differences were observed when comparing the two treatment times, i.e. 30 min and 2 h.

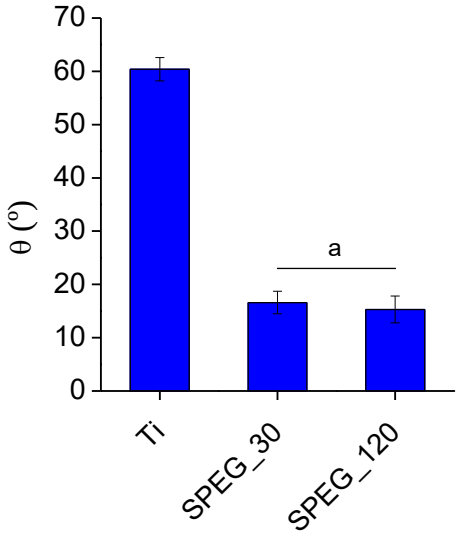

Figure 4.1. Water contact angle of the PEG-silane coated samples. *a* indicates statistically significant differences compared to Ti

The values obtained in previous studies reported higher water contact angles. For instance, Guo *et al.* developed a silanization of PEG on silicon wafers and found values of 37.8º after 30min of immersion and 33.8º after 2h of immersion [6]. In another study, Schlapak *et al.* used a coupling technique between the terminal amines of a functionalized PEG and the aldehydes groups on the surface of a glass substrate and found values around 40º for the PEG-modified sample [7]. Another example of the water contact angle of PEG was reported by Ito *et al.* for the use of photoimmobilization of PEG on titanium, and a value of 39º was found for the coated sample [8].

Despite the fact that the water contact angle measured for the silanized PEG is lower than the reported in previous studies, differences on the processing (reactants,

solvents) and the substrates used may lead to differences on the water contact angle. One fact that should be taken into account is the reduction of the contact angle when comparing the bare titanium and the PEG-coated sample. It is related to the properties of the polymer when immobilized to a surface and to the antifouling properties of the coatings.

4.1.2. Chemical composition

ATR-FTIR spectra (Figure 4.2) revealed the presence of the main peaks associated with PEG, i.e. C-H stretching at 2950cm^{-1} and C-O stretching at 1100cm^{-1}. Another peak at 1050cm^{-1} can be attributed to the Si-OCH_3 stretching from the silane presence [9,10].

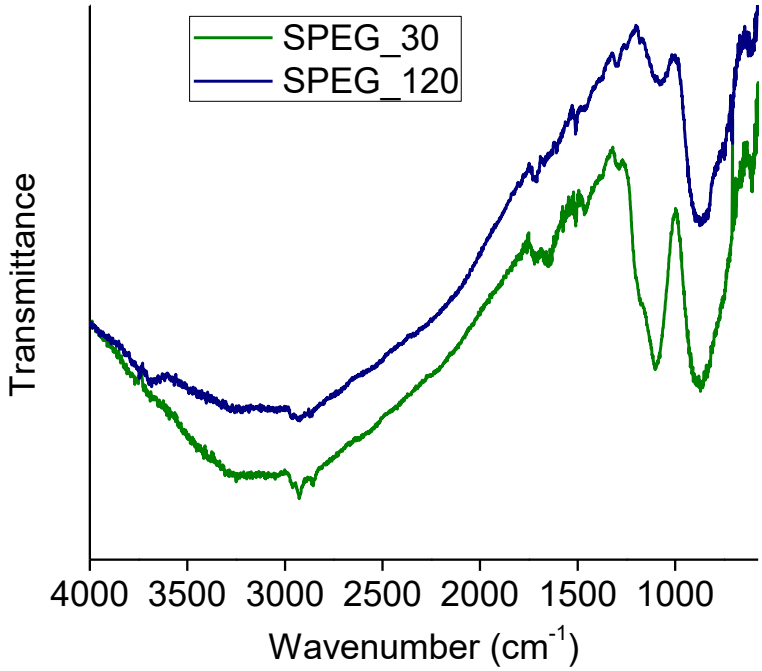

Figure 4.2. ATR-FTIR of the SPEG30 and SPEG120

The composition of the surface was assessed by XPS on Ti, the plasma activated sample (ArPA200_5) and SPEG120 (Table 4.1). The main components found were carbon, oxygen and titanium for the Ti and the ArPA200_5, while for the SPEG120, silicon and chloride were also found. As reported in section 3.2, plasma activation reduces the amount of carbon present and, subsequently, increases the amount of titanium, since the signal from the substrate is less attenuated. Regarding the SPEG120, an increase on the C1s signal is observed, showing the presence of an organic layer on the titanium substrate. The presence of the coating can be observed also from the decrease on the Ti2p signal. The increase on the Si2p signal may be indicative of the silanization process, as well as the increase on the Cl2p signal. These results are in accordance with the ones found by Sharma *et al.* [5] for the coating of silicon wafers with silanized PEG. The thickness of the PEG-silane coated sample was 1.8 nm as calculated by the attenuation of the substrate signal by XPS (section 2.6.3.3). This value is similar to the previous one obtained for this coatings on silicon wafers [3,11].

Table 4.1. % atomic composition by XPS of Ti, plasma activated titanium and SPEG120

	C1s	O1s	N1s	Si2p	Cl2p	Ti2p
Ti	23.5 ± 0.8	59.6 ± 0.8	0.6 ± 0.1	0.2 ± 0.0	0.1 ± 0.1	16.0 ± 0.1
ArPA200_5	15.0 ± 0.7	62.1 ± 0.7	0.3 ± 0.1	0.3 ± 0.0	0.0 ± 0.1	22.3 ± 0.1
SPEG120	17.7 ± 0.5	57.7 ± 0.8	0.3 ± 0.0	10.9 ± 1.2	1.8 ± 0.0	13.4 ± 0.9

The decomposition of the C1s signal revealed the presence of three main peaks (Table 4.2). The peak at 285.0eV is related to the presence of hydrocarbons (C-C). The one at 286.5eV is related to the presence of ether bonds (C-O) and the last one at 288.0eV is related to carbonyl or carboxyl moieties (C=O, O-C=O).

Table 4.2. Contribution of the peaks on the XPS spectra of C1s

Binding Energy (eV)	285.0	286.5	288.0
Ti	58.9 ± 1.6	32.2 ± 0.9	9.0 ± 0.8
Ti_ArPA200_5	58.7 ± 1.4	34.7 ± 1.4	6.5 ± 0.1
SPEG120	44.5 ± 0.9	46.9 ± 0.7	8.5 ± 0.8

ToF-SIMS analysis of the sample was performed in SPEG120 in order to check the functionalization of the surface compared to the bare titanium. The main peaks of the positive spectra (Figure 4.3) were assigned according to previous references with similar coatings [12].

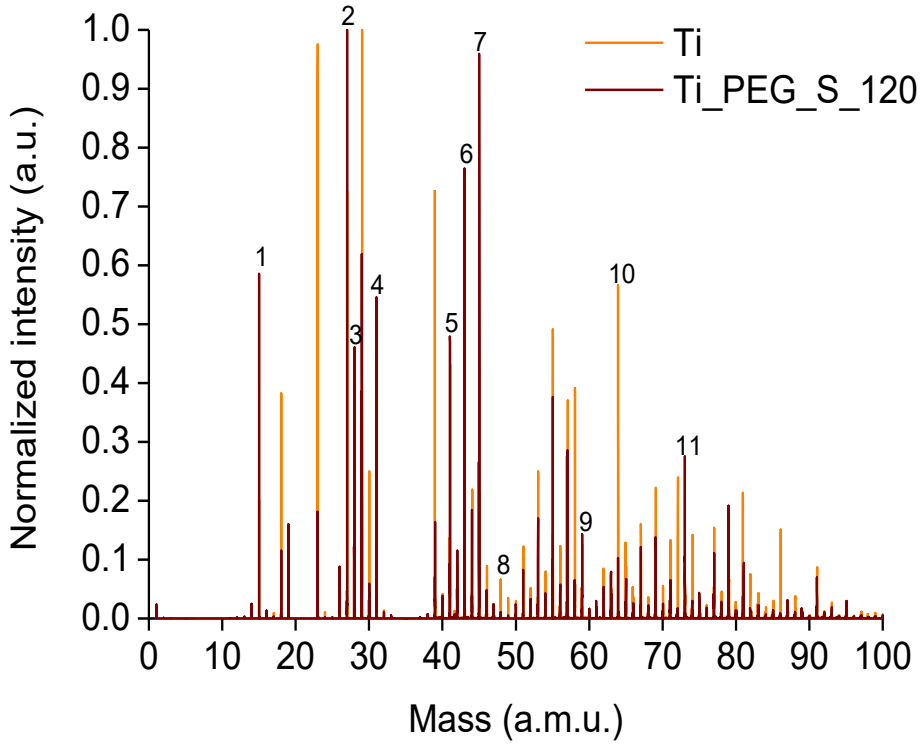

Figure 4.3. Positive spectra for Ti and SPEG120. Peak assignation can be found in Table 4.3

The presence of PEG can be observed by the characteristic peak of the polymer fragmentation, $C_2H_5O^+$. Other peaks from PEG can also be observed, such as CH_3O^+ or $C_3H_7O^+$. A reduction on the intensity of the peaks from the substrate (Ti and TiO) when

comparing the PEG coated sample and the bare titanium confirms the presence of a layer covering the substrate (Table 4.3).

Table 4.3. Peak assignation of the positive spectra of Ti and SPEG120

Peak number	Peak assignation	Mass (a.m.u.)
1	CH_3	15.0234
2	C_2H_3	27.0234
3	C_2H_4	28.0313
4	CH_3O	31.0183
5	C_2HO	41.0027
6	C_2H_3O	43.0183
7	C_2H_5O	45.0340
8	Ti	47.9479
9	$SiCH_3O$	58.9953
10	TiO	63.9428
11	$C_3H_5O_2$	73.0289

An imaging of the composition of the layer by ToF-SIMS (Figure 4.4) revealed the homogeneous composition of the coating, since the different fragments observed were distributed on the surface. Moreover, the predominant peak is the characteristic one for the PEG fragmentation, C_2H_5O. Both signals from the substrate, Ti and TiO were almost undetectable.

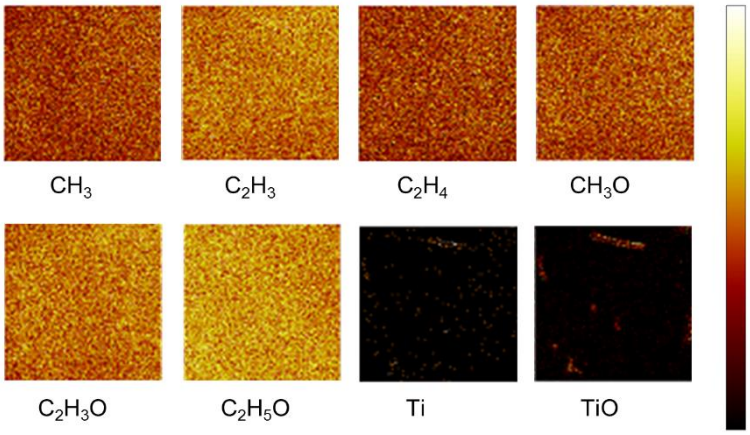

Figure 4.4. Representative peaks from the positive imaging of SPEG120. Field of view is 500x500 μm^2

4.2. Biological characterization

4.2.1. Cytotoxicity

Eluents from the silanized samples did not show any toxic effects for human fibroblasts (*Figure 4.5*), since the cell viability after 48h in contact with the eluent is not significantly affected, and it is for all the cases, higher than 80% [13].

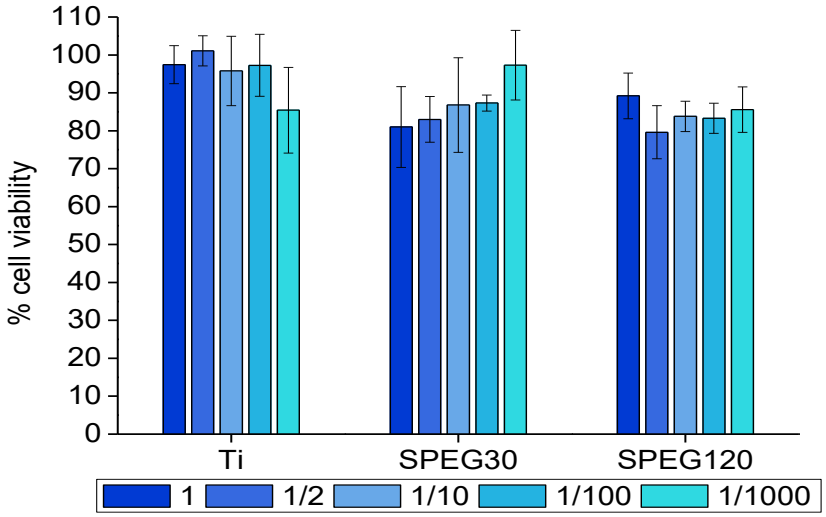

Figure 4.5. Cell viability of hFFs after 48h in contact with the eluents of the silanized samples

4.2.2. Protein adsorption: FTIC-BSA

BSA adsorption was studied by labeling the protein with FITC (Figure 4.6). The fluorescence intensity is lower for the PEG coated samples, showing a decrease on the protein adsorption. The same trend was reported by Sharma *et al.* in PEG-silane functionalized silicon wafer [4]. The antifouling effect is higher when increasing the immersion time of the titanium samples in the silanization process, in accordance to previous studies [14].

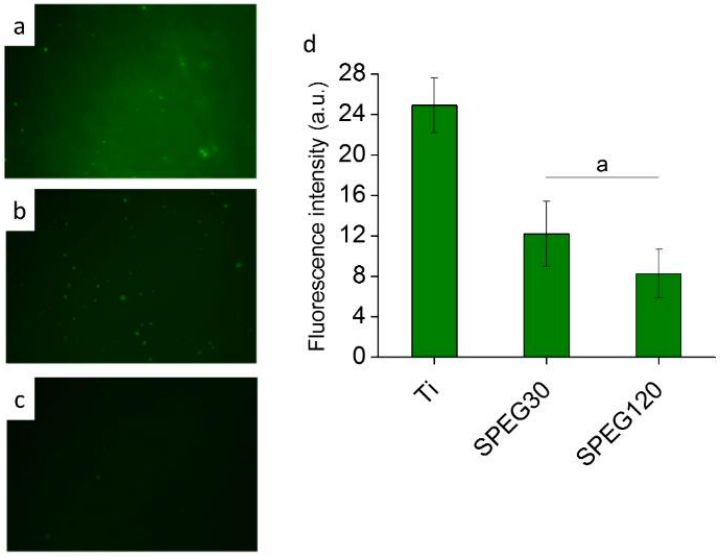

Figure 4.6. Representative fluorescence images of FITC-BSA adsorption on Ti (a), SPEG30 (b) and SPEG120 (c). Quantification of the fluorescence intensity (d). *a* indicates statistically significant differences compared to Ti ($p<0.05$)

4.2.3. Bacterial adhesion

Regarding the bacterial adhesion of *S. sanguinis* and *L. salivarius* on the coated samples, a decrease can be observed for both time conditions, SPEG30 and SPEG120. The decrease on the bacterial adhesion follows a trend with the time of immersion of the titanium on the silane-PEG solution, in the same manner as the albumin adsorption. This fact can be associated with the higher grafting density that might be obtained at longer immersion times, as reported in previous studies [14].

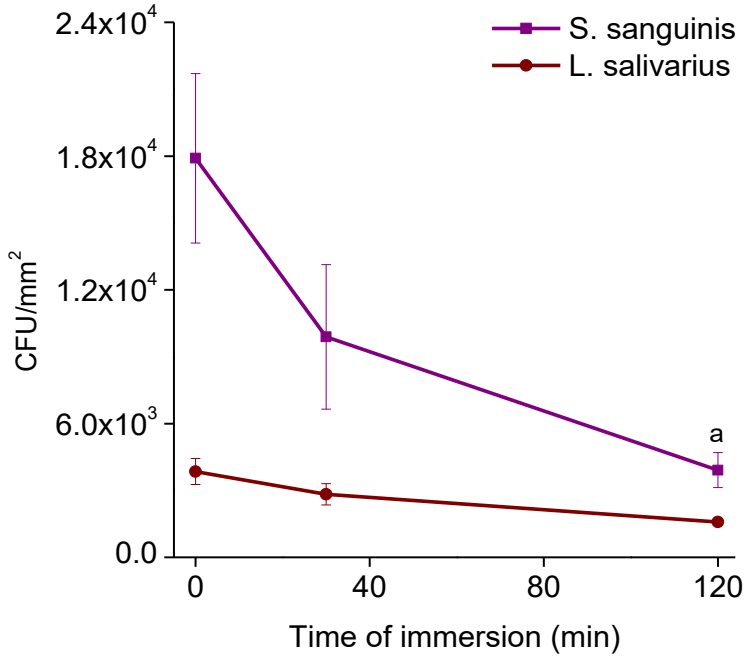

Figure 4.7. Bacterial adhesion of *S. sanguinis* and *L. salivarius* on Ti and PEG-silane coated samples. *a* indicates statistically significant differences compared to Ti in each assay ($p<0.05$)

4.3. RGD functionalization

SPEG120 was functionalized with the cell adhesion peptide RGD by physisorption, i.e. immersion in a solution of the peptide in PBS. A change in the water contact angle from a value of 15º to 30º is detected.

XPS analysis (Table 4.4) was performed in order to detect the RGD incorporation. An increase on the carbon signal can be observed, while the titanium and silicon signal is reduced. These differences may be indicative of the presence of the RGD peptide. The decrease on the silicon and titanium signal of the SPEG120_RGD compared to the SPEG120 is due to the attenuation of the substrate signal, which is characteristic of the presence of an organic layer.

Table 4.4. XPS atomic % of the PEG coated sample without and with physisorbed RGD

	C1s	O1s	N1s	Si2p	Cl2p	Ti2p
SPEG120	17.7 ± 0.5	57.7 ± 0.8	0.3 ± 0.0	10.9 ± 1.2	1.8 ± 0.0	13.4 ± 0.9
SPEG120_RGD	25.8 ± 1.8	58.9 ± 1.0	0.4 ± 0.1	5.2 ± 0.6	1.7 ± 0.3	8.0 ± 0.5

4.3.1. Cell adhesion

Cell adhesion of hFFs was tested in both the PEG coated samples with and without RGD (Figure 4.8). While the presence of the silanized PEG coating reduces the cell adhesion, the incorporation of RGD in the coating increases the cell adhesion up to the level of bare titanium. Regarding the cell spreading observed by SEM (Figure 4.8a-c) no differences were found among the different conditions.

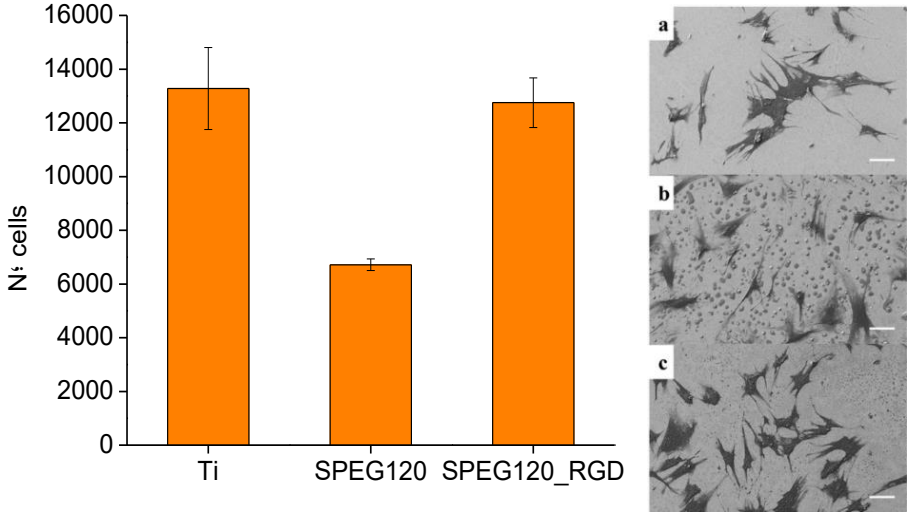

Figure 4.8. hFFs adhesion on the PEG coated sample with and without RGD. Scale bar represents 50µm

4.3.2. Bacterial adhesion

Bacterial adhesion with *S. sanguinis* and *L. salivarius* (Figure 4.9) was not significantly affected by the presence of RGD on the coating either on the titanium or the PEG-coated sample. Despite the fact that some pathogenic bacterial strains have adhesins able to interact with extracellular matrix proteins, no increase in the adhesion of the two studied bacterial strains has been observed.

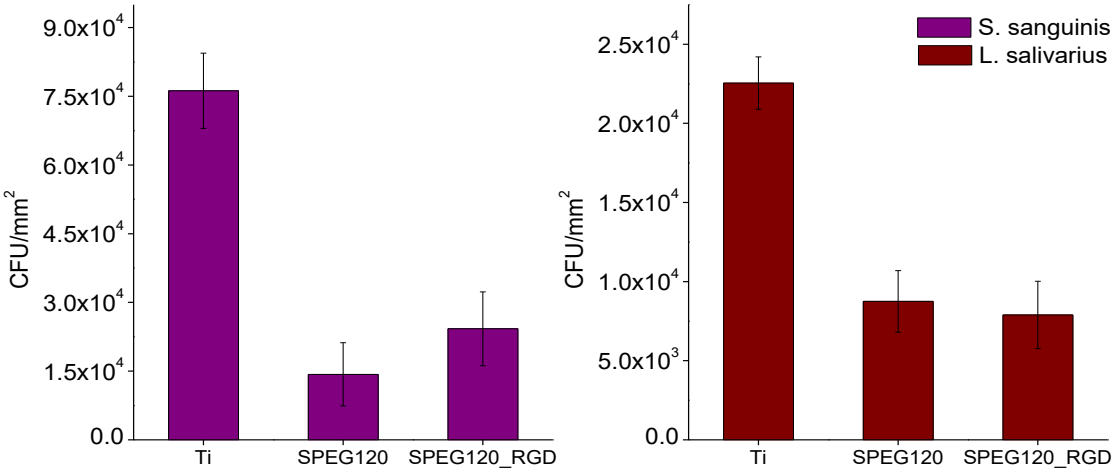

Figure 4.9. Bacterial adhesion of *S. sanguinis* and *L. salivarius*

4.4. References

[1] W.-C. Chen, C.-L. Ko, *Roughened titanium surfaces with silane and further RGD peptide modification in vitro*, Mater. Sci. Eng. C. Mater. Biol. Appl. 33 (2013) 2713–22. doi:10.1016/j.msec.2013.02.040.

[2] M. Godoy-Gallardo, J. Guillem-Marti, P. Sevilla, J.M. Manero, F.J. Gil, D. Rodriguez, *Anhydride-functional silane immobilized onto titanium surfaces induces osteoblast cell differentiation and reduces bacterial adhesion and biofilm formation*, Mater. Sci. Eng. C. Mater. Biol. Appl. 59 (2016) 524–32. doi:10.1016/j.msec.2015.10.051.

[3] K.C. Popat, S. Sharma, T.A. Desai, Quantitative XPS *Analysis of PEG-Modified Silicon Surfaces*, J. Phys. Chem. B. 108 (2004) 5185–5188. doi:10.1021/jp049260j.

[4] S. Sharma, K.C. Popat, T. a. Desai, *Controlling nonspecific protein interactions in silicon biomicrosystems with nanostructured poly(ethylene glycol) films*, Langmuir. 18 (2002) 8728–8731. doi:10.1021/la026097f.

[5] S. Sharma, R.W. Johnson, T.A. Desai, *XPS and AFM analysis of antifouling PEG interfaces for microfabricated silicon biosensors*, Biosens. Bioelectron. 20 (2004) 227–39. doi:10.1016/j.bios.2004.01.034.

[6] Z. Guo, S. Meng, W. Zhong, Q. Du, L.L. Chou, *Self-assembly of silanated poly(ethylene glycol) on silicon and glass surfaces for improved haemocompatibility*, Appl. Surf. Sci. 255 (2009) 6771–6780. doi:10.1016/j.apsusc.2009.02.034.

[7] R. Schlapak, P. Pammer, D. Armitage, R. Zhu, P. Hinterdorfer, M. Vaupel, *et al.*, *Glass surfaces grafted with high-density poly(ethylene glycol) as substrates for DNA oligonucleotide microarrays*, Langmuir. 22 (2006) 277–85. doi:10.1021/la0521793.

[8] Y. Ito, H. Hasuda, M. Sakuragi, S. Tsuzuki, *Surface modification of plastic, glass and titanium by photoimmobilization of polyethylene glycol for antibiofouling*, Acta Biomater. 3 (2007) 1024–32. doi:10.1016/j.actbio.2007.05.010.

[9] M. Isabel Tejedor-Tejedor, and Liana Paredes, M.A. Anderson, *Evaluation of ATR−FTIR Spectroscopy as an "in Situ" Tool for Following the Hydrolysis and Condensation of Alkoxysilanes under Rich H2O Conditions*, (1998). doi:10.1021/CM980146L.

[10] R. Banga, J. Yarwood, A.M. Morgan, B. Evans, J. Kells, *FTIR and AFM Studies of the Kinetics and Self-Assembly of Alkyltrichlorosilanes and (Perfluoroalkyl)trichlorosilanes onto Glass and Silicon*, Langmuir. 11 (1995) 4393–4399. doi:10.1021/la00011a036.

[11] A. Alexander Papra, Nikolaj Gadegaard, N.B. Larsen, A. Papra, N. Gadegaard, N.B. Larsen, *Characterization of Ultrathin Poly(ethylene glycol) Monolayers on Silicon Substrates*, Langmuir. 17 (2001) 1457–1460. doi:10.1021/la000609d.

[12] K. Norrman, A. Papra, F.S. Kamounah, N. Gadegaard, N.B. Larsen, *Quantification of grafted poly(ethylene glycol)-silanes on silicon by time-of-flight secondary ion mass spectrometry*, J. Mass Spectrom. 37 (2002) 699–708. doi:10.1002/jms.330.

[13] International Organization for Standardization, *ISO 10993-5: Biological evaluation of medical devices-Part 5: Tests for in vitro cytotoxicity*, (2009).

[14] S. Sharma, T.A. Desai, Nanostructured *Antifouling Poly(ethylene glycol) Films for Silicon-Based Microsystems*, J. Nanosci. Nanotechnol. 5 (2005) 235–243. doi:10.1166/jnn.2005.030.

5. PULSED PEG ELECTRODEPOSITION

Electrodeposition is a process where an external applied electric field attracts charged particles towards the electrode. This process has some advantages such as the short processing time, the possibility of operate at room temperature and the use of a fluid (usually water) as a solvent [1]. Electrochemical processes can be applied to obtain polymeric coatings, using the current to attract monomers to the substrate, where the polymerization takes place. Some examples of polymeric coatings on titanium are the deposition of composite coatings of alginate and chitosan [1] or the electropolymerization of dopamine [2]. The strategy that is reported in this chapter is based on the use of a partially charged polymer, specifically a PEG amine-terminated. Pulsed electrodeposition was the selected method for the preparation of the coatings, using different pulse time and potential. The electrodeposited coatings were used for the functionalization with two antimicrobial peptides, human lactoferrin1-11 (hLF1-11) and magainin 2.

5.1. Coating characterization

5.1.1. Wettability

Wettability was increased by the plasma activation treatment leading to a superhydrophilic surface (Figure 5.1). After applying the electrodeposition process, water contact angle increased to 25-45º. This values are in the range of the previously found by several authors [3,4], and they indicate the presence of a hydrophilic coating on the surface.

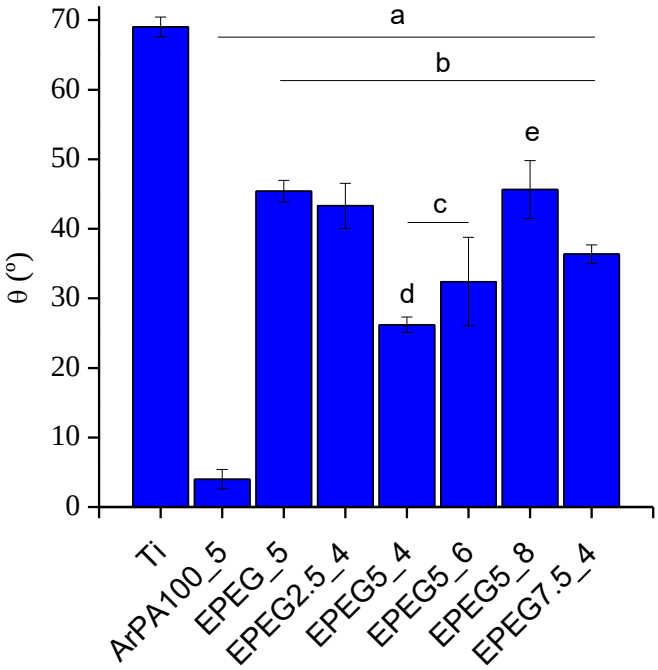

Figure 5.1. Water contact angle of the control and PEG-coated samples. *a* indicates statistically significant differences compared to Ti, *b* compared to ArPA100_5, *c* compared to EPEG_5, *d* compared to EPEG2.5_4, *e* compared to EPEG5_4 ($p<0.05$)

5.1.2. Chemical composition

ATR-FTIR spectra (Figure 5.2) presented the characteristic peaks for a PEG coating. The peaks were attributed to CH_2 bending at 963, 1342, 1455 and 1465cm^{-1}, to CO stretching at 1106 and 1060cm^{-1} and to C-C stretching at 1149cm^{-1} [5].

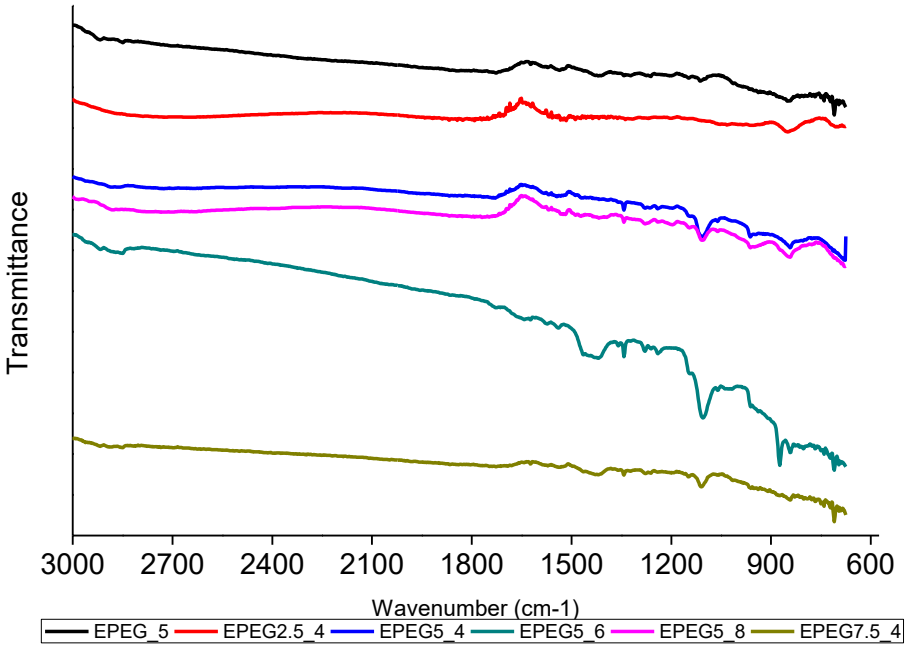

Figure 5.2. ATR-FTIR of electrodeposited samples

XPS analysis of the samples revealed the presence of titanium, carbon, oxygen and nitrogen (Table 5.1). The presence of carbon, oxygen and nitrogen can be associated to the presence of the PEG-amine coating, since the polymer contains the three elements. The titanium substrate is naturally covered by a titanium oxide layer which accounts for the titanium and oxygen presence. Both carbon and oxygen detection may also be associated to adventitious contamination adsorbed on the surface.

As previously reported, a decrease on the C1s signal can be observed when comparing Ti and ArPA100_5 samples, due to the decontamination of the samples during the plasma activation process [6]. Continuous electrodeposition (EPEG_5) rendered an increase on the C1s signal with respect of the non-coated samples, with similar values to the ones obtained by Tanaka *et al.* [7]. Subsequently, a decrease on the Ti2p signal can be observed due to the attenuation of the substrate signal.

The coatings obtained in pulsed conditions (EPEG2.5_4, EPEG5_4, EPEG5_6, EPEG5_8 and EPEG7.5_4) presented a higher amount of carbon compared to the coating obtained in the continuous mode, which showed the higher yield of the pulsed processes. Among the pulsed conditions, EPEG7.5_4 was the one with less carbon amount. In the pulsed mode the Ti2p signal was undetectable except for the PEG7.5_4. The values for the atomic composition of the layers obtained by pulses are comparable to the theoretical values for an amino-terminated PEG with a molecular weight of 1500. This fact supports the presence of the polymer on the surface.

Differences on the nitrogen amount may be due to the surface depth analysis of XPS, since the polymer layers are thicker than the analysis depth and part of the nitrogen might be in direct contact with the titanium surface. This fact can be observed on the N/Ti ratio, which is higher for the pulsed electrodeposited samples. The higher presence of nitrogen on the outermost layer of the coating is a good indicator of the suitability of the coating for the further functionalization through the bond with the terminal amine of PEG.

Table 5.1. Atomic % of the main components found on the titanium samples before electrodeposition and with the different conditions studied (XPS)

	C 1s	O 1s	N 1s	Ti 2p	N/Ti
Ti	23.5 ± 0.8	59.6 ± 0.8	0.6 ± 0.1	16.3 ± 0.1	0.04
ArPA100_5	15.0 ± 0.7	62.1 ± 0.7	0.3 ± 0.1	22.6 ± 0.1	0.01
Ti-PEG-cont	38.1 ± 0.9	47.7 ± 1.0	1.2 ± 0.1	13.9 ± 0.1	0.09
Ti-PEG-2.5-4	73.6 ± 1.0	24.8 ± 0.9	1.1 ± 0.1	0.1 ± 0.2	11
Ti-PEG-5-4	70.8 ± 0.5	26.3 ± 0.5	1.0 ± 0.1	1.2 ± 0.4	0.83
Ti-PEG-5-6	68.3 ± 0.2	29.2 ± 0.2	1.5 ± 0.4	0.5 ± 0.2	3.00
Ti-PEG-5-8	71.9 ± 0.6	26.2 ± 0.9	1.1 ± 0.1	0.7 ± 0.7	1.57
Ti-PEG-7.5-4	63.7 ± 0.3	30.1 ± 0.2	1.4 ± 0.7	4.7 ± 0.3	0.30
Theoretical-PEG	67.3	30.8	1.9	-	

In the decomposition of the C1s signal of XPS spectra (Figure 5.3), three different peaks can be found, corresponding to C-C bonds at 285eV, C-O bonds at 286.5eV and C=O peaks at 288eV.

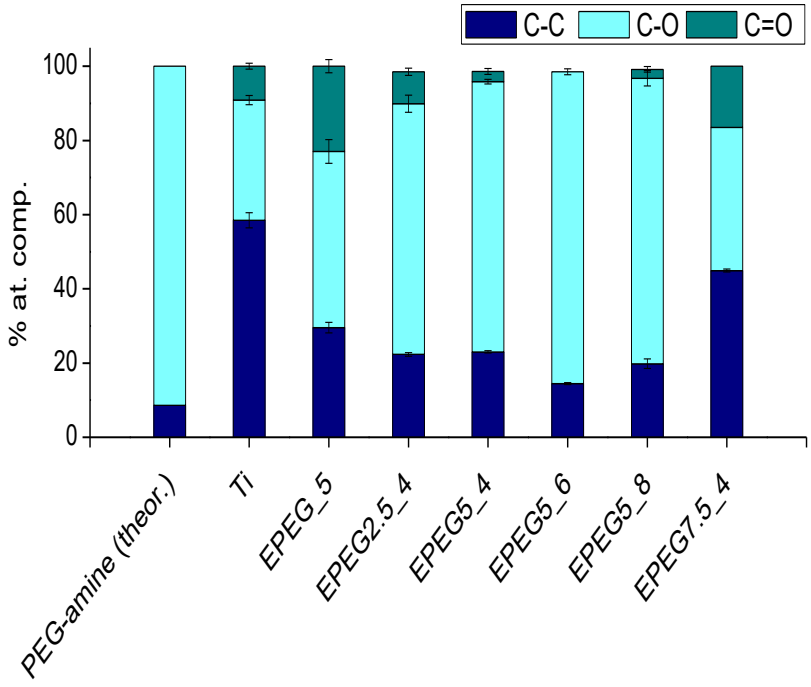

Figure 5.3. Components contribution (as atomic %) to the C1s peak for the XPS decomposition. Theoretical atomic composition is shown for comparison (PEG-amine theor.)

An increase of the presence of the C-O bond for the coated samples is indicative of the presence of PEG, and an increase of this peak for the pulsed conditions suggest a higher grafting density of the polymer chains, as previously indicated by Sharma *et al.* and Sofia *et al.* [8,9]. However, EPEG7.5_4 has less presence of this peak, which suggests a lower density of polymer chains when applying a polarity inversion. Theoretical composition calculated for the PEG amine (M_w=1500) is showed for comparison. The presence of more oxidized CO bonds may account for the presence of contamination.

5.1.3. Film thickness

The thickness of the pulsed electrodeposited films cannot be estimated by the attenuation of the substrate signal in the XPS analysis because the coatings are thicker than the depth penetration of the photoelectrons. Cross sections of the coatings were prepared by FIB in EPEG_5 and EPEG5_6 samples in order to analyze differences between the pulsed and the continuous process (Figure 5.4). The value of the thickness approximated by the images is around 15 nm for the EPEG_5 and 25 nm for the EPEG5_6.

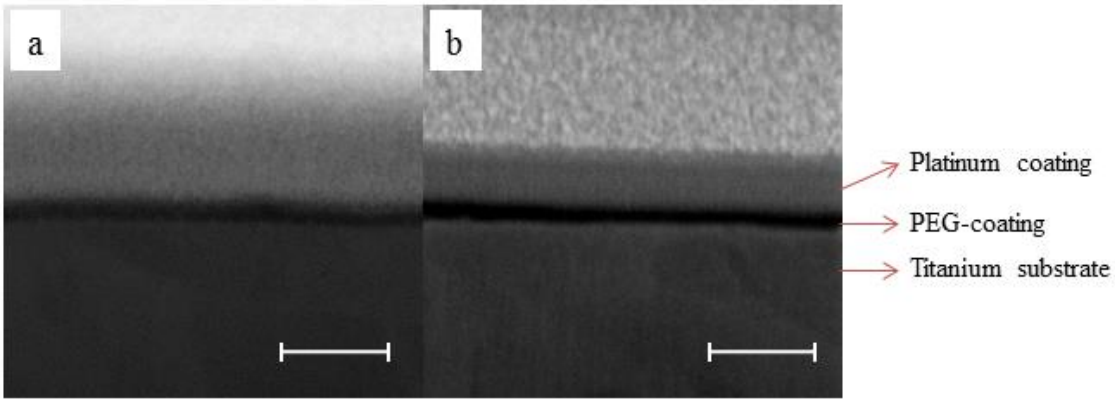

Figure 5.4. FIB image of the coating. a) Ti-PEG-cont, b) Ti-PEG-5-6 (Scale bar indicates 200nm)

5.2. Biological characterization

5.2.1. Cytotoxicity and cell adhesion

Indirect cytotoxicity of the PEG-coated samples (Figure 5.5a) revealed no toxic effect of the eluents of the samples, as the viability of the hFFs is higher than 80%. hFFs adhesion (Figure 5.5b) showed no significant differences of the PEG-coated samples when compared to the Ti for the EPEG2.5_4, EPEG5_4 and EPEG5_6, while the adhesion for the other conditions is a 60% of the adhesion on titanium. According to these results, a better biocompatibility of the EPEG2.5_4, EPEG5_4 and EPEG5_6 can be expected. Indeed, fibronectin adsorption analyzed by XPS showed a decrease on the amount of nitrogen content on the PEG-coated samples (from 8% of nitrogen on Ti to less than 5% on the PEG-coated samples both in continuous and pulsed mode) due to the decrease on the adsorption of the protein in the PEG-coated samples both in

continuous and pulsed mode. This results are in agreement with the studies of Altankov *et al.* and Röttgermann *et al.* [10,11]. In their studies, the capability of PEG coating to adsorb fibronectin was shown. The protein adsorption facilitated a certain degree of cell adhesion and spreading, making the coatings viable for tissue integration applications such as dental implants.

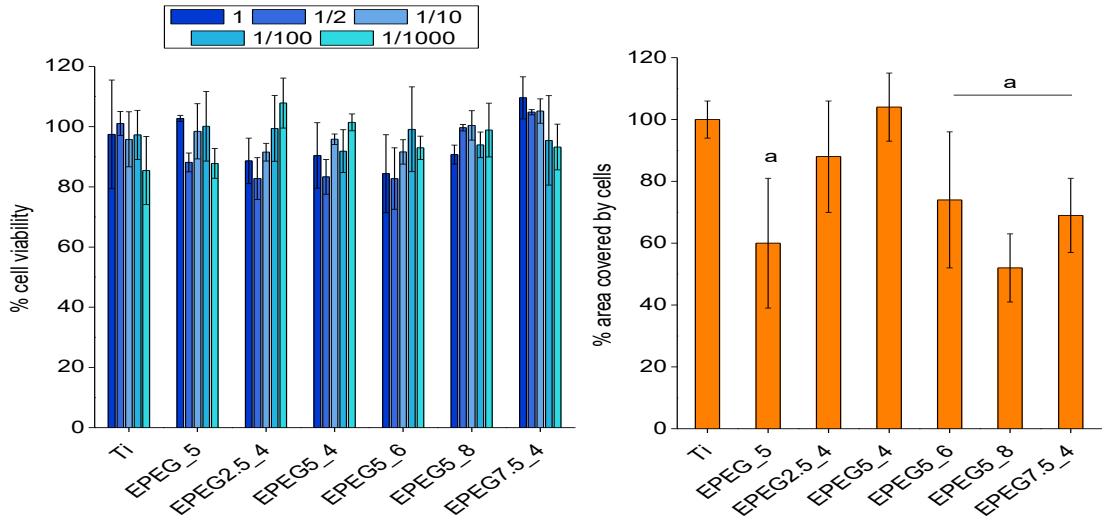

Figure 5.5. Cytotoxicity of the treated samples (a) and cell adhesion of hFFs (b). *a* indicates statistically significant differences compared to Ti ($p<0.05$)

5.2.2. Bacterial adhesion

Regarding bacterial adhesion with *S. aureus* and *E. coli*, a decrease can be observed when comparing control samples and PEG-coated samples (Figure 5.6). This behavior was previously observed by Tanaka *et al.* [12] in a continuous-mode electrodeposited sample.

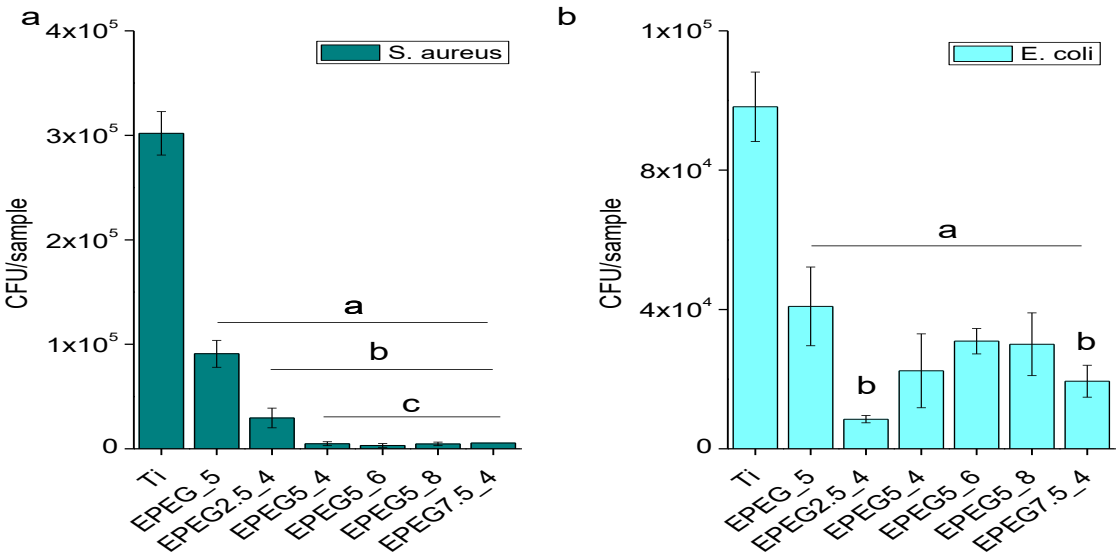

Figure 5.6. Bacterial adhesion on the coated samples. a) *S. aureus* adhesion, b) *E. coli* adhesion. *a* indicates statistically significant differences compared to Ti, *b* compared to EPEG_5 and *c* compared to EPEG2.5_4 ($p<0.05$).

A significant decrease can be also observed when comparing the continuous-mode electrodeposited sample (EPEG_5) to the pulsed ones in the *S. aureus* adhesion. However, this behavior was only observed for the *E. coli* adhesion in the samples with a t_{on}=t_{off}=4ms, i.e. EPEG2.5_4, EPEG5_4 and EPEG7.5_4. The values obtained in the continuous process are comparable to the ones reported for PEG coatings by several authors [13].

The morphological features of the bacteria adhering to the substrates were observed by SEM. Regarding *S. aureus* adhesion (Figure *5.7*), a decrease was observed when comparing Ti samples to the PEG-coated samples. Images confirm the trend previously reported for the bacterial adhesion by CFU counting assay (Figure 5.6). Biofilm formation involves the quorum sensing of the bacteria, which needs a short distance between the bacteria. In the Ti sample, the bacteria started producing the extracellular matrix, since a polymeric compound is observed under the bacteria in the images of this sample (Figure *5.7*a).

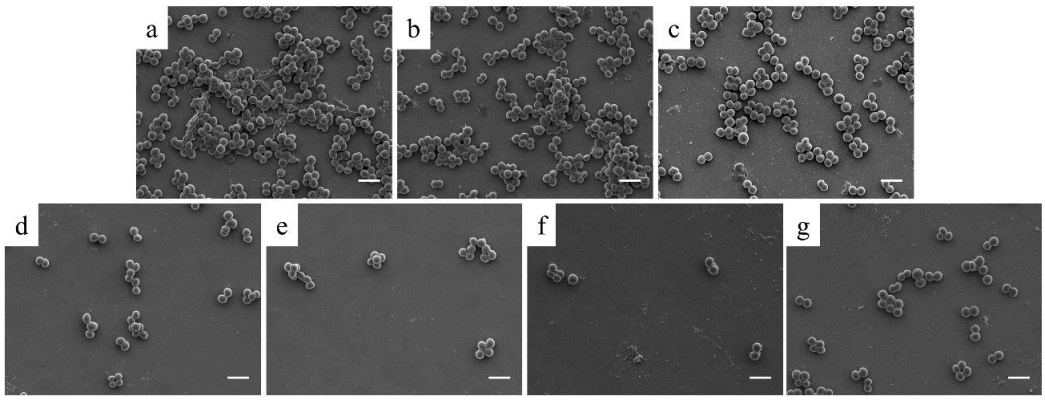

Figure 5.7. Representative SEM images of *S. aureus* adhering to Ti (a), EPEG_5 (b), EPEG_2.5_4 (c), EPEG_5_4 (d), EPEG_5_6 (e), EPEG_5_8 (f), EPEG_7.5_4 (g). Scale bar represents 2µm.

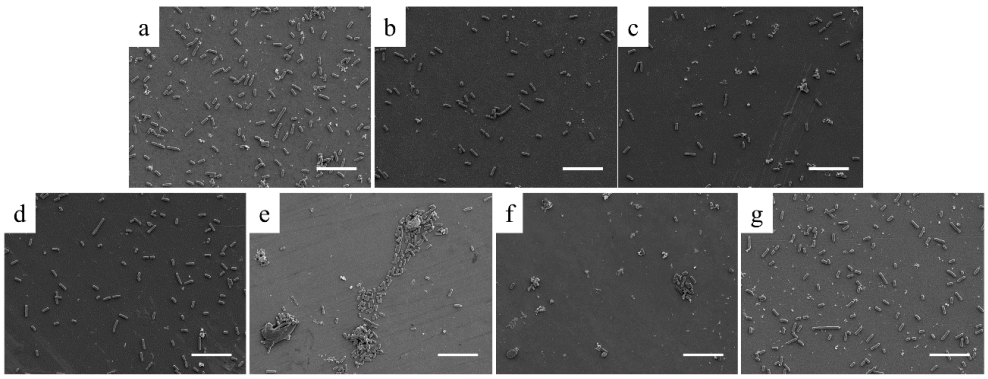

Figure 5.8. Representative SEM images of *E. coli* adhering to Ti (a), EPEG_5 (b), EPEG_2.5_4 (c), EPEG_5_4 (d), EPEG_5_6 (e), EPEG_5_8 (f), EPEG_7.5_4 (g). Scale bar represents 10µm.

In the SEM images of *E. coli* adhesion on the Ti and PEG-coated surfaces (Figure *5.8*), the trend observed in the CFU counting assay was also confirmed. For this strain, the reduction on the bacterial adhesion was lower than the one found for *S. aureus*. The

number of adhering bacteria is low enough for the bacteria to be separated. Therefore, biofilm formation was not observed.

E. coli has fimbriae, which are appendages that the bacteria use to adhere to other bacteria, to eukaryotic cells or to inanimate surfaces. Fimbriae are also related to the ability of bacteria to withstand shear forces and to the possibility to form a biofilm. These structures are observed in some cells in the control surface, but not in the PEG-coated samples (Figure 5.9). Therefore, it may be concluded that the biofilm formation by *E. coli* will be hampered on the PEG-coated surfaces.

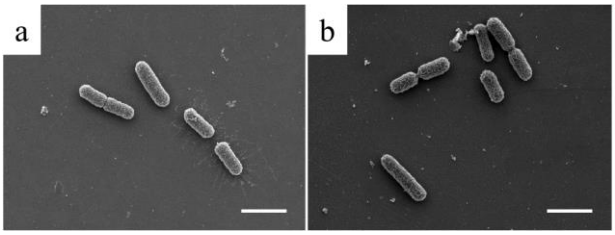

Figure 5.9. SEM images of E.coli adhesion on Ti (a) and EPEG_5_4 (b), showing the presence of fimbriae in the bacteria adhered on the Ti sample but not on the EPEG_5_4 sample. Scale bar represents 2µm.

5.2.1. Co-culture studies

Co-culture assays with bacteria and hFFs are a good way to reproduce *in vitro* the "race for the surface" mechanism described by Gristina [14]. This assay was developed and validated by Zhao *et al.* [15] in order to test different dental materials. They found out that the best material to promote a biosealing was the smooth titanium. Since the assay allows the bacteria to colonize the surface in the first place, it was used in this study to evaluate the efficacy of the antifouling coating to repel the bacterial adhesion while allowing the eukaryotic cells adhesion. The area covered by cells on the PEG coatings in presence of bacteria (Figure 5.10) was lower than the same condition without bacteria, since the presence of the coating is not able to inhibit completely the bacterial adhesion.

However, the presence of the PEG coating increased the area percentage covered by cells, showing the efficacy of the coatings to overcome the bacterial adhesion while allowing a certain degree of cell adhesion.

When taking into account the cell spreading (Figure 5.12), the cells in the mono-culture presented a good spreading on the surface, either in presence of the PEG coating or in titanium. In presence of *E. coli* the cells are less spread than in the mono-culture. However, in presence of *S. aureus* the cells are even more rounded. This fact can be related to several factors. On the one hand, the presence of the PEG coating is reducing but not completely inhibiting the bacterial adhesion. The remaining bacteria might impair the cell adhesion on the substrate. On the other hand, differences in the growth rate of the two strains might induce a different number of bacteria which can be responsible of the differences in the cell number and the cell spreading on *S. aureus* and *E. coli*.

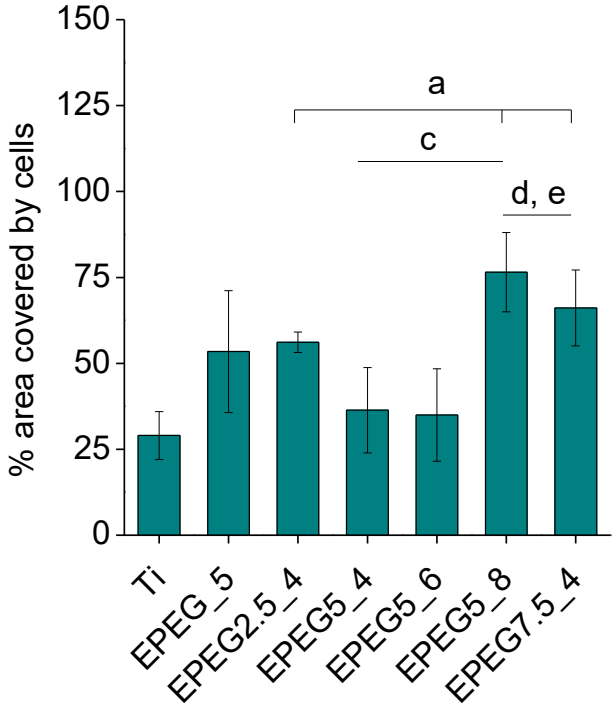

Figure 5.10. Area covered by cells in presence of *S. aureus* respect the area covered by cells in the sample of the same condition without bacteria. *a* indicates statistically significant differences compared to Ti, *b* compared to EPEG_5, *c* compared to EPEG2.5_4 and *d* compared to EPEG5_4

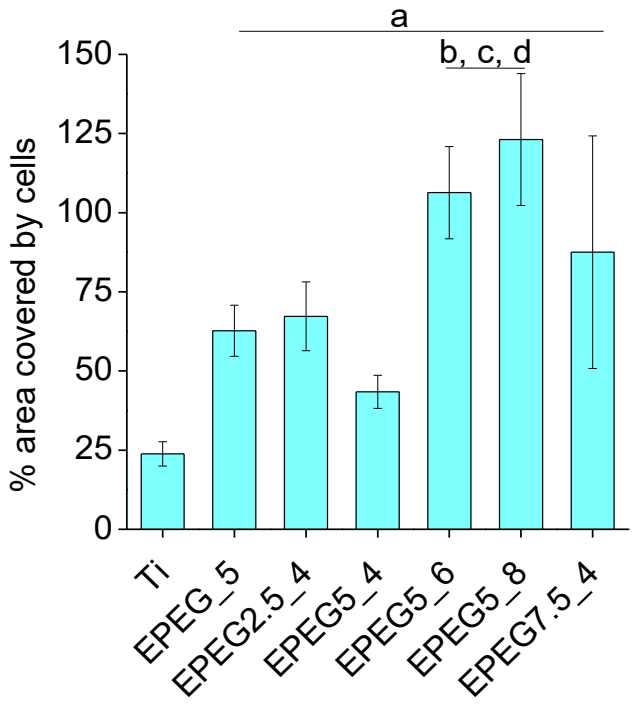

Figure 5.11. Area covered by cells in presence of *E. coli* respect the area covered by cells in the sample of the same condition without bacteria. *a* indicates statistically significant differences compared to Ti, *b* compared to EPEG_5, *c* compared to EPEG2.5_4 and *d* compared to EPEG5_4

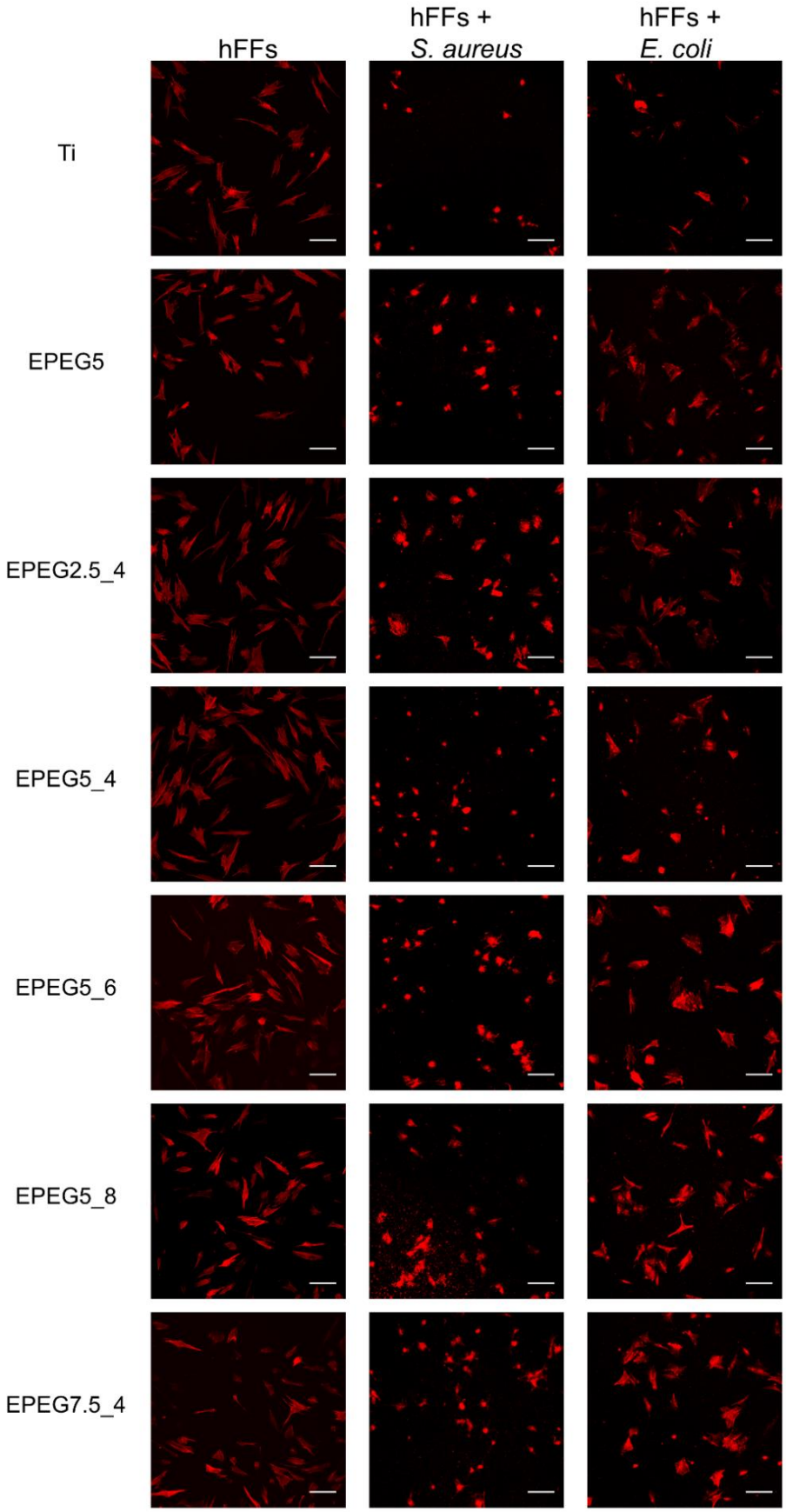

Figure 5.12. Fluorescence images of the hFFs actin filaments on the samples in mono-culture (hFFs), in co-culture with *S. aureus* (hFFs + *S. aureus*) and in co-culture with *E.coli* (hFFs + *E. coli*)

5.3. AMP immobilization

5.3.1. Minimum inhibitory concentration

The antibacterial effect of the peptides in solution was performed by the microdilution method using 2-fold dilutions of the studied peptides (Figure 5.13). The concentration of 1mM, which is much higher than the effective values found by other authors, was used as a control. *S. aureus* growth was hampered by all the peptides, since the final absorbance is lower than the absorbance of the positive control (*S. aureus* without AMP). The minimum inhibitory concentration (MIC) is usually reported as the lowest concentration of the tested antibacterial agent that completely inhibits the growth or produces at least 90% reduction of the absorbance in comparison to the absorbance of the positive control [16]. In this sense, the MIC_{90} of the peptide MG-1 was 1mM (Figure 5.13a) and the MIC of the peptide MG-2 was 128µM (Figure 5.13b). However, for the hLF1-11, none of the studied concentrations reached the 90% of reduction, showing a reduction in absorbance at the highest concentration of 50% for LF1 (Figure 5.13c) and 65% for LF2 (Figure 5.13d).

Previous studies of the activity of both magainin 2 and hLF1-11 reported lower MIC values than the ones found in this study. For instance, Zasloff [17] and Matsuzaki [18] reported a MIC of magainin 2 in the range of 2-50µM. A value of 100 µM was reported by Ge *et al.* [19] for a magainin analogue. This value is in the range of the one that is shown in this study.

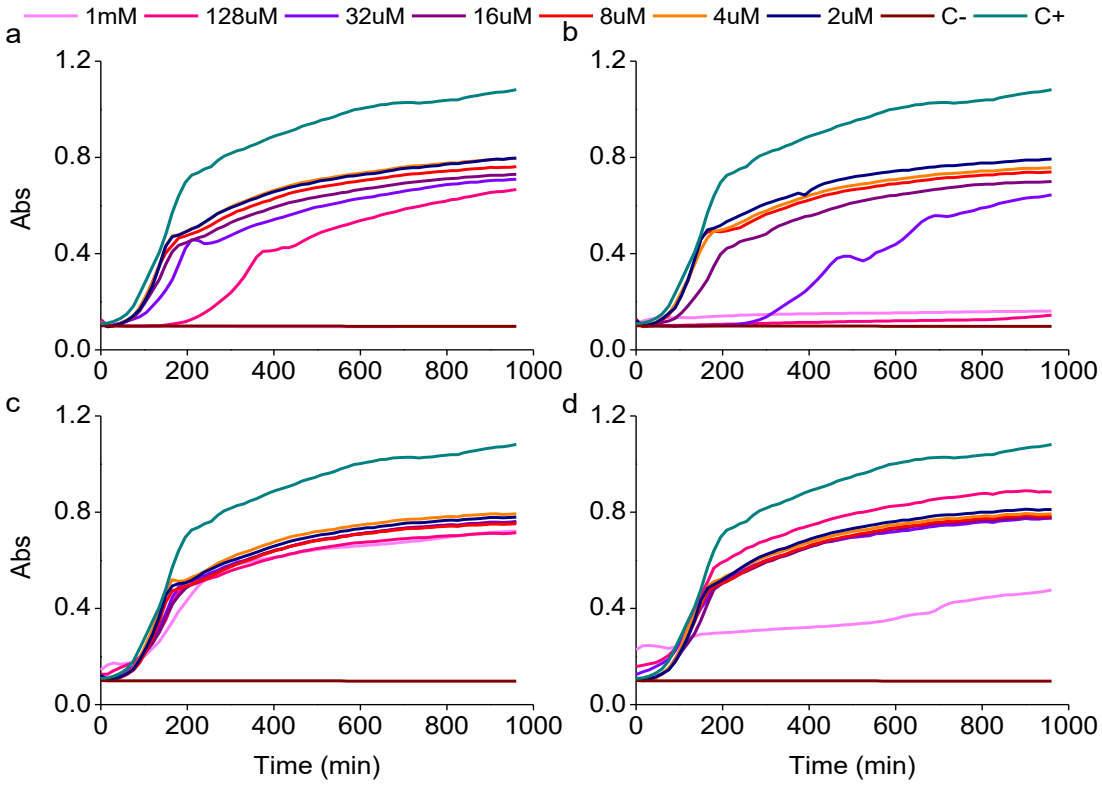

Figure 5.13. Growth curves of *S. aureus* in contact with increasing concentrations of MG1 (a), MG2 (b), LF1 (c), LF2 (d)

Differences on the MIC values might be due to differences in the experimental set-up, like the initial number of bacteria used for the growth curves. Moreover, the activity of the AMPs *in vitro* is not always indicative of the peptide performance *in vivo*. In this line, Nibbering *et al.* [20] reported a better performance of different human lactoferrin derivatives when tested in mice than the *in vitro* response in the microdilution method. This behavior might be attributed to a synergy of the peptide with other serum proteins, local factors (pH, ion concentration) or interactions with host cells that are not taken into account when running a susceptibility assay *in vitro*.

5.3.2. Selection of the immobilization technique by XPS

The AMP immobilization method was tested by XPS on EPEG_5 (*Table 5.2*). The main changes observed were in the carbon, the nitrogen and the sulfur signal from the peptides. The three elements showed an increase when comparing the EPEG_5 sample to all the AMP-functionalized coatings. Subsequently, a decrease in the titanium and the oxygen signal from the titanium oxide of the substrate was observed for the functionalized samples. As previously reported (section 5.1.3), EPEG_5 is the electrodeposited sample with the lowest thickness. This sample was selected for the study of the peptide immobilization technique because the signal from the substrate was not completely attenuated and, as a consequence, all the immobilized peptide could be detected.

Table 5.2. XPS results as %atomic of EPEG_5 and the AMP with the two functionalization strategies

	C 1s	O 1s	N 1s	Ti 2p	S2p
Ti	23.5 ± 0.8	59.6 ± 0.8	0.6 ± 0.1	16.3 ± 0.1	-
ArPA100_5	15.0 ± 0.7	62.1 ± 0.7	0.3 ± 0.1	22.6 ± 0.1	-
EPEG_5	38.1 ± 0.9	47.0 ± 1	1.2 ± 0.1	13.9 ± 0.1	-
LF-1	51.5 ± 0.8	33.7 ± 0.1	8.3 ± 0.5	6.3 ± 0.1	0.2 ± 0.1
MG-1	50.2 ± 0.1	36.0 ±0.4	7.5 ± 0.6	6.2 ± 0.2	0.1 ± 0.1
LF-2	49.1 ± 0.2	33.1 ±0.1	11.9 ± 0.5	5.2 ± 0.1	0.7 ± 0.1
MG-2	51.4 ± 0.3	32.8 ±0.7	9.6 ± 0.4	5.6 ± 0.3	0.5 ± 0.1

The yielding of the two studied coupling methods may be estimated by taking into account the N1s and the S2p signals. According to the results, the linking with the N-terminal by the crosslinking of the thiol moiety of the aminoacid cysteine yield a higher peptide concentration in the outermost layer of the coating, since both the N1s and the S2p atomic concentration is higher for the AMPs coupled by this method (MG-2 and LF-2). Thus, the crosslinking with the maleimide group is a better option than the esterification of the carboxylate with NHS/EDC.

5.3.3. Cytotoxicity of the PEG-AMP coatings

Indirect cytotoxicity of the AMP was checked to link both EPEG_5 and EPEG_5_4 (Figure 5.14). No toxic effects were observed in the samples, showing the biocompatibility of the coatings.

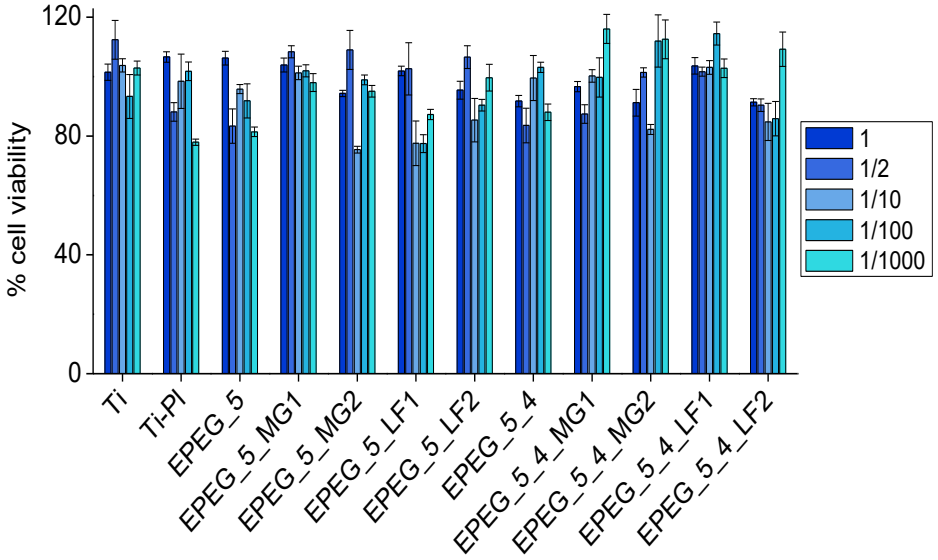

Figure 5.14. Indirect cytotoxicity of the AMP immobilized on EPEG_5 and EPEG5_4

5.3.4. Bacterial adhesion

Bacterial adhesion was checked with *S. aureus* for the AMP functionalization on EPEG_5 and EPEG_5_4 (Figure 5.15). As previously reported (section 5.2.2), the antifouling effect of the PEG coatings is higher when preparing the sample in pulsed conditions.

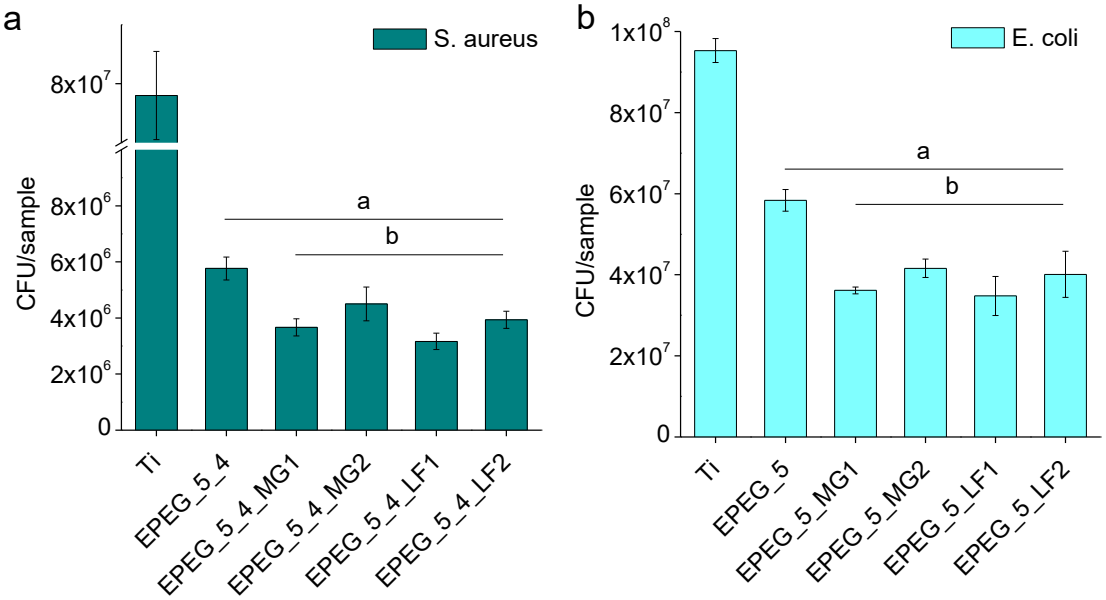

Figure 5.15. Bacterial adhesion *S. aureus* on the AMP functionalized EPEG_5 (a) and AMP functionalized EPEG_5_4 (b). *a* indicates statistically significant differences compared to Ti, and *b* compared to EPEG_5_4 ($p<0.05$)

Regarding the AMP activity, both magainin 2 and hLF1-11 showed a better antibacterial activity when immobilized by the crosslinking with the maleimide group by the N-terminal of the peptide (MG1 and LF1). This result is related to the aminoacid sequence of the peptides. The antibacterial activity of the AMP is related to the presence of positively charged aminoacids (basically, arginine and lysine). The positive charges

on the two peptides used for this study are closer to the C-terminal than to the N-terminal (Table 5.3).

Table 5.3. Aminoacid sequence of the peptides used in this study. Positively charged aminoacids (Arginine, R and Lysine, K) are in bold to highlight their position.

Peptide name	Aminoacid sequence
Magainin 2	GIG**K**FLHSA**KK**FG**K**AFVGEIMNS
hLF1-11	G**RRRR**SVQWCA

Hence, the linking of the peptide by the C-terminal may reduce the availability of the positively charged aminoacids and the antibacterial activity. However, the results might also be related to the yield of the linking protocol. As shown by the XPS results, a higher yield was observed with LF-1 and MG-1, which are the peptides showing the better antibacterial activity after the immobilization.

5.3.5. Biofilm formation: live-dead test

In order to evaluate the AMP activity, samples from the bacterial adhesion test were stained with a Live-dead kit (Figure 5.16). This kit contains two nucleic acid stains, SYTO® 9 green and propidium iodide. SYTO® stains all bacteria in green, while propidium iodide, which labels in red, is only able to penetrate bacteria with damaged membranes.

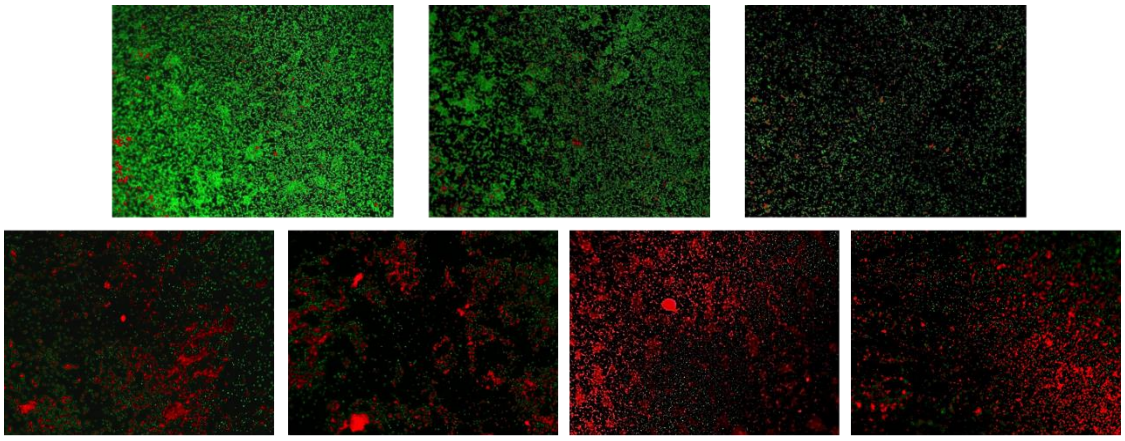

Figure 5.16. Live-dead images of the PEG-coated and the PEG + AMP coated samples. Ti (a), EPEG_5 (b), EPEG_5_4 (c), EPEG5_4_LF1 (d), EPEG5_4_LF2 (e), EPEG5_4_MG1 (f), EPEG5_4_MG2

Bare titanium (Figure 5.16a) is the surface showing the higher bacteria presence, with almost all the bacteria with intact membranes. EPEG5 (Figure 5.16b) and EPEG5_4 (Figure 5.16c) showed a lower presence of bacteria, confirming the results from the bacterial adhesion test. PEG is an antifouling polymer and has no antibacterial effect, thus almost all the bacteria observed in the assay are intact. Even though the samples with AMP had a similar amount of bacteria when compared to the EPEG5_4, the presence of red-stained bacteria reveals the ability of the peptides to disrupt the bacterial membrane. The results obtained in the bacterial adhesion test and the live-dead test show the feasibility of AMP functionalized PEG coatings as a combination of bactericidal and antifouling coatings.

5.4. References

[1] Z. Wang, X. Zhang, J. Gu, H. Yang, J. Nie, G. Ma, *Electrodeposition of alginate/chitosan layer-by-layer composite coatings on titanium substrates*, Carbohydr. Polym. 103 (2014) 38–45. doi:10.1016/j.carbpol.2013.12.007.

[2] J. Wang, B. Li, Z. Li, K. Ren, L. Jin, S. Zhang, *et al.*, *Electropolymerization of dopamine for surface modification of complex-shaped cardiovascular stents*, Biomaterials. 35 (2014) 7679–89. doi:10.1016/j.biomaterials.2014.05.047.

[3] P.K. Thalla, A. Contreras-García, H. Fadlallah, J. Barrette, G. De Crescenzo, Y. Merhi, *et al.*, *A versatile star PEG grafting method for the generation of nonfouling and nonthrombogenic surfaces*, Biomed Res. Int. 2013 (2013) 962376. doi:10.1155/2013/962376.

[4] A. Alexander Papra, Nikolaj Gadegaard, N.B. Larsen, A. Papra, N. Gadegaard, N.B. Larsen, *Characterization of Ultrathin Poly(ethylene glycol) Monolayers on Silicon Substrates*, Langmuir. 17 (2001) 1457–1460. doi:10.1021/la000609d.

[5] Z. Boru, E. Thomas, G. Rico, L. Deborah, *Chain-length dependence of the protein and cell resistance of oligo(ethylene glycol)-terminated self-assembled monolayers on gold*, J. Biomed. Mater. Res. 56 (2001) 406–416.

[6] J. Buxadera-Palomero, C. Canal, S. Torrent-Camarero, B. Garrido, F. Javier Gil, D. Rodríguez, *Antifouling coatings for dental implants: Polyethylene glycol-like coatings on titanium by plasma polymerization*, Biointerphases. 10 (2015) 29505. doi:10.1116/1.4913376.

[7] Y. Tanaka, H. Doi, Y. Iwasaki, S. Hiromoto, T. Yoneyama, K. Asami, *et al.*, *Electrodeposition of amine-terminated poly(ethylene glycol) to titanium surface*, Mater. Sci. Eng. C. 27 (2007) 206–212. doi:10.1016/j.msec.2006.03.007.

[8] S. Sharma, R.W. Johnson, T.A. Desai, *XPS and AFM analysis of antifouling PEG interfaces for microfabricated silicon biosensors*, Biosens. Bioelectron. 20 (2004) 227–39. doi:10.1016/j.bios.2004.01.034.

[9] S. Sofia, V. Premnath, E. Merrill, *Poly(ethylene oxide) Grafted to Silicon Surfaces: Grafting Density and Protein Adsorption*, Macromolecules. 31 (1998) 5059–70. doi:10.1021/ma971016l.

[10] G. Altankov, V. Thom, T. Groth, K. Jankova, G. Jonsson, M. Ulbricht, *Modulating the biocompatibility of polymer surfaces with poly(ethylene glycol): Effect of fibronectin*, J. Biomed. Mater. Res. 52 (2000) 219–230. doi:10.1002/1097-4636(200010)52:1<219::AID-JBM28>3.0.CO;2-F.

[11] P.J.F. Röttgermann, S. Hertrich, I. Berts, M. Albert, F.J. Segerer, J.-F. Moulin, *et al.*, Cell *Motility on Polyethylene Glycol Block Copolymers Correlates to Fibronectin Surface Adsorption*, Macromol. Biosci. 14 (2014) 1755–1763. doi:10.1002/mabi.201400246.

[12] Y. Tanaka, K. Matin, M. Gyo, A. Okada, Y. Tsutsumi, H. Doi, *et al.*, *Effects of electrodeposited poly(ethylene glycol) on biofilm adherence to titanium*, J. Biomed. Mater. Res. A. 95 (2010) 1105–13. doi:10.1002/jbm.a.32932.

[13] S. Gonçalves, A. Leirós, T. van Kooten, F. Dourado, L.R. Rodrigues, *Physicochemical and biological evaluation of poly(ethylene glycol) methacrylate grafted onto poly(dimethyl siloxane) surfaces for prosthetic devices*, Colloids Surfaces B Biointerfaces. 109 (2013) 228–235. doi:10.1016/j.colsurfb.2013.03.050.

[14] A. G. Gristina, *Biomaterial-centered infection: microbial adhesion versus tissue integration*, Science. 237 (1987) 1588–95. doi:10.1126/science.3629258.

[15] B. Zhao, H.C. van der Mei, G. Subbiahdoss, J. de Vries, M. Rustema-Abbing, R. Kuijer, *et al.*, *Soft tissue integration versus early biofilm formation on different dental implant*

materials, Dent. Mater. 30 (2014) 716–27. doi:10.1016/j.dental.2014.04.001.

[16] G.-X. Wei, A.N. Campagna, L.A. Bobek, *Effect of MUC7 peptides on the growth of bacteria and on Streptococcus mutans biofilm*, J. Antimicrob. Chemother. 57 (2006) 1100–1109. doi:10.1093/jac/dkl120.

[17] M. Zasloff, *Magainins, a class of antimicrobial peptides from Xenopus skin: isolation, characterization of two active forms*, and partial cDNA sequence of a precursor, Proc. Natl. Acad. Sci. U. S. A. 84 (1987) 5449–53.

[18] K. Matsuzaki, K. Sugishita, M. Harada, N. Fujii, K. Miyajima, *Interactions of an antimicrobial peptide, magainin 2, with outer and inner membranes of Gram-negative bacteria*, Biochim. Biophys. Acta - Biomembr. 1327 (1997) 119–130. doi:10.1016/S0005-2736(97)00051-5.

[19] Y. Ge, D.L. MacDonald, K.J. Holroyd, C. Thornsberry, H. Wexler, M. Zasloff, *In vitro antibacterial properties of pexiganan, an analog of magainin*, Antimicrob. Agents Chemother. 43 (1999) 782–8.

[20] P.H. Nibbering, E. Ravensbergen, M.M. Welling, L.A. Van Berkel, P.H.C. Van Berkel, E.K.J. Pauwels, *et al.*, *Human lactoferrin and peptides derived from its N terminus are highly effective against infections with antibiotic-resistant bacteria*, Infect. Immun. 69 (2001) 1469–1476. doi:10.1128/IAI.69.3.1469-1476.2001.

6. PEG-LIKE COATINGS ON TITANIUM BY LOW PRESSURE PLASMA POLYMERIZATION

Plasma treatments are a suitable technique for the production of polymeric layers on different substrates, such as polymers [1–3] or stainless steel [4]. Plasma-based methods are solvent-free, allow the treatment of several samples at the same time and are suitable for the treatment of complex geometries. The properties of plasma coatings can be controlled by modifying the parameters of the plasma treatment such as the pressure, plasma power and the type of precursor used, among others [2]. In this chapter the use of low-pressure plasma for the production of PEG-like coatings from two different monomers is described. In the first part, a plasma polymerized tetra(ethylene glycol) dimethyl ether (tetraglyme) coatings is characterized. The second part deals with the use of di(ethylene glycol) dimethyl ether (diglyme) as the plasma polymerization precursor. The coatings obtained with Diglyme are used in the third part as a drug delivery system for an antibiotic (doxycycline).

6.1. Plasma polymerization of tetraglyme

6.1.1. Surface characterization

6.1.1.1. Wettability

Water contact angle of the plasma polymerized samples (Figure 6.1) shows the hydrophilic character of the PEG-like coating, with water contact angles ranging between 10-30º.

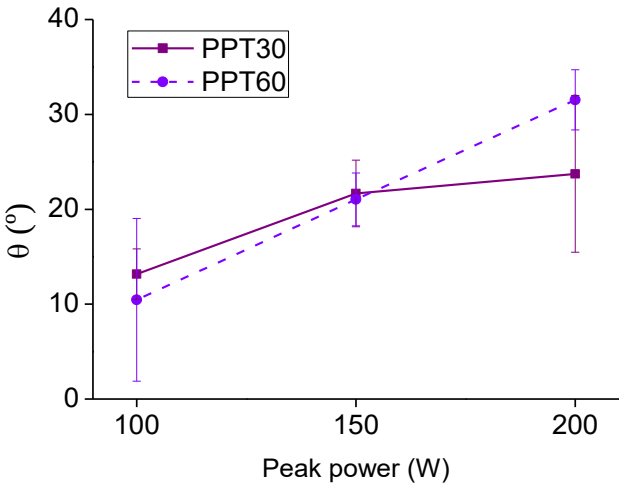

Figure 6.1. Water contact angle of the tetraglyme pulsed plasma coated samples at different plasma peak power.

The values obtained are slightly lower than the range of values found in literature [5–9]. All the coatings have been produced on plasma activated samples without breaking the vacuum for the subsequent low pressure plasma polymerization treatment.

6.1.1.2. Topography

The roughness of the samples by optical interferometry had similar values before and after coating (from a R_a value of 45 ± 5 nm before the polymerization to a value of 46 ± 4 nm). This fact was confirmed by SEM, where no changes on the topography were either observed (Figure 6.2).

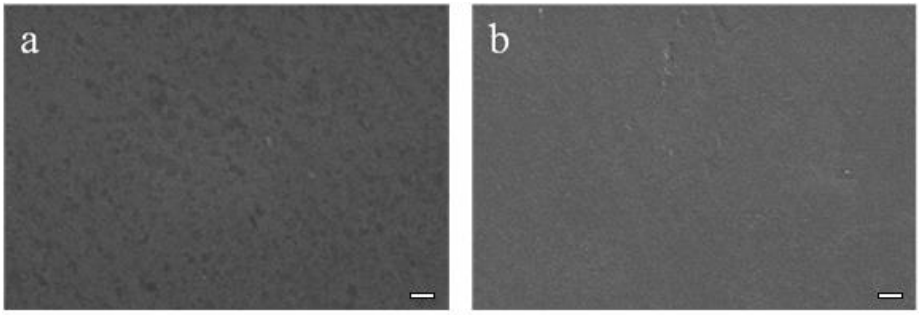

Figure 6.2. SEM image of Ti (a) and PP100_1 (b). Scale bar indicates 2 µm

6.1.1.3. Chemical composition

FTIR spectra of the tetraglyme plasma polymerized coatings (Figure 6.3) show the characteristic peaks for a PEG-like coating obtained by plasma polymerization. For comparison, the spectra of a commercial PEG with M_w=1000 was also recorded.

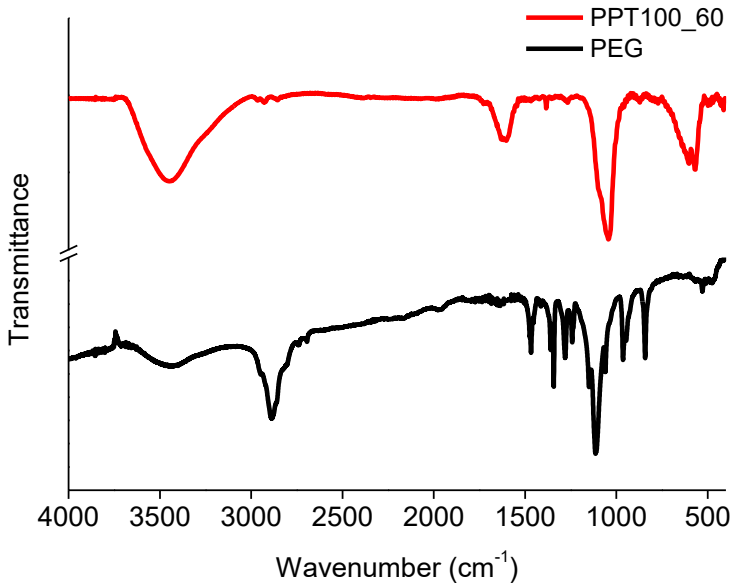

Figure 6.3. FTIR spectra of the plasma polymerized sample at 100W, 1h. Two main peaks can be observed, st(C-O) at 1100cm^{-1} and st(C-H) at 2950cm^{-1}.

For the reference spectra, the characteristic bonds of the polymer can be identified [8,10–12]. PEG presents two kinds of oxygen functionalities, ether groups (C-O-C) and alcohol groups in the terminals of the polymer (C-OH). Other bonds that can be found are C-C and C-H, from the carbon functionalities (Table 6.1). Specifically, the bands above 2900cm^{-1} are associated to C-H stretching bonds from single bonds (CH_2 and CH_3). The presence of bands from 1440 to 1380cm^{-1} account for the C-H bending mode,

and the bands centered at 1100cm^{-1} are associated to the stretching modes of C-O and C-O-C, which are characteristic of PEG.

Table 6.1. Band assignation for the FTIR spectra of the reference PEG and the PEG coating obtained by plasma polymerization

	PEG (ν (cm^{-1}))	PEG coating (ν (cm^{-1}))
C-H in plane bending	842, 961	777, 871
C-O-C stretching	1060, 1113	1039, 1100
C-C stretching	1237, 1282, 1340, 1365	Not observed
C-H stretching	2803, 2888, 2952	2853, 2932, 2971
O-H stretching	3451	3451

Some of the bands are absent or reduced in intensity if compared to the reference PEG. This might be an indication of cross-linking for the plasma polymerized coating, with changes in the C-H bands, through the reduction of the C-H stretching bands and the C-C stretching bands. The cross-linking can also be observed from a shifting on the bands centered at 1100cm^{-1}. It indicates a change on the chemical structure of the plasma polymerized coating when compared with the precursor. FTIR analysis did not allow recording any differences between the different polymerization conditions. The cross-linking is a good tool to decrease the solubility of the plasma polymerized tetraglyme layers [10,13].

The atomic concentration of the elements in the outer surface was recorded by XPS (Table 6.2). When comparing the plasma polymerized tetraglyme samples with the plasma activated ones, an increase of the carbon amount can be observed while the titanium peak decreases. The increase on the C/Ti ratio reflects the formation of a PEG-like coating on the surface, which is further confirmed by the high-resolution decomposition of the carbon peak (Table 6.2). Moreover, longer polymerization times rendered a higher C/Ti ratio, showing a higher yielding of the polymerization.

Table 6.2. Atomic concentration (in atomic%) of carbon, oxygen and titanium obtained by XPS, and C/Ti ratio

% at. Comp.	C 1s	O 1s	Ti 2p	C/Ti
Ti	23.5 ± 1.3	59.0 ± 0.5	17.5 ± 0.8	1.3 ± 0.1
ArPA5_100	15.6 ± 0.4	62.8 ± 1.0	21.6 ± 0.7	0.7 ± 0.0
PP100_30	39.3 ± 13.8	46.9 ± 10.1	13.7 ± 3.6	1.9 ± 0.0
PP100_60	38.9 ± 0.0	51.8 ± 0.7	10.1 ± 0.4	3.8 ± 0.1
PP150_30	48.3 ± 0.8	44.8 ± 0.6	6.9 ± 0.5	6.9 ± 0.2
PP150_60	50.8 ± 0.7	43.9 ± 0.4	5.2 ± 0.7	9.7 ± 0.0
PP200_30	45.5 ± 0.19	46.4 ± 0.1	8.1 ± 0.3	5.6 ± 0.2
PP200_60	53.2 ± 0.5	41.6 ± 0.5	5.1 ± 0.0	10.3 ± 0.0

In the fitting of the C1s peak (Table 6.3), four different peaks can be found. The peaks correspond respectively to hydrocarbon bonds (C-H, C-C) at 284.8 eV, ether

bonds (C-O-C) at 286.5 eV, carboxyl bonds (O-C-O) at 288 eV and carboxylic bonds (O-C=O) at 289 eV. The peak at 286.5 eV is the most characteristic of PEG as it is associated with ether bonds. This peak shows a decrease with increasing power and time of polymerization. The peaks at 288 eV and 289 eV can be related to the fragmentation of the precursor during the polymerization.

Table 6.3. Components (in atomic %) of the C 1s peak according to the carbon environment in the coated samples

	C-H, C-C	C-O-C	O-C-O	O-C=O
Ti	63.95 ± 1.2	16.31 ± 2.1	19.74 ± 0.5	-
ArPA5_100	65.5 ± 2.2	27.63 ± 2.1	7.36 ± 0.8	-
PPT100_30	1.38 ± 1.3	67.20 ± 3.4	20.61 ± 1.7	10.82 ± 3.0
PPT100_60	14.28 ± 1.7	59.03 ± 2.0	11.97 ± 2.8	14.74 ± 3.0
PPT150_30	23.63 ± 11.1	45.74 ± 3.1	25.02 ± 12.7	5.62 ± 1.6
PPT150_60	18.37 ± 1.7	41.28 ± 1.1	32.46 ± 2.2	7.89 ± 0.6
PPT200_30	13.63 ± 0.1	47.97 ± 2.4	32.40 ± 2.7	6.01 ± 0.4
PPT200_60	20.97 ± 8.3	43.61 ± 0.4	28.88 ± 7.7	6.55 ± 1.1

XPS results (Table 6.2) show an increase in the carbon amount due to the deposition of the PEG-like coating on the surface [14,15]. This is a consequence of attenuation of the substrate photoelectrons by the polymeric coating [16]. The C/Ti ratio is therefore a good indicator of the thickness of the coating [17], therefore a higher amount of PEG-like coating can be detected for the samples polymerized at 150W and 200W (PPT150_60 and PPT200_60). A higher amount of PEG can be observed at constant power for the samples polymerized at 1h. However, it should be taken into account that this results are an approximation, since the presence of adventitious contamination might be slightly different among the samples.

From the XPS results, it can be concluded that the higher the power and time of polymerization, the thicker the coating obtained. The results of the ratio C/Ti were further contrasted with the approximation of the thickness by the attenuation of the substrate signal (Figure 6.4). According to these results, the thickest coatings were produced at 150W and 1h (PP150_60).

Comparing the fitted XPS spectra of C 1s of the parameters used in the process (Figure 6.5), it can be observed that the main peak in the Ti samples and the plasma activated samples is the C-H peak at 285 eV, while in the plasma polymerized samples the main peak is the C-O peak at 286.5 eV. Due to the PEG chemical structure, the carbon peak can be fitted in four peaks, each for every different chemical environments found in a PEG-like coating, i.e, hydrocarbons (C-C or C-H), ether (C-O-C), carbonyl groups (C=O) and carboxylic groups (O-C=O).

PEG has a XPS spectrum with one peak at 286.5 eV, which shows the presence of ether bonding and of another peak at 285 eV, corresponding to the C-C bonds [18]. Thus, the ether peak is indicative of the PEG character of the coating and its decrease can be related to the fragmentation process during the plasma polymerization as a

consequence of the formation of more oxidized functional groups. The coatings with the higher ether peak are the ones obtained at 100W (PPT100_30 and PPT100_60), and they show the lower fragmentation of the precursor at lower plasma power [2,19,20].

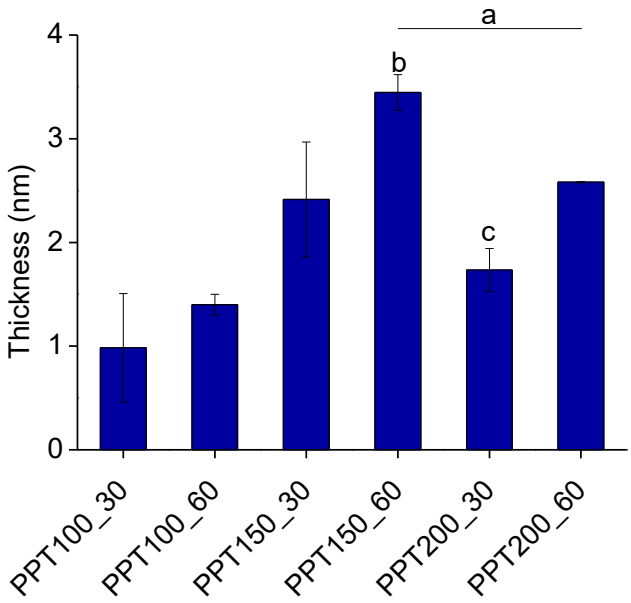

Figure 6.4. Thickness of the coatings as calculated by the attenuation of the Ti2p signal from the substrate. *a* indicates statistically significant differences compared to PPT100_30, *b* indicates statistically significant differences compared to PPT100_60 and *c* indicates statistically significant differences compared to PPT150_60 ($p<0.05$)

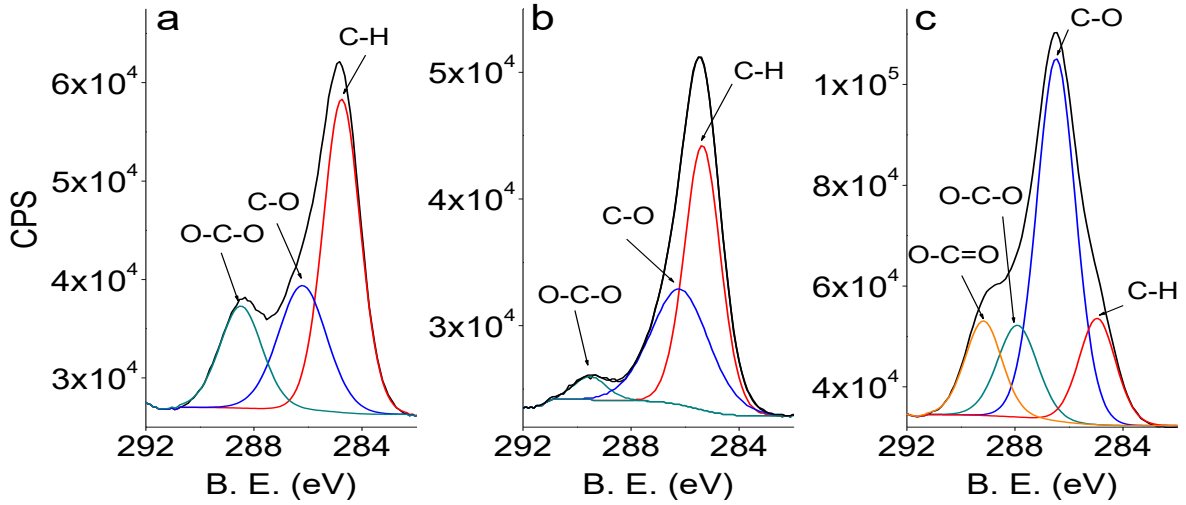

Figure 6.5. High resolution C 1s XPS spectra for the Ti (a), ArPA100_5 (b) and PP100_60 (c). The bonds corresponding to the carbon fitted peaks are indicated in the figure

6.1.2. Biological characterization

The biological performance of the samples was evaluated regarding their cytotoxicity, antifouling properties against protein and bacteria, as well as regarding their interactions with cells relevant to the dental tissue.

6.1.2.1. Cytotoxicity

After immersing the samples in cell medium and exposing the cells to such medium, cell viability showed no decrease at any dilution when tested with fibroblasts and osteoblasts (Figure 6.6). All the studied surfaces and the plasma polymerization conditions have cell viability ratios over 80%, showing the good biocompatibility of the coatings.

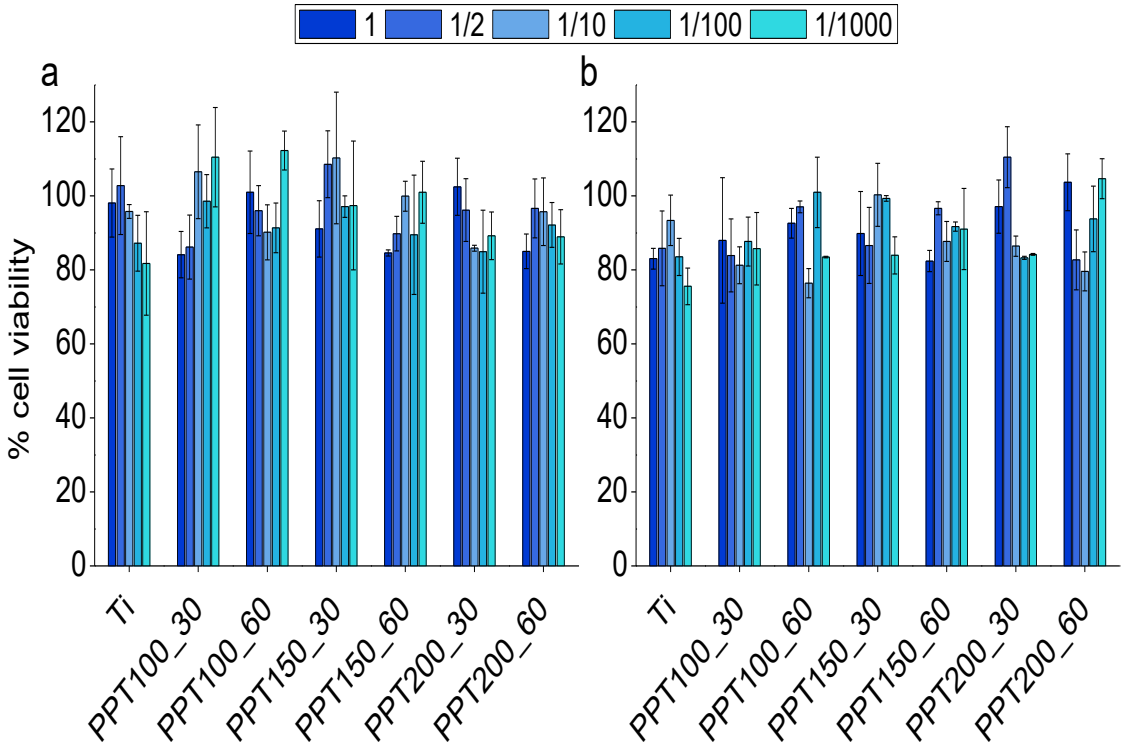

Figure 6.6. Cell viability of the hFFs (a) and the SAOS-2 (b) in contact with the eluents from the plasma polymerized samples

6.1.2.1. Cell adhesion

Cell adhesion assays with hFFs (Figure 8(a)) showed no difference between Ti and PP samples, while for SAOS-2 (Figure 8(b)) a slight decrease was measured. In terms of cell morphology (Figure 9), no differences were observed in any of the cell lines studied.

The biocompatibility of the coating was studied with cytotoxicity assays and cell adhesion assays. The lixiviates eluted by the plasma polymerized coatings obtained at the studied conditions did not show any toxicity (Figure 6.6), as the cell viability overcomes the 80% in all cases, and most generally over 90%. In terms of the fibroblast adhesion, no statistically significant differences were observed between the tetraglyme plasma polymerized samples and the Ti. No differences were observed either in the cell morphology observed by SEM images (Figure 5.10). Although this result could seem surprising, the parameters used for the plasma polymerization can lead to these results because the use of higher plasma power can lead to surfaces with a good cell adhesion [2,30,31]. Considering the application of the PEG-like coating on titanium for dental

implants, this kind of coatings could lead to a biocompatible and integrated implant with a lower incidence of infections.

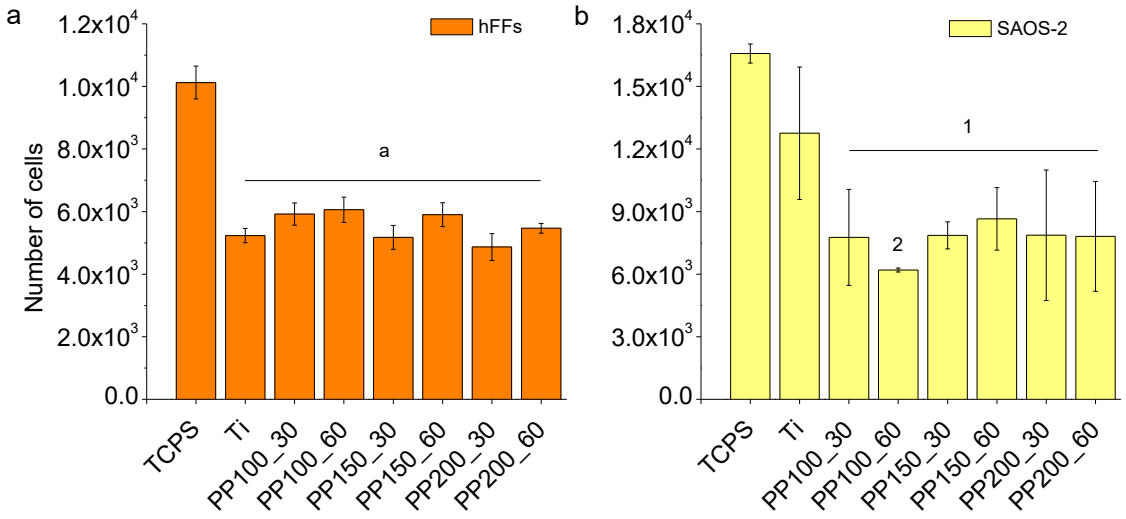

Figure 6.7 Cell adhesion of hFFs (a) and SAOS-2 (b) on the Ti and PP samples. For hFFs assay, *a* indicates statistically significant differences compared to TCPS. For SAOS-2 assay, *1* indicates statistically significant differences compared to TCPS and *2* compared to Ti ($p<0.05$)

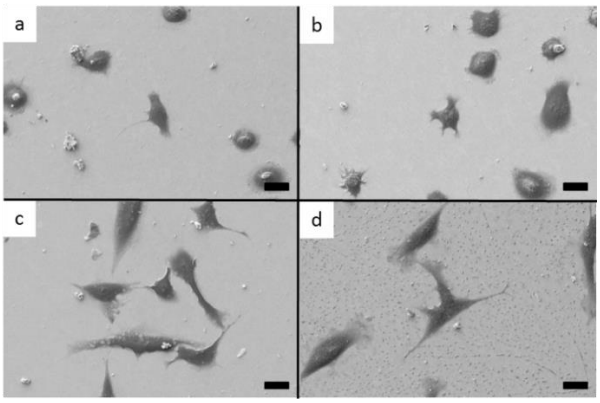

Figure 6.8. SEM images of the cell adhesion on the Ti and a PP sample. (a) SAOS-2 on Ti, (b) SAOS-2 on PPT100_60, (c) hFFs on Ti, (d) hFFs on PPT100_60. Scale bar indicates 20 µm

6.1.2.2. Protein adsorption

Protein adsorption with BSA was tested in fluorescence assays (Figure 6.9). Fluorescence intensity is an indicator of the protein presence, as FTIC molecules are bonded to the BSA. While plasma polymerization treatments of 30 min at any of the process powers evaluated showed similar protein adsorption than the untreated titanium, the plasma polymerization conditions of 1h of treatment showed lower protein adsorption than control titanium (PP100_60, PP150_60 and PP200_60). The result is interesting because avoiding unspecific protein adsorption leads to a better control of the implant integration.

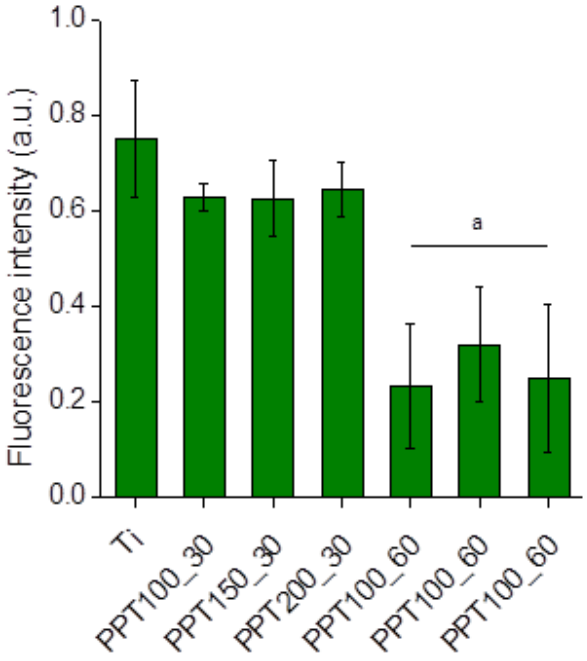

Figure 6.9. Fluorescence intensity detected for the different samples after being in contact with FITC-BSA. *a* indicates statistically significant differences compared to Ti, PPT100_30, PPT150_30 and PPT200_30 ($p<0.05$).

6.1.2.3. Bacterial adhesion

Bacterial adhesion assays showed a decreased bacterial adhesion for all PP samples both for the *S. sanguinis* (Figure 6.10a) and the *L. salivarius* (Figure 6.10b). Ti samples and plasma activated samples ArPA100_5 were used as controls. An increased bacterial adhesion was observed for the PA sample compared to Ti.

Several authors reported an increased bacterial adhesion on the hydrophobic surfaces [21,22]. However, the correlation between the wettability and the bacterial adhesion was not found in other studies [23,24]. The increase in bacterial adhesion may be related to the change on the surface charge when activating the sample with plasma. Plasma activation has been related to the formation of hydroxyl groups on the surfaces [25–27].

According to the results of McDonald *et al.* [28], the surface charge of a plasma activated titanium was positive at acidic pH (pH=3-5) and negative at higher values of pH. This change on the surface charge may be explained by the protonation and deprotonation of the hydroxyl groups. Another factor influencing the bacterial adhesion is the presence of a conditioning layer of proteins. Mackintosh *et al*. [29] reported an increased bacterial adhesion on charged surfaces with the presence of proteins.

Regarding the bacterial adhesion on the plasma polymerized tetraglyme samples, no trend was found for the different parameters of time and power of the plasma treatment. *S. sanguinis* adhesion was lower on the samples prepared at 100W

(PPT100_30 and PPT100_60) and at 150W (PPT150_30 and PPT150_60). However, for *L. salivarius*, the adhesion of the sample prepared at 150W during 1h was higher.

This, in conjunction with the lower BSA adsorption, is a very interesting result indicating an antifouling performance of the obtained coatings [30,31]. The surfaces processed at lower plasma power had better performance in terms of bacterial adhesion. These results are, in agreement with the XPS results, showing that a higher ether character (peak at 286.5eV). Thus, more PP-PEG produces a coating with less bacterial adhesion [19,32–35].

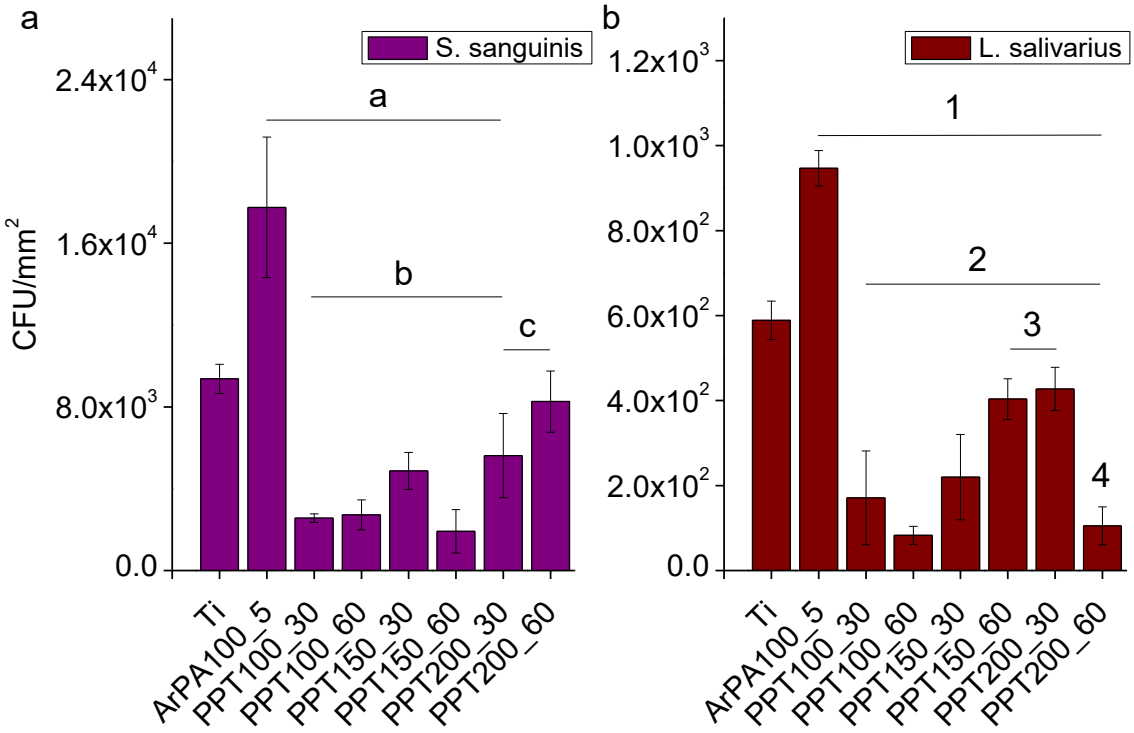

Figure 6.10. Bacterial adhesion on Ti, PA and PP samples of *S. sanguinis* (a) and *L. salivarius b* (b). For *S. sanguinis* assay, *a* indicates statistically significant differences compared to Ti, compared to ArPA100_5 and *c* compared to PPT100_30, PPT100_60 and PPT150_60. For *L. salivarius* assay, *1* indicates statistically significant differences compared to Ti, *2* compared to ArPA100_5, *3* compared to PPT100_60 and *4* compared to PPT150_60 and PPT200_30 ($p<0.05$)

Among the different plasma coatings produced on Ti, the ones produced at lower powers (100W and 150W) and longer times (1h) rendered a higher monomer retention in terms of the ether peak in XPS, a lower protein adsorption and lower bacterial adhesion. The thickness of the coating was higher for the samples prepared at 150W.

6.2. Diglyme plasma polymerization

6.2.1. Surface characterization

Diglyme plasma polymerization has been studied in terms of single and multiple steps treatments. With this aim, the samples have been polymerized during 1 h at 150 W using one step (PPD150_60), two steps (PPD150_2x30) and three steps (PPD150_3x20). Surface characterization of the diglyme plasma polymerized samples

has been done in terms of the wettability, chemical composition, thickness and degradation of the coating in simulated physiological conditions.

6.2.1.1. Water contact angle

Water contact angle (Figure 6.11) of the plasma polymerized samples employing diglyme as a precursor is slightly higher than the one of titanium, and much higher than the plasma activated sample that was used as a substrate for the deposition, indicating the presence of a coating on the surface.

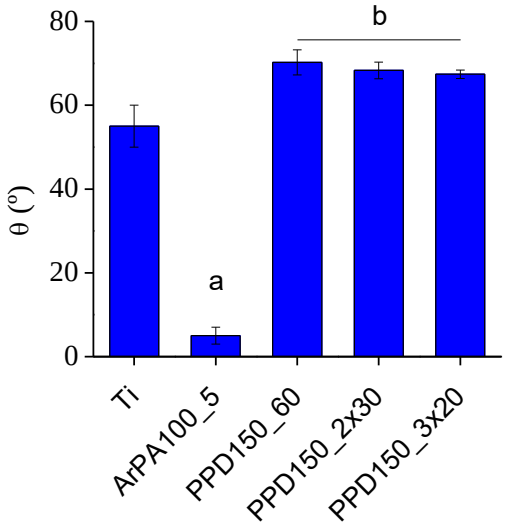

Figure 6.11. Water contact angle of the diglyme plasma polymerized samples. *a* indicates statistically significant differences compared to Ti and *b* indicates statistically significant differences compared to ArPA100_5 ($p<0.05$).

The water contact angles reported are slightly higher (around 10º higher) than the ones reported in the literature. On the one hand, Azevedo *et al.* [36] studied the plasma polymerization of diglyme at different pressures (ranging from 0.15 to 60 mbar) and reported a decrease on the water contact angle from 50º to 30º. On the other hand, Brétagnol *et al.* [37] studied the properties of diglyme plasma polymerized coatings, and found that that the wettability of the coatings obtained in continuous mode is lower than the wettability obtained for the pulsed discharges, changing from the value of 60º in continuous to 48º in pulsed mode. The following sections are aimed at elucidate the chemical composition of the coatings on order to explain such differences.

6.2.1.2. Chemical composition

ATR-FTIR spectra (Figure 6.12) showed the presence of some of the main peaks of PEG, as summarized in Table 6.1.

The peaks associated to the stretching and bending modes of the C-H bond are also present. The peak associated to the alcohol band is not detected in the plasma polymerized sample. This results are in accordance to the previously found in previous studies for the plasma polymerization of PEG precursors [36,38], as detailed in section 6.1.1.3.

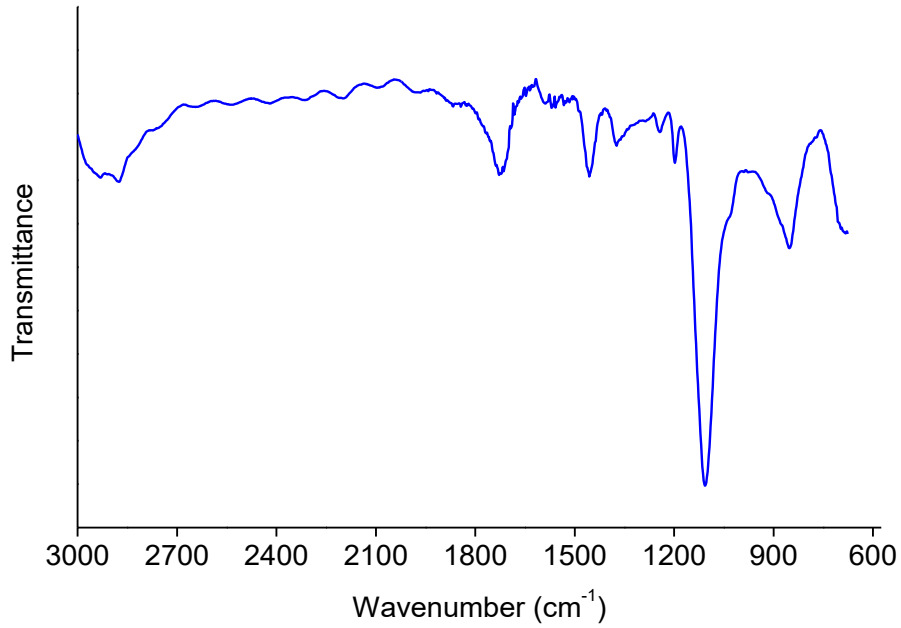

Figure 6.12. ATR-FTIR of Ti_PP_D_60, showing the characteristic peaks of a PEG-like coating

Table 6.4. Peak assignation of PPD150_60 compared to the transmission spectra of PEG with M_w=1000

	PEG (ν (cm^{-1}))	PPD150_60 (ν (cm^{-1}))
C-H in plane bending	842, 961	850
C-O-C stretching	1060, 1113	1059, 1121
C-C stretching	1237, 1282, 1340, 1365	1235, 1282, 1340
C-H stretching	2803, 2888, 2952	2809, 2884, 2954
O-H stretching	3451	Not observed

XPS analysis of the diglyme plasma polymerized samples (*Table 6.5*) showed the presence of three elements: carbon, oxygen and titanium. The presence of carbon is increased with the presence of the polymeric coating. In turn, the titanium from the substrate is undetectable for the coated samples. This means that the signal from the substrate is completely attenuated by the coating and hence, the coating is thicker than 10nm. No differences between the different plasma polymerization treatments were observed in terms of the chemical composition of the outer part of the coating. When comparing the carbon and oxygen amount with the theoretical one, it can be seen that the O/C ratio is higher than expected according to the theoretical value of diglyme.

Table 6.5. XPS atomic % of the Diglyme plasma polymerized samples

	C1s	O1s	Ti2p	O/C
Ti	9.3 ± 1.5	51.0 ± 0.7	39.7 ± 0.8	
Diglyme (theoretical)	66.7	33.3	-	0.5
PPD150_60	42.2 ± 0.0	57.6 ± 0.1	0.2 ± 0.0	1.36
PPD150_2x30	41.9 ± 0.1	57.8 ± 0.1	0.2 ± 0.0	1.37
PPD150_3x20'	42.4 ± 0.2	57.4 ± 0.3	0.2 ± 0.0	1.35

In this case, the thickness of the coating cannot be calculated from the attenuation of the substrate signal, a cross-section of the coating was done by FIB for the plasma polymerized coating in one step (PPD150_60). An approximate thickness of 30nm was measured by this technique (Figure 6.13).

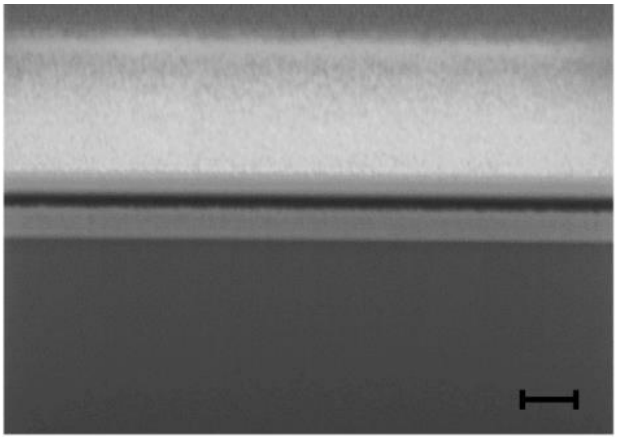

Figure 6.13. FIB Cross-section of PPD150_60. Scale bar indicates 200nm

This thickness is higher than the one obtained for the tetraglyme plasma polymerized coatings. This could be attributed to the difference on the vapor pressure of the two precursors. The difference on the physical properties of the precursor leads to a higher concentration of precursor on the plasma phase for the diglyme. The thicker coating obtained with this monomer might be suitable for use as a barrier for drug delivery systems. The thickness of the coating is comparable to the thickness of diglyme coatings obtained in the continuous mode by other authors [39].

C1s fitting (Table 6.6) presents 4 different peaks at 284.8eV (hydrocarbon bonds), 286.5eV (ether or alcohol), 287.5eV (aldehydes and ketones) and at 288.8eV (carboxylates).

Table 6.6. Atomic % of the C1s components for the diglyme plasma polymerized samples

Binding Energy (eV)	284.8	286.5	287.5	288.8
PPD150_60	25.6 ±1.2	66.2 ± 1.3	5.4 ± 0.1	2.8 ± 0.1
PPD150_2x30	23.6 ± 1.4	65.3 ± 4.1	7.6 ± 1.4	3.6 ± 1.4
PPD150_3x20	28.4 ± 1.0	62.5 ± 0.2	5.6 ± 0.5	3.6 ± 0.3

The most predominant peak is the one at 286.5eV corresponding to the ether peak, which is the characteristic peak for PEG. The presence of a significant peak in the region of hydrocarbon species might be explained by the use of continuous plasma, which could induce a higher degree of fragmentation [14].

The stability of the coatings was tested by immersion in PBS for 72h at 37ºC. No significant changes were detected on the XPS spectra of the samples (Figure 6.14). This fact reveals that the coatings are still present and do not present significant modifications on the chemical composition of the outer surface. No delamination of the coating was observed after immersion.

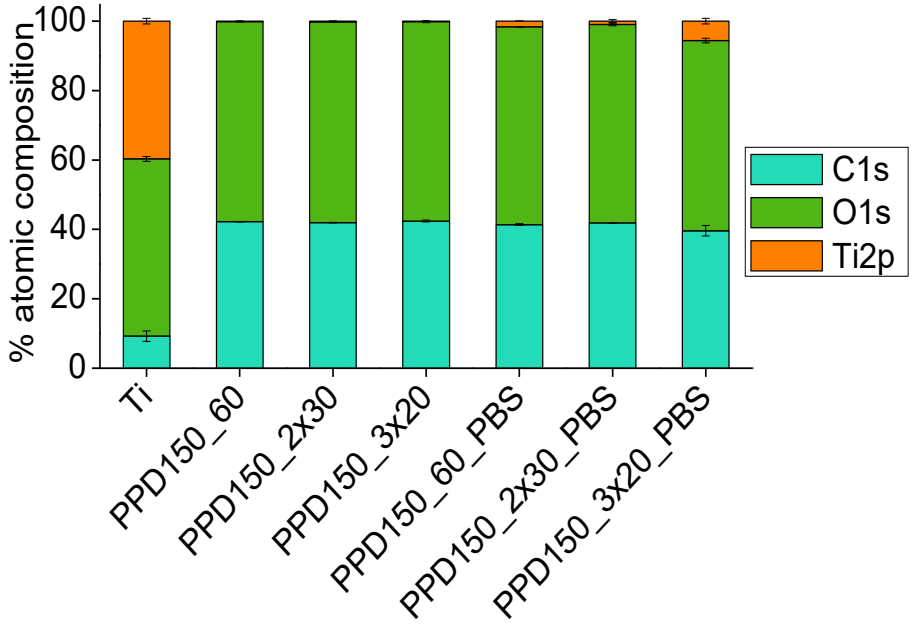

Figure 6.14. XPS atomic percentage of the diglyme plasma polymerized samples before and after immersion in PBS

6.2.2. Biological characterization

The biological performance of the diglyme plasma polymerized samples was tested by means of the cytotoxicity and cell adhesion in order to assess the biocompatibility and the bacterial adhesion of *S. aureus* in order to assess the antifouling properties of the coating in presence of a clinically relevant bacterial strain.

6.2.2.1. Cytotoxicity

No toxic effects of the eluents from the diglyme plasma polymerized coatings were observed, since the cell viability was higher than 80% in all cases (Figure 6.15). This fact indicates that no toxic substances are eluted from the samples, or that the concentration of the possible toxic substances is below the toxicity range.

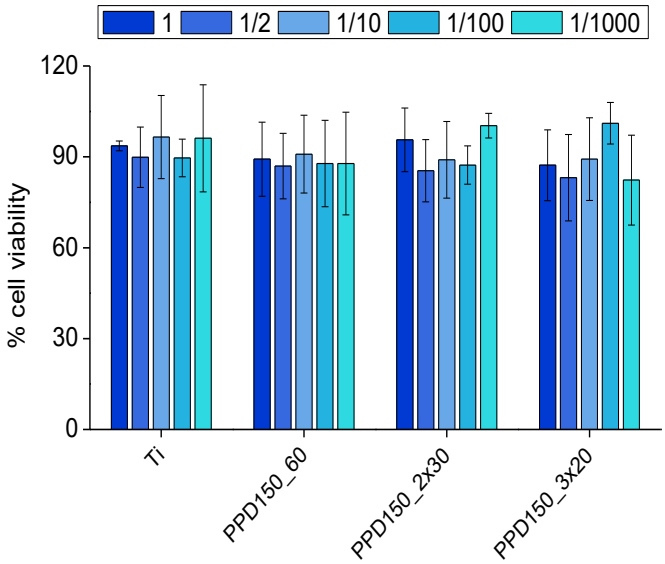

Figure 6.15. Indirect cytotoxicity of the diglyme plasma polymerized samples

6.2.2.2. Cell adhesion

Regarding the fibroblast adhesion on the diglyme plasma polymerized samples (Figure 6.16), no differences were found between the untreated titanium and the coated samples with any of the studied conditions, which was also observed with our coatings produced with tetraglyme (section 6.1.2.1). This results are opposite to the ones reported in previous studies with PEG coatings [40].

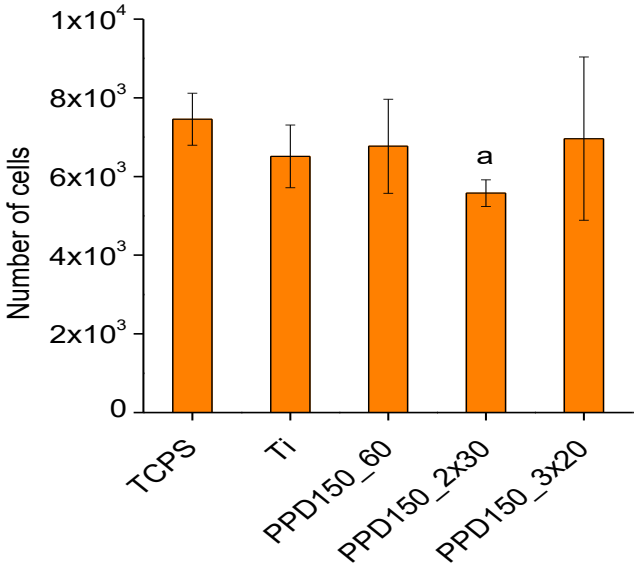

Figure 6.16. hFFs adhesion on diglyme plasma polymerized samples. *a* indicates statistically significant differences compared to TCPS ($p<0.05$)

6.2.2.3. Bacterial adhesion

The adhesion of *S. aureus* on the PEG-like coated samples using diglyme as a precursor (Figure 6.17) revealed a substantial decrease on the bacterial adhesion for all the studied conditions, showing the antifouling character of all the samples.

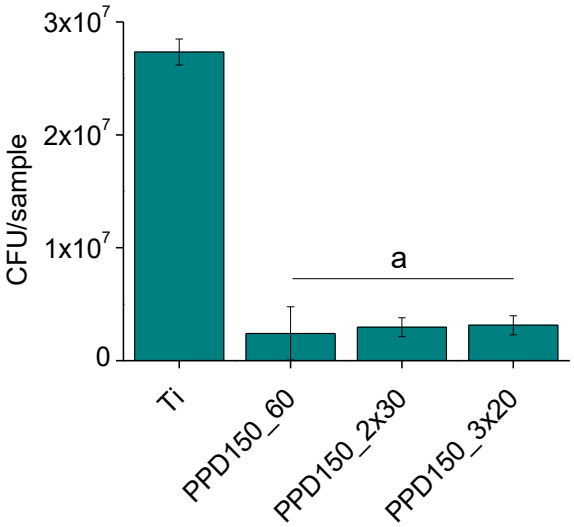

Figure 6.17. *S. aureus* adhesion on diglyme plasma polymerized samples. *a* indicates statistically significant differences compared to Ti ($p<0.05$)

Even though no significant differences were observed between the studied conditions, it seems that the treatments by steps (PPD150_2x30 and PPD150_3x20) tends to have a higher adhesion than the one step treatment (PPD150_1h).

6.3. Drug release from diglyme plasma polymerized coatings

The drug release studies have been performed with doxycycline, which was adsorbed on the titanium surface before applying the plasma polymerization treatment (section 2.4.1). Doxycycline is a tetracycline antibiotic used in dentistry to treat peri-implantitis, because of their efficacy against periodontopathic bacteria and their low cellular damage on the host cells [Suzuki 2006]. It has been also reported the beneficial effects of doxycycline regarding the bone regeneration, which can also enhance the treatment and prevention of peri-implantitis [Pastorino 2014]. A drug release study by UV-Vis have been performed in order to assess the influence of the plasma polymerized diglyme coating. Moreover, a growth curve and an agar diffusion test was carried out to check the antibacterial activity of the antibiotic after the plasma treatment.

6.3.1. Drug release studies

Drug release (Figure 6.18) was checked with the double well test as described in section (2.7.3.4). The release from the titanium sample without the polymer coating takes place immediately after soaking the sample in liquid, while for the coated samples the release is slowed down, limiting the extent of the burst release, reaching the 100% of the initial concentration of antibiotic after 16h. No differences were observed when comparing the different plasma treatments.

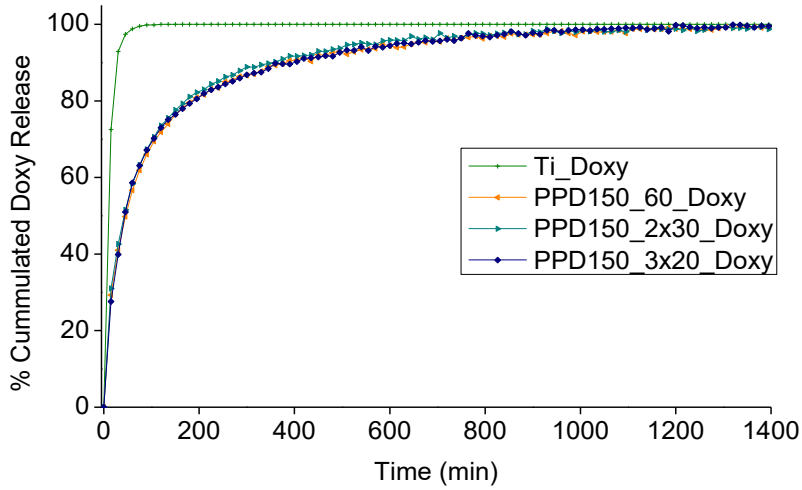

Figure 6.18. Doxycycline release from titanium and diglyme plasma polymerized titanium

6.3.2. Growth curve

Bacteria growth curve was analyzed in the same experiment set-up than the drug release assay (Figure 6.19). As expected, the plasma polymerized sample without doxycycline (PPD150_60) presented no effect on the bacterial growth, while the samples with antibiotic (PPD150_60_Doxy, PPD150_2x30_Doxy and PPD150_3x20)

completely inhibits the growth of the bacteria. This assay also showed that the activity of the antibiotic is not significantly affected by the plasma process.

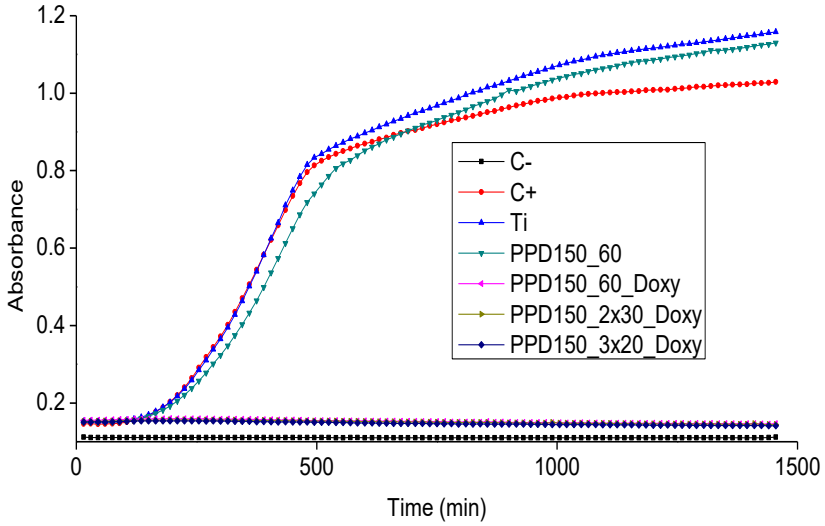

Figure 6.19. Growth curve of a suspension of *S. aureus* in contact with plasma polymerized samples without and with doxycycline

6.3.3. Agar diffusion test

In order to complete the study of the antibacterial effect of the released antibiotic, an agar diffusion test was performed with the coated samples with doxycycline (Figure 6.19). All the samples presented an inhibition zone, showing the antibacterial effect of the released antibiotic.

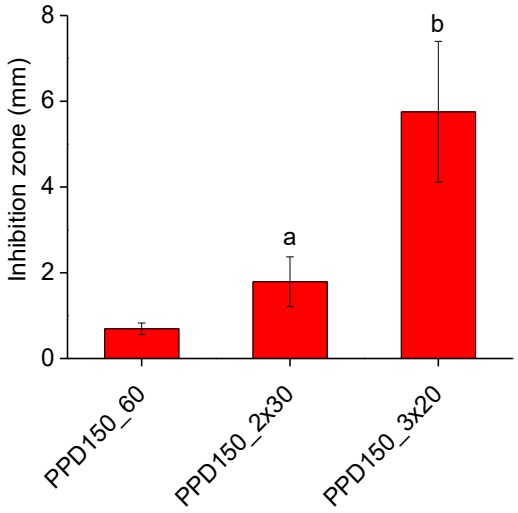

Figure 6.20. Agar diffusion test with plasma polymerized titanium loaded with doxycycline. *a* indicates significantly differences compared to PPD150_60 and b compared to PPD150_2x30 ($p<0.05$)

6.3.4. Bacterial adhesion

In order to test the potentially synergic effect of the antifouling effect with the drug release of the antibiotic, *S. aureus* adhesion was tested on the samples with and without the antibiotic (Figure 6.21).

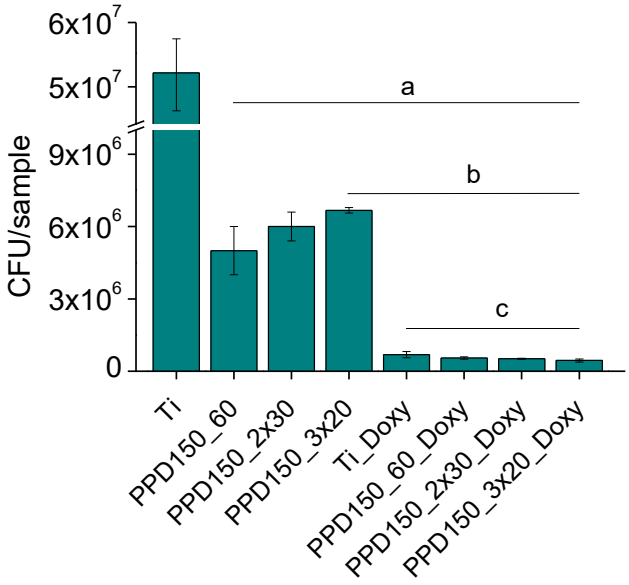

Figure 6.21. *S. aureus* adhesion on the samples with and without doxycycline. *a* indicates statististically significant differences compared to Ti, *b* compared to PPD150_60 and *c* compared to PPD150_2x30 and PPD150_3x20 ($p<0.05$)

A reduction of the bacterial adhesion was observed for all the coated samples. It can be observed that the reduction of the bacterial adhesion is higher for the samples containing the antibiotic, with a similar number of adhered bacteria on the samples non-treated with plasma (Ti_Doxy) and the samples coated with plasma.

6.4. References

[1] D. Beyer, W. Knoll, H. Ringsdorf, J.H. Wang, R.B. Timmons, P. Sluka, *Reduced protein adsorption on plastics via direct plasma deposition of triethylene glycol monoallyl ether*, J. Biomed. Mater. Res. 36 (1997) 181–9.

[2] F. Brétagnol, M. Lejeune, A. Papadopoulou-Bouraoui, M. Hasiwa, H. Rauscher, G. Ceccone, *et al.*, *Fouling and non-fouling surfaces produced by plasma polymerization of ethylene oxide monomer*, Acta Biomater. 2 (2006) 165–72. doi:10.1016/j.actbio.2005.11.002.

[3] C. Labay, J.M. Canal, M. Modic, U. Cvelbar, M. Quiles, M. Armengol, *et al.*, *Antibiotic-loaded polypropylene surgical meshes with suitable biological behaviour by plasma functionalization and polymerization*, Biomaterials. 71 (2015) 132–44. doi:10.1016/j.biomaterials.2015.08.023.

[4] A.R. Denes, E.B. Somers, a. C.L. Wong, F. Denes, *12-Crown-4-Ether and Tri(Ethylene Glycol) Dimethyl-Ether Plasma-Coated Stainless Steel Surfaces and Their Ability To Reduce Bacterial Biofilm Deposition*, J. Appl. Polym. Sci. 81 (2001) 3425–3438. doi:10.1002/app.1799.

[5] G.M. Harbers, K. Emoto, C. Greef, S.W. Metzger, H.N. Woodward, J.J. Mascali, *et al.*, *A functionalized poly(ethylene glycol)-based bioassay surface chemistry that facilitates bio-immobilization and inhibits non-specific protein, bacterial, and mammalian cell adhesion*, Chem. Mater. 19 (2007) 4405–4414. doi:10.1021/cm070509u.

[6] R. Schlapak, P. Pammer, D. Armitage, R. Zhu, P. Hinterdorfer, M. Vaupel, *et al.*, *Glass surfaces grafted with high-density poly(ethylene glycol) as substrates for DNA oligonucleotide microarrays*, Langmuir. 22 (2006) 277–85. doi:10.1021/la0521793.

[7] S.R. Kane, P.D. Ashby, L.A. Pruitt, *Microscale wear behavior and crosslinking of PEG-like coatings for total hip replacements*, J. Mater. Sci. Mater. Med. 21 (2010) 1037–45. doi:10.1007/s10856-009-3935-6.

[8] E.E. Johnston, J.D. Bryers, B.D. Ratner, *Plasma deposition and surface characterization of oligoglyme, dioxane, and crown ether nonfouling films*, Langmuir. 21 (2005) 870–881. doi:10.1021/la036274s.

[9] F. Rupp, L. Scheideler, N. Olshanska, M. de Wild, M. Wieland, J. Geis-Gerstorfer, *Enhancing surface free energy and hydrophilicity through chemical modification of microstructured titanium implant surfaces*, J. Biomed. Mater. Res. A. 76 (2006) 323–34. doi:10.1002/jbm.a.30518.

[10] D. Sakthi Kumar, M. Fujioka, K. Asano, A. Shoji, A. Jayakrishnan, Y. Yoshida, *Surface modification of poly(ethylene terephthalate) by plasma polymerization of poly(ethylene glycol)*, J. Mater. Sci. Mater. Med. 18 (2007) 1831–5. doi:10.1007/s10856-007-3033-6.

[11] G. Wells, *Understanding the synthesis of ethylene glycol pulsed plasma discharges*, Plasma Process. 10 (2013) 119–135. doi:10.1002/ppap.201200066.

[12] Y.J. Wu, R.B. Timmons, J.S. Jen, F.E. Molock, *Non-fouling surfaces produced by gas phase pulsed plasma polymerization of an ultra low molecular weight ethylene oxide containing monomer*, Colloids Surfaces B Biointerfaces. 18 (2000) 235–248. doi:10.1016/S0927-7765(99)00150-2.

[13] S. Mutlu, D. Çökeliler, M. Mutlu, *Modification of food contacting surfaces by plasma polymerization technique. Part II: Static and dynamic adsorption behavior of a model protein "bovine serum albumin" on stainless steel surface*, J. Food Eng. 78 (2007) 494–499. doi:10.1016/j.jfoodeng.2005.10.028.

[14] Y. Li, B.W. Muir, C.D. Easton, L. Thomsen, D.R. Nisbet, J.S. Forsythe, *A study of the initial film growth of PEG-like plasma polymer films via XPS and NEXAFS*, Appl. Surf. Sci. 288 (2014) 288–294. doi:10.1016/j.apsusc.2013.10.022.

[15] A. Michelmore, P. Gross-Kosche, S.A. Al-Bataineh, J.D. Whittle, R.D. Short, *On the effect of monomer chemistry on growth mechanisms of nonfouling PEG-like plasma polymers*, Langmuir. 29 (2013) 2595–601. doi:10.1021/la304713b.

[16] R. Michel, S. Pasche, M. Textor, D.G. Castner, *Influence of PEG architecture on protein adsorption and conformation*, Langmuir. 21 (2005) 12327–32. doi:10.1021/la051726h.

[17] P.J. Cumpson, *The Thickogram: a method for easy film thickness measurement in XPS*, Surf. Interface Anal. 29 (2000) 403–406. doi:10.1002/1096-9918(200006)29:6<403::AID-SIA884>3.0.CO;2-8.

[18] M. Manso, A. Valsesia, M. Lejeune, D. Gilliland, G. Ceccone, F. Rossi, *Tailoring surface properties of biomedical polymers by implantation of Ar and He ions*, Acta Biomater. 1 (2005) 431–40. doi:10.1016/j.actbio.2005.03.003.

[19] A. Roosjen, H.J. Kaper, H.C. van der Mei, W. Norde, H.J. Busscher, *Inhibition of adhesion of yeasts and bacteria by poly(ethylene oxide)-brushes on glass in a parallel plate flow chambe*r, Microbiology. 149 (2003) 3239–46.

[20] V. Zoulalian, S. Zürcher, S. Tosatti, M. Textor, S. Monge, J.-J. Robin, *Self-assembly of poly(ethylene glycol)-poly(alkyl phosphonate) terpolymers on titanium oxide surfaces: synthesis, interface characterization, investigation of nonfouling properties, and long-term stability*, Langmuir. 26 (2010) 74–82. doi:10.1021/la902110j.

[21] E. Sinde, J. Carballo, *Attachment of Salmonella spp. and Listeria monocytogenes to stainless steel, rubber and polytetrafluorethylene: the influence of free energy and the effect of commercial sanitizers*, Food Microbiol. 17 (2000) 439–447. doi:10.1006/fmic.2000.0339.

[22] A.E. Zeraik, M. Nitschke, *Influence of growth media and temperature on bacterial adhesion to polystyrene surfaces*, Brazilian Arch. Biol. Technol. 55 (2012) 569–576. doi:10.1590/S1516-89132012000400012.

[23] M.S. Chae, H. Schraft, L. Truelstrup Hansen, R. Mackereth, *Effects of physicochemical surface characteristics of Listeria monocytogenes strains on attachment to glass*, Food Microbiol. 23 (2006) 250–259. doi:10.1016/j.fm.2005.04.004.

[24] J. Li, L.. McLandsborough, *The effects of the surface charge and hydrophobicity of Escherichia coli on its adhesion to beef muscle*, Int. J. Food Microbiol. 53 (1999) 185–193. doi:10.1016/S0168-1605(99)00159-2.

[25] Y.J. Kim, I.-K. Kang, M.W. Huh, S.-C. Yoon, *Surface characterization and in vitro blood compatibility of poly(ethylene terephthalate) immobilized with insulin and/or heparin using plasma glow discharge*, Biomaterials. 21 (2000) 121–130. doi:10.1016/S0142-9612(99)00137-4.

[26] N. Özden, H. Ayhan, S. Erkut, G. Can, E. Piskin, *Coating of silicone-based impression materials in a glow-discharge system by acrylic acid plasma*, Dent. Mater. 13 (1997) 174–178. doi:10.1016/S0109-5641(97)80120-0.

[27] T.G. Vargo, E.J. Bekos, Y.S. Kim, J.P. Ranieri, R. Bellamkonda, P. Aebischer, *et al.*, *Synthesis and characterization of fluoropolymeric substrata with immobilized minimal peptide sequences for cell adhesion studies*. I, J. Biomed. Mater. Res. 29 (1995) 767–778. doi:10.1002/jbm.820290613.

[28] D.E. MacDonald, B.E. Rapuano, H.C. Schniepp, *Surface oxide net charge of a titanium alloy: Comparison between effects of treatment with heat or radiofrequency plasma glow discharge*, Colloids Surfaces B Biointerfaces. 82 (2011) 173–181. doi:10.1016/j.colsurfb.2010.08.031.

[29] E.E. MacKintosh, J.D. Patel, R.E. Marchant, J.M. Anderson, *Effects of biomaterial surface chemistry on the adhesion and biofilm formation of Staphylococcus epidermidis in vitro*, J. Biomed. Mater. Res. Part A. 78A (2006) 836–842. doi:10.1002/jbm.a.30905.

[30] G. Da Ponte, E. Sardella, F. Fanelli, A. Van Hoeck, R. d'Agostino, S. Paulussen, *et al.*,

Atmospheric pressure plasma deposition of organic films of biomedical interest, Surf. Coatings Technol. 205 (2011) S525–S528. doi:10.1016/j.surfcoat.2011.03.112.

[31] G. Da Ponte, E. Sardella, F. Fanelli, R. d'Agostino, R. Gristina, P. Favia, *Plasma Deposition of PEO-Like Coatings with Aerosol-Assisted Dielectric Barrier Discharges*, Plasma Process. Polym. 9 (2012) 1176–1183. doi:10.1002/ppap.201100201.

[32] P. Kingshott, J. Wei, D. Bagge-Ravn, N. Gadegaard, L. Gram, *Covalent Attachment of Poly(ethylene glycol) to Surfaces, Critical for Reducing Bacterial Adhesion*, Langmuir. 19 (2003) 6912–6921. doi:10.1021/la034032m.

[33] Y. Tanaka, K. Matin, M. Gyo, A. Okada, Y. Tsutsumi, H. Doi, *et al.*, *Effects of electrodeposited poly(ethylene glycol) on biofilm adherence to titanium*, J. Biomed. Mater. Res. A. 95 (2010) 1105–13. doi:10.1002/jbm.a.32932.

[34] W.J. Yang, T. Cai, K.-G. Neoh, E.-T. Kang, G.H. Dickinson, S.L.-M. Teo, *et al.*, *Biomimetic anchors for antifouling and antibacterial polymer brushes on stainless steel*, Langmuir. 27 (2011) 7065–76. doi:10.1021/la200620s.

[35] B. Nisol, G. Oldenhove, N. Preyat, D. Monteyne, M. Moser, D. Perez-Morga, *et al.*, *Atmospheric plasma synthesized PEG coatings: non-fouling biomaterials showing protein and cell repulsion*, Surf. Coatings Technol. 252 (2014) 126–133. doi:10.1016/j.surfcoat.2014.04.056.

[36] T.C.A.M. Azevedo, M.A. Algatti, R.P. Mota, R.Y. Honda, M.E. Kayama, K.G. Kostov, *et al.*, *Wettability, optical properties and molecular structure of plasma polymerized diethylene glycol dimethyl ether*, J. Phys. Conf. Ser. 167 (2009) 12053. doi:10.1088/1742-6596/167/1/012053.

[37] F. Brétagnol, L. Ceriotti, M. Lejeune, A. Papadopoulou-Bouraoui, M. Hasiwa, D. Gilliland, *et al.*, *Functional Micropatterned Surfaces by Combination of Plasma Polymerization and Lift-Off Processes*, Plasma Process. Polym. 3 (2006) 30–38. doi:10.1002/ppap.200500071.

[38] S.C. Pathak, D.W. Hess, *Dissolution and Swelling Behaviour of Plasma-Polymerized Polyethylene Glycol-Like Hydrogel Films for use as Drug Delivery Reservoirs*, ECS Trans, ECS, 2008: pp. 1–12. doi:10.1149/1.2831339.

[39] S. Bhatt, J. Pulpytel, M. Mirshahi, F. Arefi-Khonsari, *Plasma co-polymerized nano coatings – As a biodegradable solid carrier for tunable drug delivery applications*, Polymer (Guildf). 54 (2013) 4820–4829. doi:10.1016/j.polymer.2013.06.054.

[40] P.D. Drumheller, J.A. Hubbell, *Densely crosslinked polymer networks of poly(ethylene glycol) in trimethylolpropane triacrylate for cell-adhesion-resistant surfaces*, J. Biomed. Mater. Res. 29 (1995) 207–215. doi:10.1002/jbm.820290211.

7. ATMOSPHERIC PRESSURE PLASMA POLYMERIZATION

Atmospheric pressure plasma has revealed, in the last years, as an interesting technique for the deposition of thin films, since it allows the use of liquids instead of gases and it is easier to industrialize than the low pressure plasma systems. In this chapter, two different atmospheric plasma systems are evaluated to produce antibacterial and antifouling coatings on Titanium.

In the first part, an aerosol-assisted dielectric barrier discharge was used to produce an ethylene plasma-polymerized coating embedding vancomycin to obtain a drug release system, in a project carried out during a 2 month stage at the University of Bari (Italy). The second part deals with the direct treatment of a liquid precursor, 2-hydroxyethylmethacrylate, with a plasma jet system, to produce an antifouling plasma polymerized coating, in a project carried out at the INP in Greifswald (Germany) during 2 months.

7.1. Vancomycin-ethylene composite coatings

Vancomycin-ethylene composite coatings were obtained by an aerosol-assisted DBD system developed at the University of Bari. The use of a pulsed or a continuous plasma process, and the presence of a protective layer to modulate the vancomycin release from the coatings were studied.

7.1.1. Concentration of the solution on the atomizer

The configuration of the atomizer involves a recirculation of the solution that is not atomized. This leads to a progressive increase of the concentration of vancomycin in the solution. For this reason, the concentration of the solution employed for the plasma process was characterized (Figure 7.1).

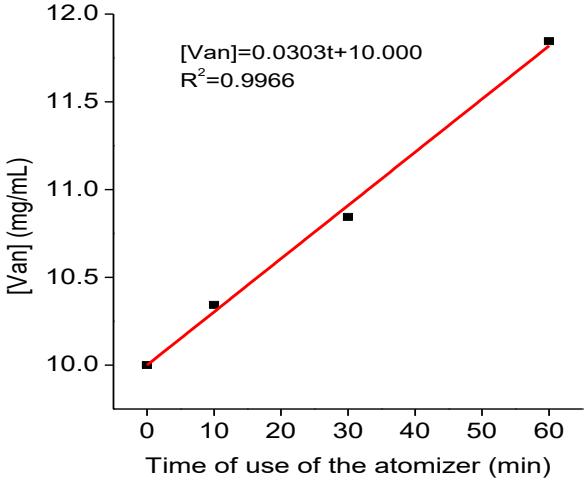

Figure 7.1. Modification on the vancomycin concentration in the atomizer over the time of use

This increase in the concentration was characterized by sampling the solution during 1h of discharge (after 10, 30 and 60 min running the atomizer with an helium

flow rate of $5 \cdot 10^3$ sccm (5 sLm) and measuring the concentration by UV-Vis. In order to maintain the concentration variation under 10% during the plasma treatments, the solution used for all the discharges was diluted every 40 min of discharge to the initial concentration, according to the trend obtained.

7.1.2. Parameters for the deposition

7.1.2.1. Deposition rate

To characterize the deposition rate, samples were produced in pulsed mode using a time on of 10 ms and a time off of 80 ms (PE_Van_10/80) and in continuous mode (PE_Van_cont) and the thickness of the coatings produced was analyzed. In order to measure the thickness of the coating, a scratch was made and the profile of the sample was measured in order to detect the step, which was taken as the thickness of the coating. The rate of deposition was calculated taking into account the measured thickness and the time of deposition, and it was found to be of 54nm/min for the PE_Van_10/80, and of 102nm/min for the PE_Van_cont, which are values in the range of previous studies dealing with ethylene plasma polymerization [1,2]. The higher deposition rate of the continuous plasma polymerization of ethylene has been already described by Yasuda *et al.* [3]. This fact can be explained by the higher energy input per monomer in the continuous mode, which in turn leads to the generation of more polymerization/deposition-forming species (i.e. more fragmentation) in the plasma state [4,5].

To modulate the release rate of vancomycin, a protective layer was polymerized on top of the composite coating. This top coating was prepared in the pulsed mode, using a mixture of ethylene and helium without the solution from the atomizer to avoid the presence of drug on the protective coating. The deposition rate was similar to the one found for the pulsed mode and the vancomycin-ethylene and helium mixture.

7.1.2.2. Chemical composition

To analyze the chemical composition of the coatings, FTIR spectra were acquired in transmission mode on silicon wafers submitted to the aforementioned atmospheric plasma treatments for the composite coating containing vancomycin in both the pulsed and the continuous mode. The spectrum of pure vancomycin and the plasma polymerized ethylene without vancomycin (PE) were recorded for comparison (Figure 7.2). Presence of the protective top coating does not modify significantly the FTIR spectra.

Vancomycin, as a glycopeptide antibiotic, contains a high concentration of amide groups, which can be assigned as amide A band centered at 3373cm^{-1}, amide I band at 1681cm^{-1} and amide II band at 1505cm^{-1}. The presence of OH groups is overlapped with the band at 3373cm^{-1}, and confirmed by the presence of the bending band at 1061cm^{-1}. The bands associated with C-H stretching are present at 3132cm^{-1} and 2909cm^{-1} for the hydrogen bonded to a sp^2 and a sp^3 carbon, respectively. Other bands are present, like

the C-O stretching in a phenol group at 1231cm^{-1} or the C-H bending at 1312cm^{-1}. The bands found in this spectrum are in good agreement with previous reports of vancomycin [2,3].

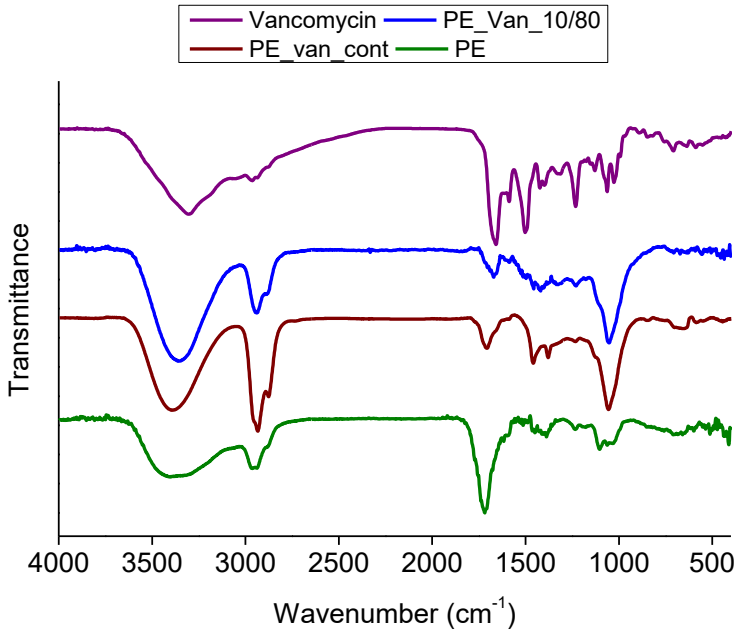

Figure 7.2. FTIR spectra of pure vancomycin, the composite coating in pulsed mode (PE_Van_10/80), the composite coating in the continuous mode (PE_Van_cont) and the plasma polymerized ethylene (PE).

Plasma polymerization of ethylene results in the presence of insaturations in the resulting plasma polymer [6]. For instance, the existence of triple bonds can be assigned to the band in the region of 3300cm^{-1}(≡C-H), 2198cm^{-1} (R'-C≡C-R) and 2101cm^{-1} (H-C≡C-R). The shoulder at 1600cm^{-1} may correspond to the presence of aromatic or cumulated C=C double bond vibrations. Single bonds are observed through the presence of symmetric and asymmetric stretching vibration bands, with the respective deformation vibrations found between 1140cm^{-1} and 1370cm^{-1}. The exposure of the samples to ambient air can be related to the presence of oxygen functional groups, such as OH vibration at 3430cm^{-1}, the carbonyl band at 1720cm^{-1} and the band at 1020cm^{-1} due to the C-COH stretching vibration.

The FTIR of the composite coatings (PE_Van_10/80 and PE_Van_cont) are similar to the plasma polymerized ethylene (PE), showing the presence of a polymeric matrix in the coatings containing vancomycin. The peaks of both plasma polymerized ethylene and vancomycin are overlapping and the vancomycin concentration is much lower compared to the polymeric matrix, so it is complicated to distinguish whether the peaks originate only from the polymer or the polymer with the vancomycin.

Samples produced in the continuous mode led to coatings with a thickness of approximately 2µm, while in the pulsed mode the thickness obtained was of approximately 1µm as determined by contact profilometry. This fact correlates with the

intensity of the FTIR spectra, which is higher for the PE_van_cont than for the PE_van_10/80.

7.1.3. Vancomycin release from titanium disks

The amount of vancomycin released from the different coatings on the titanium disks was measured after 1h of immersion in water. In order to check the total amount of vancomycin remaining on the coating, the samples were sonicated for 15min in water (Figure 7.3). The release after one hour from the sample polymerized in continuous mode (PE_Van_cont) is higher than the one from the pulsed sample (PE_Van_10/80). Moreover, after sonication, the amount of remaining vancomycin was lower for the pulsed polymerized sample than for the continuous one. This can be related to the thickness of the coating, which might be also related to the amount of vancomycin present in the sample.

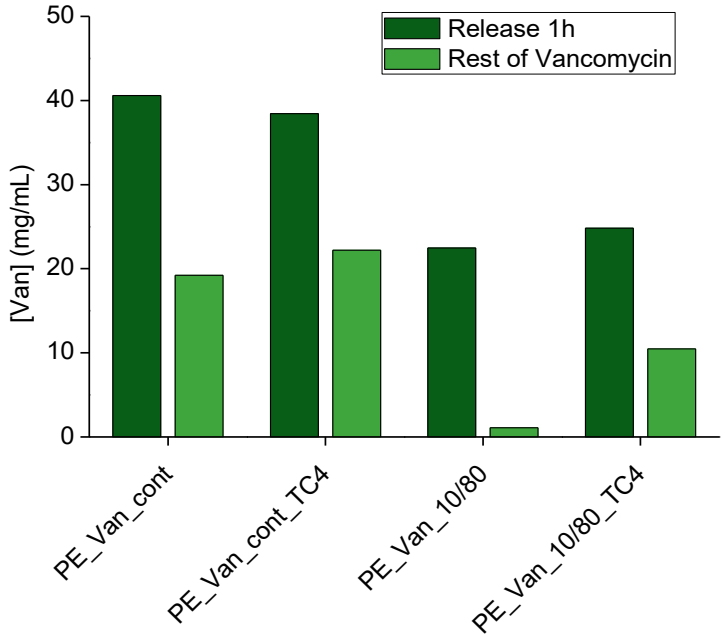

Figure 7.3. Vancomycin release from the plasma polymerized titanium samples in either continuous or pulsed mode without/with protective coating

The other parameter that was taken into account was the presence of the protective coating. This coating was able to reduce the release after one hour for both the continuous (PE_Van_cont_TC4) and the pulsed sample (PE_Van_10/80_TC4). After the sonication, the remaining vancomycin was also higher for the samples with the top coating. This seems to indicate that, plasma polymerized ethylene forms a hydrophobic layer on top of the composite layer that reduces the diffusion of the drug [7,8].

7.1.4. Characterization of the antibacterial properties

The growth of *S. aureus* was tested by the double-well test (section 2.7.3.4). The control samples, i.e. bare titanium and plasma polymerized ethylene on titanium did not alter the growth of *S. aureus*, showing that neither the titanium nor the plasma

polymerized ethylene samples have any effect on the bacteria viability. Regarding the samples containing vancomycin and the protective coating (PE_van_cont_TC4 and PE_van_10/80_TC2), a slight increase on the optical density was found in the first 2 h, which indicates that the growth was not completely inhibited at the beginning of the experiment. This can be related to the presence of the protective coating, which delays the release of the vancomycin.

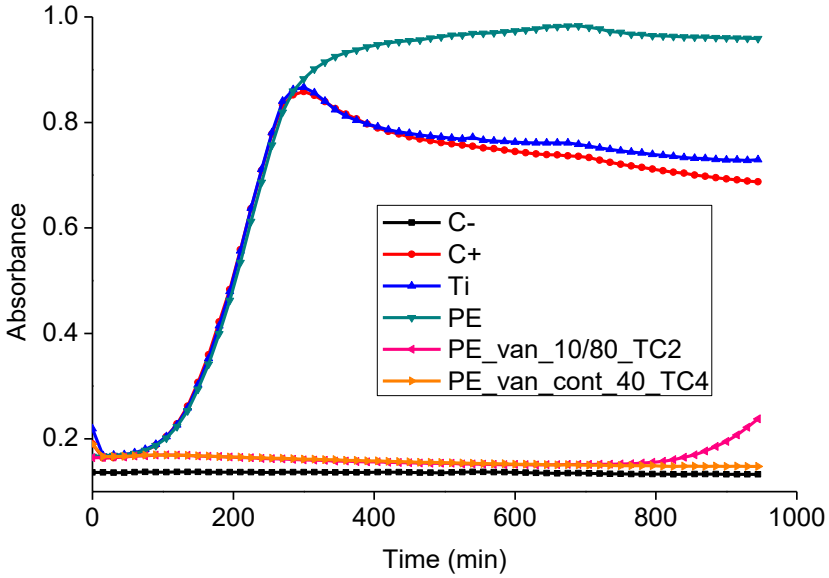

Figure 7.4. Growth curve of *S. aureus* tested in the double-well test

After this time, a decrease on the optical density was observed, probably because the vancomycin concentration was higher at this point. However, for the pulsed sample (PE_van_10/80_TC2), a growth of the bacteria was observed at the end of the experiment. This means that some viable bacteria were present even in presence of the vancomycin, and, hence, the concentration of the antibiotic was not high enough to completely inhibit the growth at the bacteria concentration used for the study.

This assay indicates the ability of the ethylene-vancomycin coatings to inhibit the initial growth of bacteria in an effective way, since over more than 10h no growth was observed. This means that the minimum inhibitory concentration for the strain used was reached for both the conditions studied [6].

7.1.5. Agar diffusion test

The agar diffusion test (Figure 7.5) showed the ability of the coatings to inhibit the growth of *S. aureus*. The assay was performed with the coating in contact with the bacteria in the agar plate, and no growth was observed in the zone directly contacting with the sample. The samples produced in the pulsed mode have a slightly lower inhibition zone, probably due to the lower thickness of the coating, which, in turn, implies lower vancomycin content. Presence of the top coating increases the inhibition zone, probably because it delays the release of the drug. This results correlates with the ones obtained in the growth curve experiment. Similar inhibition zones were obtained in previous studies with a lysozyme in composite coatings [9].

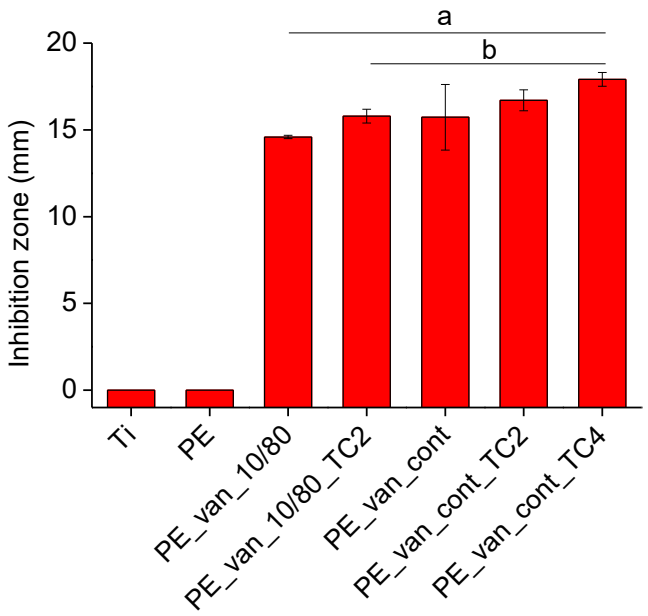

Figure 7.5. Agar diffusion test. *a* indicates statistically significant differences compared to Ti and PE, and *b* compared to PE_van_10/80 ($p<0.05$)

According to the results obtained, a plasma polymerized ethylene coating containing vancomycin was prepared on the titanium surface. The typical FTIR bands for an ethylene plasma polymerized coating were found, indicating the presence of the coating. The *in vitro* results with *S. aureus* revealed the suitability of the coating to inhibit the bacterial growth in an effective way.

7.2. Liquid phase plasma polymerized poly(2-hydroxyethyl methacrylate)

A plasma jet system developed at the INP Greifswald was used to evaluate the possibility of polymerizing 2-hydroxyethylmethacrylate (HEMA) in liquid state on the titanium sample at atmospheric pressure. The coating was prepared by placing a drop of the liquid HEMA on the sample and treating the sample during 5 min with an argon plasma. Different plasma power, gas flow rate, distance between the sample and the electrode and drop volume of monomer (HEMA) were tested.

7.2.1. Characterization of the coating

7.2.1.1. Surface free energy

The surface free energy of the plasma polymerized HEMA coatings was calculated by measuring the contact angle with distilled water, diiodomethane and ethylene glycol (Figure 7.6). Two different regions of the sample were studied: the center and the edge, being the center the part of the sample placed right under the jet and the edge the part of the sample potentially less affected by the jet. The values obtained were similar for the four conditions tested, and no significant differences were observed when comparing the center and edge positions, indicating that the treatment was sufficiently uniform on the whole diameter of the sample (10 mm).

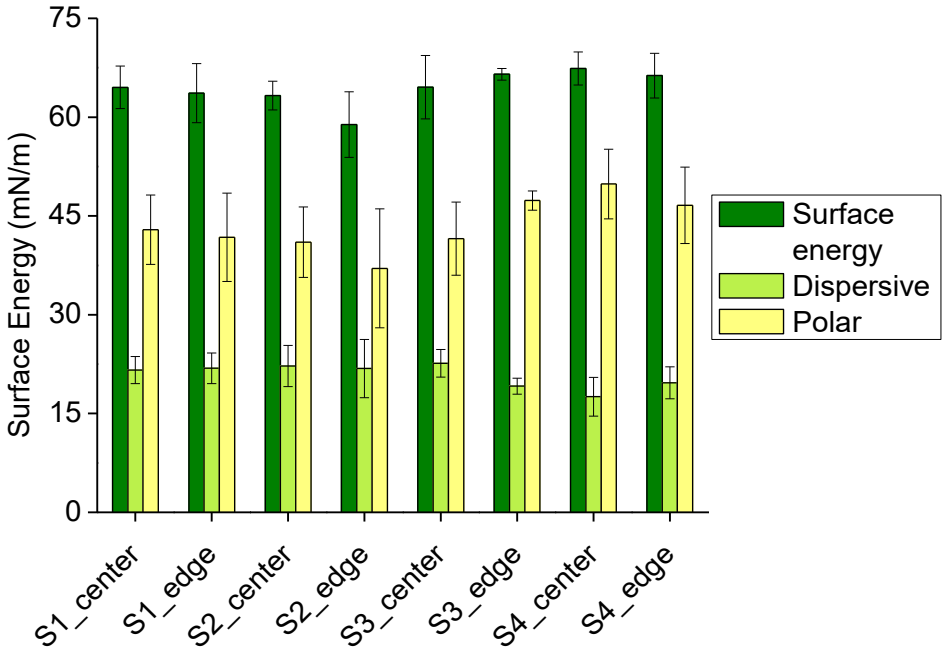

Figure 7.6. Surface energy of the plasma polymerized HEMA coated samples and its dispersive and polar components.

The coatings produced displayed higher surface energy compared to previous studies [10,11], with a higher polar component and lower dispersive component. This indicates that the plasma polymerized coatings have a higher amount of polar groups on the surface than the polymer synthesized conventionally. For instance, a previous study dealing with the plasma treatment of the PHEMA has been reported to enhance the wettability of the polymer, reaching similar values to the ones reported here [12,13]. On the other hand, PHEMA is a moderately swellable polymer system, in which the swelling equilibrium depends on the polymerization mechanism [14]. The increase on the wettability might depend on the increase on polar functional groups and the degree of crosslinking that is induced by the plasma treatment. This enhanced wettability makes the coating suitable for biomedical applications [15,16].

The stability in water of the coated samples was tested by measuring the water contact angle of the sample as-treated and after an immersion of 48h in water (Figure 7.7). In all the samples, a slight increase on the water contact angle was detected, indicating a change on the wettability of the sample. This can be associated to dissolution of the less stable groups in water. Another factor which adds to the previous one can be the hydrophobic recovery by reorganization of the polymer chains after drying the samples. In the sample treated in two stages (S4), the contact angle increase is higher, probably because the treatment time of the liquid was divided (half of the HEMA volume was added after 2.5 min of the plasma treatment). Hence, the treatment with the plasma was shorter, leaving to a decrease on the wettability [17].

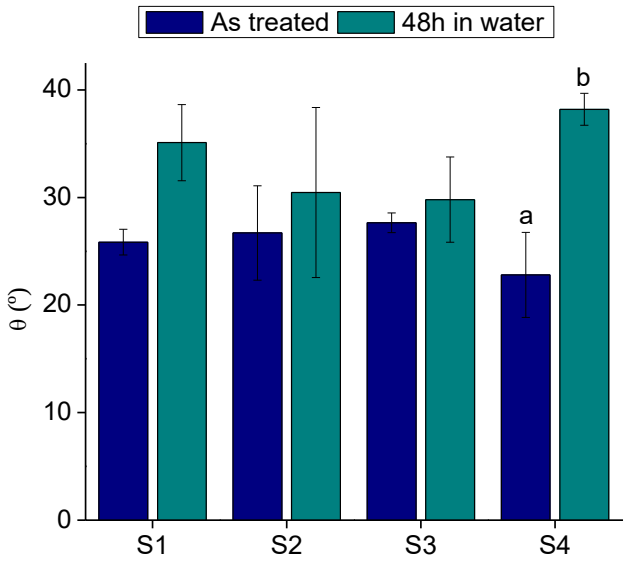

Figure 7.7. Water contact angle of the plasma polymerized HEMA coatings just after treating with plasma (as treated) and after 48h immersion in water. *a* indicates statistically significant differences compared to S1 after 48h in water, and *b* indicates statistically significant differences with all the samples as treated and S2 after 48h in water.

7.2.1.2. Chemical composition

The chemical composition of the plasma polymerized HEMA was tested by FTIR in the ATR mode (Figure 7.8). All the conditions rendered an organic coating on the surface.

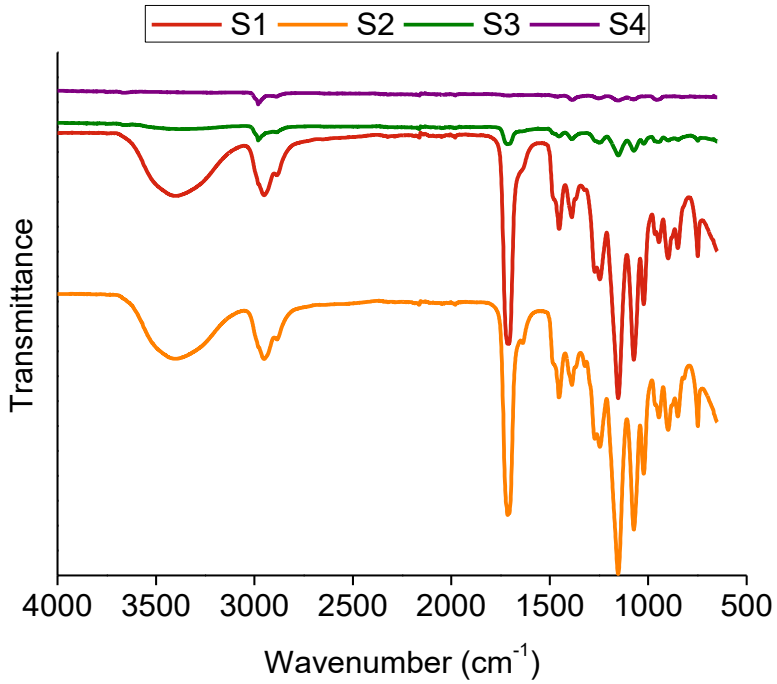

Figure 7.8. ATR-FTIR spectra of the plasma polymerized HEMA coating

The bands found in the spectra correspond to the bands found in the liquid precursor (structure described in section 1.5.2), namely, the alcohol bands (stretching at 3422cm^{-1} and bending at 1022cm^{-1}), and the ester band (stretching C=O at 1728cm^{-1} and stretching C-O at 1275cm^{-1}). The hydrocarbon bands were also found (Table 7.1).

Table 7.1. Peak assignation for the FTIR spectra of the plasma polymerized HEMA coatings

Wavenumber (cm^{-1})	Peak assignation
3422	OH stretching
3097	Vinyl stretching
2954-2888	C-H stretching
1712	C=O stretching
1637	C=C stretching
1160	C-O stretching
1456	C-H bending
1022	C-O bending

Even though ATR-FTIR is not a quantitative technique, some conclusions can be extracted from the intensity of the signal. The samples S1 and S2 are the ones with the most intense signal, and that can be associated with a thicker coating. These samples were produced at a higher distance between the plasma jet and the sample (4 mm instead of 3 mm for S3 and S4). The distance between the plasma and the jet influences the energy input on the substrate, which in turn is a consequence of the heat flux and the inelastic interactions of plasma species with the substrate. Hence, the smaller distances may induce a degradation of the coating that can explain the lower signal in the ATR-FTIR spectra [18].

Surface chemical composition was assessed by XPS, and 8 measurements were performed in a profile of the sample, covering the part of the HEMA that was directly treated with plasma (central part of the sample) and the part surrounding this area (Figure 7.9). This measurement was carried out on silicon wafers as a model material. Three elements were found in the general XPS spectra: carbon and oxygen from the polymer and silicon from the substrate. The composition of the plasma polymerized coatings resembles the theoretical one for a PHEMA coating (63% C1s and 37% O1s), as indicated as dashed lines in Figure 7.9, with a slightly higher amount of carbon and, subsequently, a slightly lower amount of oxygen. This can be associated to the presence of organic contaminants (hydrocarbons). The composition found for these coatings is in good correspondence with the ones found in previous studies dealing with PHEMA coatings obtained by plasma [7–9]. The signal from the substrate is not visible due to the attenuation of the photoelectrons generated by the substrate material. At some points the substrate is visible, with the subsequent diminution of the carbon signal, probably because a scratch done during the sample preparation. Moreover, the efficiency of the polymerization is higher in the center of the sample, i.e. the zone with the higher incidence of the jet.

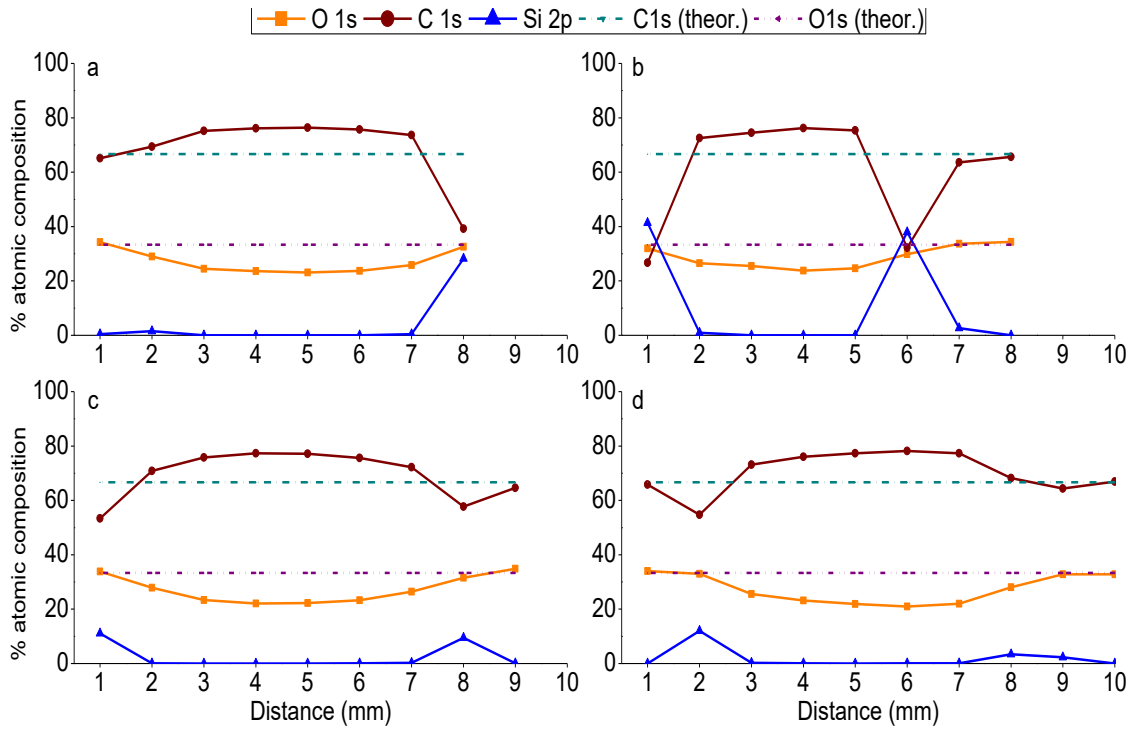

Figure 7.9. Composition of the plasma polymerized HEMA coatings in a profile of the sample. (a) S1, (b) S2, (c) S3 and (d) S4. The dashed lines indicate the theoretical composition for a traditionally synthesized PHEMA. Measurements were taken in the central part of the sample, doing one measurement per mm.

The corresponding high resolution C1s spectra (Figure 7.10) were decomposed into five different components which can be assigned to the presence of hydrocarbon bonds (C-C, C-H), CH_2-C=O groups, ether and hydroxyl bonds (C-O), carbonyl bonds (C=O) and carboxyl bonds (COO).

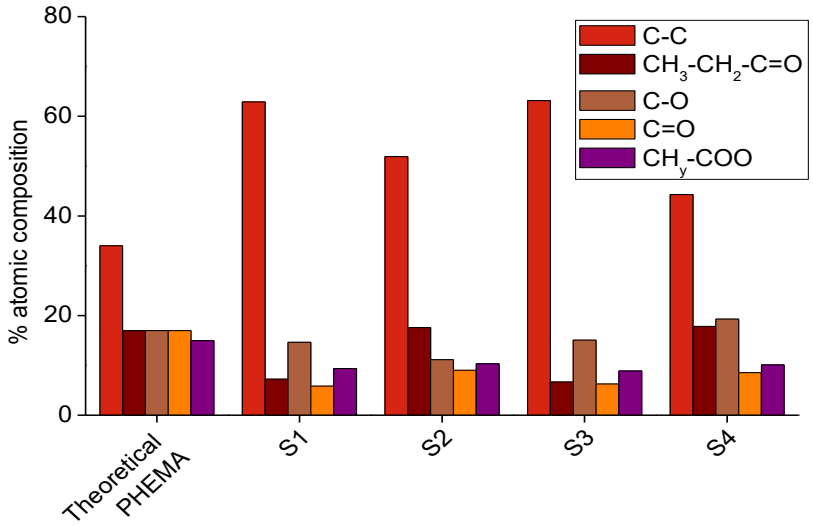

Figure 7.10. High resolution XPS C1s peak fitting components

The results obtained showed a higher presence of C-C bonds, which can correspond to the organic contamination. The stoichiometry of the different carbon-

oxygen bonds is slightly different to the theoretical one, indicating that some changes on these functionalities might have occurred due to the plasma treatment.

The stability of the samples was tested by ATR-FTIR measuring the same sample before and after an immersion in water for 24h (Figure 7.11). Even though the intensity of the bands was lower after the water immersion, the characteristic bands for PHEMA can be observed (Table 7.1), showing that part of the coating is lost but not completely.

The sample showing a higher intensity after the immersion is S2, which is the sample treated in the mildest conditions, i.e. low plasma power (7 W), gas flow (0.7 sLm) and high distance between the substrate and the jet. This can be related to the lower power input of this condition, and thus, the lower degradation of the coating.

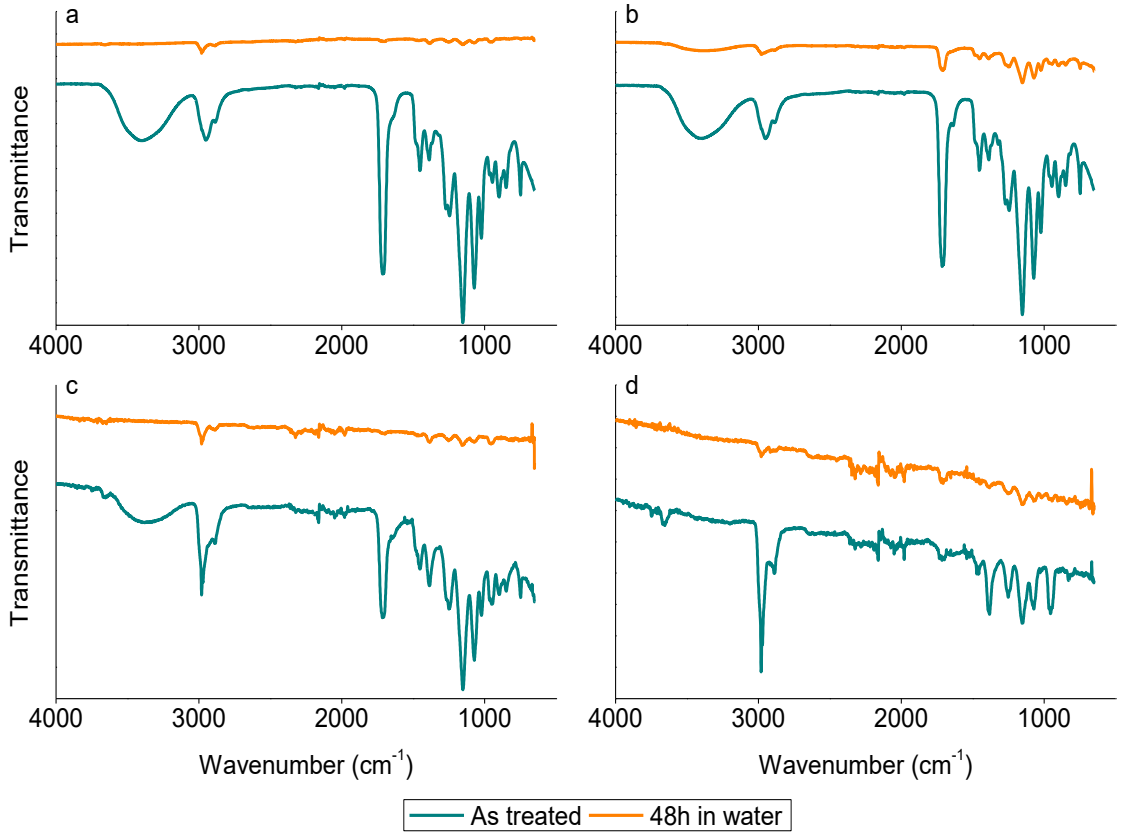

Figure 7.11. ATR-FTIR spectra of the samples before and after an immersion in water (a) S1, (b) S2, (c) S3, (d) S4

To evaluate the stability of the coatings under different conditions, one of the samples was selected (S2) for the XPS analysis (Figure 7.12). This sample was selected because it was the most stable according to the ATR-FTIR study. The stability of this sample was tested in air for 24 and 48h, in water immersion for 24 and 48h and in an ultrasonic bath for 5min. A change in the atomic concentrations after an ultrasonic bath can be seen: carbon content dropped slightly whereas a remarkable increase in oxygen and a decrease in nitrogen were detected. According to the increased portion of oxygen after the ultrasonic bath, an increase in the percentage amount of functional groups is

shown. Furthermore, swelling but no dissolution of the films has been observed after storage in water.

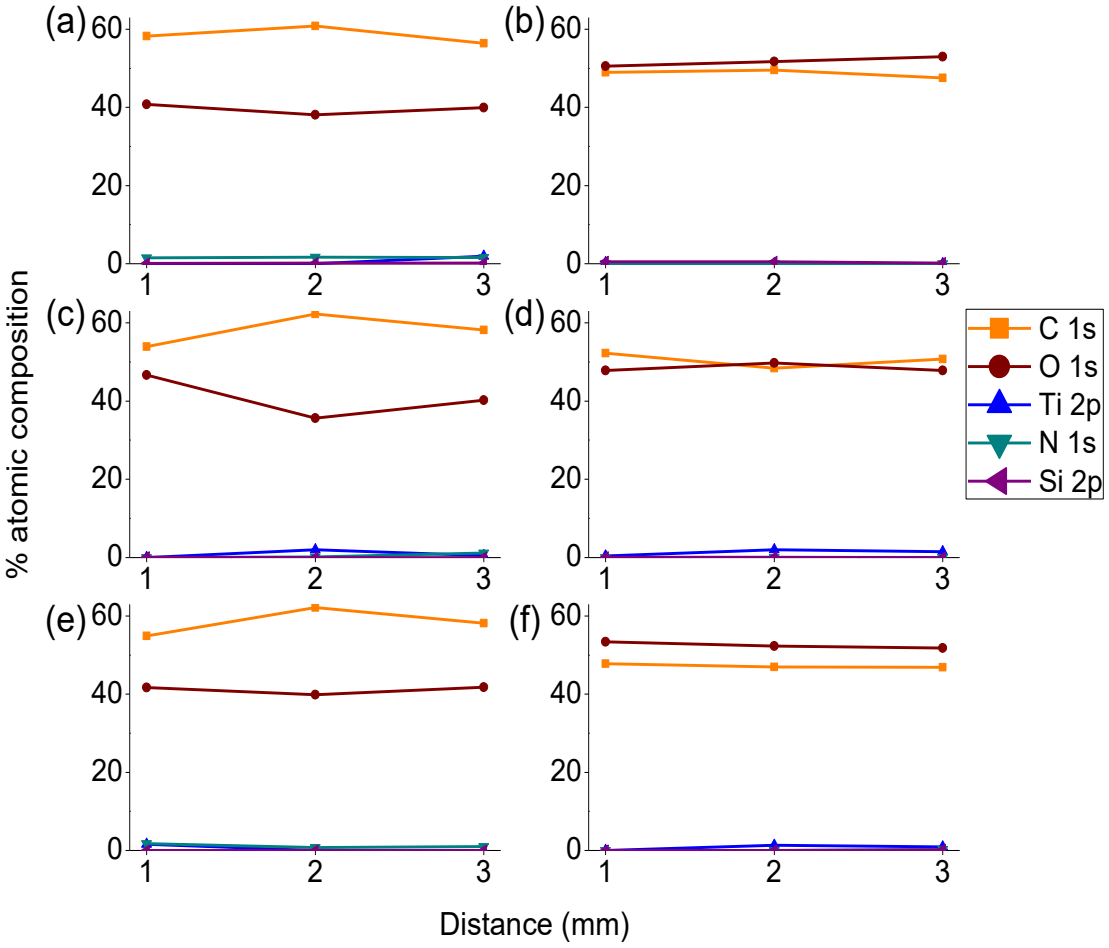

Figure 7.12 Composition of the plasma polymerized HEMA coatings in a profile of the sample for all the aging conditions. (a) S2, (b) S2 after a 5 min ultrasound treatment in water, (c) S2 stored in air for 24 h, (d) S2 stored in water for 24 h, (e) S2 stored in air for 48 h, (f) S2 stored in water for 48 h

7.2.2. Biocompatibility: cytotoxicity and cell adhesion

In this section, the biocompatibility of the coatings was assessed by means of the toxicity of the eluents and the adhesion of human fibroblast on the samples. No toxic effects were observed on the hFFs in contact with the eluents of the samples (Figure 7.13), with cell viability above 80% in all cases. This fact shows that during the plasma process, no toxic molecules were produced or if so, the concentration was too low to exert cell toxicity.

The hFFs adhesion was tested after 6 h and 24 h in contact with the coated samples (Figure 7.15). The assay revealed higher adhesion on the plasma polymerized HEMA samples than on titanium. Regarding the cell proliferation after 24h, the increase on the cell number was higher on the titanium than on the coated samples in most conditions, which may indicate that the polymeric coating is not completely favorable for the tissue integration. However, the increase on the cell number after 6 h and 24 h is

significant, making this material suitable for dental implant applications. Similar results with PHEMA coatings were found by other authors [7,10].

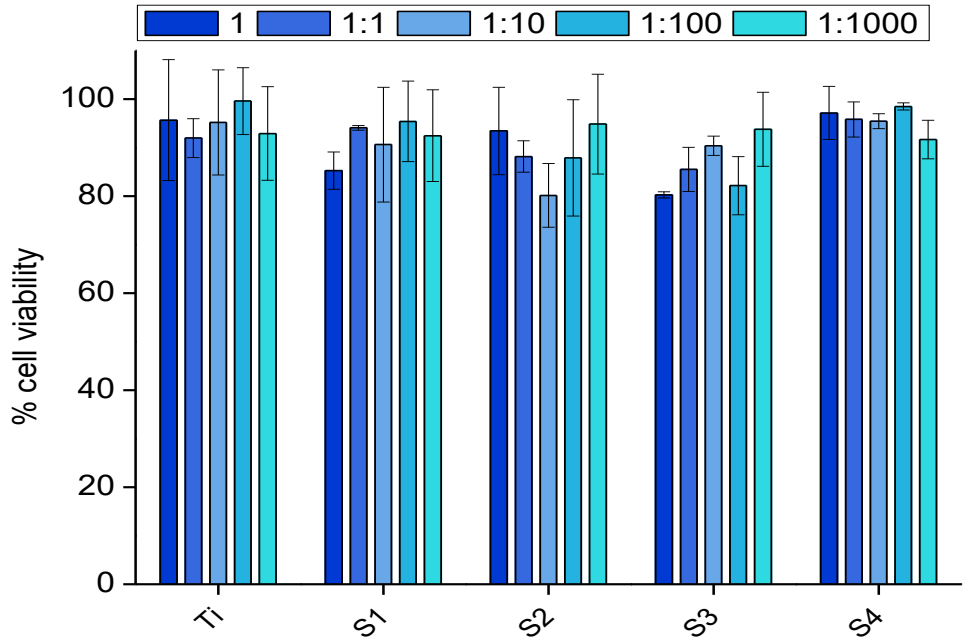

Figure 7.13. Cytotoxicity of the plasma polymerized HEMA coated samples

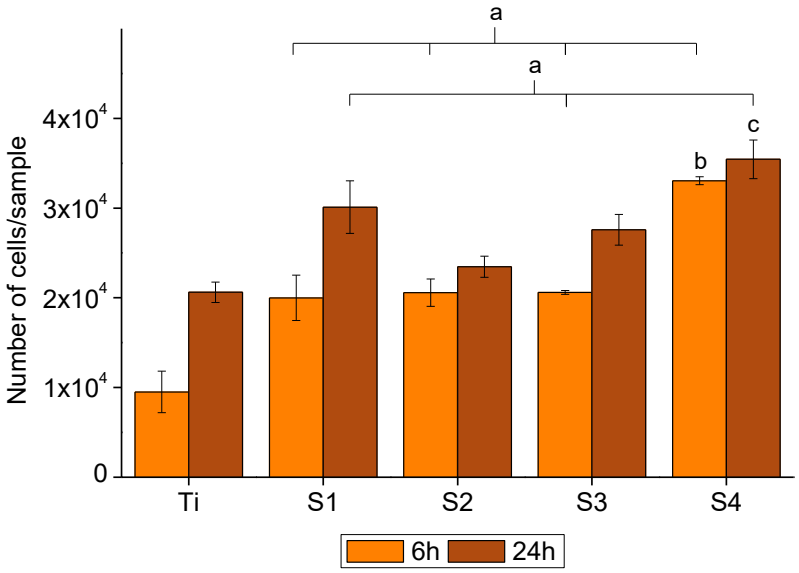

Figure 7.14. hFFs adhesion on the PP-HEMA coated samples. For each time point, *a* indicates statistically significant differences compared to Ti, *b* compared to S1, S2 and S3 and *c* compared to S2, S3 ($p<0.05$).

7.2.3. Bacterial adhesion

Bacterial adhesion of *S. aureus* and *E. coli* is lower on the plasma polymerized HEMA coatings, showing a 50% of reduction compared to the titanium (Figure 7.15). The antifouling properties of PHEMA films are related to high water retention (as this is a hydrogel coating), which translates to a lower polymer chains mobility and a steric hindrance for the bacterial adhesion [11–13], which is very interesting for the applications aimed at in this thesis.

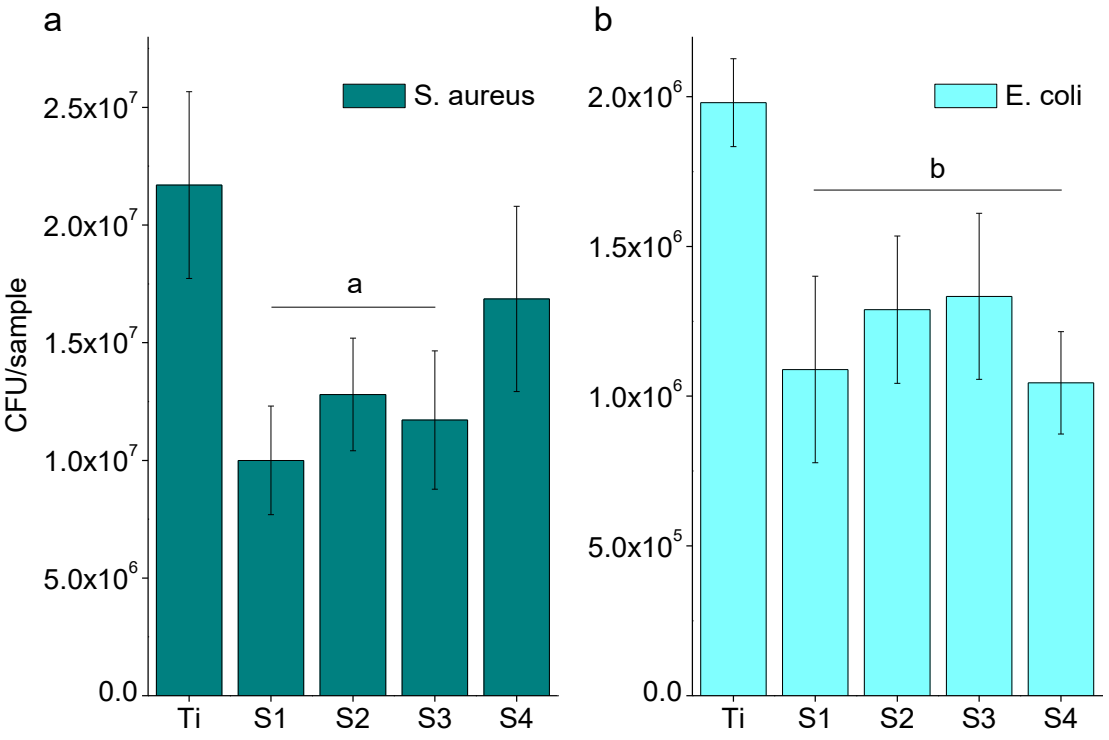

Figure 7.15. *S. aureus* (a) and *E. coli* (b) adhesion on the PP-HEMA samples

7.3. References

[1] H. Yasuda, C.R. Wang, *Plasma polymerization investigated by the substrate temperature dependence*, J. Polym. Sci. Polym. Chem. Ed. 23 (1985) 87–106. doi:10.1002/pol.1985.170230110.

[2] K.G. Donohoe, T. Wydeven, *Plasma polymerization of ethylene in an atmospheric pressure-pulsed discharge*, J. Appl. Polym. Sci. 23 (1979) 2591–2601. doi:10.1002/app.1979.070230905.

[3] H. Yasuda, T. Hsu, *Some aspects of plasma polymerization investigated by pulsed R.F. discharge*, J. Polym. Sci. Polym. Chem. Ed. 15 (1977) 81–97. doi:10.1002/pol.1977.170150109.

[4] Y.-R. Wang, W.-C. Ma, J.-H. Lin, H.-H. Lin, C.-Y. Tsai, C. Huang, *Deposition of fluorocarbon film with 1,1,1,2-tetrafluoroethane pulsed plasma polymerization*, Thin Solid Films. 570 (2014) 445–450. doi:10.1016/j.tsf.2014.03.026.

[5] A.E. Lefohn, N.M. Mackie, E.R. Fisher, *Comparison of Films Deposited from Pulsed and Continuous Wave Acetonitrile and Acrylonitrile Plasmas*, Plasmas Polym. 3 (1998) 197–209. doi:10.1023/A:1021850604696.

[6] I. Retzko, J.F. Friedrich, A. Lippitz, W.E.S. Unger, *Chemical analysis of plasma-polymerized films: The application of X-ray photoelectron spectroscopy (XPS), X-ray absorption spectroscopy (NEXAFS) and fourier transform infrared spectroscopy (FTIR)*, J. Electron Spectros. Relat. Phenomena. 121 (2001) 111–129. doi:10.1016/S0368-2048(01)00330-9.

[7] K.S. Siow, L. Britcher, S. Kumar, H.J. Griesser, *Plasma Methods for the Generation of Chemically Reactive Surfaces for Biomolecule Immobilization and Cell Colonization - A Review*, Plasma Process. Polym. 3 (2006) 392–418. doi:10.1002/ppap.200600021.

[8] T.C.A.M. Azevedo, M.A. Algatti, R.P. Mota, R.Y. Honda, M.E. Kayama, K.G. Kostov, *et al., Wettability, optical properties and molecular structure of plasma polymerized diethylene glycol dimethyl ether*, J. Phys. Conf. Ser. 167 (2009) 12053. doi:10.1088/1742-6596/167/1/012053.

[9] F. Palumbo, G. Camporeale, Y.W. Yang, J.S. Wu, E. Sardella, G. Dilecce, *et al., Direct Plasma Deposition of Lysozyme-Embedded Bio-Composite Thin Films*, Plasma Process. Polym. 12 (2015) 1302–1310. doi:10.1002/ppap.201500039.

[10] G. Bayramoğlu, M. Yakup Arıca, *Surface energy components of a dye-ligand immobilized pHEMA membranes: Effects of their molecular attracting forces for non-covalent interactions with IgG and HSA in aqueous media*, Int. J. Biol. Macromol. 37 (2005) 249–256. doi:10.1016/j.ijbiomac.2005.12.005.

[11] M. Kiremitçi-Gümü, *Microbial adhesion to ionogenic PHEMA, PU and PP implants*, Biomaterials. 17 (1996) 443–449. doi:10.1016/0142-9612(96)89662-1.

[12] H. Lim, Y. Lee, S. Han, J. Cho, K.-J. Kim, *Surface treatment and characterization of PMMA, PHEMA, and PHPMA*, J. Vac. Sci. Technol. A Vacuum, Surfaces, Film. 19 (2001) 1490–1496. doi:10.1116/1.1382650.

[13] Sabine Paulussen, Dirk Vangeneugden, Olivier Goossens, Erik Dekempeneer, *Antimicrobial Coatings Obtained in an Atmospheric Pressure Dielectric Barrier Glow Discharge*, MRS Proc. 724 (2002) N8.13. doi:10.1557/PROC-724-N8.13.

[14] E. De Giglio, D. Cafagna, M. Giangregorio, M. Domingos, M. Mattioli-Belmonte, S. Cometa, *PHEMA-based thin hydrogel films for biomedical applications*, J. Bioact. Compat. Polym. 26 (2011) 420–434. doi:10.1177/0883911511410460.

[15] V.P. Bavaresco, C.A.C. Zavaglia, S.M. Malmonge, M.C. Reis, *Viability of pHEMA Hydrogels as Coating in Human Synovial Joint Prosthesis*, Mater. Res. 5 (2002) 481–484. doi:10.1590/S1516-14392002000400014.

[16] L. Indolfi, F. Causa, P.A. Netti, *Coating process and early stage adhesion evaluation of poly(2-hydroxy-ethyl-methacrylate) hydrogel coating of 316L steel surface for stent applications.*, J. Mater. Sci. Mater. Med. 20 (2009) 1541–51. doi:10.1007/s10856-009-3699-z.

[17] L.-C. Xu, C.A. Siedlecki, *Effects of surface wettability and contact time on protein adhesion to biomaterial surfaces*., Biomaterials. 28 (2007) 3273–83. doi:10.1016/j.biomaterials.2007.03.032.

[18] K.-D. Weltmann, E. Kindel, R. Brandenburg, C. Meyer, R. Bussiahn, C. Wilke, *et al.*, *Atmospheric Pressure Plasma Jet for Medical Therapy: Plasma Parameters and Risk Estimation*, Contrib. to Plasma Phys. 49 (2009) 631–640. doi:10.1002/ctpp.200910067.

8. GENERAL DISCUSSION

The main aim of this thesis was to develop polymeric antibacterial coatings for titanium dental implants. In this chapter, the main results obtained are discussed and compared in order to highlight the contributions made to the field of antibacterial coatings for titanium dental implants. During the last years, different strategies have been studied in order to achieve antibacterial surfaces, including changes in the topography [1,2] or the chemical composition [3–6] and the incorporation of different antibacterial molecules on the titanium surface, including antibiotics [7–9] and antimicrobial peptides [10,11]. Another strategy that has been explored in literature is to coat the titanium surface with polymers, which can be antifouling or antibacterial. Combinations of the different strategies might offer an interesting approach to improve the performance of the coatings.

This thesis focuses on the preparation of antibacterial polymeric coatings on titanium, to achieve a surface with antibacterial properties and a proper cell response for a good biosealing of the head of the implant. This is based on the theory of "the race for the surface", which postulates a competition between the cell tissue integration and the bacterial adhesion. According to this theory, if the biomaterial surface is colonized by the host cells, it will be more difficult for the bacteria to colonize the surface [12].

8.1. Comparison of the antibacterial coating strategy

The main strategies used till now in the field of the polymeric antibacterial coatings are the bactericidal surfaces, which kill the bacteria, the bacteria-resistant surfaces, which avoid the interaction and adhesion with the bacteria and the bacteria-releasing surfaces, which facilitates the release of attached bacteria by external forces [13]. The three methods have inherent advantages and disadvantages. For instance, bacteria-resistant and bacteria-releasing surfaces can prevent the initial attachment of bacteria, but none of the coatings developed till date inhibit completely the bacterial adhesion and, hence, the bacteria that are not killed may colonize the surface. Bactericidal surfaces, in turn, prevent the formation of biofilms but the remaining dead bacteria on the surface may trigger an immunological response and inflammation. Moreover, biocides included in this kind of coating have problems of cytotoxicity towards non-targeted species like mammalian cells. For this reason, a combination of these strategies might be a way to obtain synergistic effects between the advantages and disadvantages of every single strategy.

In this thesis, combined coatings have been prepared using antifouling coatings as a base coating. With this aim, antifouling coatings based either on PEG or PHEMA have been prepared. PEG coatings were further functionalized with a cell-adhesion peptide for the enhancement of the biocompatibility of the coatings. Antimicrobial peptides were also immobilized on the PEG surface in order to achieve a combination

of antifouling and antibacterial properties. In the same line, PEG was combined with an antibiotic in order to achieve a controlled drug release system. Another drug release system, combining an antibiotic in a plasma polymerized ethylene matrix was also developed.

As previously reported (section 1.4.2.1), antifouling coatings are generated with polymers that are electrically neutral, possess hydrogen bond donors and render hydrophilic surfaces [14]. This kind of polymers, when immobilized on a surface, form a hydrated coating that inhibits the bacterial adhesion by steric repulsion [15]. The interaction of an implant with the surrounding tissues is ultimately determined by its physical and chemical properties. In this regard, the wettability, topography and chemical composition are intended to play a role on the interaction between the material surface and the cells, either prokaryotic or eukaryotic.

The wettability of the implant surface is known to have an influence on the *in vitro* and *in vivo* response [16–20]. When an implant is coated with a polymeric coating there is a change on the chemical composition of the surface that determines the final measure of the contact angle. For this reason, contact angle measurements were used as an indication of the presence of the coating.

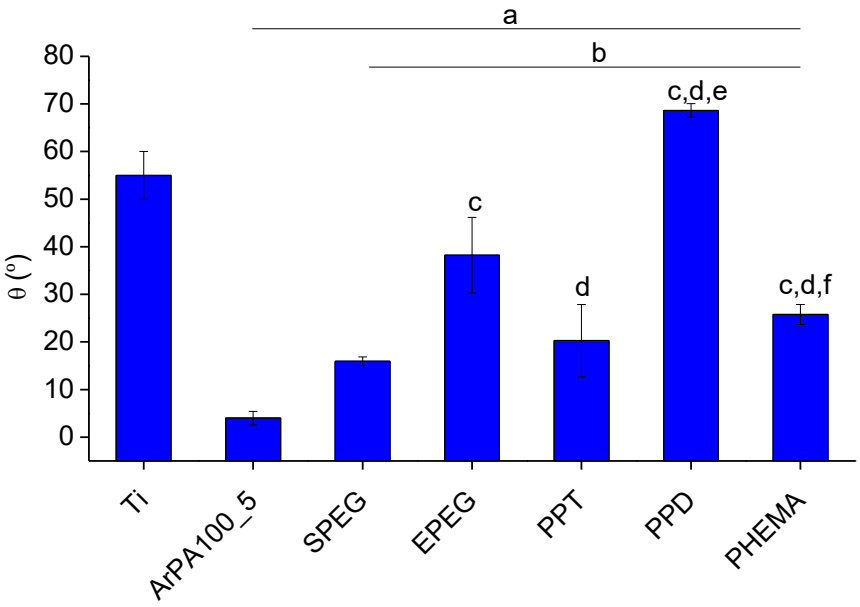

Figure 8.1. Average value of the water contact angle for all the coatings prepared in the thesis

The average values of the water contact angle (Figure 8.1) are different depending on the technique used for the preparation of the coating, with values ranging from superhydrophilic to 70º. Plasma activated sample (ArPA100_5) presented a value of water contact angle lower that 10º. Within the PEG coatings, the most hydrophilic coatings are the silanized (SPEG) and the plasma polymerized tetraglyme (PPT). On the other hand, electrodeposited coatings (EPEG) and plasma polymerized diglyme coatings (PPD) are thicker and less hydrophilic. It should be pointed out that the two coatings

prepared with low pressure plasma polymerization have a great difference between the values of the water contact angle (section 6.1.1.1 and section 6.2.1.1). This fact could be explained by the operation mode, since the PPT was prepared in pulsed mode while PPD was prepared in continuous mode. Using a continuous plasma treatment implies a higher crosslinking of the polymer and, thus, a less hydrophilic surface [21,22]. Plasma polymerized HEMA (PHEMA) is also hydrophilic. The hydrophilic character of the antifouling coatings is explained by the structure of the polymer, which has an intrinsic trend to bond water.

The changes on the hydrophilicity of the PEG coatings can be explained by the grafting density of the coatings, calculated as the contribution of the ether peak on the C1s XPS spectra (*Figure 8.2*). In this regard, the coating that presented a larger contribution on the C-O peak have a higher grafting density [23], and hence, a higher water contact angle.

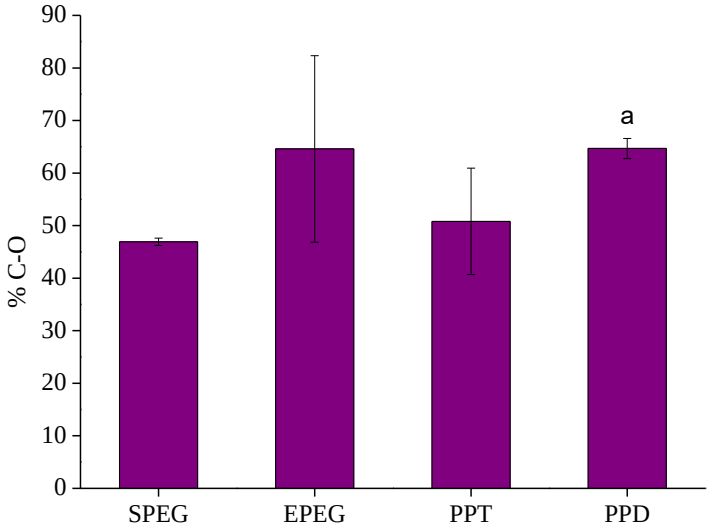

Figure 8.2. Average contribution of the C-O peak on the C1s XPS high resolution spectra. *a* indicates statistically significant differences compared to SPEG ($p<0.05$)

Regarding the *in vitro* biological performance of the coated samples, the protein adsorption, human fibroblast adhesion and bacterial adhesion was assessed in order to investigate the antifouling properties of the coatings. Protein adsorption is considered the most important factor of the interaction between biomaterials and tissues or body tissues, since proteins are the first biological molecules that cover the artificial surface when implanted into the body [19,24]. Generally, the adsorption is fast and non-specific and may lead to denatured protein that can cause a cascade of undesired events known as foreign body reaction [25].

The interaction of proteins with the biomaterial surface is also an important event in the colonization by bacteria. The relationship between the implant, the tissue integration and the biomaterial is determined by the binding characteristics [26]. This process was described as *the race for the surface* by Gristina [12]. If the binding is done

by a tissue cell, the implant will be integrated and protected and therefore the implant surface will be less available for bacterial colonization.

The factors controlling protein adsorption can be divided into external parameters, protein properties and surface properties. The external parameters include temperature, pH, and ionic strength, and are mainly fixed in the body [27]. The protein properties influence the way that the protein can adapt to the surface. Small proteins are more rigid and not able to adapt to the surface, while higher molecules can be decomposed into individual domains with specific properties, like hydrophilicity, polarity or charge, and can change their conformation to adapt to the surface properties [28,29]. Therefore, surface properties also play an important role on the interaction of the proteins with the surfaces. Proteins tend to adsorb more strongly to non-polar, high surface energy and charged surfaces [27,30,31]. Antifouling coatings are able to repulse the adsorption of proteins by a steric repulsion, since the presence of the protein on the surface reduces the conformational freedom of the polymeric chains and is thermodynamically unfavorable.

Several methods have been reported for the assessment of the protein presence on a surface, including the radiolabeling [32,33], labeling with fluorescent molecules [34–36], and the quartz microbalance with dissipation [37,38]. In this thesis, two different methods have been used, namely, the labeling of BSA with FITC and the observation with fluorescence microscopy and the XPS analysis of fibronectin.

FITC-BSA adsorption is a method based on the fluorescence microscopy images analysis. In the present work, it was used to compare the PEG coating methods, specifically tetraglyme plasma polymerization, electrodeposition and silanization (Figure 8.3). The fluorescence intensity of the images is related to the amount of adsorbed protein present on the sample [35,39].

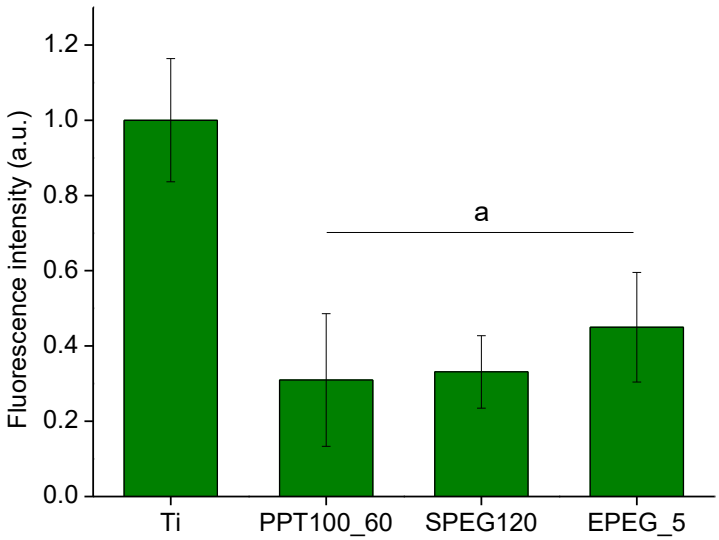

Figure 8.3. Quantification of the fluorescence signal on microscopy images of the samples with adsorbed FITC-BSA. *a* indicates statistically significant differences compared to Ti

In this regard, the protein adsorption was reduced on all the PEG coatings compared to the titanium samples. The results when comparing the different PEG coatings present no statistically significant differences. This result shows the ability to confer antifouling properties to the titanium surface, which have been already described for immobilized PEG by different techniques. For instance, Menzies *et al.* [40] prepared a plasma polymerized PEG and assessed the albumin adsorption by ToF-SIMS, finding a reduced amount of protein adsorbed on the PEG-coated samples. Wang *et al.* [41] Thalla *et al.* [42] used labeled albumin and found a lower fluorescence intensity for the PEG-coated samples compared to the control. The last paper also reported a 79% reduction of fibrinogen assessed by QCM-D, which is a comparable value to the ones obtained in this thesis with the FITC-BSA assay.

An important issue for the biocompatibility of titanium implant is the cytotoxicity of the possible eluents from the samples, such as remainings of the organic solvents used for the preparation of the coating, low molecular weight compounds produced by the coating process (for example, during plasma polymerization) and other non-bond molecules that may exert toxicity. Cell toxicity was tested for all the coatings as indicated in the ISO standard 10993-5. With this aim, the samples were immersed on cell media and after a certain time, the cell medium was placed with human fibroblast to test the cell survival. None of the coatings presented cytotoxic effects, since the cell survival ratio was higher than 80%.

In a recent study by Liu *et al.* [43], the cytotoxicity of PEG was tested. By checking different molecular weight polymers and oligomers, they found out that the polymers with a molecular weight between 400 and 2000 are non-toxic and, hence, are a good choice for the synthesis of biocompatible materials. In this thesis, different molecular weight PEG have been used. For instance, the polymers used for the silanization or the electrodeposition have a molecular weight in the range reported for non-toxic polymers. Regarding the plasma polymers, the molecular weight of the precursors was lower, which have been associated to toxic and mutagenic effects [44]. However, the plasma polymerization increase the molecular weight and changes the precursor structure, making the coating non-toxic for the cells. Moreover, the fact that the polymer is linked to the titanium substrate would reduce the concentration of the PEG molecules in the solution, and hence, increases the viability of the coatings. With the results obtained, it can be deduced that the concentration of the possible toxic molecules is lower than the minimum toxic concentrations for the cells used in this thesis.

Regarding the toxicity of HEMA, it has been reported that this monomer exert cell toxicity *via* apoptosis, among other effects on the cells [45–47]. However, the polymer PHEMA did not appear to show significant intrinsic surface toxicity [48,49]. This fact have a good correlation with the non-toxic results obtained in the cytotoxicity assay for the plasma polymerized HEMA on titanium.

Cell adhesion to the coated samples is also an important parameter for the tissue integration. The selected cells for the studies in this thesis were the human fibroblasts, which play a role on the new tissue formation after implantation and in the maintenance of a proper sealing between the oral environment and the peri-implant tissue [39,50,51]. Fibroblast adhesion on the coated samples compared to the titanium sample was lower for all the PEG coatings. However, PHEMA coatings reported a higher adhesion on all the studied conditions.

Due to the importance attributed to the existence of a proper biological sealing, an additional assay was performed in order to check the effects on cells of the cell adhesion peptide RGD on the PEG coatings (Figure 8.4). An increase on the number of cells adhered was observed for the plasma polymerized tetraglyme and the PEG silanized sample. Electrodeposited samples had a similar behavior with the presence of RGD or without the peptide, which in turn was similar to the titanium sample.

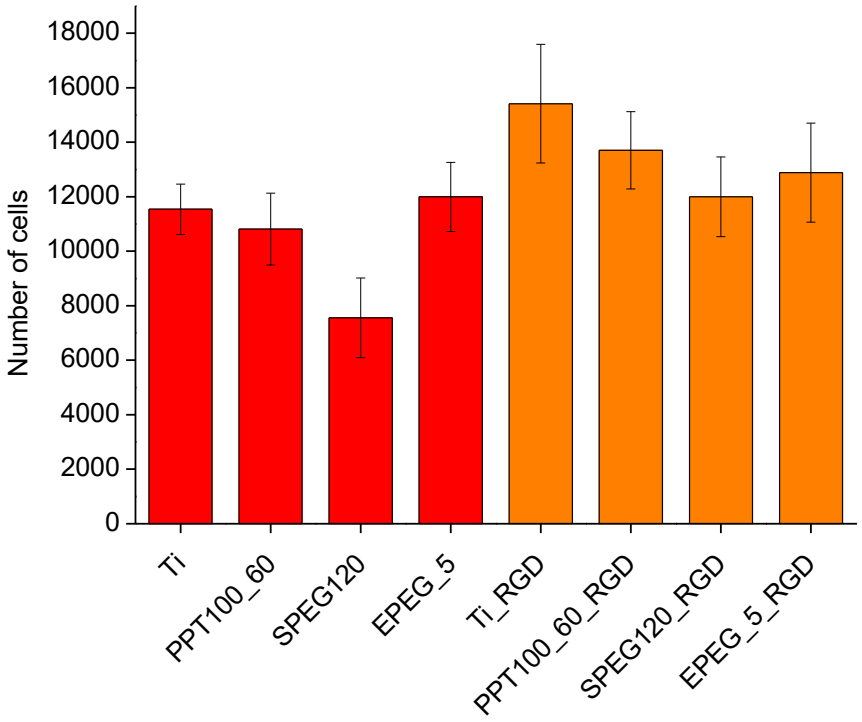

Figure 8.4. hFFs adhesion on selected PEG samples without and with RGD

The increased cell adhesion on the PEG coated samples has not been reported in previous studies, in which a reduced cell adhesion was found [52–55]. This fact can be related to the protein adsorption on the samples. Even though the protein adsorption was reduced by the presence of the PEG coatings, the amount of protein adsorbed could be enough to promote a specific binding of the cells [56]. Similar results were reported by Saldarriaga-Fernandez *et al.* [57]. In their study, a higher cell adhesion was found on PEG coatings when the protein concentration in the media was higher.

Bacterial adhesion was tested with four different strains, namely, *Streptococcus sanguinis*, *Lactobacillus salivarius*, *Staphylococcus aureus* and *Escherichia coli*. As

reported in section 1.3, *S. sanguinis* is a primary colonizer associated with dental infections and *L. salivarius* plays an important role on the biofilm maintenance. *S. aureus* and *E. coli* were selected as a model for Gram positive and Gram negative bacteria. Moreover, *S. aureus* have been found in some peri-implant pockets of infected patients, showing that it has a role on the dental implant related infections.

Regarding the results of the bacterial adhesion assays, a significant reduction of the adhesion was found for all the tested samples (Table 8.1). It has been assumed that the reduction of the bacterial adhesion was due to the antifouling characteristics associated with PEG coatings, since no bacteriostatic nor bactericidal effect of the polymer can be expected. This point is supported with the live/dead assay on the electrodeposited samples (section 5.3.5). In this assay, a reduction on the number of bacteria adhered to the sample was observed, but the coating was not bactericidal against the bacteria able to adhere.

Table 8.1. Bacterial adhesion (% normalized vs Ti) for selected conditions of each type of coating

	S. sanguinis	*L. salivarius*	*S. aureus*	*E. coli*
Ti	100.0 ± 21.2	100.0 ± 15.1	100.0 ± 6.9	100.0 ± 10.1
SPEG_120	21.9 ± 4.4	41.02 ± 2.0	-	-
EPEG5	28.3 ± 9.7	42.5 ± 5.7	-	-
EPEG5_4	-	-	7.5 ± 0.6	28.7 ± 1.8
EPEG5_4_MG1	-	-	4.5 ± 0.3	18.3 ± 2.3
PP150_30	37.3 ± 17.1	52 ± 9.7	-	-
PPD150_60	-	-	9.6 ± 1.9	-
PPD150_60_Doxy	-	-	1.1 ± 0.1	-
S4			52.7 ± 8.6	

Comparing the PEG coated samples, the ones showing the better performance are EPEG in the pulsed mode and PPD. These samples showed a higher thickness and hence, surface coverage, leading to a better antifouling activity. As expected, the best results were obtained with the AMP functionalized EPEG and the Doxycycline containing PPD, showing the better performance of a dual-function coating combining an antifouling and antibacterial agent.

Several parameters have been described in order to explain the reduced bacterial adhesion on PEG-coated samples. For instance, the hydrophilicity of the PEG coatings is one of the factors affecting the adhesion. In general, a higher bacterial adhesion have been detected on more hydrophobic surfaces [58,59]. The hydrophilic character of the coating is due to the water adsorption which acts as a steric barrier. Another factor is the individual steric repulsion exerted by the individual PEG chains, which hampers the approximation of the bacteria to the surface [60,61].

It has been reported that the adhesion force of the bacteria adhering to a PEG-coated surface is lower than the force to adhere to non-coated substrates [62–64]. This

fact, which contributes to a lower biofilm formation and to an easy biofilm removal, is attributed to the attenuation of the Van der Waals interaction forces of the bacteria membrane by the polymer. Moreover, since the PEG is a neutrally charged polymer, the electrostatic attraction forces between the bacteria and the substrate are also reduced by the presence of the coating [56].

The thicker PEG coatings prepared in this thesis (electrodeposited PEG and plasma polymerized diglyme) present a higher reduction of bacterial adhesion, since the interaction between the bacteria and the substrate is reduced. Regarding the reduction on the bacterial adhesion, values in the range of 70-90% have been reported [57,60,63,65]. This values are in the same range of the ones obtained in this thesis for the electrodeposited PEG and the plasma polymerized diglyme. Moreover, the use of AMPs or doxycycline enhanced the performance of the coatings, reaching reductions of 95-99%.

8.2. Comparison of deposition methods

Sample preparation for coating involves a grinding and polishing process, which contaminates the titanium surface. Therefore, this process is followed by a solvent cleaning process, which removes part of the surface contamination, such as grinding residues or organic contaminants. The cleaned surface presented a water contact angle around 60º and a surface carbon content of 25% as reflected in the XPS analysis. Treatment of the surface with acid or basic solutions may reduce the contamination, making the surface suitable for coating [66]. However, these techniques require the use of chemicals and temperature and are time consuming. For this reason, plasma activation was the selected method for the pre-treatment of the titanium samples before applying the coatings. Plasma activation is a well-known procedure for the cleaning and activation of the first nanometers of the surface metals, polymers and ceramics without altering their bulk properties [67].

In chapter 3, the results of the optimization of the plasma activation of the titanium surface were described. The activation rendered a superhydrophilic surface, with water contact angles below 5º, and carbon contents below 15% in the XPS analysis, a fact that can be related to the decrease on the organic contaminants and to the increase on the polar species on the titanium oxide, for instance, hydroxyl or carbonyl species [68–70].

Chapters 4, 5 and 6 described the results of coating the titanium surface with polyethylene glycol (PEG) through different methods. PEG was the polymer selected for the preparation of the coatings for the well-known antifouling properties of the coatings prepared with this polymer [71–74]. The application of PEG coatings on certain medical devices is intended to decrease bacterial adhesion in order to reduce the rate of infections related to the implantation [75,76]. In the case of dental and orthopedic applications, cell adhesion should be maintained in order to achieve a proper integration

and stability of the implant while obtaining antifouling properties with regards bacteria [77,78].

Till now, several strategies to produce polymeric coatings have been studied. All the methods proposed have advantages and disadvantages. For instance, grafting and self-assembled monolayers are compatible with specific substrates (such as gold or silicon) [79–81]. Physisorbed coatings typically require a charged or hydrophobic substrate and are liable to be desorbed under certain conditions [64,82,83]. Many coating methods require a multiple step process which might be difficult to control [84].

Even though several deposition methods have been investigated for the obtention of PEG coatings on titanium, a simple and effective method is still lacking. For instance, the production of comb-like copolymer of poly-L-lysine (PLL) and PEG [85], silica-polyethylene glycol hybrid [86] or a photoreactive PEG by co-polymerization of methacrylate- PEG and acryloyl 4-azidobenzene [87] involve complex synthesis routes for the preparation of the polymer prior the immobilization. With the aim to avoid this complexity, three different methods of deposition, namely, silanization, electrodeposition and plasma polymerization, which were firstly developed for the coating of titanium for dental implant applications, namely, silanization, electrodeposition and plasma polymerization. These methods represent three different coating strategies: a wet chemical technique, an electrochemical technique and a chemical vapor deposition. These methods were selected because they do not involve time-consuming synthesis routes or expensive reactants.

The use of silane chemistry has been widely developed for silicon surfaces. It is based on the reactivity of the silane coupling agents with the hydroxyl groups found in the surface. The strategy used in this thesis was not using an organosilane coupling agent but bonding a silicon atom to the terminal alcohol in PEG, which is a novel strategy for coating titanium. Silane groups have a high tendency to hydrolyze, and hence, the process must be carried out in vacuum and organic solvents (toluene). This requisite represents a drawback in economic and environmental terms. However, this strategy presents the advantage that the bonding of the PEG to the titanium is made in one step just after the preparation of the silanized PEG.

Electrochemical methods are also a good option in the environmental and economic costs, since they can be carried out in aqueous based solutions and, of course, the vacuum is not necessary. For the electrochemical deposition of PEG, an amine terminated PEG was used, as previously reported by Tanaka *et al.* [88–90]. The amine groups are partly protonated in water solution, which creates a positive charge in the end group of the polymer that is attracted towards the cathode of the electrolytic cell. One of the major advantages of this method is the short time of treatment, in the order of minutes, but the low charge density of the polymer represents a low yielding of the method. In order to increase the yielding of the process, a pulsed process was

successfully developed and tested in this thesis, probing that a thicker and more effective coating was prepared by pulsed electrodeposition.

The third method employed for the preparation of PEG coatings has been plasma polymerization. Plasma polymerization has been studied for a long time on model substrates such as silicon or gold and on polymers [52,91–95]. However, the application of this method on titanium substrates had not been explored. Plasma polymerization is based on the cleavage and recombination of bonds in a low molecular weight precursor in order to obtain a polymeric layer on the substrate that resembles the structure and properties of the precursor [96–99]. The conditions of the plasma treatment are a key parameter for the proper performance of the polymeric coating produced. In this thesis, two different precursors for PEG-like coatings have been studied (tetraglyme and diglyme). The two precursors have been shown to produce PEG-like coatings under suitable plasma conditions [100–103], so the feasibility of the polymerized layers was studied focusing on the dental implants applications.

The second part of the thesis (Chapter 7) was centered on the use of atmospheric pressure plasma for the preparation of polymeric antibacterial coatings on titanium substrates. One of the main advantages of using atmospheric pressure plasma is the possibility of using liquids in direct contact with the plasma [93,104–106]. Two different plasma systems were used, an aerosol-assisted dielectric barrier discharge and a plasma jet.

Aerosol-assisted DBD plasmas at atmospheric pressure are an interesting approach for the coating of biomedical devices. On the one hand, the processing at atmospheric pressure allows for the treatment of hydrogels and porous materials without the need of a long vacuum degassing time. On the other hand, the use of an aerosol allows for the use of precursors with high boiling point and even precursors containing suspended molecules or nanoparticles [107]. A plasma jet configuration in direct contact with liquids is also an attractive strategy, providing the possibility to treat directly any kind of liquid precursor and polymerize it on the surface in a short time of treatment and with control on the film properties. It is also a suitable technique for a continuous process in the industry.

8.3. Future work

In this thesis, several modifications for the preparation of antibacterial polymeric coatings on titanium have been reported. The surface characterization showed the presence of the coating in all the strategies undertaken, taking into account the physical properties and the chemical properties. A research on the mechanical properties and the long-term stability of the coatings should be carried out in order to assess the proper performance of the coatings *in vivo* or in clinical applications.

The *in vitro* characterization done in this thesis showed the good performance of the antifouling coatings and the combination of such coatings with antibacterial

molecules. Even though the co-culture experiment performed in this thesis (section 5.2.1) is considered a good approach to mimic the clinical conditions, an *in vivo* study would be determining to achieve an insight of the performance of the coating in a complex biological environment. Further *in vitro* studies would also be helpful, such as dynamic protein adsorption assays or dynamic bacterial adhesion assays.

Further studies on the drug release systems either at low or at atmospheric pressure could also be done, in order to achieve release rates and times suitable for clinical situations. For instance, the use of multi-layer coatings with different polymers would delay the drug release and hence, increase the suitability of such coatings. The dose of the antibiotic should also be studied carefully in order to achieve the MIC of the bacteria without exceeding the threshold concentration of toxicity towards mammalian cells. Finally, the characterization of the atmospheric pressure plasma coatings should be completed, in order to assess the influence of the processing steps on the *in vitro* results.

8.4. References

[1] C. Lüdecke, J. Bossert, M. Roth, K.D. Jandt, *Physical vapor deposited titanium thin films for biomedical applications: Reproducibility of nanoscale surface roughness and microbial adhesion properties*, Appl. Surf. Sci. 280 (2013) 578–589. doi:10.1016/j.apsusc.2013.05.030.

[2] L. Badihi Hauslich, M.N. Sela, D. Steinberg, G. Rosen, D. Kohavi, *The adhesion of oral bacteria to modified titanium surfaces: role of plasma proteins and electrostatic forces*, Clin. Oral Implants Res. 24 (2013) 49–56. doi:10.1111/j.1600-0501.2011.02364.x.

[3] M. Godoy-Gallardo, A.G. Rodríguez-Hernández, L.M. Delgado, J.M. Manero, F. Javier Gil, D. Rodríguez, *Silver deposition on titanium surface by electrochemical anodizing process reduces bacterial adhesion of Streptococcus sanguinis and Lactobacillus salivarius*., Clin. Oral Implants Res. 0 (2014) 1–10. doi:10.1111/clr.12422.

[4] X.B. Tian, Z.M. Wang, S.Q. Yang, Z.J. Luo, R.K.Y. Fu, P.K. Chu, *Antibacterial copper-containing titanium nitride films produced by dual magnetron sputtering*, Surf. Coatings Technol. 201 (2007) 8606–8609. doi:10.1016/j.surfcoat.2006.09.322.

[5] M. Yoshinari, Y. Oda, T. Kato, K. Okuda, *Influence of surface modifications to titanium on antibacterial activity in vitro*, Biomaterials. 22 (2001) 2043–2048. doi:10.1016/S0142-9612(00)00392-6.

[6] G. McDonnell, A.D. Russell, *Antiseptics and disinfectants: activity, action, and resistance*., Clin. Microbiol. Rev. 12 (1999) 147–79.

[7] S. Radin, P. Ducheyne, *Controlled release of vancomycin from thin sol-gel films on titanium alloy fracture plate material*., Biomaterials. 28 (2007) 1721–9. doi:10.1016/j.biomaterials.2006.11.035.

[8] M. Stigter, K. de Groot, P. Layrolle, *Incorporation of Tobramycin into biomimetic hydroxyapatite coating on titanium*, *Biomaterials*. 23 (2002) 4143–4153.

[9] M. Stigter, J. Bezemer, K. de Groot, P. Layrolle, *Incorporation of different antibiotics into carbonated hydroxyapatite coatings on titanium implants, release and antibiotic efficacy*., J. Control. Release. 99 (2004) 127–37. doi:10.1016/j.jconrel.2004.06.011.

[10] M. Gabriel, K. Nazmi, E.C. Veerman, A. V Nieuw Amerongen, A. Zentner, *Preparation of LL-37-grafted titanium surfaces with bactericidal activity*., Bioconjug. Chem. 17 (2006) 548–50. doi:10.1021/bc050091v.

[11] G. Gao, D. Lange, K. Hilpert, J. Kindrachuk, Y. Zou, J.T.J.J. Cheng, *et al.*, *The biocompatibility and biofilm resistance of implant coatings based on hydrophilic polymer brushes conjugated with antimicrobial peptides*, Biomaterials. 32 (2011) 3899–3909. doi:10.1016/j.biomaterials.2011.02.013.

[12] A. G. Gristina, *Biomaterial-centered infection: microbial adhesion versus tissue integration*., Science. 237 (1987) 1588–95. doi:10.1126/science.3629258.

[13] Q. Yu, Z. Wu, H. Chen, *Dual-function antibacterial surfaces for biomedical applications*, Acta Biomater. 16 (2015) 1–13. doi:10.1016/j.actbio.2015.01.018.

[14] J.L. Dalsin, P.B. Messersmith, *Bioinspired antifouling polymers*, Mater. Today. 8 (2005) 38–46. doi:10.1016/S1369-7021(05)71079-8.

[15] A. Utrata-Wesoek, *Antifouling surfaces in medical application*, Polimery. 58 (2013) 685–696. doi:10.14314/polimery.2013.685.

[16] F. Rupp, R.A. Gittens, L. Scheideler, A. Marmur, B.D. Boyan, Z. Schwartz, *et al.*, *A review on the wettability of dental implant surfaces I: theoretical and experimental aspects*., Acta Biomater. 10 (2014) 2894–906. doi:10.1016/j.actbio.2014.02.040.

[17] A. Sethuraman, M. Han, R.S. Kane, G. Belfort, *Effect of surface wettability on the adhesion of proteins*., Langmuir. 20 (2004) 7779–88. doi:10.1021/la049454q.

[18] J.I. Rosales-Leal, M.A. Rodríguez-Valverde, G. Mazzaglia, P.J. Ramón-Torregrosa, L.

Díaz-Rodríguez, O. García-Martínez, *et al.*, *Effect of roughness, wettability and morphology of engineered titanium surfaces on osteoblast-like cell adhesion*, Colloids Surfaces A Physicochem. Eng. Asp. 365 (2010) 222–229. doi:10.1016/j.colsurfa.2009.12.017.

[19] L.-C. Xu, C.A. Siedlecki, *Effects of surface wettability and contact time on protein adhesion to biomaterial surfaces*., Biomaterials. 28 (2007) 3273–83. doi:10.1016/j.biomaterials.2007.03.032.

[20] R.A. Gittens, L. Scheideler, F. Rupp, S.L. Hyzy, J. Geis-Gerstorfer, Z. Schwartz, *et al.*, *A review on the wettability of dental implant surfaces II: Biological and clinical aspects*., Acta Biomater. 10 (2014) 2907–18. doi:10.1016/j.actbio.2014.03.032.

[21] A.E. Lefohn, N.M. Mackie, E.R. Fisher, *Comparison of Films Deposited from Pulsed and Continuous Wave Acetonitrile and Acrylonitrile Plasmas*, Plasmas Polym. 3 (1998) 197–209. doi:10.1023/A:1021850604696.

[22] C. Tendero, C. Tixier, P. Tristant, J. Desmaison, P. Leprince, *Atmospheric pressure plasmas: A review*, Spectrochim. Acta Part B At. Spectrosc. 61 (2006) 2–30. doi:10.1016/j.sab.2005.10.003.

[23] K.C. Popat, S. Sharma, T.A. Desai, *Quantitative XPS Analysis of PEG-Modified Silicon* Surfaces, J. Phys. Chem. B. 108 (2004) 5185–5188. doi:10.1021/jp049260j.

[24] Q. Wei, T. Becherer, S. Angioletti-Uberti, J. Dzubiella, C. Wischke, A.T. Neffe, *et al.*, *Protein interactions with polymer coatings and biomaterials*., Angew. Chem. Int. Ed. Engl. 53 (2014) 8004–31. doi:10.1002/anie.201400546.

[25] R. Michel, S. Pasche, M. Textor, D.G. Castner, *Influence of PEG architecture on protein adsorption and conformation*., Langmuir. 21 (2005) 12327–32. doi:10.1021/la051726h.

[26] J.M. Anderson, *Chapter 4 Mechanisms of inflammation and infection with implanted devices*, Cardiovasc. Pathol. 2 (1993) 33–41. doi:10.1016/1054-8807(93)90045-4.

[27] M. Rabe, D. Verdes, S. Seeger, *Understanding protein adsorption phenomena at solid surfaces*., Adv. Colloid Interface Sci. 162 (2011) 87–106. doi:10.1016/j.cis.2010.12.007.

[28] Q. Wei, T. Becherer, S. Angioletti-Uberti, J. Dzubiella, C. Wischke, A.T. Neffe, *et al.*, *Protein Interactions with Polymer Coatings and Biomaterials*, Angew. Chemie Int. Ed. 53 (2014) 8004–8031. doi:10.1002/anie.201400546.

[29] M.S. Lord, M. Foss, F. Besenbacher, *Influence of nanoscale surface topography on protein adsorption and cellular response*, Nano Today. 5 (2010) 66–78. doi:10.1016/j.nantod.2010.01.001.

[30] E.A. Vogler, *Protein adsorption in three dimensions*., Biomaterials. 33 (2012) 1201–37. doi:10.1016/j.biomaterials.2011.10.059.

[31] F. Poncin-Epaillard, T. Vrlinic, D. Debarnot, M. Mozetic, A. Coudreuse, G. Legeay, *et al.*, *Surface treatment of polymeric materials controlling the adhesion of biomolecules*., J. Funct. Biomater. 3 (2012) 528–43. doi:10.3390/jfb3030528.

[32] D.L. Elbert, J.A. Hubbell, *Self-assembly and steric stabilization at heterogeneous, biological surfaces using adsorbing block copolymers*, Chem. Biol. 5 (1998) 177–183. doi:10.1016/S1074-5521(98)90062-X.

[33] Z. Bai, M.J. Filiaggi, J.R. Dahn, *Fibrinogen adsorption onto 316L stainless steel, Nitinol and titanium*, Surf. Sci. 603 (2009) 839–846. doi:10.1016/j.susc.2009.01.040.

[34] H. Flores-Villaseñor, A. Canizalez-Román, M. Reyes-Lopez, K. Nazmi, M. de la Garza, J. Zazueta-Beltrán, *et al.*, *Bactericidal effect of bovine lactoferrin, LFcin, LFampin and LFchimera on antibiotic-resistant Staphylococcus aureus and Escherichia coli*., Biometals. 23 (2010) 569–78. doi:10.1007/s10534-010-9306-4.

[35] E. Molena, C. Credi, C. De Marco, M. Levi, S. Turri, G. Simeone, *Protein antifouling and fouling-release in perfluoropolyether surfaces*, Appl. Surf. Sci. 309 (2014) 160–167. doi:10.1016/j.apsusc.2014.04.211.

[36] P.-H. Chua, K.-G. Neoh, E.-T. Kang, W. Wang, *Surface functionalization of titanium with hyaluronic acid/chitosan polyelectrolyte multilayers and RGD for promoting osteoblast functions and inhibiting bacterial adhesion*., Biomaterials. 29 (2008) 1412–21. doi:10.1016/j.biomaterials.2007.12.019.

[37] M. Pegueroles, C. Tonda-Turo, J.A. Planell, F.-J. Gil, C. Aparicio, *Adsorption of Fibronectin, Fibrinogen, and Albumin on TiO 2 : Time-Resolved Kinetics, Structural Changes, and Competition Study*, Biointerphases. 7 (2012) 48. doi:10.1007/s13758-012-0048-4.

[38] V. Hlady, J. Buijs, H.P. Jennissen, *Methods for Studying Protein Adsorption*, Methods Enzymol. 309 (1999) 402–429.

[39] I.-S. Moon, T. Berglundh, I. Abrahamsson, E. Linder, J. Lindhe, *The barrier between the keratinized mucosa and the dental implant. An experimental study in the dog*, J. Clin. Periodontol. 26 (1999) 658–663. doi:10.1034/j.1600-051X.1999.261005.x.

[40] D.J. Menzies, M. Jasieniak, H.J. Griesser, J.S. Forsythe, G. Johnson, G.A. McFarland, *et al., A ToF-SIMS and XPS study of protein adsorption and cell attachment across PEG-like plasma polymer films with lateral compositional gradients*, Surf. Sci. 606 (2012) 1798–1807. doi:10.1016/j.susc.2012.07.017.

[41] H. Wang, J. Ren, A. Hlaing, M. Yan, *Fabrication and anti-fouling properties of photochemically and thermally immobilized poly(ethylene oxide) and low molecular weight poly(ethylene glycol) thin films*., J. Colloid Interface Sci. 354 (2011) 160–7. doi:10.1016/j.jcis.2010.10.018.

[42] P.K. Thalla, A. Contreras-García, H. Fadlallah, J. Barrette, G. De Crescenzo, Y. Merhi, *et al., A versatile star PEG grafting method for the generation of nonfouling and nonthrombogenic surfaces*, Biomed Res. Int. 2013 (2013) 962376. doi:10.1155/2013/962376.

[43] G. Liu, Y. Li, L. Yang, Y. Wei, X. Wang, Z. Wang, *et al., Cytotoxicity study of polyethylene glycol derivatives*, RSC Adv. (2017), 7, 18252-18259, doi:10.1039/c7ra00861a.

[44] O. Biondi, S. Motta, P. Mosesso, *Low molecular weight polyethylene glycol induces chromosome aberrations in Chinese hamster cells cultured in vitro*, Mutagenesis. 17 (2002) 261–264. doi:10.1093/mutage/17.3.261.

[45] M. Gallorini, A. Cataldi, V. di Giacomo, *HEMA-induced cytotoxicity: oxidative stress, genotoxicity and apoptosis*, Int. Endod. J. 47 (2014) 813–818. doi:10.1111/iej.12232.

[46] A. Bakopoulou, T. Papadopoulos, P. Garefis, *Molecular Toxicology of Substances Released from Resin–Based Dental Restorative Materials*, Int. J. Mol. Sci. 10 (2009) 3861–3899. doi:10.3390/ijms10093861.

[47] S. Krifka, G. Spagnuolo, G. Schmalz, H. Schweikl, *A review of adaptive mechanisms in cell responses towards oxidative stress caused by dental resin monomers*, Biomaterials. 34 (2013) 4555–4563. doi:10.1016/j.biomaterials.2013.03.019.

[48] S.I. Ertel, B.D. Ratner, A. Kaul, M.B. Schway, T.A. Horbett, *In vitro study of the intrinsic toxicity of synthetic surfaces to cells*, J. Biomed. Mater. Res. 28 (1994) 667–675. doi:10.1002/jbm.820280603.

[49] M. Prasitsilp, T. Siriwittayakorn, R. Molloy, N. Suebsanit, P. Siriwittayakorn, S. Veeranondha, *Cytotoxicity study of homopolymers and copolymers of 2-hydroxyethyl methacrylate and some alkyl acrylates for potential use as temporary skin substitutes*, J. Mater. Sci. Mater. Med. 14 (2003) 595–600. doi:10.1023/A:1024066806347.

[50] H.L. Myshin, J.P. Wiens, *Factors affecting soft tissue around dental implants: A review of the literature*, J. Prosthet. Dent. 94 (2005) 440–444. doi:10.1016/j.prosdent.2005.08.021.

[51] A. Sculean, R. Gruber, D.D. Bosshardt, *Soft tissue wound healing around teeth and*

dental implants., J. Clin. Periodontol. 41 Suppl 1 (2014) S6-22. doi:10.1111/jcpe.12206.
[52] B. Nisol, G. Oldenhove, N. Preyat, D. Monteyne, M. Moser, D. Perez-Morga, *et al.*, *Atmospheric plasma synthesized PEG coatings: non-fouling biomaterials showing protein and cell repulsion*, Surf. Coatings Technol. 252 (2014) 126–133. doi:10.1016/j.surfcoat.2014.04.056.
[53] J. Chen, J. Cao, J. Wang, M.F. Maitz, L. Guo, Y. Zhao, *et al.*, *Biofunctionalization of titanium with PEG and anti-CD34 for hemocompatibility and stimulated endothelialization*., J. Colloid Interface Sci. 368 (2012) 636–47. doi:10.1016/j.jcis.2011.11.039.
[54] E. Lih, S.H. Oh, Y.K. Joung, J.H. Lee, D.K. Han, *Polymers for cell/tissue anti-adhesion*, Prog. Polym. Sci. 44 (2015) 28–61. doi:10.1016/j.progpolymsci.2014.10.004.
[55] F. Zhang, G. Li, P. Yang, W. Qin, C. Li, N. Huang, *Fabrication of biomolecule-PEG micropattern on titanium surface and its effects on platelet adhesion*., Colloids Surf. B. Biointerfaces. 102 (2013) 457–65. doi:10.1016/j.colsurfb.2012.02.018.
[56] E.A. Burton, K.A. Simon, S. Hou, D. Ren, Y.-Y. Luk, *Molecular Gradients of Bioinertness Reveal a Mechanistic Difference between Mammalian Cell Adhesion and Bacterial Biofilm Formation*, Langmuir. 25 (2009) 1547–1553. doi:10.1021/la803261b.
[57] I.C. Saldarriaga Fernández, H.C. van der Mei, M.J. Lochhead, D.W. Grainger, H.J. Busscher, *The inhibition of the adhesion of clinically isolated bacterial strains on multi-component cross-linked poly(ethylene glycol)-based polymer coatings*, Biomaterials. 28 (2007) 4105–4112. doi:10.1016/j.biomaterials.2007.05.023.
[58] A. Fournier, L. Payant, R. Bouclin, *Adherence of Streptococcus mutans to orthodontic brackets*, Am. J. Orthod. Dentofac. Orthop. 114 (1998) 414–417. doi:10.1016/S0889-5406(98)70186-6.
[59] B. Li, B.E. Logan, *Bacterial adhesion to glass and metal-oxide surfaces*, Colloids Surfaces B Biointerfaces. 36 (2004) 81–90. doi:10.1016/j.colsurfb.2004.05.006.
[60] K.D. Park, Y.S. Kim, D.K. Han, Y.H. Kim, E.H.B. Lee, H. Suh, *et al.*, *Bacterial adhesion on PEG modified polyurethane surfaces*, Biomaterials. 19 (1998) 851–859. doi:10.1016/S0142-9612(97)00245-7.
[61] A. Roosjen, H.J. Kaper, H.C. van der Mei, W. Norde, H.J. Busscher, *Inhibition of adhesion of yeasts and bacteria by poly(ethylene oxide)-brushes on glass in a parallel plate flow chamber*., Microbiology. 149 (2003) 3239–46.
[62] A. Kawawe, I. Nakagawa, Z. Kanno, Y. Tsutsumi, T. Hanawa, T. Ono, *Evaluation of biofilm formation in the presence of saliva on poly(ethylene glycol)deposited titanium*, Dent. Mater. J. 33 (2014) 638–47. doi:10.4012/dmj.2014-025.
[63] A. Roosjen, H.J. Busscher, W. Norde, H. van der Mei, *Bacterial factors influencing adhesion of Pseudomonas aeruginosa strains to a poly(ethylene glycol) brush*, Microbiology. 152 (2006) 2673–2682.
[64] Anneta Razatos, Yea-Ling Ong, Fabienne Boulay, Donald L. Elbert, Jeffrey A. Hubbell, Mukul M. Sharma, *et al.*, *Force Measurements between Bacteria and Poly(ethylene glycol)-Coated Surfaces*, (2000). doi:10.1021/LA000818Y.
[65] N.P. Desai, S.F.A. Hossainy, J.A. Hubbell, *Surface-immobilized polyethylene oxide for bacterial repellence*, Biomaterials. 13 (1992) 417–420. doi:10.1016/0142-9612(92)90160-P.
[66] X. Liu, P.K. Chu, C. Ding, *Surface modification of titanium, titanium alloys, and related materials for biomedical applications*, Mater. Sci. Eng. R Reports. 47 (2004) 49–121. doi:10.1016/j.mser.2004.11.001.
[67] P.. Chu, J.. Chen, L.. Wang, N. Huang, *Plasma-surface modification of biomaterials*, Mater. Sci. Eng. R Reports. 36 (2002) 143–206. doi:10.1016/S0927-796X(02)00004-9.
[68] P. Cools, N. De Geyter, E. Vanderleyden, P. Dubruel, R. Morent, *Surface Analysis of*

Titanium Cleaning and Activation Processes: Non-thermal Plasma Versus Other Techniques, Plasma Chem. Plasma Process. 34 (2014) 917–932. doi:10.1007/s11090-014-9552-2.

[69] S. Zhang, F. Awaja, N. James, D.R. McKenzie, A.J. Ruys, *Autohesion of plasma treated semi-crystalline PEEK: Comparative study of argon, nitrogen and oxygen treatments*, Colloids Surfaces A Physicochem. Eng. Asp. 374 (2011) 88–95. doi:10.1016/j.colsurfa.2010.11.013.

[70] M.C. Kim, S.H. Yang, J.-H. Boo, J.G. Han, *Surface treatment of metals using an atmospheric pressure plasma jet and their surface characteristics*, Surf. Coatings Technol. 174 (2003) 839–844. doi:10.1016/S0257-8972(03)00560-7.

[71] Peter K. Working, Mary S. Newman, Judy Johnson, Joel B. Cornacoff, *Poly(ethylene glycol)*, American Chemical Society, Washington, DC, 1997. doi:10.1021/bk-1997-0680.

[72] S. Krishnan, C.J. Weinman, C.K. Ober, *Advances in polymers for anti-biofouling surfaces*, J. Mater. Chem. 18 (2008) 3405. doi:10.1039/b801491d.

[73] I. Szleifer, *Protein Adsorption on Surfaces with Grafted Polymers*, Biophys. J. 72 (1997) 595–612. doi:10.1016/S0006-3495(97)78698-3.

[74] S. Chen, L. Li, C. Zhao, J. Zheng, *Surface hydration: Principles and applications toward low-fouling/nonfouling biomaterials*, Polymer (Guildf). 51 (2010) 5283–5293. doi:10.1016/j.polymer.2010.08.022.

[75] E. Byun, J. Kim, S.M. Kang, H. Lee, D. Bang, H. Lee, *Surface PEGylation via native chemical ligation.*, Bioconjug. Chem. 22 (2011) 4–8. doi:10.1021/bc100285p.

[76] S. Saxer, C. Portmann, S. Tosatti, K. Gademann, S. Zürcher, M. Textor, *Surface Assembly of Catechol-Functionalized Poly(l -lysine)- graft -poly(ethylene glycol) Copolymer on Titanium Exploiting Combined Electrostatically Driven Self-Organization and Biomimetic Strong Adhesion*, Macromolecules. 43 (2010) 1050–1060. doi:10.1021/ma9020664.

[77] R.R. Maddikeri, S. Tosatti, M. Schuler, S. Chessari, M. Textor, R.G. Richards, *et al.*, *Reduced medical infection related bacterial strains adhesion on bioactive RGD modified titanium surfaces: a first step toward cell selective surfaces.*, J. Biomed. Mater. Res. A. 84 (2008) 425–35. doi:10.1002/jbm.a.31323.

[78] K. Oya, Y. Tanaka, H. Saito, K. Kurashima, K. Nogi, H. Tsutsumi, *et al.*, *Calcification by MC3T3-E1 cells on RGD peptide immobilized on titanium through electrodeposited PEG.*, Biomaterials. 30 (2009) 1281–6. doi:10.1016/j.biomaterials.2008.11.030.

[79] L. Deng, M. Mrksich, G.M. Whitesides, Self-Assembled Monolayers of Alkanethiolates Presenting Tri(propylene sulfoxide) Groups Resist the Adsorption of Protein, J. Am. Chem. Soc. 118 (1996) 5136–5137. doi:10.1021/ja960461d.

[80] N.-J. Lin, H.-S. Yang, Y. Chang, K.-L. Tung, W.-H. Chen, H.-W. Cheng, *et al.*, Surface Self-Assembled PEGylation of Fluoro-Based PVDF Membranes via Hydrophobic-Driven Copolymer Anchoring for Ultra-Stable Biofouling Resistance, Langmuir. 29 (2013) 10183–10193. doi:10.1021/la401336y.

[81] N. Faucheux, R. Schweiss, K. Lützow, C. Werner, T. Groth, Self-assembled monolayers with different terminating groups as model substrates for cell adhesion studies., Biomaterials. 25 (2004) 2721–30. doi:10.1016/j.biomaterials.2003.09.069.

[82] A.K. Muszanska, E.T.J. Rochford, A. Gruszka, A.A. Bastian, H.J. Busscher, W. Norde, *et al.*, Antiadhesive Polymer Brush Coating Functionalized with Antimicrobial and RGD Peptides to Reduce Biofilm Formation and Enhance Tissue Integration, Biomacromolecules. 15 (2014) 2019–2026. doi:10.1021/bm500168s.

[83] P. Alexandridis, T. Alan Hatton, *Poly(ethylene oxide)-poly(propylene oxide)-poly(ethylene oxide) block copolymer surfactants in aqueous solutions and at interfaces:*

thermodynamics, structure, dynamics, and modeling, Colloids Surfaces A Physicochem. Eng. Asp. 96 (1995) 1–46. doi:10.1016/0927-7757(94)03028-X.

[84] G.M. Harbers, K. Emoto, C. Greef, S.W. Metzger, H.N. Woodward, J.J. Mascali, *et al.*, *A functionalized poly(ethylene glycol)-based bioassay surface chemistry that facilitates bio-immobilization and inhibits non-specific protein, bacterial, and mammalian cell adhesion*., Chem. Mater. 19 (2007) 4405–4414. doi:10.1021/cm070509u.

[85] G.L. Kenausis, J. Vörös, D.L. Elbert, N. Huang, R. Hofer, L. Ruiz-Taylor, *et al.*, *Poly(l -lysine)-g-Poly(ethylene glycol) Layers on Metal Oxide Surfaces: Attachment Mechanism and Effects of Polymer Architecture on Resistance to Protein Adsorption*, J. Phys. Chem. B. 104 (2000) 3298–3309. doi:10.1021/jp993359m.

[86] M. Catauro, F. Bollino, F. Papale, M. Gallicchio, S. Pacifico, *Synthesis and chemical characterization of new silica polyethylene glycol hybrid nanocomposite materials for controlled drug delivery*, J. Drug Deliv. Sci. Technol. 24 (2014) 320–325. doi:10.1016/S1773-2247(14)50069-X.

[87] Y. Ito, H. Hasuda, M. Sakuragi, S. Tsuzuki, *Surface modification of plastic, glass and titanium by photoimmobilization of polyethylene glycol for antibiofouling*., Acta Biomater. 3 (2007) 1024–32. doi:10.1016/j.actbio.2007.05.010.

[88] Y. Tanaka, K. Matin, M. Gyo, A. Okada, Y. Tsutsumi, H. Doi, *et al.*, *Effects of electrodeposited poly(ethylene glycol) on biofilm adherence to titanium*., J. Biomed. Mater. Res. A. 95 (2010) 1105–13. doi:10.1002/jbm.a.32932.

[89] Y. Tanaka, H. Doi, Y. Iwasaki, S. Hiromoto, T. Yoneyama, K. Asami, *et al.*, *Electrodeposition of amine-terminated poly(ethylene glycol) to titanium surface*, Mater. Sci. Eng. C. 27 (2007) 206–212. doi:10.1016/j.msec.2006.03.007.

[90] Y. Tanaka, Y. Matsuo, T. Komiya, Y. Tsutsumi, H. Doi, T. Yoneyama, *et al.*, *Characterization of the spatial immobilization manner of poly(ethylene glycol) to a titanium surface with immersion and electrodeposition and its effects on platelet adhesion*., J. Biomed. Mater. Res. A. 92 (2010) 350–8. doi:10.1002/jbm.a.32375.

[91] Y.J. Wu, R.B. Timmons, J.S. Jen, F.E. Molock, *Non-fouling surfaces produced by gas phase pulsed plasma polymerization of an ultra low molecular weight ethylene oxide containing monomer*, Colloids Surfaces B Biointerfaces. 18 (2000) 235–248. doi:10.1016/S0927-7765(99)00150-2.

[92] G. Clarotti, F. Schue, J. Sledz, K.E. Geckeler, W. Göpel, A. Orsetti, *Plasma deposition of thin fluorocarbon films for increased membrane hemocompatibility*, J. Memb. Sci. 61 (1991) 289–301. doi:10.1016/0376-7388(91)80022-X.

[93] F. Fanelli, A.M. Mastrangelo, F. Fracassi, *Aerosol-Assisted Atmospheric Cold Plasma Deposition and Characterization of Superhydrophobic Organic–Inorganic Nanocomposite Thin Films*, Langmuir. 30 (2014) 857–865. doi:10.1021/la404755n.

[94] F. Brétagnol, M. Lejeune, A. Papadopoulou-Bouraoui, M. Hasiwa, H. Rauscher, G. Ceccone, *et al.*, *Fouling and non-fouling surfaces produced by plasma polymerization of ethylene oxide monomer*., Acta Biomater. 2 (2006) 165–72. doi:10.1016/j.actbio.2005.11.002.

[95] P. Chu, *Plasma-surface modification of biomaterials*, Mater. Sci. Eng. R Reports. 36 (2002) 143–206. doi:10.1016/S0927-796X(02)00004-9.

[96] F.F. Shi, *Recent advances in polymer thin films prepared by plasma polymerization Synthesis, structural characterization, properties and applications*, Surf. Coatings Technol. 82 (1996) 1–15. doi:10.1016/0257-8972(95)02621-5.

[97] H.K. Yasuda, *Some Important Aspects of Plasma Polymerization*, Plasma Process. Polym. 2 (2005) 293–304. doi:10.1002/ppap.200400071.

[98] H. Yasuda, T. Hsu, *Some aspects of plasma polymerization investigated by pulsed R.F. discharge*, J. Polym. Sci. Polym. Chem. Ed. 15 (1977) 81–97.

doi:10.1002/pol.1977.170150109.

[99] A. Michelmore, C. Charles, R.W. Boswell, R.D. Short, J.D. Whittle, *Defining plasma polymerization: new insight into what we should be measuring*., ACS Appl. Mater. Interfaces. 5 (2013) 5387–91. doi:10.1021/am401484b.

[100] M. Salim, G. Mishra, G.J.S. Fowler, B. O'sullivan, P.C. Wright, S.L. McArthur, *Non-fouling microfluidic chip produced by radio frequency tetraglyme plasma deposition*., Lab Chip. 7 (2007) 523–525. doi:10.1039/b615328c.

[101] M. Shen, M.S. Wagner, D.G. Castner, B.D. Ratner, T.A. Horbett, *Multivariate Surface Analysis of Plasma-Deposited Tetraglyme for Reduction of Protein Adsorption and Monocyte Adhesion* , Langmuir. 19 (2003) 1692–1699. doi:10.1021/la0259297.

[102] E.E. Johnston, J.D. Bryers, B.D. Ratner, *Plasma deposition and surface characterization of oligoglyme, dioxane, and crown ether nonfouling films*, Langmuir. 21 (2005) 870–881. doi:10.1021/la036274s.

[103] T.C.A.M. Azevedo, M.A. Algatti, R.P. Mota, R.Y. Honda, M.E. Kayama, K.G. Kostov, *et al., Wettability, optical properties and molecular structure of plasma polymerized diethylene glycol dimethyl ether*, J. Phys. Conf. Ser. 167 (2009) 12053. doi:10.1088/1742-6596/167/1/012053.

[104] B. Nisol, C. Poleunis, P. Bertrand, F. Reniers, *Poly(ethylene glycol) Films Deposited by Atmospheric Pressure Plasma Liquid Deposition and Atmospheric Pressure Plasma-Enhanced Chemical Vapour Deposition: Process, Chemical Composition Analysis and Biocompatibility*, Plasma Process. Polym. 7 (2010) 715–725. doi:10.1002/ppap.201000023.

[105] L. O'Neill, L.-A. O'Hare, S.R. Leadley, A.J. Goodwin, *Atmospheric Pressure Plasma Liquid Deposition - A Novel Route to Barrier Coatings*, Chem. Vap. Depos. 11 (2005) 477–479. doi:10.1002/cvde.200404209.

[106] F. Fanelli, A.M. Mastrangelo, F. Fracassi, *Aerosol-Assisted Atmospheric Cold Plasma Deposition and Characterization of Superhydrophobic Organic–Inorganic Nanocomposite Thin Films,* Langmuir. 30 (2014) 857–865. doi:10.1021/la404755n.

[107] G. Da Ponte, E. Sardella, F. Fanelli, R. D'Agostino, R. Gristina, P. Favia, Plasma *Deposition of PEO-Like Coatings with Aerosol-Assisted Dielectric Barrier Discharges,* Plasma Process. Polym. 9 (2012) 1176–1183. doi:10.1002/ppap.201100201.

CONCLUSIONS

9. CONCLUSIONS

This thesis has evaluated different methods for the coating of titanium for dental implants, allowing to identify different relevant tools to confer enhanced properties to the implants, which are summarized in the following conclusions.

Optimum activation conditions for titanium by means of plasma treatments were found by employing argon as the discharge gas, which led to superhydrophilic surfaces with a reduced amount of organic contaminants on the surface.

Silanized PEG was synthesized and successfully grafted onto the titanium surface, giving an ultra-thin coating able to withstand BSA adsorption and *S. sanguinis* and *L. salivarius* adhesion. The impaired fibroblast adhesion due to the presence of the antifouling coating has been improved by means of the incorporation of the cell adhesion peptide RGD to the coating. Moreover, the bacterial adhesion of the two tested strains has not been significantly modified by the presence of RGD.

An electrodeposited PEG bis(aminopropyl) terminated coating has been prepared by means of continuous and pulsed electrodeposition. Surface characterization reported a thicker coating when using pulses, with a higher surface coverage, demonstrating the higher yield of this process compared to the continuous one. This fact is also reflected in the *in vitro* results, either in mono- or co-culture experiments, showing the efficacy of the coatings to favor the fibroblast adhesion over the bacteria adhesion. Both Magainin 2 and Lactoferrin 1-11 have been successfully immobilized on the electrodeposited PEG coating by two different bonding strategies. The use of the coating as a platform for the AMP immobilization improved the *in vitro* response of the coatings, by decreasing the bacterial adhesion.

A PEG-like plasma polymerized coating has been achieved on the titanium surface. Both tetraglyme and diglyme precursors are suitable for the preparation of the coatings. This coating reduces the bacterial adhesion while maintaining the cellular adhesion, giving a biocompatible coating suitable for dental implants applications. Some differences can be observed in terms of the chemical composition, but these differences do not show a significant difference on the biological performance *in vitro* of the coatings. Plasma polymerized diglyme is a suitable coating to achieve a dual-function system, by combining the antifouling properties of the coating and the antibacterial activity of the doxycycline.

Atmospheric pressure plasma for the direct treatment of liquid in a different approach to prepare coatings. A vancomycin-containing plasma polymerized ethylene coating has been prepared by aerosol-assisted dielectric barrier discharge plasma, in order to prepare a drug delivery system. The coating showed a delayed release, and the antibacterial properties of the vancomycin were maintained after the plasma treatment. On the other hand, a HEMA plasma polymerized coating has been successfully prepared by treating the monomer with an atmospheric pressure plasma jet system. The coating showed a retained wettability and chemical composition compared to the precursor. The

coating was stable after immersion in water and sonication. Fibroblast adhesion was enhanced with the polymer, while the bacterial adhesion of *S. aureus* an *E. coli* was reduced, and therefore the coating is suitable for dental implant applications.